

Association of spectroscopic and rs-fMRI markers with vulnerability factors, endophenotypes and clinical dimensions and conditions of affective disorders

Dissertation Zur Erlangung des akademischen Grades
doctor rerum naturalium (Dr. rer. nat.) genehmigt durch
die Fakultät für Naturwissenschaften der Otto-von-Guericke
Universität Magdeburg

von Mag. Biol. **Lejla Colic**
geboren am 16.12.1985. in Tuzla

eingereicht am 27.11.2018.

verteidigt am 15.08.2019.

Betreuer& Gutachter: Prof. Dr. med. Martin Walter

Gutachter: Prof. Dr. med. Franz X. Vollenweider

“Making knowledge is not simply about making facts but about making worlds, or rather, it is about making specific worldly configurations – not in the sense of making them up ex nihilo, or out of language, beliefs, or ideas, but in the sense of materially engaging as part of the world in giving it specific material form.”

Karen Barad

“Take this pink ribbon off my eyes
I'm exposed
And it's no big surprise
Don't you think I know
Exactly where I stand
This world is forcing me
To hold your hand
'Cause I'm just a girl, little ol' me
Well don't let me out of your sight
Oh, I'm just a girl, all pretty and petite
So don't let me have any rights
Oh, I've had it up to here!”

No Doubt

Table of Contents

Table of Contents	1
Abstract	7
Zusammenfassung	9
List of Abbreviations	11
List of Figures	15
List of Tables	16
List of Supplementary Figures	17
List of Supplementary Tables	18
Chapter 1. General Introduction	19
1.1. Biomarkers.....	20
1.2. The Cingulate Cortex	22
1.2.1. Anterior Cingulate Cortex (ACC).....	23
1.2.2. Posterior Cingulate Cortex (PCC).....	24
1.2.3. Cingulate cortex in affective pathologies	25
1.3. Vulnerabilities - personality and genetic polymorphisms	26
1.4. Pathological affective states: Major Depressive Disorder.....	27
1.5. Intervention: Ketamine as a prototypical glutamate modulator and potential antidepressant agent	28
1.5.1. Ketamine pharmacology	29
1.5.2. Ketamine metabolism.....	29
1.5.3. Ketamine administration.....	30
1.5.4. Mechanisms of antidepressant action.....	31
1.5.5. Implications of ketamine mechanisms in MDD	33
1.6. Outline of the studies	33
Chapter 2. Materials and Methods	36
2.1. Anatomical scans	36
2.1.1. Anatomical scan at 3T.....	36
2.1.2. Anatomical scan at 7T	37
2.1.3. Anatomical data preprocessing and analysis	37
2.2. Magnetic Resonance Spectroscopy (MRS).....	37
2.2.1. Intro to MRS - What is MRS	37

2.2.2.Principles of MRS.....	38
2.2.3.MRS data acquisition	39
2.2.4.Comparison of the 3T and 7T sequences	41
2.2.5.MRS data acquisition and processing at 3T	42
2.2.6.MRS data acquisition and processing at 7T	43
2.2.7.Reliability of quality exclusion criteria	45
2.3. Resting state functional magnetic resonance imaging.....	47
2.3.1.Principles of Magnetic Resonance Imaging.....	47
2.3.2.Resting state fMRI	49
2.3.3.Indices of resting state	49
2.3.4.rs-fMRI data acquisition and analysis.....	51
2.3.5.Challenges at high-field imaging	54
2.4. Summary of general methods.....	58
Chapters 3 - 6: Individual studies (pp. 60-157)	59
Chapter 3. Study 1: Metabolite and connectivity correlates of alexithymia in DMN and SN	60
3.1. Introduction to Study 1	60
3.1.1.Sex differences in alexithymia	61
3.1.2.Alexithymia in neuroimaging.....	61
3.1.3.The self- and the other- distinction in alexithymia.....	62
3.2. Specific materials and methods of Study 1.....	64
3.2.1.Participants.....	64
3.2.2.Psychometric assessment	64
3.2.3.3T MRS acquisition and processing	65
3.2.4.7T rs-fMRI acquisition and preprocessing	65
3.2.5.Statistical analysis	65
3.3. Results of Study 1 Alexithymia	66
3.3.1.Demographic data	66
3.3.2.TAS-20 total score associates with metabolites in DMN in women, and in salience network in men	67
3.3.3.TAS-20 is not associated with cortical thickness	68
3.3.4.TAS-20 scales mirror main effects of alexithymia	69
3.3.5.TAS-20 correlates with FC of gyri and sulci mid-dACC seeds towards large medial frontal area.....	71
3.3.6.Sex differences were present only in the FC of the gyri seeds.....	74
3.4. Discussion of Study 1	75

3.4.1. Demographic properties.....	75
3.4.2. 3T metabolite study.....	75
3.4.3. 7T connectivity study	78
3.4.4. Alexithymia and disorders of affect regulation: an unspecific cross-relationship	81
3.5. Limitations of Study 1	81
3.6. Conclusions of Study 1	83
Chapter 4. Study 2: Genetic and sex effects of anxiety-related endophenotypes in the pgACC	84
4.1. Introduction to Study 2.....	84
4.2. Specific materials and methods of Study 2	87
4.2.1. Participants.....	87
4.2.2. Genotyping	87
4.2.3. Personality questionnaire	89
4.2.4. 7T MRS and rs-fMRI acquisition.....	90
4.2.5. Statistical analysis	90
4.3. Results of Study 2	92
4.3.1. Demographic data	92
4.3.2. Genotype differences in the local neuronal activity	95
4.3.3. <i>GAD2</i> polymorphism rs2236418 and sex show effect on the GABA/Glu ratio in the pgACC.....	96
4.3.4. In women GABA/Glu ratio correlates negatively with harm avoidance.....	99
4.3.5. PgACC GABA/Glu mediates relationship between <i>GAD2</i> rs2236418 genotype and harm avoidance but only in women.....	100
4.4. Discussion of Study 2.....	101
4.5. Limitations of Study 2.....	105
4.6. Conclusions of Study 2.....	106
Chapter 5. Study 3: Glutamatergic imbalance in pgACC depends on symptom severity in major depressive disorder	107
5.1. Introduction to Study 3.....	107
5.2. Study 3 specific materials and methods	111
5.2.1. Participants.....	111
5.2.2. 7T MRS and rs-fMRI acquisition	112
5.2.3. Statistical analyses	113
5.3. Results Study 3.....	114
5.3.1. Demographics	114

5.3.2.Variance of the pgACC metabolites is equal between the MDD and the healthy control group.....	115
5.3.3.Gln/Glu ratio was increased in the MDD	115
5.3.4.Severity displays a moderated relationship with Gln/Glu levels in the pgACC116	
5.3.5.Glutamine levels drive the metabolite associations to anhedonia	117
5.3.6.Medication use does not affect metabolite levels in the pgACC.....	118
5.4. Discussion Study 3 MDD	119
5.5. Limitations of Study 3.....	123
5.6. Conclusions of Study 3.....	123

Chapter 6. Study 4: Ketamine infusion in healthy participants induces delayed changes in glutamatergic levels in the pgACC, peripheral blood markers and long-term safety outcomes 125

6.1. Introduction	126
6.2. Study 4 specific materials and methods	130
6.2.1.Study design.....	130
6.2.2.Participants	131
6.2.3.Study Medication	131
6.2.4.Study procedure	131
6.2.5.MR measurements	133
6.2.6.Blood marker measurement and analysis	134
6.2.7.Safety blood measurement and analysis.....	135
6.2.8.Statistical analyses	136
6.3. Results Study 4 Ketamine.....	137
6.3.1.Demographics.....	137
6.3.2.Sex predicts baseline levels of Acet-Tub/TRF, their absolute levels, haemoglobin and number of erythrocytes and thrombocytes	139
6.3.3.Glutamate levels in the pgACC change 24 h after ketamine infusion.....	140
6.3.4.Change of Acet-Tub/TRF levels after ketamine is sex specific	141
6.3.5.Relative changes of Acet-Tub/TRF and Glu/tCr correlate negatively after ketamine infusion	143
6.3.6.Thrombocyte number increases 14 days after ketamine infusion	143
6.3.7.Demographic factors do not predict relative increase of investigated parameters	146
6.3.8.Acute Dissociative symptoms do not associate to the magnitude of changes within the ketamine group.....	146
6.4. Discussion Study 4 Ketamine	147
6.4.1.Baseline sex differences.....	147

6.4.2. Ketamine-induced effects are general for Glu/tCr change, but sex specific for Acet-Tub/TRF change	147
6.4.3. Safety considerations	149
6.4.4. Hyper-acute dissociative symptoms	154
6.5. Limitations Study 4 Ketamine	155
6.6. Conclusion Study 4 Ketamine	156
Chapter 7. General conclusion & Critical outlook	158
7.1. Summary	158
7.2. Regional and metabolite convergence	158
7.3. Demographic diversity as an asset and not a confound	160
7.4. Clinical heterogeneity	161
7.5. Ketamine mechanisms of action and future applications	162
7.6. Methodological considerations	164
References	165
Appendix	i
I. Supplementary Material	i
I.A. Supplementary Figures	i
I.B. Supplementary Tables	vii
II. Publications	xxvi
III. Ehrenerklärung	xxix

Abstract

Magnetic resonance spectroscopy (MRS) and resting state functional magnetic resonance imaging (rs-fMRI) present opportunities to investigate the brain in a non-invasive manner, via metabolite and functional activity at rest. Imaging measures can be furthermore used as biomarkers of predisposition to develop affective disorders, correlates of clinical conditions, *e.g.* major depressive disorder (MDD), or measures of activity under pharmacological interventions. Therefore, imaging markers of these three levels were examined in the pregenual anterior cingulate cortex (pgACC), a well described region governing affect processing in health and disease including depression.

In this work, I investigated the suitability and additive evidence derived from multimodal imaging parameters in affect-related dimensions and depression, elaborating their responsiveness to therapeutic effects and susceptibility to participant factors, such as clinical stages and potential control parameters.

Studies 1 and 2 investigated healthy study samples, in relation to affect-related features. Study 1 applied MRS and fMRI in alexithymia as an exemplary personality dimension related to affect processing deficits, while Study 2 looked at a genetic variation in the γ -aminobutyric acid (GABA) synthesizing enzyme glutamate decarboxylase (GAD65) in connection to an anxiety-related phenotype. Both studies found that metabolite levels in the pgACC associate to the respective personality parameter. Expression of alexithymia correlated with N-acetylaspartate, a marker of neuronal integrity. Moreover, metabolite levels and connectivity profiles in other cingulate regions differed between men and women. Further, association of different GAD65 SNPs to altered GABA/Glutamate (Glu) levels was also observed, which was related to harm avoidance trait. Here an influence of sex was also found.

Study 3 compared glutamatergic markers between healthy and major depressive disorder (MDD) participants, additionally including clinical dimensions, depressive symptom severity and anhedonia as factors of interest. MDD patients showed higher levels of Glutamine (Gln)/Glu, reflecting pathophysiological processes in the Gln-Glu cycle. Moreover, depression severity and anhedonia showed a moderating function to the glutamatergic status.

Lastly, Study 4 looked at glutamatergic and peripheral biomarker response 24 h after ketamine infusion in controls, a supposed peak time point of antidepressant response. Glu/total Creatine (tCr) decreased, and this further correlated to an increase in peripheral marker of synaptic plasticity, namely Acetyl-Tubulin/Transferrin (Acet-Tub/TRF), more evidently in women. Additionally, safety parameters were inspected. Thrombocyte levels were increased two weeks after infusion marking that careful monitoring is needed especially for at-risk patients.

In conclusion, changes in levels of different metabolite systems that are related to affective processes, that are impaired in depression and that are modulated after antidepressant treatment, overlapped in the pgACC together with functional activities. This confirmed the importance of the pgACC in affective disorders and supported the relevance of this region as a biomarker for investigating pathological affective processes. On the other hand, there was no clear metabolite overlap between alexithymia, anxiety-related traits and depression, which demonstrated the distinctiveness of the investigated predispositions and affective disorder in regard to the neurobiological information in the pgACC. Moreover, there was strong evidence that factors such as sex and clinical heterogeneity need to be accounted for, especially in pharmacological trials and biomarker studies.

Zusammenfassung

Magnetresonanzspektroskopie (MRS) und funktionelle Magnetresonanztomographie im Ruhezustand (rs-fMRI) bieten die Möglichkeit, das Gehirn auf nicht-invasivem Wege basierend auf dessen metabolischer und funktioneller Aktivität im Ruhezustand zu untersuchen. Maße die der Bildgebung entstammen können weiterhin als Biomarker für die Prädisposition affektive Erkrankungen zu entwickeln, sowie als Korrelate von Erkrankungen wie zum Beispiel Majorer Depression (MDD), oder als Messgröße für Aktivität während pharmakologischer Interventionen benutzt werden. Im Folgenden wurden Bildgebungsmaße auf diesen drei Leveln im prägenualen anterioren zingulären Kortex (pgACC), einer gut beschriebenen Region, die für Affektverarbeitung in physiologischen und pathologischen Stadien (zB im Verlauf einer MDD) verantwortlich ist, untersucht.

In der vorliegenden Arbeit habe ich die Tauglichkeit von multimodalen Bildgebungsmaßen sowie darauf basierende zusätzliche Evidenz sowohl in affektbezogenen Dimensionen also auch der Depression untersucht; wobei auch deren Ansprechschwelle zu therapeutischen Effekten und Suszeptibilität bezüglich subjektiver Faktoren, wie zum Beispiel klinischer Stadien und potentiellen Kontrollparametern berücksichtigt wurden.

Studien eins und zwei betreffen affekt-bezogenen Eigenschaften von gesunden Kontrollprobanden. Während in Studie eins MRS und fMRI in Alexithymie, einer exemplarischen Persönlichkeitsdimension die mit Defiziten in der Verarbeitung von Affekt einhergeht, untersucht wurde, betrachtete ich in Studie zwei das Zusammenspiel zwischen dem angstbezogenen Phänotyp und einer genetische Variationen von GAD65, einer γ -Aminobuttersäure (GABA) synthetisierenden Glutamat-Decarboxylase. Beide Studien ergaben, dass die metabolischen Spiegel im pgACC mit dem jeweiligen Persönlichkeitsmarker assoziiert sind. Die Ausprägung von Alexithymie war mit N-acetylaspartat, einem Marker für neuronale Integrität, korreliert. Desweiteren unterschieden sich die metabolischen Spiegel und Konnektivitätsprofile zwischen Männern und Frauen. Eine Assoziation verschiedener GAD65 Einzelnukleotidpolymorphismen (SNPs) mit verändertem GABA/Glutaminsäure (Glu) Spiegel wurde auch beobachtet. Diese stand im

Zusammenhang mit dem Persönlichkeitsmerkmal Schadensvermeidung; wobei desweiteren ein zusätzlicher Einfluss des Geschlechtes gefunden wurde.

Studie drei verglich glutamaterge Marker zwischen gesunden Kontrollprobanden und MDD Patienten. Zusätzlich waren klinische Dimensionen, Symptomschweregrad und Anhedonie als Faktoren von Interesse inkludiert.

Letztlich betrachtete Studie vier die Reaktion glutamaterger und peripherer Biomarker in gesunden Kontrollprobanden 24 Stunden nach einer Infusion mit Ketamin, und damit zum angenommenen zeitlichen Höhepunkt einer antidepressiven Wirkung des Medikamentes. Das Verhältnis von Glu zu Creatinin (tCr) war verringert, und desweiteren insbesondere bei Frauen mit dem Anstieg eines peripheren Markers für synaptische Plastizität, namens Acetyl-Tubulin/Transferrin (Acet-Tub/TRF) korreliert. Zusätzlich wurde der Langzeiteffekt auf einen klinischen Sicherheitsparameter untersucht. Zwei Wochen nach der Infusion zeigte der Thrombozytenspiegel einen Anstieg; was zeigt, dass ein sorgfältiges Überwachen besonders bei Risikopatienten ratsam ist.

Zusammengefasst lässt sich sagen, dass Veränderungen in verschiedenen metabolischen Spiegeln, die im Zusammenhang mit affektiven Prozessen stehen, bei der MDD beeinträchtigt sind und weitere Veränderungen nach antidepressiver Behandlung zeigen. Diese Veränderungen sind im pgACC lokalisiert mit funktionellen Aktivitätsmaßen. Diese Befunde unterstreichen die Bedeutung des pgACC in affektiven Störungen und unterstützen die Relevanz dieser Region als Biomarker für die Untersuchung pathologisch veränderter affektiver Prozesse. Andererseits ergab sich kein Überlapp in den metabolischen Spiegeln zwischen Alexithymie, angst-bezogenen Persönlichkeitsmerkmalen und der Depression, was demonstriert, dass die untersuchten Prädispositionen und affektiven Störungen in Bezug auf die neurobiologischen Informationen im pgACC zu unterscheiden sind. Nichtsdestotrotz ergab sich eine starke Evidenz für zusätzliche Faktoren wie Geschlecht und klinische Heterogenität, welche zukünftig besonderes Augenmerk erhalten sollten, besonders in Anbetracht von pharmakologischen Untersuchungen und Studien zu Biomarkern.

List of Abbreviations

AAL	Automated Anatomical Labelling
ACC	Anterior cingulate cortex
Acet-Tub	Acetylated α -tubulin
ALFF	Amplitude of low frequency fluctuations
aMCC	Anterior mid cingulate cortex
AMPA	α -amino-3-hydroxy-5-methyl-4-isoxazolepropionic acid receptor
ANCOVA	Analysis of co-variance
ANOVA	Analysis of variance
APA	American Psychiatric Association
BDNF	Brain derived neurotrophic factor
BMI	Body mass index
BOLD	Blood oxygenation level dependent
boot	Bootstrapped
bp	Base pairs
CADSS	Clinician administered dissociative states scale
CBF	Cerebral blood flow
CC	Cingulate cortex
CEN	Central executive network
CI	Confidence interval
CNS	Central nervous system
COMT	Catechol-O-methyltransferase
CRLB	Cramer-Rao lower bound
CSF	Cerebrospinal fluid
CTh	Cortical thickness
dACC	Dorsal anterior cingulate cortex
DAN	Dorsal attention network
dIPFC	Dorsolateral prefrontal cortex
DMN	Default mode network
DNA	Deoxyribonucleic acid
DPARSF	Data Processing Assistant for Resting-State fMRI
dPCC	Dorsal posterior cingulate cortex
DSM	Diagnostic and Statistical Manual of Mental Disorders
EAAT	Excitatory amino acid transporter

EDTA	Ethylenediaminetetraacetic acid
EEG	Electroencephalogram
EPI	Echo planar imaging
FA	Flip angle
fALLF	Fractional amplitude of low frequency fluctuations
FC	Functional connectivity
FCD	Functional connectivity density
FD	Framewise displacement
fMRI	Functional magnetic resonance imaging
FOV	Field of view
FWE	Family wise error
FWHM	Full width at half maximum
GABA	γ -aminobutyric acid
GAD	Glutamate decarboxylase
Gln	Glutamine
GLS	Glutaminase
Glu	Glutamate
Glx	Glutamate + glutamine
GM	Gray matter
GS	Global signal
GSR	Global signal regression
HA	Harm avoidance
HAMD	Hamilton rating scale for depression
HC	Healthy controls
HR	Haemodynamic response
HRF	Haemodynamic response function
ICA	Independent component analysis
KCC	Kendall's coefficient of concordance
LC	Locus coeruleus
M.I.N.I.	Mini International Neuropsychiatric Interview
MCC	Mid cingulate cortex
MDD	Major depressive disorder
Met	Methionine
MFG	Middle frontal gyrus
MNI	Montreal Neurological Institute
mPFC	Medial prefrontal cortex

MPRAGE	Magnetization prepared rapid gradient echo
MR	Magnetic resonance
MRI	Magnetic resonance imaging
mRNA	Messenger ribonucleic acid
MRS	Magnetic resonance spectroscopy
MTG	Middle temporal gyrus
NAA	N-acetylaspartate
NbN	Neuroscience based Nomenclature
NCBI	National Center for Biotechnology Information
NEX	Number of excitations
NMDAR	N-methyl-D-aspartate receptor
PCC	Posterior cingulate cortex
PCR	Polymerase chain reaction
PFC	Prefrontal cortex
pgACC	Pregenual anterior cingulate cortex
ppm	Parts per million
PSF	Point-spread function
PTM	Post-translational modification
ReHo	Regional homogeneity
RF	Radio frequency
rmANCOVA	Repeated measures analysis of co-variance
rmANOVA	Repeated measures analysis of variance
ROI	Region of interest
rs-fMRI	Resting state functional magnetic resonance imaging
SD	Standard deviation
SFG	Superior frontal gyrus
SHAPS	Snaith-Hamilton pleasure scale
SN	Saliency network
SNP	Single nucleotide polymorphism
SPM	Statistical Parametric Mapping
SPSS	Statistical Package for the Social Sciences
SSRI	Selective serotonin reuptake inhibitor
STAR*D	Sequenced Treatment Alternatives to Relieve Depression
STG	Superior temporal gyrus
T	Tesla
TCI	Temperament and Character Inventory

tCr	Total creatine
TE	Echo time
TM	Mixing time
TMS	Tetramethylsilane
TR	Repetition time
TRF	Transferrin
Val	Valine
VBM	Voxel Based Morphometry
vPCC	Ventral posterior cingulate cortex
WM	White matter

List of Figures

Figure 1.1. Schema of imaging markers.	22
Figure 1.2. Cingulate cortex subregions.	23
Figure 1.3. Schema of the studies that were performed in the thesis, and their respective topics.....	34
Figure 2.1. Example of a high-resolution anatomical scan.	36
Figure 2.2. Simplified schematic depiction of the MRS acquisition sequences.	40
Figure 2.3. Single voxel ¹ H MRS measured in 3T.	43
Figure 2.4. Single voxel 1H MRS measured in 7T.....	44
Figure 2.5. Example of a raw spectra from an individual pgACC voxel.....	44
Figure 2.6. Examples of spectra processed with the LCMoel.	45
Figure 2.7. Simplified schematic depiction of the BOLD signal.	48
Figure 2.8. Schema of the preprocessing steps of the 7T resting state EPIs.	54
Figure 2.9. Regions of interest for the FC analysis in Study 1.	54
Figure 2.10. Frequencies of excluded volumes based on the FD Jenkinson threshold.	56
Figure 2.11. Differences in preprocessing strategies.....	57
Figure 3.1. Correlations of TAS-20 and FC of mid cingulate seeds.	71
Figure 3.2. Differences in correlations of TAS-20 and FC of mid cingulate seeds between men and women.	74
Figure 4.1. Difference in the resting-state fMRI indices for the <i>GAD2</i> rs2236418.	96
Figure 4.2. Differences in the GABA/Glu ratio for the <i>GAD2</i> rs2236418.....	98
Figure 4.3. Correlation slopes of harm avoidance and pgACC GABA/Glu residuals.	100
Figure 4.4. Mediation model moderated by sex.	101
Figure 5.1. Main effect of the MDD on glutamatergic metabolites.....	115
Figure 5.2. Moderation by HAMD groups between HAMD scores and metabolites.....	116
Figure 5.3. Influence of the MDD intermediate severity groups.	117
Figure 5.4. Moderation by SHAPS groups between SHAPS scores and metabolites.	118
Figure 5.5. Effect of the medication on glutamatergic metabolites.	119
Figure 6.1. Ketamine study schema.	133
Figure 6.2. Example of an Infrared Western Blot for Acet-Tub/TRF.....	135
Figure 6.3. Diagram of the trial based on the CONSORT 2010 recommendations.....	138
Figure 6.4. Significant interaction of time points and group for the Glu/tCr residuals measured in the pgACC.	141
Figure 6.5. Relative increase for Acet-Tub/TRF and absolute values in women.....	142
Figure 6.6. Correlation between relative change of Glu/tCr and Acet-Tub/TRF.....	143
Figure 6.7. Results of the rmANOVA for the thrombocyte levels.	144

List of Tables

Table 2.1. Comparison of MRS acquisition sequences.....	41
Table 2.2. Population characteristics for the 7T GABA/Glu residuals with different inclusion criteria.....	46
Table 3.1. TAS-20 values in both studies, for the whole sample and split by sex.....	67
Table 3.2. Correlation coefficients and difference in slopes between the sexes for the TAS-20 total score and metabolites.	68
Table 3.3. Correlation coefficients and difference in slopes between the sexes for the TAS-20 total score and cortical thickness.	69
Table 3.4. Correlation differences between the sexes for the TAS-20 subscales.....	70
Table 3.5. Positive correlations between TAS-20 total score and FC of mid cingulate seeds..	72
Table 4.1 Study sample demographics for the <i>GAD2</i> rs2236418.....	93
Table 4.2. Analyses sample characteristics for the <i>GAD2</i> rs2236418.....	94
Table 4.3. Study sample characteristics for additional polymorphisms.....	95
Table 4.4. Analyses of the GABA/Glu levels within the ACC subregions for the five investigated SNPs.....	97
Table 4.5. Post hoc analyses of the GABA/Glu levels within the ACC subregions.	98
Table 4.6. Exploratory ANCOVAs for GABA/tCr and Glu/tCr levels within the ACC subregions.	99
Table 5.1. Demographic and clinical properties of MDD and control participants.	114
Table 6.1. Demographic data of the trial.....	139
Table 6.2. Results of the rmANOVA for Glu/tCr residualized for gray matter partial volume.	140
Table 6.3. Results of the rmANOVA for Acet-Tub/TRF levels.	142
Table 6.4. Results of the rmANOVAs for safety parameters.....	144
Table 6.5. Results of the univariate ANOVA between CADSS groups and placebo.....	146

List of Supplementary Figures

Figure S2. 1. Comparison of inclusion criteria for the GABA/Glu ratio measured in 7T.	i
Figure S3. 1. Significant correlations of TAS-20 total score and metabolites.....	ii
Figure S4. 1. Additive mediation model with pgACC GABA/Glu and ALFF.....	iii
Figure S4. 2. Additive mediation model with pgACC GABA/Glu and ReHo.....	iii
Figure S4. 3. Moderated mediation with ALFF.	iv
Figure S4. 4. Moderated mediation with ReHo.	iv
Figure S6. 1. Baseline sex and contraception differences in Acet-Tub/TRF.....	v
Figure S6. 2. Correlation of the changes in the glutamatergic and the peripheral system 24 h after ketamine.....	vi
Figure S6. 3. Frequency of participants exceeding reference range for thrombocytes.	vi

List of Supplementary Tables

Table S3. 1. Inter scale correlation matrix for the TAS-20 questionnaire for both studies.	vii
Table S3. 2. Metabolite and cortical thickness values for the 3T study.	viii
Table S3. 3. Difference in the correlation slopes between women and men for TAS-20 and FC maps of ACC inferior seeds.	ix
Table S4. 1. Comparison of the pgACC GABA/Glu levels in women between all five SNPs.	x
Table S5. 1. Medication list for the 23 MDD patients.	xi
Table S5. 2. Demographic and clinical properties of the MDD divided by the HAMD clinical cut-off 18 and control participants.	xii
Table S5. 3. Demographic and clinical properties of the MDD divided by the SHAPS cut- off 4 and control participants.	xiii
Table S5. 4. Demographic and clinical properties of the MDD divided by medication status and control participants.	xiv
Table S6. 1. Reference ranges for hematological and biochemical values included in the analysis.	xv
Table S6. 2. Results of the linear regression (enter-method) for the baseline measures in the ketamine study.	xv
Table S6. 3. Results of the rmANOVA for the absolute peripheral markers.	xxi
Table S6. 4. Results of the repeated measures ANCOVA for blood safety parameters.	xxi
Table S6. 5. Results of the linear regression (enter method) for the relative increase of.....	xxii
Table S6. 6. Demographic data for the CADSS groups: there were no differences between the groups.	xxv

Chapter 1. General Introduction

In the last thirty years, advancements in imaging technology and methods have provided a platform for the development of individualized psychiatry. Individually tailored psychiatry is necessary since clinical diagnosis are often broad and equivocal, and do not recognize variability and symptom interactions, which can ultimately lead to a decrease in treatment efficacy. However, meaningful translational interpretation of neuroimaging findings and use of imaging parameters as a standard clinical practice has not been reached yet. More recently, translational research efforts have shifted towards using big data and machine learning approaches, but so far, they also have not accomplished clinical utility (Walter *et al.*, 2018).

To move forward the generalizability of imaging parameters, we first need to establish their neurobiological plausibility and predictive validity. Ideally, these imaging markers should also capture heterogeneity of clinical assessments and be robust to other demographic factors. In other words, results from focused and thorough investigations of suitability of brain regions or imaging parameters that are susceptible to disease predisposition, manifestation and progress or therapeutic modification should form the basis of computational approaches. Afterwards, such derived disease surrogate markers could become factors of treatment decision.

Thus, Studies in this Thesis comprised of multimodal and multilevel investigations of neurobiological markers of vulnerability factors for affective disorders, affective disease and pharmacological challenge. Imaging methods were task free measurements, magnetic resonance spectroscopy (MRS) and resting state functional magnetic imaging (rs-fMRI). Further on, personality and clinical status were examined, together with peripheral markers after pharmacological intervention. By integrating results from the abovementioned analyses, regional and metabolite overlap of imaging markers was addressed, also considering demographic variables such as sex, age, or clinical status.

First and second chapter provide a general overview of terminology, levels of investigations, and methods description, respectively. Chapter three to six include individual studies. Final chapter summarizes main findings and provides an outlook for future investigations.

1.1. Biomarkers

In a broad sense, a biomarker is a measurable characteristic of a biological condition. Biomarkers are used to assess regular biological processes, pathological conditions and pharmacological responses (Group *et al.*, 2001). Conversely, biomarkers reflect the internal factors of a disease/symptom/trait, or the effects of an external mediator. On the contrary, they do not reflect causality of a disease/symptom/trait, they can be state dependent, and do not necessarily contain a genetic component (Lenzenweger, 2013). For example, studies have detected neuroimaging biomarkers which are disease state- but not trait-related (Maalouf *et al.*, 2011). In biomedical research biomarkers are furthermore used for disease classification, prognosis and prediction of treatment success, yet such putative neuroimaging biomarkers for affective disorders have been virtually absent (Lener and Iosifescu, 2015; Perkovic *et al.*, 2018).

In pharmacological studies, biomarkers contribute to early assessments of efficacy and safety of a treatment, and can be ideally used as surrogate endpoints for monitoring and clinical response (Group *et al.*, 2001). Following, they must comply with certain criteria such as sensitivity and specificity to the treatment and replicability (Group *et al.*, 2001).

Biomarkers are a broad categorization, and there is more specific terminology to describe subtype of internal biomarkers of a disease/symptom/trait.

Endophenotypes and intermediate phenotypes

The endophenotype is a term used to congregate specific components into a stable construct that in part, has a clear genetic component. The term was first coined by entomologists investigating grasshopper populations (John and Lewis, 1966). In psychiatry, endophenotypes describe the bridge between the disease occurrence (measurable phenotype) and the genetic variability, mostly associated with single nucleotide polymorphisms (SNP) (Gottesman and Gould, 2003; Flint and Munafò, 2007). Endophenotypes can be neuroanatomical, endocrine, neurophysiological or neuropsychological (Gottesman and Gould, 2003; Lenzenweger, 2013). There are clear criteria for an endophenotype: it is connected to a disease/symptom/trait in a population; it is independent of a state disease; it has a clear genetic component and is heritable; within families, it is present more in the family members suffering from a disease/symptom/trait, but it is present at a higher rate within the affected family

than in general population; it is measured reliably and does not overlap with other conditions (Lenzenweger, 2013; Glahn *et al.*, 2016). Thus, it is mostly used for heritable psychiatric disorders, such as schizophrenia (Beauchaine, 2009). However, there is a growing interest to discover endophenotypes also in affective disorders, with multiple bio- and psychopathological dimension. For example, based on neuroimaging studies there is some progress for major depressive disorder, where glutamatergic deficits, cortical thinning or aberrant resting state activity have been found to repeatedly associate to clinical symptoms of the disease (Hasler *et al.*, 2004; Hasler and Northoff, 2011). Notwithstanding, majority of studies do not include all requirements for a measured variable to be termed the endophenotype, especially co-segregation within affected families, and co-segregation within a population (Hasler *et al.*, 2004; Glahn *et al.*, 2016).

Another similar term without a clear genetic component or proven heritability is “intermediate phenotype”. Intermediate phenotype thus also refers to a type of internal biomarker which can be associated with a disease/symptom/trait in a population and is somehow causally related to it. It is also used to describe certain pathological dimensions of a well-defined pathological phenotype. For instance, healthy first-degree relatives of schizophrenia patients show similar brain response deficits in striatal regions as patients, during a reward anticipation fMRI paradigm (Grimm *et al.*, 2014). There are no distinct guidelines for intermediate phenotypes, as opposite to endophenotypes. Finally, although there is a clear distinction between the two; the terminology is often used interchangeably, especially in cases of complex disorders with multi-gene contributions (Meyer-Lindenberg and Weinberger, 2006; Glahn *et al.*, 2016) (Figure 1.1.).

In conclusion, there is lot of room for advancement in validation of neuroimaging endophenotypes, and in general biomarkers, of affective disorders, especially considering disease or symptom specificity and heritability.

Nevertheless, there are certain regional commonalities between risk-phenotypes and intermediate phenotypes in healthy population and affective disorders patients. Based on PET, structural and fMRI studies, regions of the cortico-limbic circuit haven been elucidated as promising imaging markers and treatment targets across affective disorders, encompassing regions such as amygdala, ventromedial prefrontal cortex and cingulate cortex (Dalglish, 2004; Lener and Iosifescu, 2015).

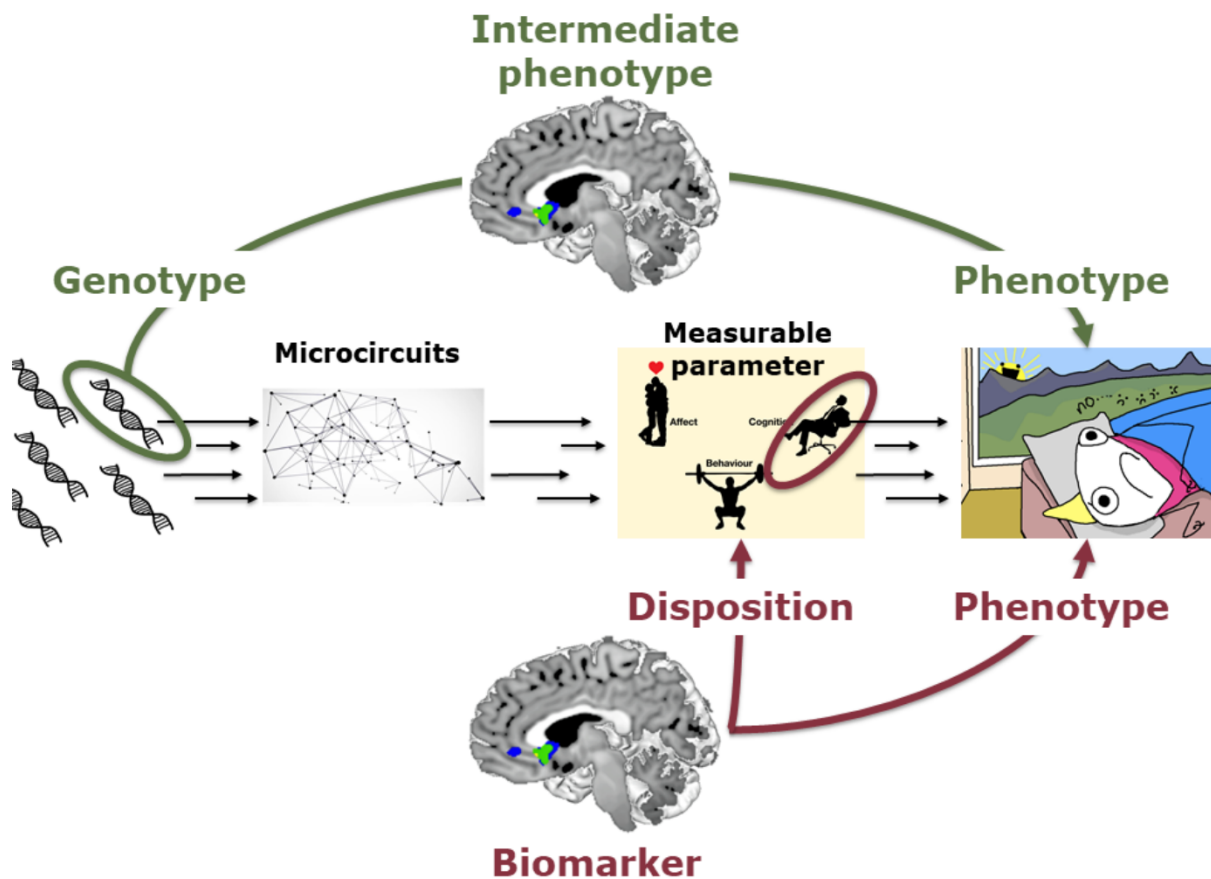


Figure 1.1. Schema of imaging markers.

Intermediate phenotypes have a discernable genetic component that can be connected to the disease phenotype (upper olive-green arrow), while biomarkers measure any biological, or behavioral characteristics or phenotypes.

1.2. The Cingulate Cortex

Cingulate cortex refers to frontal and posterior parts of cortex that surround the corpus callosum. Broad division consist of Anterior CC (ACC) and Posterior CC (PCC) (Vogt *et al.*, 1995), sometimes with a further inclusion of Mid CC (MCC). Seminal work by Vogt, B.A. on the histological architecture and the receptor distribution has demonstrated further division within these larger cingulate components. ACC was divided to: subgenual ACC (sgACC), pregenual ACC (pgACC), dorsal ACC (dACC) and posterior dorsal ACC (pdACC) (Vogt, 2005; Palomero-Gallagher *et al.*, 2009; Vogt and Palomero-Gallagher, 2012), while the PCC to dorsal (dPCC) and ventral (vPCC) (Vogt, Vogt and Laureys, 2006). It needs to be noted that there has been some confusion regarding different terminology, where for instance the dACC is interchangeably used with anterior MCC (aMCC), or the pdACC with posterior MCC

(pMCC). Nevertheless, the position of these subregions is defined, especially in their anatomical relation to the corpus callosum (Figure 1.2.).

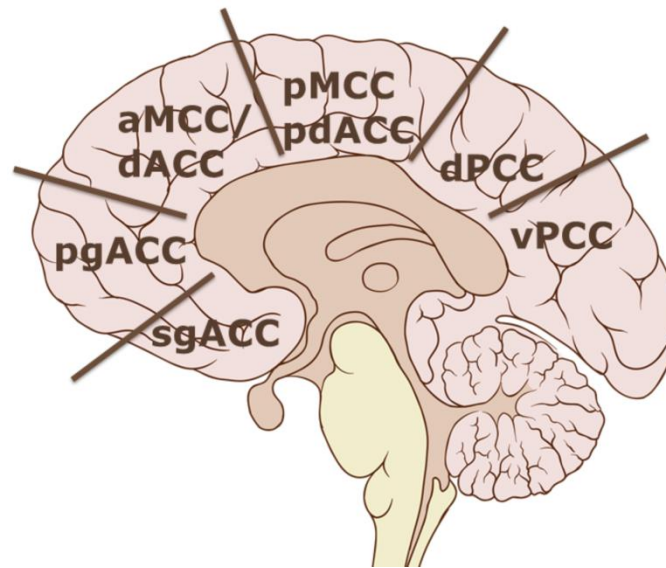


Figure 1.2. Cingulate cortex subregions.

Subregional divisions were made based on Vogt, et al., (Vogt, 2005). The underlying brain picture is "Courtesy of Patrick J. Lynch, medical illustrator".

1.2.1. Anterior Cingulate Cortex (ACC)

The ACC consists of Brodmann areas 24, 32 and 33. The BA later split to subsection (a, b, c) based on the cortical layer organization (Vogt *et al.*, 1995; Vogt, 2005; Palomero-Gallagher *et al.*, 2009). Interestingly, a histological particularity of the ACC are spindle neurons, evolutionary young type of neurons that occurs in animals with sophisticated social structures like humans, apes and elephants (von Economo and Koskinas, 1925; Nimchinsky *et al.*, 1999; Allman *et al.*, 2011). High density of these neurons in the ACC is thought to highlight the role in processing complex tasks, but also increase vulnerability to stressors which might contribute to later development of psychopathologies (Allman *et al.*, 2001, 2011).

Data from electrophysiological recordings and imaging research has attributed variety of functions to the ACC, ranging from autonomic functions (Critchley *et al.*, 2003; Luu and Posner, 2003; Azevedo *et al.*, 2017), attention processing (Pardo *et al.*, 1990), conflict monitoring & decision making (Botvinick, Cohen and Carter, 2004; Critchley *et al.*, 2005; Kool *et al.*, 2010), pain (Fuchs *et al.*, 2014; Wager *et al.*, 2016) and emotion processing (Vogt, 2005).

The ACC is characterized by a rostro-caudal division (Devinsky, Morrell and Vogt, 1995; Bush, Luu and Posner, 2000) that roughly delineates affective (rostral) and cognitive and monitoring (caudal) functional separation. The subregions are demarcated by the receptor distribution (Palomero-Gallagher *et al.*, 2008; Palomero-Gallagher *et al.*, 2009) and metabolite composition (Dou *et al.*, 2013). Moreover, the functional connectivity profiles are also distinct between the subregions (Margulies *et al.*, 2007; Yu *et al.*, 2011; Torta *et al.*, 2013). Recently, investigations have detected that even within a subregion, cytoarchitectonic areas differ in their connectivity profiles, as for example in the pgACC (Palomero-Gallagher *et al.*, 2018).

The pgACC shows strong anatomical connections to limbic and reward areas (Yu *et al.*, 2011; Palomero-Gallagher *et al.*, 2018). It is implicated in broad bottom-up and top-down affect processing and regulation (Amit Etkin, Egner and Kalisch, 2011), that includes emotion recognition (Grimm *et al.*, 2006), valence evaluation (Walter *et al.*, 2008; Victor *et al.*, 2013) and, in association with amygdala, fear regulation (Etkin *et al.*, 2006). Imaging research has reported activations during self-reflection, and self-processing (Northoff *et al.*, 2006; Davey, Pujol and Harrison, 2016). The pgACC is part of the default mode network (DMN) (Raichle *et al.*, 2001; Schilbach *et al.*, 2008; Smith *et al.*, 2009), a network that is active during internal processing, but down-regulated during task execution or externally oriented attention (Raichle *et al.*, 2001; Fransson, 2006).

The dorsal ACC / anterior MCC is the region related mostly to error detection and attentional functions (Bush *et al.*, 2002; Botvinick, Cohen and Carter, 2004). It's anatomically connected to areas of the prefrontal and parietal cortex, and motor regions, so some theories propose its role in mediating momentary behavioural performance (Sheth *et al.*, 2012). Next to Anterior Insula, it was moreover described as a region of salience detection, that identifies relevant stimuli and instates (de)activation of other networks, mainly central executive (CEN) and default mode network (DMN) (Menon and Uddin, 2010). It was thus ascribed to the salience (SN) and cognition network (DAN) (Seeley *et al.*, 2007; Taylor, Seminowicz and Davis, 2009; Menon and Uddin, 2010).

1.2.2. Posterior Cingulate Cortex (PCC)

The PCC was divided to dorsal PCC (dPCC) and ventral PCC (vPCC). The PCC includes Brodmann areas 23 and 31, and as within the ACC, these were further

divided BA subsections based on their cortical layer organization (Vogt, Vogt and Laureys, 2006). It has anatomical connections to parts of paralimbic structures and temporal lobes, as well as to the ACC (Vogt, Vogt and Laureys, 2006). The PCC is metabolically highly active structure (Buckner, Andrews-Hanna and Schacter, 2008; Fransson and Marrelec, 2008). Subregions of the PCC are functionally distinct (Vogt, Vogt and Laureys, 2006; Leech and Sharp, 2014), and there are even indications that they might belong to different networks (dPCC to central executive network and vPCC to DMN) (Leech and Sharp, 2014; Fan *et al.*, 2018). The dPCC is mainly connected to motor actions and attention and the vPCC to actions regarding memory and self-attributional processes (Maddock, Garrett and Buonocore, 2001; Leech and Sharp, 2014; Davey, Pujol and Harrison, 2016).

1.2.3. Cingulate cortex in affective pathologies

In the context of affective disorders, core imaging findings have been predominantly connected to the (dys)function of the ACC, precisely of the ventral part, pgACC. Results from various modalities showed that the activity of the pgACC is intricately connected to the symptomatology of the MDD, including aberrant functional (de)activations during processing of affective cues (Drevets, 2001; Grimm *et al.*, 2009; Groenewold *et al.*, 2013) or hedonic information (Walter *et al.*, 2008, 2009; Abler *et al.*, 2011; Price and Drevets, 2012). What is moreover intriguing is that across disease diagnosis the pgACC was denoted as a neuronal substrate of psychopathologies (Marusak *et al.*, 2016). For instance, in another group of disorders, the anxiety-related disorders, both hyper- and hypoactivation during rest or emotional tasks have been found for post-traumatic stress disorder (PTSD) (Etkin and Wager, 2007; Martin *et al.*, 2009), or for other anxiety disorders (Zhao *et al.*, 2007).

One of the most compelling models of mood disorders circuits has put forward the pgACC as juxtaposition between limbic and high-order cortical structures (Kober *et al.*, 2008; Kupfer, Frank and Phillips, 2012). The focus of the studies described in this thesis has therefore been heavily tendentious towards investigating metabolite and functional role of the ACC, especially the pgACC, in relation to affective vulnerabilities and affective endophenotypes in healthy individuals, as well as in MDD patients.

1.3. Vulnerabilities - personality and genetic polymorphisms

Vulnerability dispositions can be considered as a liability to develop a psychopathology. Therefore, it is worth investigating the regional, functional, and metabolic congruence of candidate psychological and biological dispositions, which may elucidate if there is veritably a metabolic or connectivity endophenotype or intermediate phenotype of affective states, or general pathological conditions.

Next to psychiatric pathologies, the glutamatergic and the GABAergic levels in the ACC have also been connected to personality traits like harm avoidance and extraversion (Kim *et al.*, 2009; Grimm *et al.*, 2012), personality construct like alexithymia (Ernst *et al.*, 2013) and risk genetic polymorphisms (Marenco *et al.*, 2010), thus denoting the possibility that the metabolite levels might be indeed considered as intermediate phenotypes connected both to risk factors and to psychopathological conditions. Here, two aspects, a personality construct and a genetic polymorphism were examined, which can be further related to imaging biomarkers of affective disorders.

General deficits in affect-related processing are features of alexithymia, a personality construct that has been associated with a variety of psychopathological conditions and has been described also as a risk factor for the development of affective disorders (Conrad *et al.*, 2009; Grynberg *et al.*, 2010; Leweke *et al.*, 2012). Neuroimaging investigations have moreover pointed towards ACC as a region of interest, identifying the same neuronal substrate for mechanisms of alexithymia and affective pathologies (Velde *et al.*, 2013).

Further, influence of genetic makeup on psychiatric disorders has been in focus for some time, and groups of genes and SNPs have been identified as promising biomarkers of disease diagnosis (Caspi *et al.*, 2003; van Rossum *et al.*, 2006) and treatment response (Domschke *et al.*, 2008; Lekman *et al.*, 2008; Licinio, Dong and Wong, 2009). Few studies have also reported connection between risk genes for schizophrenia and metabolite levels (Yoo *et al.*, 2009; Radulescu *et al.*, 2013).

However, there is a clear lack of investigations correlating target SNPs with neuroimaging and personality phenotypes of affective or anxiety disorders. For example, genes coding for major neurotransmitters, GABA or Glu would be ideal Vulnerabilities - personality and genetic polymorphismsdepression, respectively.

1.4. Pathological affective states: Major Depressive Disorder

Major depressive disorder is chronic, burdensome, prevalent and universally common illnesses, with large individual and societal costs, and that is most importantly reducing quality of life of patients and their surroundings if not treated adequately (Nemeroff, 2007; Kessler, 2012; Ferrari *et al.*, 2013). It is a recurrent disease, frequently co-morbid with other medical conditions, like coronary diseases, and can grievously be lethal. Like other affective disorders it disproportionately affects women (Kessler, 2003). Patients often do not respond to the available treatments, hence there is a growing necessity to disentangle putative biomarkers of the disease, which would improve patient stratification and guide the development of alternative treatment options.

MDD patients unfortunately constitute a highly heterogeneous patient population, and show diverse psychological and physiological symptoms, reflecting the plurality of possible etiopathology, ranging from genetic predisposition, hyper-inflammation (Setiawan *et al.*, 2015; Kim, 2018), personality predispositions (Bienvenu *et al.*, 2004) or hyper-reactivity to stress (Burke *et al.*, 2005). Based on the ICD criteria, core symptoms of depression include persistent sadness, anhedonia (loss of pleasure or interest) and fatigue. Additional factors such as sleep patterns, changes in appetite or cognitive retardation are often evaluated as well, and there have been extensive attempts to connect different features to biological and imaging endophenotypes (Hasler *et al.*, 2004).

Nevertheless, there are certain neurobiological markers which are shared within the MDD population, the most striking one being metabolite and glutamatergic deficits in the prefrontal cortex (Drevets, 2000; Yüksel and Öngür, 2010; Arnone *et al.*, 2012; Luykx *et al.*, 2012; Moriguchi *et al.*, 2018), accompanied by deficits in synaptic plasticity, thoroughly investigated in animal models of depression (Sanacora, Treccani and Popoli, 2012; Duman *et al.*, 2016). Glutamatergic metabolites have been correlated with brain network functional connectivity differences to control populations (Horn, Yu, Steiner, Buchmann, Kaufmann and Osoba, 2010; Demenescu *et al.*, 2017), functional response to tasks (Berpohl *et al.*, 2009; Grimm *et al.*, 2009; Walter *et al.*, 2009), cortical thickness (van Tol *et al.*, 2013; Li *et al.*, 2014), facets of clinical symptoms (Walter *et al.*, 2009) and duration of illness (Portella *et al.*, 2011; Abdallah *et al.*, 2014). These evidences support the notion that the glutamatergic system changes are intrinsically connected to the disease phenomenon and progress.

Course of glutamatergic deficits in the MDD is not known, but current theories propose that overt stress conditions firstly induce over-activation in regions susceptible to stress such as hippocampus and prefrontal cortex. High levels of extracellular glutamate in turn trigger excitotoxicity (Murphy-Royal *et al.*, 2017). This, in conjunction with astrocyte dysfunction in Gln-Glu cycling, adversely affects synaptic configuration and plasticity, induces neuronal atrophy (Duman *et al.*, 2016; Rial *et al.*, 2016), leading to a low resting prefrontal glutamate transmission (Banasr and Duman, 2008; Sanacora and Banasr, 2013). Moreover, this general pattern of glutamatergic synaptic changes in MDD is thought to be shaped by additional factors such as genetic predispositions, environment (e.g. childhood trauma) and length of disease.

In the last fifteen years, the emergence of this so-called glutamatergic hypothesis of depression has thus led to a research wave investigating glutamatergic modulators as potential antidepressants for various patient groups.

1.5. Intervention: Ketamine as a prototypical glutamate modulator and potential antidepressant agent

Antidepressants targeting monoamine receptors (like Selective serotonin reuptake inhibitors, SSRI) have low recovery rate and long remission time and a substantial proportion of patients do not remit after treatment (around 30%) (Gaynes *et al.*, 2009). Following, there is a gap for fast-acting antidepressants, which will also be effective for patients who do not respond to available treatment options. Compounds targeting N-methyl-D-aspartate receptor (NMDAR), such as ketamine, riluzole, GLYX-13 and Lanicemine have first shown promising results, but the efficacy and replicability in larger trials have exhibited mixed success.

Ketamine, an NMDAR antagonist, is one of such compounds that has been first discovered. Until today, it also remains the most investigated one, both in human clinical trials, and basic research related to neurobiological mechanisms of action. At sub-anesthetic doses ketamine exerts rapid antidepressant response, even in individuals with treatment-resistant depression (Berman *et al.*, 2000; Zarate *et al.*, 2006; Murrough *et al.*, 2013). Peak antidepressant activity is achieved 24 hours after administration, and the effects fade up to a week after infusion (Zarate *et al.*, 2006; Caddy *et al.*, 2014).

1.5.1. Ketamine pharmacology

Chemically, ketamine is an arylcyclohexylamine derivative. Its main mode of action is as a non-competitive NMDAR antagonist, where it binds to the dizocilpine (MK-801) site next the channel pore (Tyler *et al.*, 2017). There are indications that it controls opening of the channel through another allosteric site too (Orser, Pennefather and MacDonald, 1997). Interestingly, it also binds to variety of other receptor types, although with lower affinity, like- dopamine receptor 2 (D2), serotonin receptor 2A (HTR-2A) (Kapur and Seeman, 2002), norepinephrine transporter (NET) or, as recently discovered, oestrogen receptor (Ho *et al.*, 2018). It is thus not unimaginable that ketamine's antidepressant properties might stem from coadjutant receptor activation.

1.5.2. Ketamine metabolism

There are two isomeric forms of ketamine; S(+) and R(-) ketamine, which differ in their pharmacological profile. S(+) has a four times higher affinity for NMDARs (Tyler *et al.*, 2017), it induces higher peripheral blood pressure and heart rate (Casoni, Spadavecchia and Adami, 2015), but elicits lower behavioural side effects (White *et al.*, 1985), although there are opposing accounts (Yang *et al.*, 2015, 2017). Thus far in research and clinical trials, the racemic compound has been in use the most (Short *et al.*, 2018) while pharmaceutical developments are targeting S-ketamine as a more promising treatment (Daly *et al.*, 2018).

Both ketamine isomers undergo extensive hepatic metabolism which involves N-demethylation by liver microsomal cytochrome P45. Rates of demethylation and clearance of S(+) isomer are larger than for R(-) or the racemate (Kharasch and Labroo, 1992). Metabolite pathway of ketamine is diverse, with several intermediate and final metabolites (Hijazi and Boulieu, 2002; Yanagihara *et al.*, 2003; Zhao *et al.*, 2012). Norketamine, the primary active metabolite, is less potent (one third to one fifth the potency of ketamine) and is subsequently hydroxylated and conjugated into water-soluble inactive metabolites that are excreted in urine (Dinis-Oliveira, 2017). There are several forms of hydroxynorketamine (HNK4a-4f) (Hijazi and Boulieu, 2002). Ketamine metabolites are present longer in the body than ketamine itself, implying that they might have a role in the observed anti-depressant effects (Zarate *et al.*, 2012; Zhao *et al.*, 2012). Remarkably, a recent publication proposed that main anti-depressant agent is indeed ketamine's metabolite- HNK4c (Zanos *et al.*, 2016).

However, due to relative short-life, ketamine and its metabolites are not present in the blood at the time of maximal antidepressant effects, 24 h after infusion.

The CYP3A4 isoform is the major enzyme responsible for ketamine N-demethylation, and CYP2C9 and CYP2B6 have a minor role in its metabolite pathway (Hijazi and Boulieu, 2002; Dinis-Oliveira, 2017). When trying to anticipate individual drug response or potential pharmacokinetic drug interactions, properties and genetic variation of these enzymes should be considered (Hijazi and Boulieu, 2002). For example, plasma levels of ketamine might be increased by enzyme inhibitors of CYP3A4 or CYP2C9 such as protease inhibitors, some antibiotics, antiarrhythmics and psychotropic agents (Pelkonen *et al.*, 2008; Peltoniemi *et al.*, 2016). On the other hand, ketamine metabolism could be enhanced by enzyme inducers for example by barbiturates and rifampicin (Pelkonen *et al.*, 2008). This is immensely important since patient populations that are target for ketamine administration, such as treatment resistant MDD, are more likely to receive polypharmacy, not just because of the need for add-on treatments for depression but also because of psychiatric and physical comorbidities (Al-Harbi, 2012; Rizvi *et al.*, 2014).

Further on, genetic polymorphisms in CYP2B6 and 2C9 could also have an impact on the rate of ketamine metabolism (Lee, Goldstein and Pieper, 2002). This was proved for other types of medication, for example anticoagulant S-warfarin (Lee, Goldstein and Pieper, 2002), or other antidepressant medicaments (Porcelli *et al.*, 2011). And surely, in vitro analysis showed a significant influence of allelic variant of CYP2B6 (Li *et al.*, 2013). Yet, so far, human studies are inconclusive about the impact of this genetic variation on ketamine effects: one study reported considerable effect on the clearance of ketamine and adverse effects between genetic variations for CYP2B6 in chronic pain patients (Li *et al.*, 2015), while another no effect at all in healthy participants (Rao *et al.*, 2016).

1.5.3. Ketamine administration

Historically, ketamine has been used in veterinary and medical practice as an anaesthetic, a post-operative analgesic, or in chronic pain diseases (Elia and Tramèr, 2005). Route of ketamine administration can be oral, nasal, sub-cutaneous and muscular (Glue *et al.*, 2011), but mostly it is applied intravenously (IV). Administration of ketamine is therefore systemic, and it affects not only targeted neuronal networks but also the periphery. Doses for antidepressant effect are sub-

anaesthetic, ranging around 0.5 mg/kg for the racemic ketamine, and 0.2-0.3 mg/kg for the S-ketamine (Glue *et al.*, 2011; Cieslik *et al.*, 2013; Xu *et al.*, 2016; Su *et al.*, 2017).

1.5.4. Mechanisms of antidepressant action

The multiple facets of ketamine pharmacokinetics pose a challenge to unequivocally reveal mechanisms of its anti-depressant mechanisms (Williams and Schatzberg, 2016), but predominant models describe that through acute blockage of NMDAR and ensuing α -amino-3-hydroxy-5-methyl-4-isoxazolepropionic acid receptor (AMPA) upregulation, a glutamatergic surge induces downstream synaptic plasticity and sustained increase in synaptic strength (Abdallah, Sanacora, *et al.*, 2018). This was observed particularly in regions important for affect regulation prefrontal cortex and hippocampus (Murrough, Abdallah and Mathew, 2017; Abdallah, Sanacora, *et al.*, 2018).

Glutamatergic surge

Ketamine acutely blocks NMDAR, but intriguingly, effects of this blockade are an acute surge in glutamate release and potentiation of glutamate synapses. There are opposing views on the exact mechanisms of this phenomenon. In short, one posits that the acute blockage of NMDAR on GABAergic neurons leads to disinhibition and activation of local glutamatergic neurons (Sanacora and Schatzberg, 2015), while other that this is achieved through blockage of extra synaptic NMDR on postsynaptic neurons, which have opposite pattern to the synaptic ones and inhibit the neuron (Abdallah, Sanacora, *et al.*, 2018). Another important feature is that other glutamate receptor, AMPAR are upregulated on postsynaptic neurons following ketamine application. AMPAR activation seems as an indispensable step in ketamine's antidepressant action (Maeng *et al.*, 2008). Interestingly, it has been also shown that ketamine metabolite (2R,6R)-HNK activates AMPAR and induces a glutamate surge bypassing NMDAR blockade (Zanos *et al.*, 2016).

Although the mechanisms of action are still under debate, authors agree that ketamine administration generates acute and transient surge in glutamate and glutamine, especially in mPFC, as repeatedly shown with several methods in animal studies (Moghaddam *et al.*, 1997; Chowdhury *et al.*, 2017).

In humans, on a macroscopic level measured with MRS, both positive and negative changes in glutamatergic metabolites have been reported (Lener *et al.*, 2017). For

example, acute surge during infusion in Glx or Glu levels in prefrontal cortex was observed (Stone *et al.*, 2012; Milak *et al.*, 2016). Opposite, no change was seen in mPFC/ACC (Taylor, Tiangga, *et al.*, 2012; Evans, Lally, *et al.*, 2018) or occipital cortex (Valentine *et al.*, 2011). The discrepancies in the findings might be due to variations in voxel locations and acquisition time points (during or post-infusion). Moreover, regional specificity of activation is another important factor, since often antidepressant effects induce opposite patterns in for example mPFC& hippocampus versus amygdala and Nucleus accumbens (Russo and Nestler, 2013). Globally, this was also exemplified for ketamine, where major increase in glucose metabolism has been recorded in the prefrontal cortex and, in contrasts, a reduction in the amygdala (Li *et al.*, 2016), habenula, insula and temporal regions (Carlson *et al.*, 2013).

Synaptic plasticity and peripheral markers

Ketamine-induced glutamatergic activation of downstream mechanisms of synaptic machinery were heavily investigated in animal models (Kavalali and Monteggia, 2012; Zanos and Gould, 2018). Several plasticity pathways were proposed, such as brain-derived neurotrophic factor (BDNF) (Yang *et al.*, 2013; Zhou *et al.*, 2014; Björkholm and Monteggia, 2016), mechanistic target of rapamycin (mTOR) (Li *et al.*, 2010; Paul *et al.*, 2014), GSK-3 (Beurel, Song and Jope, 2011) and eukaryotic elongation factor 2 kinase (eEF2K) (Autry *et al.*, 2011; Monteggia, Gideons and Kavalali, 2013).

Measuring changes in neuroplasticity via protein levels in human brain *in vivo* is not viable. Therefore, studies in humans have used surrogate brain markers, such as changes in EEG readouts (Duncan *et al.*, 2013), cortical excitability measured with MEG (Cornwell *et al.*, 2012) and resting state brain networks reconfiguration (Scheidegger *et al.*, 2012; Evans, Szczepanik, *et al.*, 2018; Li *et al.*, 2018) to detected ketamine neuroplasticity effects. Alternative to imaging markers are peripheral blood markers. BDNF was so far the most common readout, and several studies showed increase in peripheral plasma or serum shortly after infusion (Duncan *et al.*, 2013; Carspecken *et al.*, 2018; Le Nedelec *et al.*, 2018). Moreover, in certain studies the increase was associated with the magnitude of antidepressant response (Haile *et al.*, 2014; Allen *et al.*, 2015).

1.5.5. Implications of ketamine mechanisms in MDD

The paragraph 1.4. described in detail glutamatergic deficits observed in human MDD patients. Deficits in the Gln-Glu cycle and the excessive glutamate release lead to a reduction in neuronal plasticity, which is observed as a loss in dendritic branching, neuronal atrophy and glial reduction, especially in prefrontal cortex and hippocampus (Kang *et al.*, 2012; Popoli *et al.*, 2012; Sanacora and Banasr, 2013; Duman *et al.*, 2016). In animal stress and depression models, the behavioural antidepressant effect of ketamine is acute and transient as it is in humans. Moreover, deficits in synaptic plasticity are reversible with treatment with glutamatergic agents, including ketamine through enhancing dendritic branching and synaptogenesis and astrocyte modification (Serafini *et al.*, 2014; Ardalan *et al.*, 2017).

Therefore, as substantiated with preclinical models, ketamine targets these two major biological patho-substrates of MDD, and could consequentially, at least for responder patients, provide “neuroplasticity window” during which, in conjunction with psychotherapy, depression circuits could be modified and stabilized (Walter, Li and Demenescu, 2014).

The problem of inadequate treatment response to glutamate-modulating agents for part of the patients however remains unresolved. Recent study explicitly confirmed that some MDD patients don't profit from ketamine administration (Daly *et al.*, 2018; Ballard *et al.*, 2018). Hence, neuroimaging studies in humans have been increasingly trying to identify proper biomarkers of ketamine's activity, not only to elucidate mechanisms of action on meso- and macroscopic levels, but also to develop surrogates of efficacy, which can, in future, be used as predictive classifiers for treatment selection.

1.6. Outline of the studies

The preceding paragraphs have outlined the problematics of classification of affective and pathological phenotypes, and related imaging biomarkers. It was also emphasized that there are indications of shared regional features (pgACC), which could be perhaps exploited in development of drug-related imaging markers of efficacy.

Therefore, the conceptual arch of the Thesis was to look for i) commonalties between imaging biomarkers of pathologies that can be explored as a function of a risk personality construct and biological components such as genetic polymorphism and

sex in controls (Studies 1&2); ii) the metabolite components of a typical affective disorder, MDD (Study 3); iii) markers of action of a prototypical glutamate modulating agent, ketamine (Study 4). All studies investigated metabolite levels with MRS, which was complemented with rs-fMRI measures in Study 1& 2 (Figure 1.3.).

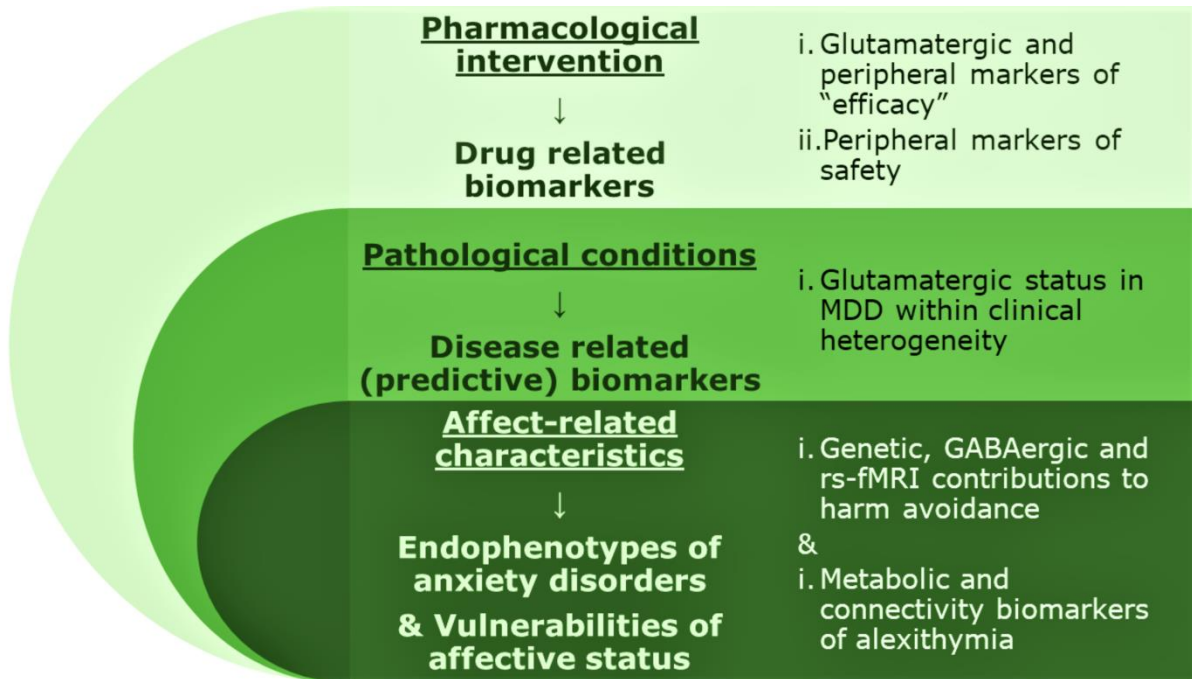


Figure 1.3. Schema of the studies that were performed in the thesis, and their respective topics.

In Study 1, Toronto Alexithymia Scale (TAS-20), a self-reported alexithymia questionnaire was correlated with measures of glutamatergic system and neuronal integrity in voxels placed through CC, separately in men and women. Moreover, functional connectivity was calculated for regions of interest (ROI) also along mid CC, with a fine rostro-caudal and ventral-dorsal direction. The similarity of affective features between alexithymia and MDD might indicate a shared neurobiological substrate. Thus, the hypothesis was that higher TAS-20 would be reflected in lower Glx levels in the DMN, and stronger between network connectivity, as was delineated for the MDD previously in our lab (Horn *et al.*, 2010).

In Study 2, a genetic polymorphism in GABA synthesizing gene, GAD2, in association to GABA/Glu ratio, baseline brain activity, and harm avoidance, a trait related to anxiety phenotype was tested. Sex was added as a moderation factor, accounting for higher prevalence of anxiety disorders in women.

Study 3 looked at group differences in glutamatergic metabolites in the pgACC between MDD patients and matched controls. Based on meta-analytical reports, lower level of Gln/Glu ratio, and to different degrees Gln/tCr and Glu/tCr were expected. To dissect clinical heterogeneity, symptom severity and anhedonia were tested with moderation models in their relationship to glutamatergic markers.

Lastly, Study 4 investigated pharmacological modulation in controls. Racemic ketamine dose of 0.5 mg/kg was given in a continuous infusion over 40 min following the most frequent administration route. To unlock the mechanism of ketamine's fast effect, characterization of markers on several phenomenological levels was done, considering individual variations and possible adverse events. Changes in glutamatergic system and peripheral proteins, was compared between placebo and ketamine 24 h after infusion. Glu/tCr was previously shown to decrease at 24 h after infusion (Li *et al.*, 2017), and the relative change was expected to positively correlate to Acetyl-Tubulin, a marker of synaptic reorganization. Additionally, changes in safety parameters were examined.

Chapter 2. Materials and Methods

In this section the general principle of magnetic resonance spectroscopy (MRS) and resting state functional magnetic imaging (rs-fMRI) will be discussed, as well as the applied measurements and preprocessing techniques.

2.1. Anatomical scans

In every study, the first MR measurement was a high resolution T1-weighted anatomical scan (Figure 2.1.). The resulting images were used: to position voxels within anatomical landmarks by an experienced technician; to calculate gray matter volume proportion (to correct the metabolite levels); to calculate cortical thickness; for the co-registration step in rs-fMRI preprocessing pipeline. Positioning of the voxels was done on-line, at the scanner, while other steps were done offline, during preprocessing of the data.

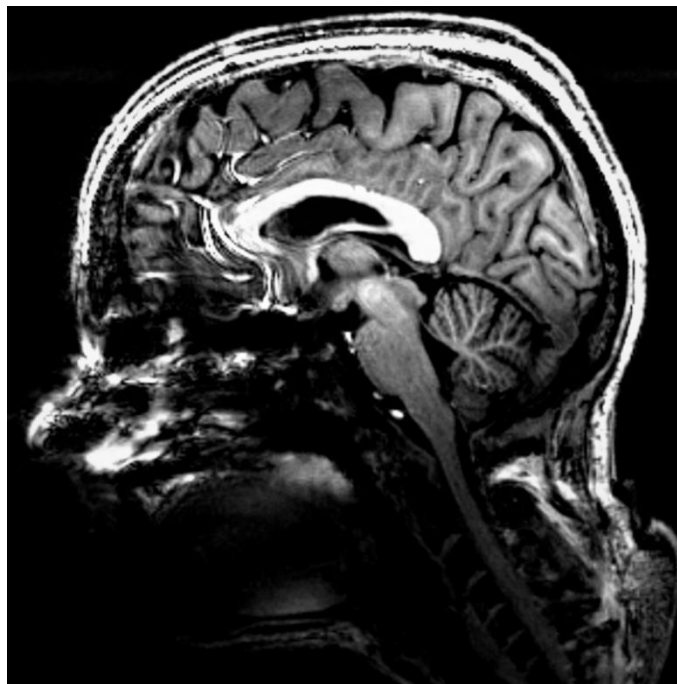


Figure 2.1. Example of a high-resolution anatomical scan.

Scanned at the 7T Siemens scanner (Siemens Healthineers, Erlangen, Germany).

2.1.1. Anatomical scan at 3T

MR images were acquired on a 3T Siemens MAGNETOM Trio scanner (Siemens, Erlangen, Germany) with an 8-channel phased-array head coil. After automated whole brain shimming, a magnetization-prepared rapid gradient echo sequence

(MPRAGE) was applied with the following parameters: echo time (TE)= 4.77 ms, repetition time (TR)= 2500 ms, inversion time (TI)= 1100 ms, flip angle= 7°, bandwidth= 140 Hz/pixel, acquisition matrix= 256x 256x 192 mm, isotropic voxel size= 1.0 mm.

2.1.2. Anatomical scan at 7T

MR images were acquired on a 7T Siemens scanner (Siemens Healthineers, Erlangen, Germany) with a 32-channel head array coil. After automated whole brain shimming, a MPRAGE sequence was applied with the following parameters: TE= 2.73 ms, TR= 2300 ms, TI= 1050 ms, flip angle= 5°, bandwidth= 150 Hz/pixel, acquisition matrix= 320x 320x 224 mm, isotropic voxel size = 0.8 mm.

2.1.3. Anatomical data preprocessing and analysis

To calculate gray matter volume proportion, to calculate cortical thickness and to use for the co-registrations step in rs-fMRI preprocessing pipeline, the individual anatomical images were segmented with VBM8 in SPM8 (www.neuro.uni-jena.de/vbm/).

Gray matter volume proportion of MRS voxels was calculated as follows: each individual MRS voxel was co-registered to the corresponding anatomical scan with SPM8 and segmented gray matter volume was divided by the total volume within the voxel.

To calculate cortical thickness, anatomical images were processed with the CIVET pipeline, developed by the McConnell Brain Imaging Centre (Zijdenbos, Forghani and Evans, 2002). Cortical thickness was extracted for the individual voxels by applying affine transformation matrix (from native space to template space in CIVET) to the individual co-registered voxel. The co-registered voxels were then projected to the normalized surface.

2.2. Magnetic Resonance Spectroscopy (MRS)

2.2.1. Intro to MRS - What is MRS

Magnetic resonance spectroscopy is a noninvasive magnetic imaging technique used to detect and quantify endogenous brain metabolites *in vivo* (Jansen *et al.*, 2006). Metabolites are present in low concentrations (< 20 mmol/L) and are measured both in intra- and extracellular space (Ende, 2015). Similar to other spectroscopy techniques, data are represented by a plot (response as a function of frequency) and

metabolite concentrations are expressed in relative concentrations or absolute concentrations (institutional units, i.u.), dependent on the preprocessing technique. MRS is used in scientific research to look at neurobiological properties of the brain regions in regard to behavior, differences between patient populations and healthy control participants or after pharmacological interventions (Brandão and Domingues, 2004), and to a lesser extent as a clinical application, for example in tumor imaging (Majós *et al.*, 2004).

2.2.2. Principles of MRS

The principle of signal detection in MRS is chemical shift. Each nucleus is in a specific position within the investigated metabolite, and hence has a unique “neighboring chemical environment” dependent on other atoms in its vicinity. The “neighboring chemical environment” of electron clouds affects local electromagnetic field properties and the resonant frequency of the nucleus, *i.e.* the electron clouds generate a small magnetic field that counters the main static magnetic field (B_0), in a process called shielding. This results in each nucleus having its chemical (frequency) shift, which is plotted relative to the reference metabolite- tetramethylsilane (TMS) (Brown, 2007).

Within the B_0 magnetic field, nuclei are aligned and anti-aligned, resulting in net magnetization (M). After the RF pulse is turned on and off, M precesses around B_0 and returns to the z axis of the B_0 field, and with that produces small electrical signals which are detected with receiver coils. Metabolites are then detected by their characteristic set of nuclei chemical shifts. The chemical shift dispersion, *i.e.* the separation of the peaks, increases with B_0 field strength and allows for better detection of metabolites (Brown, 2007).

The hydrogen proton (^1H) is the most commonly used nucleus for MRS due to abundance of H in organic matter. In contrast to standard MR images, the signal of interest in MRS does not come from water or fat, but from the “rest” of less abundant molecules, scaled to the micromolar range (Ende, 2015). Other nuclei, such as carbon (^{13}C), sodium (^{23}Na) and phosphorous (^{31}P), can also be used for MRS measurements with addition of specific coils tuned to the preferred nucleus. Usage of ^1H is, however, favored since it is present in most of metabolites in the brain, has a high abundance in organic matter and thus has a fairly high signal to noise ratio (SNR), and in addition, standard MR imaging coils can be employed to measure it.

The acquired signal is transformed to the frequency domain by Fourier transformation. The x-axis of a spectrum in ppm shows the chemical shift relative to the reference metabolite (TMS). The vertical axis shows the amplitude of metabolites in arbitrary units and height under the peak marks the metabolite concentration. Frequently quantified metabolites with already known frequency distribution (peak position) are: NAA, creatine (Cr), myo-Inositol (MI), choline (Cho), glutamate (Glu), glutamine (Gln), GABA, Lactate (Lac). Some metabolites have a strong and clear peak independent of the field strength: NAA, Cr and Cho, while some, due to similar molecular structure (such as Glu and Gln) require high-field or a specific TE/TR for proper detection (Godlewska *et al.*, 2017).

2.2.3. MRS data acquisition

The first step in the acquisition of MRS is local shimming. This refers to electrical and mechanical adjustments performed to ensure better homogeneity of the magnetic field within the measurement field. If the external field is inhomogeneous it will give distortion to the spectra, thus shimming improves linewidth and SNR (Zhu and Barker, 2011).

After shimming, depending on the sequence, water suppression pulses are applied. Water contains hydrogen and is >1000-fold more abundant in the brain than metabolites of interest (Ende, 2015), thus without suppressing water signal would obscure other metabolite spectroscopic peaks. There are several water suppression techniques, for example chemical shift selective water suppression (CHESS; Haase *et al.*, 1985). A spectrum without water suppression is also measured for eddy current correction and for absolute quantification.

There are two main principles of obtaining MRS data, single voxel spectroscopy (SVS) and magnetic resonance spectroscopic imaging (MRSI) (also known as chemical shift imaging; Brown, Kincaid and Ugurbil, 1982)). In SVS, a single volume is placed in a defined region of interest, with low spatial resolution (usually > 1 cm³). On the other hand, MRSI is covering larger areas divided into voxels, from which the spectral data is obtained concurrently. SVS is more robust to artefacts, since larger areas are required for the MRSI, which are then also prone to poor shimming and “signal bleeding”. MRSI is advantageous in situations where a spatial distribution of metabolites is required, for example to examine stroke effects on larger areas around a focal point (Nelson, Vigneron and Dillon, 1999). Recent advancements in MR

technology brought in another choice, which is functional MRS (fMRS). fMRS measures fluctuations in metabolites, for example glutamate, during task execution (Stanley and Raz, 2018). With this, functional neuronal response to stimuli can be compared between participants with psychiatric conditions and healthy controls regardless of vascular changes (Taylor *et al.*, 2015), as well as temporal metabolite changes to pharmacological interventions. Nevertheless, SVS is still the predominantly applied MRS technique which was also used in the here described studies.

The two mostly used sequences for SVS are point-resolved spectroscopy (PRESS; Ordidge and Gordon, 1985; Bottomley, 1987) and stimulated echo acquisition mode (STEAM; Frahm *et al.*, 1989)). The difference between the two sequences is in the combination of RF and gradient pulses to achieve localization (Figure 2.2.), and duration of TE and TR. TE is particularly important parameter, since each metabolite has characteristic T2 relaxation time.

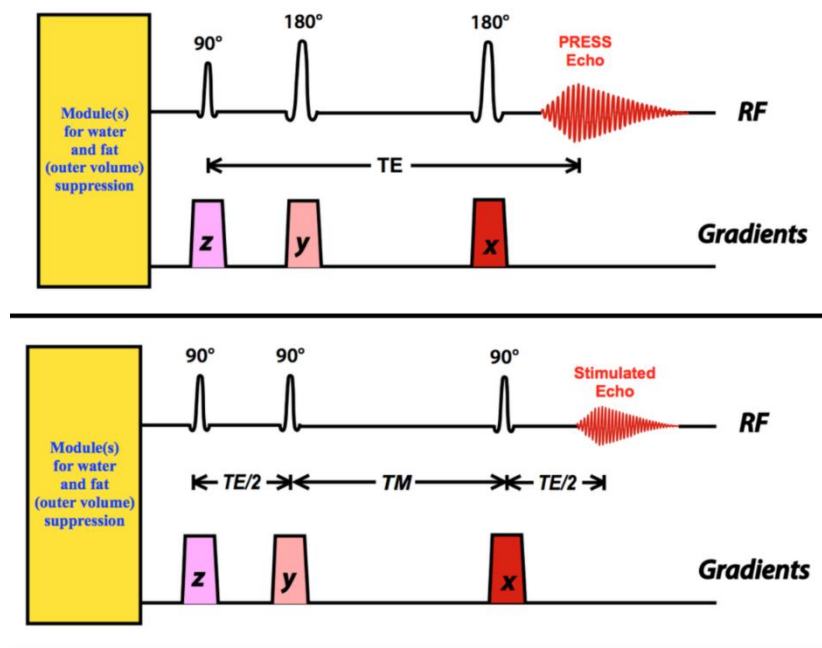


Figure 2.2. Simplified schematic depiction of the MRS acquisition sequences.

PRESS (upper panel) and the STEAM (lower panel) SVS sequence. The pictures were "Courtesy of Allen D. Elster, MRIquestions.com".

Therefore, long TE (> 135 ms) is suited for metabolites with long T2 relaxation time, (NAA, Cr and Cho) resulting in few pronounced and clear peaks, while short TE (< 35 ms) allows quantification of more metabolites and has better SNR. PRESS is

favorable over STEAM at same TEs, since it recovers the full signal and has better SNR. In contrast, a short TE can be applied with STEAM resulting in reduced spectral artefacts, and separation of overlapping signals (Zhu and Barker, 2011). Comparison of these two acquisition methods is shown in Table 2.1.

Table 2.1. Comparison of MRS acquisition sequences.

	PRESS	STEAM
Signal to noise (SNR)	High	50% of PRESS
	Small number of signal averages	Large number of signal averages
Specific absorption rate (SAR)	High	Low
Short TE	Difficult	Possible
Localization	Large VOI	Small VOI

2.2.4. Comparison of the 3T and 7T sequences

Based on previous research (Dou *et al.*, 2015), two different sequences were used for the 3T and 7T measurements. Sequences were selected to optimize quality of the spectra and acquisition time.

At 3T, a PRESS sequence was used to maximize SNR and collect robust signal for the metabolites with a well-defined peak: Glx, NAA and Cr. The molecular structure of Glu and Gln is similar, so the magnetic resonance fingerprint of these metabolites is almost the same. As a result, at lower field strengths, separation of Glu - Gln signals presents a challenge due to low signal dispersion (Jansen *et al.*, 2006). Following, Glx, a joint measurement of glutamate and glutamine (with minor contributions of GABA and glutathione) was used instead of Glu only. Glx represents the total neuronal and astrocyte glutamatergic pool, that is available for both neurotransmitter and metabolite purposes (Rothman *et al.*, 2003; Maddock and Buonocore, 2011). Spectra were measured in four regions, thus, a tradeoff between time acquisition tolerable for participants and long acquisition sequences to obtain individual spectral signal had to be made for Study 1.

In contrast, a STEAM sequence was chosen for the 7T MRS. Firstly, combination of small voxel size and high-field innately increased SNR ratio and spectral resolution, adjusting for using STEAM. Secondly, application of short TE/TM and sufficiently long acquisition time allowed separating Glx signal to Glu, Gln and GABA (Dou *et al.*, 2015). This metabolite distinction was indispensable for Studies 2-4, since the research questions concerned explicitly GABA or glutamatergic cycling (see introduction, paragraph 1.6).

In both scanners, ACC voxels were placed based on the established anatomical landmarks, following a paper by Dou *et al.*, 2013 (Dou *et al.*, 2013). MPRAGE images were placed to anterior commissure (AC)-posterior commissure (PC) plane. The pgACC voxel was placed on the lower edge of the genu of the corpus callosum, posterior bordering the anterior border of the genu of the corpus callosum as tilted in the AC-PC plane. The aMCC was set to the posterior border of the genu of the corpus callosum and it was oriented in parallel to the hippocampal axis, while the limitation in the z-axis was the upper limits of the corpus callosum. The PCC voxel was placed following individual orientation of the central sulcus, centering the visible separation of fornix and corpus callosum for the AC-PC plane. Voxels in the ACC were placed on the sagittal midline to increase the coverage of the gray matter.

Additionally, in Study 1, metabolites were measured in a voxel placed in the left dlPFC. The position of this voxel was also determined based on anatomical landmarks.

2.2.5. MRS data acquisition and processing at 3T

Study 1 was done on a 3T MAGNETOM Trio scanner (Siemens, Erlangen, Germany). ^1H MRS were acquired in four different regions: i) bilateral pgACC $10 \times 20 \times 20 \text{ mm}^3 = 4.0 \text{ ml}$, ii) bilateral dACC/ aMCC $10 \times 20 \times 20 \text{ mm}^3 = 4.0 \text{ ml}$, iii) bilateral PCC $10 \times 20 \times 20 \text{ mm}^3 = 4.0 \text{ ml}$ and iv) left dlPFC $20 \times 20 \times 10 \text{ mm}^3 = 4.0 \text{ ml}$ (Figure 2.3.). Region specific shimming was performed manually for each voxel separately with a shim routine (between 1-5 min per voxel). The parameters of PRESS sequence were: number of excitations (NEX)= 256 averages, TE= 80 ms, TR= 2000 ms, TM= , bandwidth= 1200 Hz, and were based on the previously published optimized parameters for ACC measurement using a faster PRESS at 3 T (Schubert *et al.*, 2004). Water reference data (TE= 80 ms, TR= 10000 ms, 4 averages) were obtained for

eddy current correction (Klose, 1990). Acquisition time for each voxel was 8.40 min, thus the total acquisition time amounted to 50 min.

To enhance accuracy of peak fitting an *in vitro* basis set was measured with same TR/TE at 3T for sixteen standard metabolites (Dou *et al.*, 2015). Obtained spectral data were fitted using LCModel version 6.1.0 (Provencher, 1993, 2001)). A measurement was considered unreliable if: 1) visual inspection of the baseline showed poor water suppression or movement; 2) the SNR was < 8 ; 3) a full-width-at-half maximum (FWHM) was > 12 Hz; 4) the Cramer-Rao lower bound estimate of the fitting error (CRLB) was $> 20\%$ (Cavassila *et al.*, 2001). Ratios of Glx and NAA to Creatine + Phosphocreatine (tCr) were used in further statistical analyses (Yildiz-Yesiloglu and Ankerst, 2006; Oz *et al.*, 2014). Furthermore, the Glx/NAA ratio was also used to check the relation between these markers (Savic *et al.*, 2000; Duncan *et al.*, 2013).

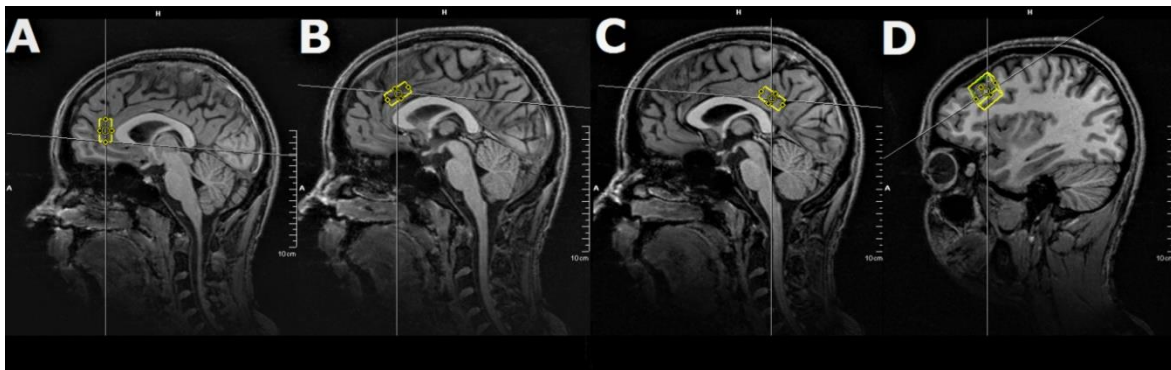


Figure 2.3. Single voxel ^1H MRS measured in 3T.

Voxels were placed in A pgACC; B dACC/aMCC; C PCC and D dlPFC measured on a 3T MAGNETOM Trio scanner (Siemens, Erlangen, Germany).

2.2.6. MRS data acquisition and processing at 7T

MRS measurements in studies 2-4 were done on a 7T scanner with a 32-channel head array coil (Siemens Healthineers, Erlangen, Germany). First, a region-specific shimming was done using an optimized vendor-provided, double-gradient echo shim technique, with the following steps: i) a B_1 map of the voxel; ii) a voxel shim with participant-specific electric tension information; iii) a field map. Thereafter, a STEAM sequence with optimized variable rate selective excitation RF pulses (Elywa *et al.*, 2012) was applied. Spectra were acquired in two different regions: i) bilateral pgACC $20 \times 15 \times 10 \text{ mm}^3 = 3.0 \text{ ml}$ and ii) bilateral dACC/ aMCC $25 \times 15 \times 10 \text{ mm}^3 = 3.75$

ml (Figure 2.4) with the following parameters: NEX= 128, TE= 20 ms, TR= 3000 ms, TM= 10 ms, bandwidth= 2800 Hz.

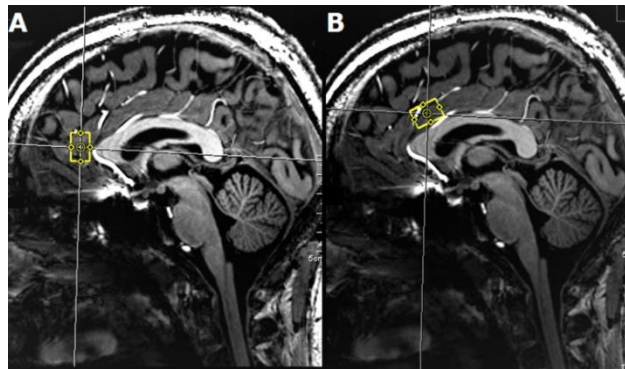


Figure 2.4. Single voxel ^1H MRS measured in 7T.

Voxels were placed in A pgACC; B dACC/ aMCC; measured on a 7T scanner (Siemens, Erlangen, Germany).

A single-average water signal served as internal reference for quantification and eddy current correction (Figure 2.5.). Acquisition time for each voxel was around 6.30 min, thus the total acquisition time including local shimming amounted to 24 min.

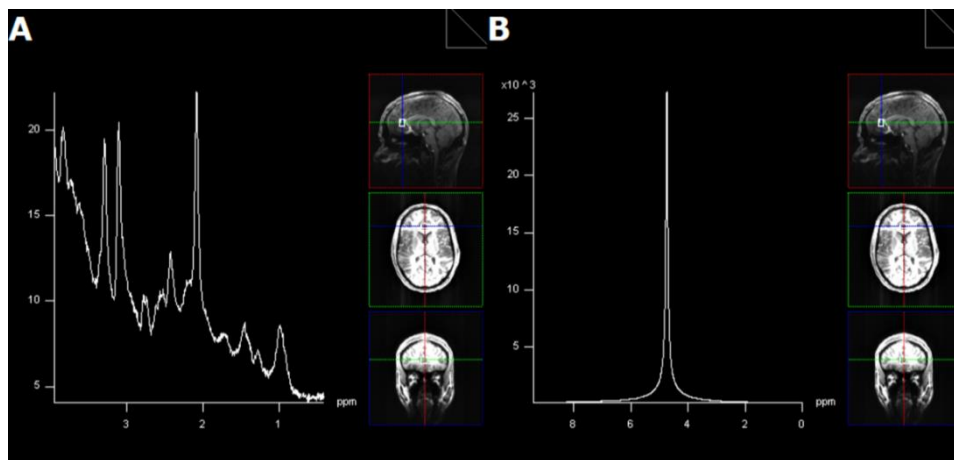


Figure 2.5. Example of a raw spectra from an individual pgACC voxel.

A neurometabolite signals; B water signal (x-axis represent chemical shift relative to the reference metabolite (TMS), y-axis shows the amplitude of metabolites in arbitrary units.

Metabolite concentrations were expressed in institutional units (*i.u.*), due to the absence of individual correction for T1 and T2 relaxation differences between in vitro and in vivo metabolites. Spectral data were analyzed with the LCModel (Stephen Provencher, Inc., Oakville, ON, Canada, V6.3.0) (Provencher, 2001). The sequence specific basis set was previously measured and described in Dou et al., (Dou *et al.*,

2015). Lipid and macromolecule signal were simulated in LCModel using the method described in Seeger et al., (Mader *et al.*, 2002). A measurement was considered unreliable if: i) visual inspection of the baseline showed poor water suppression; ii) SNR was < 20 ; iii) FWHM was > 24 Hz; iv) CRLB was $> 20\%$ (Cavassila *et al.*, 2001).

To test study specific hypotheses, the following metabolites were used: i) Study 2- GABA/Glu, GABA/tCr and Glu/tCr; ii) Study 3- Gln/Glu, Gln/tCr and Glu/tCr; iii) Study 4- Glu/tCr.

2.2.7. Reliability of quality exclusion criteria

Despite the advantages of MRS measurement at high field 7T, some participants were excluded due to insufficient MRS quality for GABA and Gln. Frequent sources of poor spectral quality were movement of the participants, scanner artefacts or unsuccessful water suppression, as visible from the appearance of the baseline (Figure 2.6.). GABA and Gln were the most affected metabolites since the peak resolution for their detection is generally lower than for other more reliable metabolites, for example NAA.

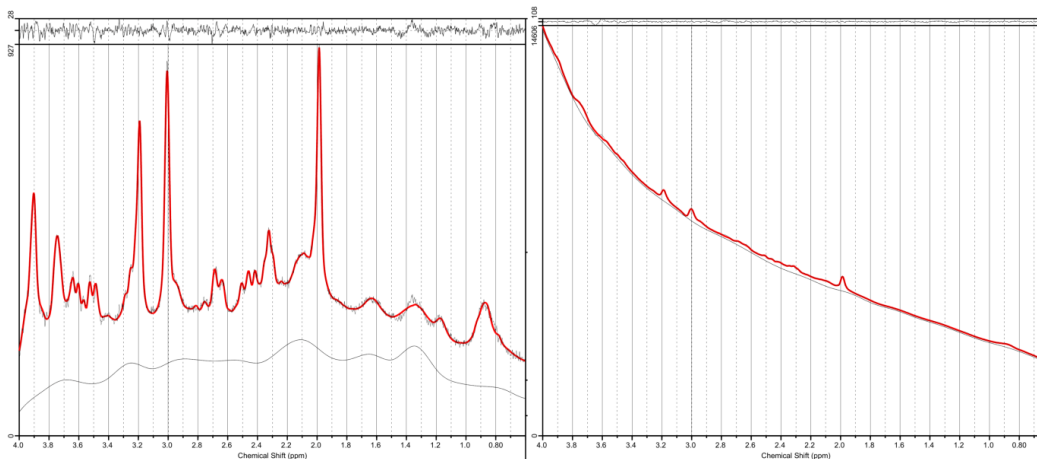


Figure 2.6. Examples of spectra processed with the LCModel.

Spectra were acquired with the STEAM sequence on a 7T scanner and processed with the LCModel; spectra that fulfilled inclusion criteria (left), and spectra for which the water suppression did not work (right).

To make sure that quality criteria did not affect the variance or means of the representative study samples, as an example, the GABA/Glu ratio used in the Study 2: Genetic and sex effects of anxiety-related endophenotypes in the pgACC was tested for inclusion criteria. Different levels of inclusion criteria were applied: whole sample, SNR (included if $\text{SNR} > 20$), SNR and CRLB (included if $\text{SNR} > 20$ and $\text{CRLB} < 20\%$)

and SNR, CRLB and baseline (included if SNR > 20, CRLB < 20% and baseline passed visual inspection) (Table 2.2.) for the analysis. Following a non-parametric Levene’s test of equality of variance between these different sample populations was calculated (Nordstokke and Zumbo, 2010). Results showed that both mean, and variance were preserved across the different levels of data quality. A non-parametric Levene’s test showed a difference in the equality of variances between samples of different inclusion criteria for aMCC GABA/Glu residuals ($F(1,3) = 3.69, p = .012$). This was due to an outlier in the whole sample population, as visible when comparing variances of the other three populations ($F(1,2) = .43, p = .654$). For pgACC GABA/Glu residuals there were no differences with and without the inclusion of outliers ($F(1,3) = .209, p = .890$; and $F(1,2) = .137, p = .872$.) (Figure S2. 1.).

Table 2.2. Population characteristics for the 7T GABA/Glu residuals with different inclusion criteria.

	Whole sample	SNR	SNR& CRLB	SNR& CRLB & baseline
aMCC				
Participants	104	99	93	77
M	$.9 \times 10^{-6}$	$-.1 \times 10^{-6}$	$-.3 \times 10^{-6}$	$.3 \times 10^{-6}$
SD	.9951	.9949	.9946	.9934
Range	8.4619	4.9059	3.9763	3.7653
Variance	.990	.990	.989	.987
pgACC				
Participants	105	101	98	91
M	$-.1 \times 10^{-6}$	$-.1 \times 10^{-6}$	$.2 \times 10^{-6}$	$.01 \times 10^{-6}$
SD	.9952	.9949	.9948	.9944
Range	5.6012	5.3006	4.9895	5.1159
Variance	.990	.990	.990	.989

The similarity in variances and mean values of residuals thus speaks for a robust measurement procedure, and more importantly show that any observed population effects are not artificially induced due to exclusion of data. Nevertheless, to ensure data reproducibility, all quality criterial were used in all studies.

2.3. Resting state functional magnetic resonance imaging

2.3.1. Principles of Magnetic Resonance Imaging

MR technology has enabled functional non-invasive investigations of brain activity, emotional and cognitive processing, neurological and psychiatric conditions. Compared to other non-invasive research methods, like electroencephalogram (EEG), it lacks temporal but has a great spatial resolution. However, recent advancements in fast sequences are also improving the former thus pushing the possibilities of functional imaging towards even very fast events such as neuronal oscillations (Lewis *et al.*, 2016).

Magnetic resonance

The basis of magnetic imaging is the interaction of magnetic properties of atomic nuclei and a strong externally applied magnetic field. Each nucleus that has odd sum of protons and neutrons, has a magnetic momentum, a spin, which interacts with a magnetic field. Spin depends on a ratio of protons and neutrons in each nucleus, which can result in a rotation around the longitudinal axis. In a static magnetic field nucleus aligns with the field but keep the spin around their axis. The spin happens in a frequency, called the Larmor frequency that depends on the applied field strength and the gyromagnetic ratio of the nucleus. Using electromagnetic radio frequency (RF) pulses, the orientation of the nuclei is then changed in the static magnetic field. After switching off the RF pulses, the absorbed energy is transmitted, thereby causing the MR signal. The nuclei return to equilibrium, in a process called relaxation. T1 relaxation is the recovery of the longitudinal magnetization, and T2 relaxation involves the dephasing of the spins. The T1 and T2 relaxation times are constant for specific tissue types, dependent on the field strength, and are used to reconstruct structural images. To obtain images with a solid spatial resolution, additional gradients are applied through a sequence of electromagnetic pulses. The most common fMRI sequence is echo-planar imaging (EPI). EPI includes rapid cycling gradients, which allow whole-brain measurements within a few seconds.

BOLD signal

The blood-oxygen level dependent (BOLD) signal is the basis of the indirect visualization of brain activity. Areas with higher neuronal activity require more oxygen and energy, which is delivered via blood (Raichle, 1987). The haemodynamic response (HR) enables rapid delivery of nutrients to active brain areas. Cell types that

control the vasodilatation/vasoconstriction and consequentially homeostasis of the HR include endothelial cells and smooth muscle cells of arterioles and capillaries, as well as astrocytes and pericytes (types of glial cells). Coupling of neuronal activity, metabolite status and cerebral blood flow (CBF) allows mapping of active brain areas (Lin *et al.*, 2010). A surge in CBF changes the ratio of oxygenated hemoglobin relative to deoxygenated hemoglobin. A functional MR image comes from the contrast in magnetic properties between the two forms of haemoglobin. Deoxygenated haemoglobin is paramagnetic (has a magnetic momentum) and interferes with local magnetic field, causing dephasing of the signal and consequentially less MR signal. In contrast, the oxygenated form of haemoglobin is diamagnetic (with two electrons bound to the Fe atom) and interferes with the local magnetic field to a lesser degree. Hence, a decrease in deoxygenated haemoglobin due to an increase in neuro-metabolite activity in a brain area is reflected in a stronger local MR signal (Raichle, 1987; Ogawa *et al.*, 1990; Chen *et al.*, 2013).

Figure 2.7. depicts the shape of a BOLD signal that follows the time course of the HR function. The analysis and interpretation of a HR is determined by the study design (block or event related for task fMRI). The statistical analysis and interpretation of BOLD signal relies on repetition of conditions, and detecting which areas are on average more active during that condition. The increase in spatial resolution, especially in high-field imaging, moreover, allows for a precise localization of brain activity. Notably, the peak of BOLD signal intensity comes 6-8 sec after a ‘stimulus’, which is compared to fast neuronal events, rather slow. Thus, the temporal resolution of task-based fMRI is limited.

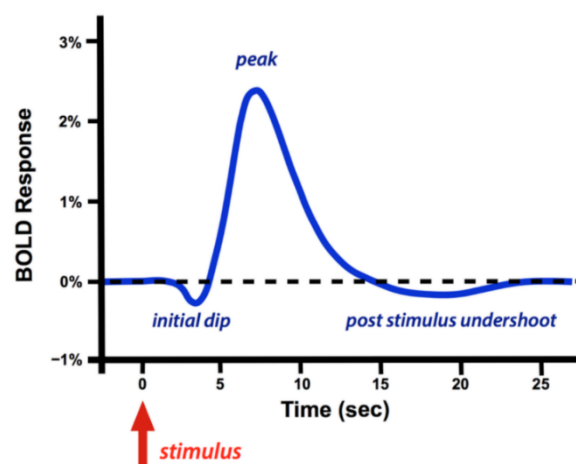


Figure 2.7. Simplified schematic depiction of the BOLD signal.

The picture is "Courtesy of Allen D. Elster, MRIquestions.com".

2.3.2. Resting state fMRI

Resting state functional magnetic resonance imaging (rs-fMRI) is a form of fMRI that is task and stimulus free. Participants are instructed to lay still and awake, with eyes closed, or open and fixated on a cross, thus it is often referred to as a free-mind-wandering task. Scanning usually takes between 5-15 min, and T2*-weighted echo-planar images are obtained.

The inception of the resting state field started form work by Biswal et al. (Biswal *et al.*, 1995) who reported a correlation of low-frequency changes in BOLD signal between motor areas in participants at rest. The authors interpreted the temporal synchronicity of these fluctuations as brain's intrinsic functional connectivity. Since this seminal work, the number of publications has steadily increased.

Resting state is thought to estimate brain's intrinsic organization. The brain is intrinsically active even when at rest, and spontaneous brain activity utilizes around 70% of brain energy (Tomasi, Wang and Volkow, 2013). Such high activity is accompanied by blood flow fluctuations. Thus, the resting state relies on the same principles as the more conventional task fMRI; the BOLD signal.

Rs-fMRI indices can evaluate connectivity based on local activations, or global functional connections and co-fluctuations (Raichle and Gusnard, 2005; Tomasi, Wang and Volkow, 2013). The appeal of resting state comes from its simplicity and the short duration of the measurement, which can be applied to all types of participants, even patients that are under anesthesia, or in vegetative state (Boly *et al.*, 2008).

2.3.3. Indices of resting state

Resting state measures can be divided to two large branches: global and local measures. Global approaches include independent component analysis (ICA), functional connectivity density (FCD), and seed based functional connectivity (FC) all of which are voxel time-series based measures. Local measures are Regional Homogeneity (ReHo) and (fractional) amplitudes of low frequency fluctuations ((f)ALFF). Global and local measures describe different properties of the intrinsic brain activity and are often complementary in describing investigated conditions.

Seed-based FC

Seed-based functional connectivity refers to correlation of BOLD time-series between spatially separated regions/ voxels. The basis of functional connectivity is that regions that have correlated time-series share certain functional properties as well (Fox *et al.*, 2005).

The common approach to analyze seed-based FC is to compute mean time-series within a seed (region of interest, ROI) and correlate it to the time series of all other voxels in the brain. The resulting participant-level connectivity maps are translated to the standardized Fischer z-transformed maps for further group level statistics.

FC and ICA studies have established a set of resting state networks that describe the intrinsic and hierarchical organization of the brain. These networks are stable and replicable over time, and recognizable in other species as well (Fransson, 2006). The most recognized rs- network that is often equalized to resting state itself is the default mode network (DMN) (Buckner, Andrews-Hanna and Schacter, 2008; Greicius *et al.*, 2009). The DMN consist of regions that are highly active during rest, but are disengaged during task executions, such as pgACC, PCC and lateral Inferior Parietal Lobe (Raichle *et al.*, 2001). Another relevant network in this thesis is the SN, which consists of dACC/anterior MCC and Anterior Insula (Seeley *et al.*, 2007). The SN guides switching between externally and internally focused attention to the most pertinent stimuli (Menon and Uddin, 2010).

FC analysis has been extensively applied in research of clinical conditions, and has provided valuable insights regarding disturbances in between-region connectivity that are related to clinical status (Greicius *et al.*, 2007; Meda *et al.*, 2012), task execution (Hampson *et al.*, 2006) and can be even related to treatment success (Fox *et al.*, 2012). It has been moreover suggested as a possible surrogate marker of pharmacological effects (Li *et al.*, 2018).

ALFF & fALFF

Amplitude of Low Frequency Fluctuations (ALFF) and fractional Amplitude of Low Frequency Fluctuations (fALFF) are measures of voxel-based spontaneous fluctuations in the BOLD signal and are reflecting the intensity of the brain activity (synaptic currents).

The calculation of these indices includes transformation of BOLD signal time series into the frequency power domain. ALFF is computed as a sum of amplitudes within a low frequency range, usually .01-.1 Hz (Zang *et al.*, 2007). FALFF is computed as a

fraction of the sum of amplitudes within low frequency range to the total frequency range ($< .01$ Hz-.25 Hz) (Zou *et al.*, 2008). Participant-level ALFF and fALFF are translated to the standardized Fischer z-transformed maps for further group level statistics.

ALFF and fALFF are correlated and are most prominent in regions of the default mode network (DMN), which are highly active at rest (Fox and Raichle, 2007). (F)ALFF activity comes mostly from the gray matter (Zuo *et al.*, 2010). FALFF is considered to be less sensitive to physiological (cardiac) noise than ALFF (Song *et al.*, 2011). On the contrary, test-retest reliability is higher for ALFF (Zuo *et al.*, 2010).

The amount of low frequency spontaneous fluctuations is assumed to be connected to neuronal and baseline metabolite activity. FALFF in particular has been suggested as a surrogate of regional glucose metabolism (Aiello *et al.*, 2015; Nugent *et al.*, 2015). Both ALFF and fALFF have been used to investigate biological processes such as aging (Hu *et al.*, 2014), or psychiatric illness (Zang *et al.*, 2007).

ReHo

Regional homogeneity is another voxel-based local resting state metric that assesses temporal similarity of the BOLD signal fluctuations, thus reflecting the coherence of a given voxel and its adjacent voxels (Zang *et al.*, 2004).

ReHo is computed via Kendall's coefficient of concordance (KCC) (Kendall and Gibbons, 1990), which estimates the similarity of the time series between a given voxel and defined nearest neighbors (cluster size 7, 19 or 27 voxles) (Zang *et al.*, 2004). Participant-level maps are created based on KCC values (Song *et al.*, 2011) and translated to the standardized Fischer z-transformed maps for further group level statistics.

Analogous to (f)ALFF, ReHo is prominent in the DMN regions during rest (Long *et al.*, 2008), and associated with glucose consumption (Nugent *et al.*, 2015). It has been also used to investigate individual differences in healthy control populations (Tian, Ren and Zang, 2012) as well as clinical conditions (Cao *et al.*, 2006).

2.3.4. rs-fMRI data acquisition and analysis

Functional images were acquired on a 7T scanner with a 32-channel head array coil (Siemens Healthineers, Erlangen, Germany). Resting state measurement was done after MRS measurements to avoid exceeding SAR limitations of the scanner and

subsequent poor detection of the spectra, but before any task measurement in order to prevent any carry-over effects of the task. Participants were instructed to lay still and awake with their eyes closed during the scanning session. Whole-brain T2*- EPIs were acquired (280 time points, 62 axial slices, TE= 22 ms, TR= 2800 ms, flip angle= 80°, bandwidth= 2246 Hz, isotropic voxel size= 2 mm, acquisition time= 13 min). Sequence parameters were optimized to circumvent intra voxel dephasing and loss of signal, particularly in the lower medial prefrontal cortex. Online motion and distortion correction were applied (Speck, Stadler and Zaitsev, 2008). Distortion correction was done using an improved point-spread function (PSF) mapping method (Chung *et al.*, 2011; In and Speck, 2012). EPIs were visually inspected for data quality (frontal and temporal signal loss) and scanning artifacts.

Like task fMRI, analysis of the rs-fMRI data involves three steps, preprocessing participant-specific first level analysis, here in the form of indices of resting state activity, and second level inferential statistic across or between groups.

Preprocessing was performed using Statistical Parametric Mapping (SPM12; Wellcome Trust Centre for Neuroimaging, London, United Kingdom) and DPARSFA toolbox V2.1 (Chao-Gan and Yu-Feng, 2010). For each participant, the first 10 volumes were discarded to allow for steady-state magnetization. Images were temporally corrected for acquisition delay with slice timing. Realignment was applied as a spatial correction for head motion. Motion parameters obtained from realignment were checked and participants with head motion exceeding voxel size (2 mm in any direction and any volume) were excluded from further analysis. Anatomical images were co-registered to the individual mean EPI image from realignment to improve the following spatial normalization into the MNI stereotactic reference frame (Montreal Neurological Institute). Next steps were adjusted for the specific rs-fMRI index that was calculated (Figure 2.8.). Normalized EPIs were smoothed using a double voxel length Gaussian kernel of 4 mm FWHM. This smoothing kernel was chosen based on the acquisition parameters and to cater to the primary target of the analyses- subregions of the ACC (see paragraph 2.3.5.). In short, a small kernel size is optimal to prevent averaging of time series signals of adjacent seeds for FC (Study 1- FC of the gyri and sulci ACC seeds, paragraph 3.2.4) as well as to detect strong local activations within the boundaries of the cytoarchitectonic subregions (Study 2- ALFF& ReHo, paragraph 4.2.4). After smoothing, regression of the mean white matter signal, the mean CSF signal and the six motion parameters

was done. Importantly, motion parameters were obtained from the realignment of the non-motion-corrected data (see paragraph 3.2.4). Global signal regression was not performed (Murphy and Fox, 2017). Temporal filtering (0.01- 0.1 Hz) was done next, followed by scrubbing. Scrubbing was computed using cubic spline interpolation for time points that exceeded a frame-wise displacement (FD) threshold of 0.5 determined with the method proposed by Jenkinson (Jenkinson *et al.*, 2002), as well as for adjacent time points. To control the number of volumes that are interpolated, and thus preserve variance in the BOLD signal, the participants who had more than 13 time points (5%) with >0.5 FD were additionally excluded from second level analyses. FD threshold and motion regression parameters were optimized to include maximum number of participants while controlling for prominent nuisance factors that could inflate results (Bright and Murphy, 2015) (see also paragraph 2.3.5.).

FC: After the scrubbing preprocessing step, seed-based functional connectivity (FC) maps were calculated and converted to z maps using Fisher's r-to-z transformation (Chao-Gan and Yu-Feng, 2010). Seeds were placed bilaterally in dACC/ a&pMCC and were defined as spheres ($r= 4$ mm) in previously reported coordinates: five spheres were placed along the cingulate gyrus and five along the cingulate sulcus on each side (Margulies *et al.*, 2007) (Figure 2.9.).

ALFF: After the nuisance regression preprocessing step, amplitude of low frequency fluctuations (Zuo *et al.*, 2010) were calculated in the frequency band of 0.01- 0.1 Hz. The ALFF metric was converted to z maps using Fisher's r-to-z transformation.

ReHo: Smoothing was not applied in the preprocessing pipeline for calculating regional homogeneity (Zang *et al.*, 2004). After scrubbing, the similarity of time-series was estimated for 19 neighboring voxels, and the result was converted to z maps using Fisher's r-to-z transformation. Z maps were then smoothed with a 4 mm Gaussian kernel.

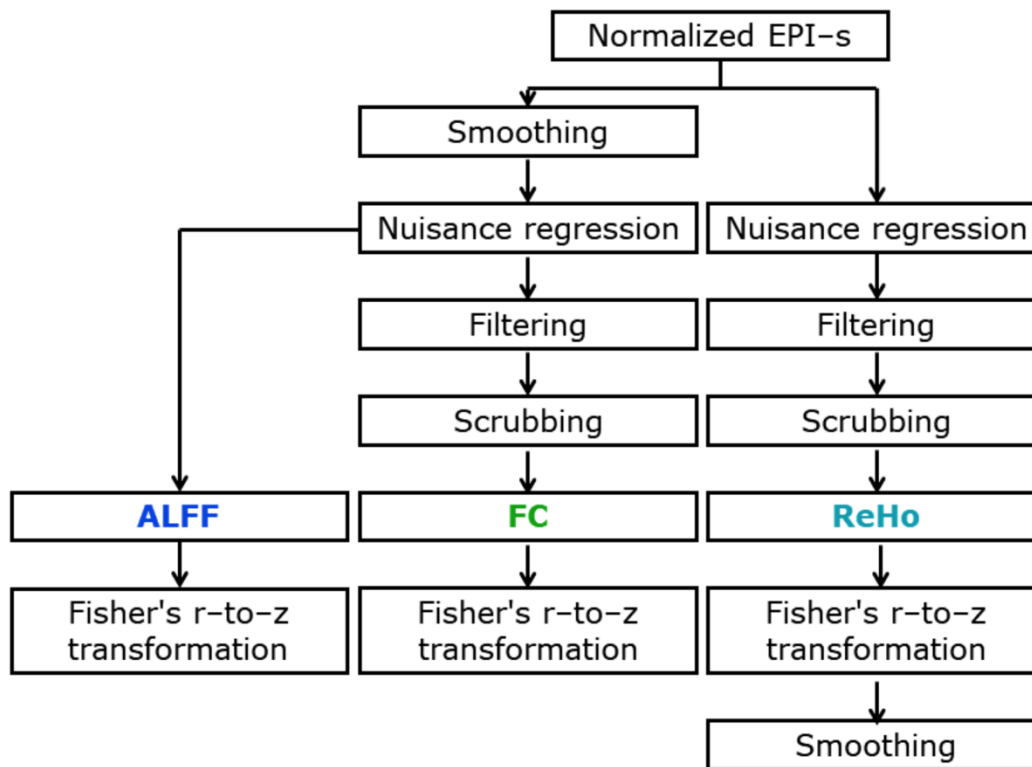


Figure 2.8. Schema of the preprocessing steps of the 7T resting state EPIs.

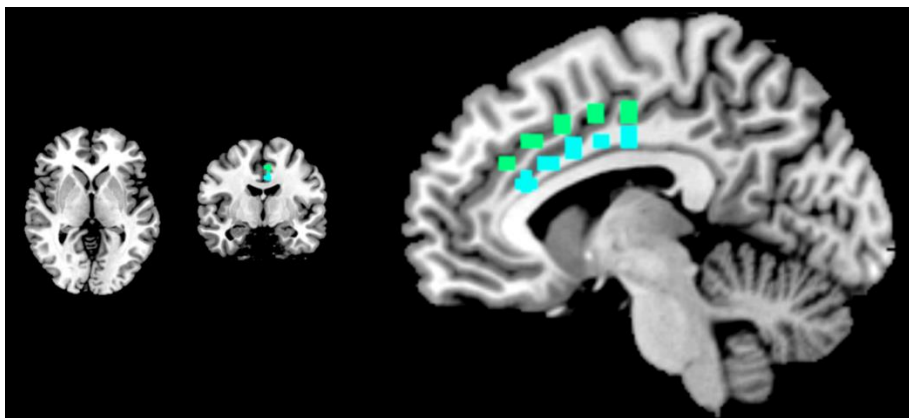


Figure 2.9. Regions of interest for the FC analysis in Study 1.

Seeds were placed along gyrus (cyan) and sulcus (aquamarine) of the mid CC. ROIs are superimposed on an MRIcron template in MNI space.

2.3.5. Challenges at high-field imaging

There were several challenges faced during preprocessing of the functional data from 7T. Firstly, the PSF method used for distortion correction has long acquisition time and is vulnerable for motion during scanning, thus some functional images had scanner artefacts which were challenging for the normalization step. Next, in some

instances, SPM12 falsely recognized the skull as a border of the brain. To circumvent this problem SPM12 segmentation was used, with templates using tissue probability maps for gray matter, white matter, cerebrospinal fluid, bone, tissue, and air. Moreover, correct co-registration and normalization were confirmed for each individual EPI by visually comparing anatomical landmarks in parallel with individual anatomical scan and canonical template. Secondly, question of “what is noise” and “what is true signal” is still an open challenge for the resting state field. Movement during scanning presents one of the prominent nuisance factors that influence quality of data and subsequent group level analysis (van Dijk, Sabuncu and Buckner, 2012; Yan *et al.*, 2013). Thus, motion needs to be accounted for during the preprocessing; for the systematic head movement by regressing out motion parameters, and for the differences between adjacent slices by removing or interpolating motion confounded time points (scrubbing) (Satterthwaite *et al.*, 2013; Power, Schlaggar and Petersen, 2015). To estimate right parameters for nuisance regression for the 7T dataset, several motion-related preprocessing options were calculated: motion regression with Rigid-body 6 and Friston 24. The Rigid-body 6 option regresses out 6 head motion parameters, while the Friston 24 option regresses out 6 head motion parameters, 6 head motion parameters one time point before, and the 12 corresponding squared items (Friston *et al.*, 1996). Friston 24 Motion parameters were used from the ‘raw’ images without the online motion correction since they stand for the real individual motion during acquisition. Online motion corrects volumes based on the preceding volume and not the first volume, approximating motion close to 0. Thereby using online motion corrected images for extracting motion parameters there is a risk of falsely inflating results. Second parameter that was tested was scrubbing. The threshold for scrubbing (cubic spline interpolation) was set by calculating outliers ($Q3 + 3 * IQR$) based on Framewise Displacement (FD) Jenkinson (Jenkinson *et al.*, 2002) of all time points of all participants. Scrubbing was thus done on 0.16 as well as on an often used but more lenient threshold of 0.5. Participants that had more than 10% of volumes above the threshold or > 4 volumes in a row were excluded (Figure 2.10.).

Then, a second level correlation between FC map of aMCC and age was done to see the influence of confounding motion factors and similarity of results. Age was chosen as an example test variable since it is often used as a covariate in group level statistics.

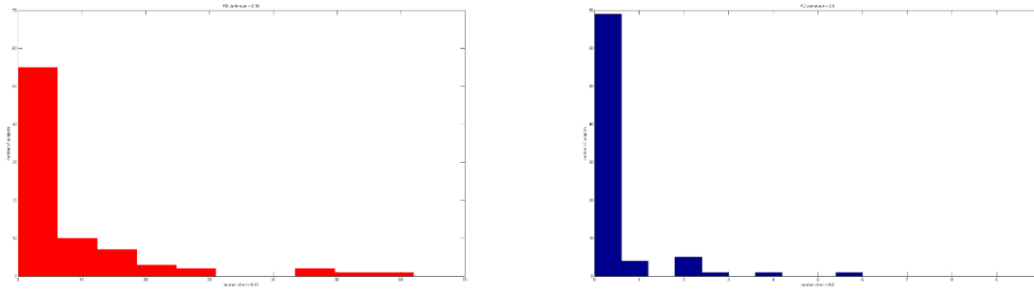


Figure 2.10. Frequencies of excluded volumes based on the FD Jenkinson threshold.

Threshold >0.16 , x-axis (0-70 volumes) (left panel); threshold >0.5 , x-axis (0-10 volumes) (right panel), y-axis (0-70 participants).

Four second level results were obtained. The number of participants that had to be excluded due to FD threshold 0.16 was 20 participants more than for 0.5. To have comparable results, overlapping participants were used for second level statistics ($n=60$). All preprocessing strategies showed similar patterns of results, with a cluster in the left Inferior Parietal Gyrus (Figure 2.11.). The cluster however differed in size and statistical significance.

Additionally, an interaction between age and motion parameters was conducted with repeated measures ANCOVA in SPSS V22 (IBM, IL). An interaction analysis between age and i) 6 realignment parameters (RP), ii) other parameters in Friston 24 model and iii) FD Jenkinson was run. Age showed i) no effect with the 6 RP by time; ii) trend significant effect of squared motion parameters of current and preceding volume by time ($F(7,72)= 2.68$ & $F(7,72)= 2.69$, $p= .083$); iii) there was no interaction between FD Jenkinson by time by age.

Results thus showed that using high threshold such as 0.16 might average the natural variance of brain signals and level out the possible relations of other variables to it. Importantly, a high number of participants must be excluded, which resulted in decreasing degrees of freedom and statistical power. In the dataset at hand there was also a significant interaction with the 12 squared motion parameters, which was not present with original motion parameters. Additional variables in motion regression, as in Friston 24, remove not only variance due to motion but also extra components possibly unrelated to it (Bright and Murphy, 2015). Although preprocessing strategies showed similar patterns of results, this optimization analysis incited to use regression

of basic 6-Rigid body motion parameters and a more lenient threshold for scrubbing (FD Jenkinson > 0.5).

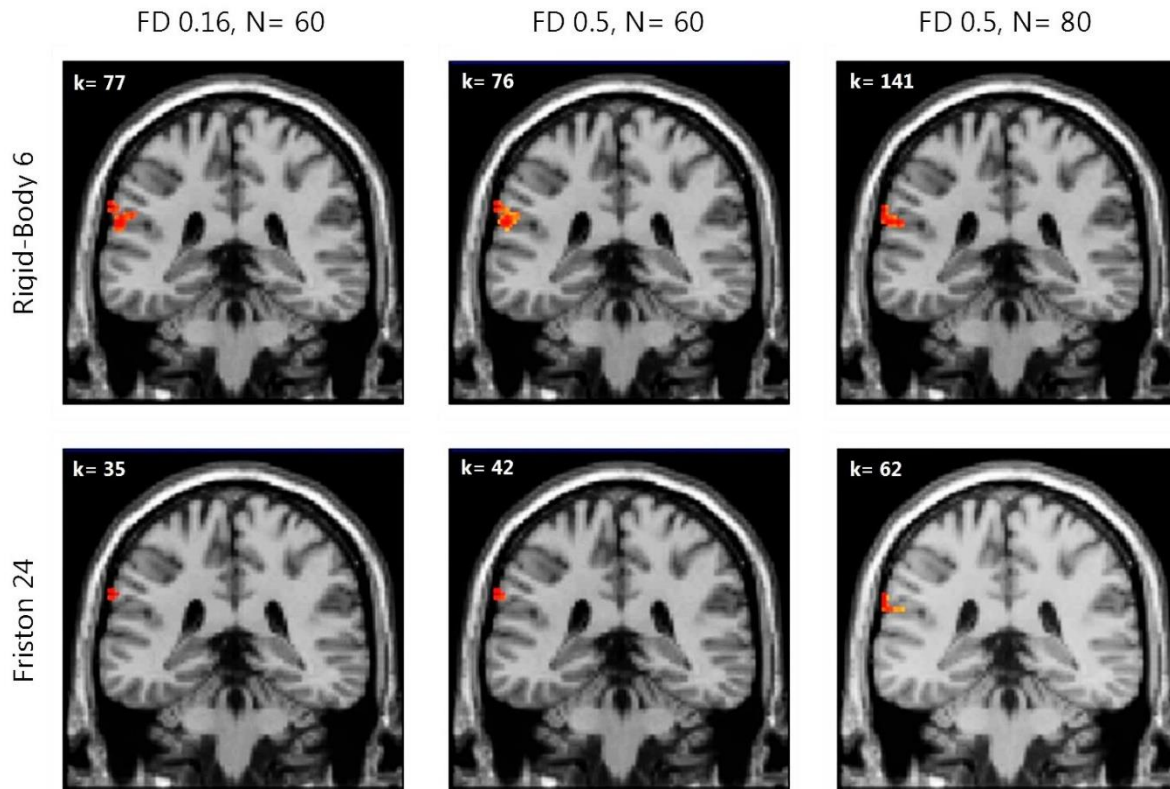


Figure 2.11. Differences in preprocessing strategies.

Positive association of age and FC aMCC towards L Inferior parietal lobule ($y=-36$) across preprocessing options, k size showed in the top left corner.

Lastly, during acquisition, tissue inhomogeneity causes voxel- dephasing which manifests as signal loss and is more pronounced at ultra-high-field strengths. One way to solve it is to increase spatial image resolution. Smaller voxel size reduces intra-voxel field inhomogeneities and leads to increased MR signal (Sladky *et al.*, 2013). For that reason, the acquisition voxel size was 2 mm isotropic. The combination of high-field and high resolution also improves signal to noise ratio (SNR) compared to the same resolution at lower field strengths (Triantafyllou *et al.*, 2005), and increases detection of signal change (in Study 1- seed time series, paragraph 3.2.4 and in Study 2 neuronal activation fluctuations, paragraph 4.2.4) (Sladky *et al.*, 2013). The increased SNR of raw images allowed employing a detection-sensitive kernel size of 2 times voxel size (Skudlarski, Constable and Gore, 1999), thus 4 mm was the local optimum. Furthermore, by using a small smoothing kernel spatial accuracy was targeted. In the Study 1 small Gaussian kernel size was

used to ensure that the extracted ROI signal in FC analyses are not averaged across gyrus/sulcus or adjacent seeds, while in the Study 2 it was used to ensure that the observed activations are well within the boundaries of the respective subregion of the ACC (pgACC versus aMCC) since, in SPM, peaks are merged if they are less than twice FWHM apart.

2.4. Summary of general methods

Each acquisition process proved to have challenges during processing. Although high-field 7T measurements for MRS and rs-fMRI improved specificity and sensitivity, number of excluded participants due to scanner artefacts was higher than for the lower field. By scanning a large number of participants in 7T measurements appropriate n sizes was nevertheless obtained.

In the following chapters (3– 6) each study will also include a brief description of the study specific methods and statistical analysis.

Chapters 3 - 6: Individual studies (pp. 60-157)

Chapter 3. Study 1: Metabolite and connectivity correlates of alexithymia in DMN and SN

In this study the goal was to examine how intrinsic brain architecture measured by the MRS and rs-fMRI relate to alexithymia, which is considered a predisposition to develop affective disorders.

The part of the following study was first published in:

Colic, L., Demenescu, L. R., Li, M., Kaufmann, J., Krause, A. L., Metzger, C., & Walter, M. (2015). Metabolite mapping reveals sex-dependent involvement of default mode and salience network in alexithymia. *Social cognitive and affective neuroscience*, 11(2), 289-298.

3.1. Introduction to Study 1

Alexithymia (Greek, “*without words for feelings*”) was coined in seventies by Sifneos to label symptoms of affect processing in patients with psychosomatic disorders (Nemiah and Sifneos, 1970). It is usually described with phrases “difficulties in identifying, analyzing and verbalizing feelings”, “restricted imaginary and dreaming states” and “limited emotional experience” (Bagby, Parker and Taylor, 1994; Bagby, Taylor and Parker, 1994; Lane *et al.*, 1998). In other words, in alexithymic participants the boundary between the cognitive and the somatic experience of feelings is blurred (Taylor, 2000). Alexithymia covers a broad range of problems in both internal (self-) and external (others-) affect attribution and expression.

Deficits in alexithymia were mostly attributed to cognitive aspects of affect processing, which are captured by the Toronto Alexithymia Scale (TAS-20) three subscales: “difficulty identifying feelings”, “difficulty describing feelings”, and “externally oriented thinking” (Bagby, Parker and Taylor, 1994; Bagby, Taylor and Parker, 1994). In recent years though, another dimension was added - “intrinsic” affective aspect of affect processing (Vorst and Bermond, 2001). This dimension is related to difficulties in experiencing immediate emotional arousal and reduced ability to fantasize (Vorst and Bermond, 2001; Velde *et al.*, 2013), and is regularly assessed by the Bermond-Vorst Alexithymia Questionnaire (BVAQ; (Vorst and Bermond, 2001).

3.1.1. Sex differences in alexithymia

In some form alexithymia is present in about 10% of general population (Honkalampi *et al.*, 2000; Moriguchi *et al.*, 2007a; Franz *et al.*, 2008), and consequentially is sometimes referred to as a *personality trait* or a *construct*. Importantly, it is considered a clinically relevant risk factor to develop affective psychopathologies (Conrad *et al.*, 2009; Honkalampi *et al.*, 2010; Leweke *et al.*, 2012). Variety of psychiatric disorders, like depression, alcohol dependence or eating-disorders, show comorbidity with alexithymia (Honkalampi *et al.*, 2001; Vanheule *et al.*, 2007; de Timary *et al.*, 2008; Pinna, Sanna and Carpiniello, 2014; Ho, Wong and Lee, 2016). Importantly, there has been a clear distinction between depressive disorders and alexithymic features (Hintikka *et al.*, 2001; Honkalampi *et al.*, 2001). In addition, high levels of alexithymia can impact everyday life and quality of interpersonal relationships (Grynberg *et al.*, 2010; Eid and Boucher, 2012; Pérusse, Boucher and Fernet, 2012). It has been more frequently reported for men than women (Mattila *et al.*, 2006; Levant *et al.*, 2009). The exact causes of such prevalence discrepancy are not known. One possible explanation might be patterns of socialization that for men include restrictive emotionality, which could contribute to the development of alexithymia (Levant *et al.*, 2003, 2009). The sex difference in prevalence is however dependent also on other predictors, such as poor education, and low health status (Mattila *et al.*, 2006; Moriguchi *et al.*, 2007a).

3.1.2. Alexithymia in neuroimaging

In short, brain regions that were repeatedly associated with alexithymic features were subregions of the ACC, Insula and Amygdala (Velde *et al.*, 2013). Insula and amygdala activations were associated with the deficits in the affective dimension (Goerlich-Dobre *et al.*, 2014; Van der Velde *et al.*, 2014). In light of unique functionality linking both cognition and emotion processing, the ACC was connected to both dimensions (Goerlich-Dobre *et al.*, 2014; Van der Velde *et al.*, 2014).

Task fMRI studies of alexithymia have reported both increase (Berthoz *et al.*, 2002; Reker *et al.*, 2010; Heinzl *et al.*, 2012) and decrease in functional activations in the ACC (Leweke *et al.*, 2004; Bird *et al.*, 2010; Reker *et al.*, 2010) during different emotional tasks. This was congruent given that the ACC subregions were involved in different aspects of awareness, regulation and affect control (Lane *et al.*, 1998; Bermond, Vorst and Moormann, 2006; McRae *et al.*, 2008; Gyurak, Gross and Etkin,

2011). PgACC and PCC, as parts of the DMN, are involved in the self- or internally related aspects of affect processing (Raichle *et al.*, 2001; Laird *et al.*, 2009; Leech and Sharp, 2014). In contrast, the dACC/MCC, as part of the SN (Seeley *et al.*, 2007; Menon and Uddin, 2010), is engaged in detection and modulation of response to both internal and external emotionally salient events, and might represent affect cues that are related both internal (self-) and external (others-).

3.1.3. The self- and the other- distinction in alexithymia

As we have seen earlier, the dorsal part of the ACC/MCC is part of the saliency network that helps switching between default mode and task ensemble network. This area is therefore involved in attribution or evaluation of both internal and external stimuli, which can be afterwards translated into affect-relevant behavior (Vogt, Berger and Derbyshire, 2003; Margulies *et al.*, 2007; Medford and Critchley, 2010; Menon and Uddin, 2010).

According to Ernst *et al.*, (Ernst *et al.*, 2013). SN is hyperactivated, and alexithymic individuals seem to have an inability to process information based on saliency cues. This further leads to inability to differentiate internal from external sensations (Lane *et al.*, 2000; Ernst *et al.*, 2013). This might trigger either excessive emotional arousal or over-down-regulation, which create impoverished conscious affect experience of emotions (Lane *et al.*, 2000).

Recently, studies have shown that the dACC/MCC displays a gradient of connectivity and activation profiles rather than an uniform one (Torta and Cauda, 2011; Torta *et al.*, 2013). Next to the well-established rostro-caudal division of the cingulate cortex (paragraph 1.2.1.), a further separation between histological profiles and functionality between cingulate gyrus and cingulate sulcus was delineated (Margulies *et al.*, 2007; Vogt, 2016). Intriguingly, based on monkey electrophysiological and human imaging studies it was proposed that mid cingulate gyrus to sulcus follows a distinction regarding others- (gyrus) and self- (sulcus) processes (Apps, Rushworth and Chang, 2016). Therefore, the reported hypo/hyperactivity in alexithymia during affective task fMRI studies could be due to problems in self- and/ or in other- affect attribution of the SN.

To elucidate neurobiological substrates of cognitive aspect of alexithymia magnetic resonance spectroscopy (MRS) and resting state fMRI (rs-fMRI) were employed. To tap into both internal and external facet of affect processing several subregions of the

cingulate cortex, - and consequently networks - were investigated. Moreover, imaging or spectroscopic studies did not investigate sex differences in brain correlates with alexithymia, so both studies tested shared and differential neuronal correlates of alexithymia between the sexes in the cingulate cortex subregions. Sex-specificity was approached in an exploratory manner, while respective statistical corrections were still applied.

3T metabolite study

An MRS study (Ernst *et al.*, 2013) described increased levels of GABA in the pgACC which indicates the inhibition of that area, and increased glutamate in the anterior insula that is congruent with the enhanced activity in this region reported by functional studies (Moriguchi and Komaki, 2013; Velde *et al.*, 2013).

First, to broaden previous findings, N-acetylaspartate (NAA), a marker of neuronal integrity, and Glx, a marker of local metabolism, were measured in an anatomically parceled subregions of the cingulate cortex (paragraph 1.2.): the pgACC, the dACC/aMCC and the PCC. Additionally, the left dorsolateral prefrontal cortex (dlPFC) was also evaluated. DLPFC was previously connected to cognitive emotion regulation (Takeuchi *et al.*, 2013), attention- task operant network, and thus might be involved in the externally oriented thinking aspect of alexithymia.

Since volumetric studies also showed changes in the ACC with alexithymia (Borsci *et al.*, 2009; Sturm and Levenson, 2011; Ihme *et al.*, 2013; Goerlich-Dobre *et al.*, 2014), cortical thickness (CTh) was calculated to control for potential macroscopic changes.

7T connectivity study

To distinguish the aspects of self- versus other- related changes with TAS-20, a FC study was done using high resolution 7T (acquisition voxel 2 mm) functional images. This allowed the distinction of time courses not only alongside the fine rostro-caudal gradient in the dACC /MCC, but also between the gyrus and the sulcus cortical areas (Margulies *et al.*, 2007). Previous rs-fMRI study found increased connectivity in frontal areas and within DMN (Liemburg *et al.*, 2012). Based on former reports, stronger associations of both gyri and sulci SN nodes and high-order frontal cognitive areas with higher TAS-20 score were hypothesized, which would bias attention towards external cues at rest or interfere with the emotion-cognition interaction. Simultaneously, lower connectivity between sulci ROIs and DMN with higher TAS-20 was expected, reflecting lower internal evaluation of feelings.

3.2. Specific materials and methods of Study 1

3.2.1. Participants

Participants included in the 3T metabolite study were eighteen women (age= 37.17± 1.27) and eighteen men (age= 32.00± 4.97). Participants included in the 7T connectivity study were thirty-one women (age= 27.32± 7.11) and twenty-eight men (age= 27.00± 6.85). participants were recruited via advertisements - between 2008 and 2012 for the spectroscopic study and between 2013 and 2015 for the rs-fMRI study. They were right handed, without any prior neurological or psychiatric disorders, as confirmed with the German Version 5.0 of the Mini International Neuropsychiatric Interview (M.I.N.I.) (Sheehan *et al.*, 1998; Ackenheil *et al.*, 1999) and by additional interviews with the study physician. Studies included psychometric assessment and MR measurements (either MRS measurement at 3T or rs-fMRI measurement at 7T). The study was approved by the Institutional Review Board of Otto von Guericke University of Magdeburg, Faculty of Medicine. The study was conducted in accordance with the Declaration of Helsinki (World Medical Association, 2002) and all participants gave written informed consent.

3.2.2. Psychometric assessment

Participants filled out German version of the Toronto Alexithymia Scale (TAS-20) (Bach *et al.*, 1996). TAS-20 is a self-reported questionnaire consisting of three subscales 'Difficulties in describing feelings', 'Difficulties in identifying feelings', and 'Externally oriented thinking style' (Bagby, Parker and Taylor, 1994). Items are rated on a five- point Likert scale (1 is strongly disagree - 5 is strongly agree), and for the subscale EOTS items are inverted. TAS-20 shows good cross item consistency and reliability (Bagby, Taylor and Parker, 1994), which was also replicated for the German version (Bach *et al.*, 1996; Franz *et al.*, 2008). Score ranges from 20 to 100, and participants are considered alexithymic if they score >61 on the total score (Parker, Taylor and Bagby, 2003). Participants in both spectroscopic and resting state study were below this clinical cut off score.

It must be noted that TAS-20 represents only cognitive dimension of alexithymia, which refers to affect processing at the cognitive cortical level, for example analyzing own or others' feelings. Other questionnaires such as Bermond-Vorst Alexithymia Questionnaire (BVAQ) also measure affective dimension (Vorst and Bermond, 2001), which encompasses affect experience, for example levels of arousal to certain

emotion-inducing events. Nevertheless, TAS-20 remains the most often used and the most reliable tool for assessing alexithymia scale, therefore it was also employed in this study.

3.2.3. 3T MRS acquisition and processing

Anatomical and MRS were collected on the 3T scanner. Details of the acquisition and preprocessing can be found in paragraphs 2.1.1., 2.1.3. and 2.2.5.

In short, spectral data were obtained with the PRESS sequence from four voxels: pgACC, dACC, dPCC and dlPFC (Figure 2.3). Glx, NAA and tCr were quantified with the LCModel, and used in further statistical analysis. Anatomical data were used for calculating cortical thickness. Moreover, the gray matter partial volume of the individual voxel was calculated as the segmented gray matter divided by the total volume within voxels.

3.2.4. 7T rs-fMRI acquisition and preprocessing

The data were obtained on the 7T scanner. Details of the acquisition and preprocessing can be found in paragraphs 2.1.2., 2.1.3. and 2.3.4.

In short, rs-fMRI data were preprocessed in a standard manner and FC was calculated for gyri and sulci seeds alongside dACC/MCC as described in paragraph 2.3.4. (Figure 2.3). The resulting Fischer transformed Maps were used for second level analysis.

3.2.5. Statistical analysis

Metabolite association of the ACC subregions with alexithymia

Statistical analysis for the 3T spectroscopic study was done in SPSS (version 15.0; SPSS, Inc., Chicago, IL, USA). Correlation between TAS-20 score and metabolites: Glx/NAA, NAA/tCr and Glx/tCr measured in the pgACC, aMCC, PCC, and dlPFC was calculated using partial rank correlations. Gray matter was used as a covariate to control for the effects of the individual voxel placement. Moreover, it was shown that age is correlated to the TAS-20 scores (Moriguchi *et al.*, 2007b) and to some metabolites (Schuff *et al.*, 2001), thus it was also added as a covariate. To control for multiple comparisons, the Family wise error (FWE) correction was applied. Since measured metabolites are not independent variables across regions, a classical Bonferroni correction have been too strict (Sankoh, Huque and Dubey, 1997). Therefore, the mean correlation coefficient of the correlation matrix of metabolites

was calculated (men $r = .387$, women $r = .395$) and the degree of metabolite interdependence was incorporated for each sex separately (number of comparisons = 12) with the following formulas: $\alpha^k = 1 - (1 - \alpha)^{1/mk}$ where $mk = K - 1 - r^{*k}$. For both sexes the significance threshold was adjusted ($p \leq .011$) standing for a corrected $p < .05$, two-sided. The difference between the sexes was calculated following Fischer's transformation and significance values were obtained from the computed Z-values.

Cortical thickness in the ACC subregions and alexithymia

To control for the underlying effects of macroscopic gray matter structure, correlation coefficients of the regional cortical thickness and the TAS-20 scales were additionally computed with partial rank correlations with age as a covariate ($p < .05$, two-tailed level).

Finally, as an exploratory analysis, correlations were also computed for TAS-20 subscales and metabolites from four regions, with the same adjusted statistical threshold of $p \leq .011$.

Functional connectivity of the dACC/MCC seeds and regression with alexithymia

A second level statistical analysis for the 7T resting state connectivity study was performed in SPM12 (SPM12; Wellcome Trust Centre for Neuroimaging, London, United Kingdom). Regression analysis with total TAS-20 score was conducted for each seed, with addition of age and sex as nuisance covariates for the whole sample regression (Kelly *et al.*, 2009; Biswal *et al.*, 2010). Further on, comparison of correlation slopes of FCs and TAS-20 between sexes was done. Statistical threshold was set at $p < .05$, FWE cluster level corrected.

3.3. Results of Study 1 Alexithymia

3.3.1. Demographic data

In both the 3T and 7T studies there were no statistically significant differences between male and female participants in TAS-20 scores (Table 3.1.), or significant correlation of age with total TAS-20 scores or separate scale scores (3T: all $p > .4$, all r/ρ coefficients $< .2$; 7T: all $p > .25$, all ρ coefficients $< .2$). Correlation coefficients in-between scales were high and similar between studies and sample, except for the scale EOTS, which had a low correlational score to other facets and some discrepancy between the two studies (Table S3. 1.). Further on, in the 3T data set there were no

significant differences between male and female participants for metabolites or cortical thickness (Table S3. 2.).

Table 3.1. TAS-20 values in both studies, for the whole sample and split by sex.

Variables are in mean± SD.

	Whole sample	Women	Men	Student's t-test or Mann-Whitney test
3T spectroscopy study				
<i>n</i>	36	18	18	/
Age	34.58± 8.37	37.17± 1.27	32.00± 4.97	$U= 126, p= .253$
Total TAS-20	4.86± 9.41	4.83± 11.18	4.89± 7.56	$t(34)= -.017, p= .986$
DDF	1.78± 3.52	1.11± 3.32	11.44± 3.68	$t(34)= -1.141, p= .262$
DIF	12.50± 4.51	13.17± 5.22	11.83± 3.70	$U= 137.5, p= .443$
EOTS	17.58± 3.82	17.56± 4.29	17.61± 3.42	$t(34)= -.043, p= .966$
7T connectivity study				
<i>n</i>	59	31	28	/
Age	27.17± 6.93	27.32± 7.11	27.00± 6.85	$U= 429.5, p= .945$
Total TAS-20	38.46± 7.37	39.74± 7.03	37.04± 7.61	$t(57)= -1.420, p= .161$
DDF	9.80± 2.68	1.16± 2.85	9.39± 2.45	$t(57)= -1.103, p= .275$
DIF	11.56± 3.30	12.23± 3.45	1.82± 3.02	$U= 342.5, p= .163$
EOTS	17.29± 3.91	17.00± 4.31	17.55± 3.57	$t(57)= -.534, p= .595$

3.3.2. TAS-20 total score associates with metabolites in DMN in women, and in salience network in men

In both sexes TAS-20 correlated negatively with the NAA/tCr in the pgACC, on an adjusted statistical threshold $p < .011$ in women ($\rho = -.71, p = .004$), and on an uncorrected trend level in men ($\rho = -.49, p = .06$; Table 3.2., Figure S3. 1.).

On a corrected threshold, in women total TAS-20 score correlated only with the Glx/NAA measured in the PCC ($\rho = -.72, p = .004$), and Fischer's test revealed significant differences of the correlation scores between sexes ($p = .018$; Table 3.2., Figure S3. 1.). Further on, for men, there was an unadjusted trend correlation for the

Glx/NAA in the dACC ($\rho = .50, p = .07$), but did not significantly differ to correlation coefficient in women ($p = .1$; Table 3.2., Figure S3. 1.). There was no association between the dlPFC metabolites and TAS-20 in either sex.

Table 3.2. Correlation coefficients and difference in slopes between the sexes for the TAS-20 total score and metabolites.

Correlations with metabolites were controlled for age and tissue composition and controlled for multiple comparisons, with an adjusted FWE correction of $p < .011$.

Region	Metabolite	Correlation with TAS-20		Fisher's test	
		Women	Men	Z Value	p value
PCC	NAA/tCr	.26	-.19	1.23	.22
	Glx/tCr	-.40	.23	-1.74	.082 #
	Glx/NAA	-.72 ^A	.28	-3.15	.002 **
dlPFC	NAA/tCr	.12	-.20	.89	.37
	Glx/tCr	.04	-.15	.51	.61
	Glx/NAA	-.13	.13	-.69	.49
pgACC	NAA/tCr	-.71 ^A	-.49 ^B	-.96	.34
	Glx/tCr	-.07	-.13	.17	.87
	Glx/NAA	.37	.11	.76	.45
dACC	NAA/tCr	-.15	-.07	-.22	.83
	Glx/tCr	.01	.45	-1.30	.19
	Glx/NAA	.03	.50 ^B	-1.42	.16

^A denotes $p < .011$, statistical threshold with the FWE correction, ^B denotes $.1 > p > .011$; Fisher's test: ** $Z > 2.58$, equivalent to $p < .01$

3.3.3. TAS-20 is not associated with cortical thickness

On a trend level TAS-20 correlated with the cortical thickness (Cth) in the PCC only in women ($\rho = .45, p = .07$). There were no further significant correlations in either sex ($p > .05$) (Table 3.3.).

Table 3.3. Correlation coefficients and difference in slopes between the sexes for the TAS-20 total score and cortical thickness.

Correlations with cortical thickness were controlled for age, with a threshold of $p < .05$.

	Correlation with TAS-20		Fisher's test	
	Women	Men	p value	
CTh	PCC	.45 ^B	.18	.42
	dIPFC	.22	.002	.54
	pgACC	.16	.07	.80
	dACC	-.001	.22	.53

^B denotes $.1 > p > .05$

3.3.4. TAS-20 scales mirror main effects of alexithymia

On an exploratory uncorrected level, TAS-20 subscales showed similar correlates as the total score. Difficulties describing feelings (DDF) correlated with the Glx/NAA in the PCC ($\rho = -.59$, $p = .027$) and the NAA/tCr in the pgACC ($\rho = -.64$, $p = .013$) in women, and with the Glx/NAA in the dACC ($\rho = .52$, $p = .06$) in men. Additionally, for women there was trend-correlation for the Glx/tCr in the PCC ($\rho = -.48$, $p = .085$), which was not present for the total score. For the DDF, sex difference between the correlation scores for the Glx/NAA in the PCC was replicated ($p = .032$) and there was an additional trend difference for the Glx/NAA in the dACC ($p = .067$). Difficulties in identifying feelings (DIF) was strongly correlated with the Glx/NAA in the PCC ($\rho = -.79$, $p = .001$) and with the NAA/tCr in the pgACC ($\rho = -.69$, $p = .007$) in women, and on a trend-level with the Glx/NAA in the dACC for men ($\rho = .46$, $p = .09$). The only robust differences between the correlation coefficients between sexes was again for the Glx/NAA in the PCC ($p = .0002$). In contrast, externally oriented thinking style (EOTS) correlated only with the NAA/tCr in the pgACC for both women and men ($\rho = -.63$, $p = .015$ and $\rho = -.49$, $p = .062$, respectively). Consistent to total score all three scales did not show any associations with the markers measured in the dlPFC (Table 3.4.).

Table 3.4. Correlation differences between the sexes for the TAS-20 subscales.

Table is restricted to results with significance of $p < .1$.

Region	Metabolite	Women	Men	DDF	Fisher's test	Women	Men	DIF	Fisher's test	Women	Men	EOTS
PCC	Glx/NAA	-0.59 ^B	.13	.032 *	-0.79 ^A	.30	.0002**					
pgACC	Glx/tCr	-0.48 ^C	.04	.16								
dACC	NAA/tCr	-0.64 ^B	-0.35	.28	-0.69 ^A	-0.26	.12	-0.63 ^B	-0.49 ^C	.58		
dACC	Glx/NAA	.025	.52 ^C	.067 [†]	.11	.46 ^C	.14					
	Glx/tCr									-0.01	-0.48 ^C	.17

^A denotes $p < .011$, statistical threshold with the FWE correction, ^B denotes $p > .05$, ^C denotes $p > .011$; Fisher test: * $p < .05$, ** $p < .005$, [†] $p < .1$

3.3.5. TAS-20 correlates with FC of gyri and sulci mid-dACC seeds towards large medial frontal area

TAS-20 total score showed a robust positive association with functional connectivity of gyri seeds R gdACC 2 and R gdACC 3 to L Medial Frontal Gyrus (MFG) ($k > 80$). Sulci seeds likewise showed positive correlation towards frontal regions: L sdACC2 to L MFG and R sdACC 4 to R Superior Frontal Gyrus (SFG) both $k > 80$). Additionally, sulci seeds showed higher connectivity to L Middle Temporal Gyrus (MTG) with higher TAS-20, particularly L sdACC 4 ($k > 80$). Other sulci seeds also showed associations with L MTG and L STG, but the cluster size did not reach corrected significance. Results are presented in Table 3.5. and Figure 3.1. for representative clusters.

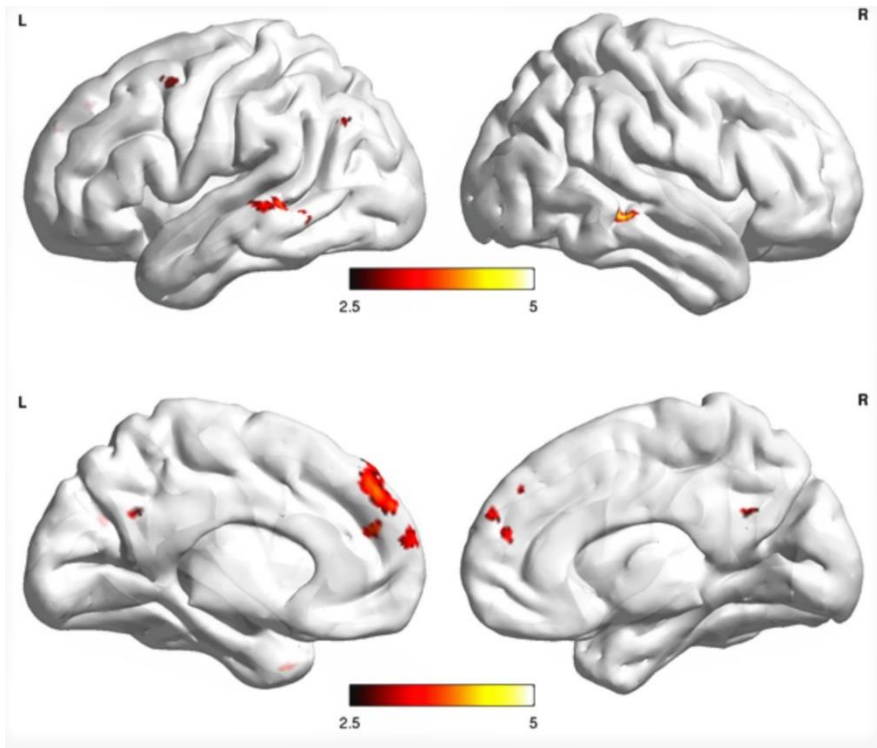


Figure 3.1. Correlations of TAS-20 and FC of mid cingulate seeds.

Representative clusters of positive correlations between TAS-20 and sulci seeds towards Middle and Superior Temporal gyrus (upper panel) and gyri & sulci seeds towards medial frontal cortex (lower panel).

Table 3.5. Positive correlations between TAS-20 total score and FC of mid cingulate seeds.

A Gyri and B Sulci ACC seeds controlled for age and sex. Results are considered significant at $p < .05$, FWE cluster level corrected, with an initial threshold of $p < .001$, uncorrected. Other non-significant results (ns) are reported here at cluster size $k > 5$, as to show consistency of the result.

ROI	<i>p</i>	<i>k</i>	MNI			Region
			<i>x</i>	<i>y</i>	<i>z</i>	
L gdACC 1	ns	32	-8	48	22	L Superior Medial Gyrus
L gdACC 2	ns	6	-8	62	20	L Superior Medial Gyrus
L gdACC 3	ns	8	-2	54	30	L Superior Medial Gyrus
L gdACC 4	ns	10	-8	32	60	L Superior Medial Gyrus
L gdACC 5	ns					/
R gdACC 1	ns	18	-66	-24	8	L Superior Temporal Gyrus
R gdACC 2	<.001	210	-8	48	22	L Superior Medial Gyrus
			0	50	40	
			-6	44	44	
	ns	19	-64	-24	6	L Superior Temporal Gyrus
			-66	-28	2	L Middle Temporal Gyrus
R gdACC 3	ns	12	-66	-22	8	L Superior Temporal Gyrus
	.003	127	-2	54	32	L Superior Medial Gyrus
R gdACC 4	ns	18	-62	-30	-6	L Middle Temporal Gyrus
			-66	-28	0	
			.105	62	8	56
	ns	49	6	58	30	
			-4	52	30	L Superior Medial Gyrus
			-12	46	32	L Superior Frontal Gyrus
	ns	27	-6	50	44	L Superior Medial Gyrus

R gdACC 5 ns 22 -14 58 24 L Superior Frontal Gyrus

ROI	<i>p</i>	<i>k</i>	MNI			Region		
			<i>x</i>	<i>y</i>	<i>z</i>			
L sdACC 1	ns	29	-66	-22	10	L Superior Temporal Gyrus		
	ns	8	-2	52	32	L Superior Medial Gyrus		
L sdACC 2	<.001	213	4	56	32	R Superior Medial Gyrus		
			-8	48	34			
			-6	50	46			
L sdACC 3	ns	33	-66	-24	8	L Superior Temporal Gyrus		
	ns	24	-66	-28	-2	L Middle Temporal Gyrus		
	ns	12	60	-32	-8	R Middle Temporal Gyrus		
	ns	32	-4	52	32	L Superior Medial Gyrus		
L sdACC 4	.028	86	-2	56	34			
			-12	8	52	L Superior Frontal Gyrus		
			-60	-40	-4	L Middle Temporal Gyrus		
L sdACC 5	ns	52	-60	-32	-6			
	ns	27	62	-32	-6	R Middle Temporal Gyrus		
R sdACC 1	ns	27	-4	48	24	L Superior Medial Gyrus		
	ns	37	14	62	24	R Superior Frontal Gyrus		
R sdACC 2	ns	12	-66	-22	8	L Superior Temporal Gyrus		
	ns	24	-62	-24	6	L Superior Temporal Gyrus		
	ns	27	-4	50	34	L Superior Medial Gyrus		
R sdACC 3	ns	10	66	-28	0	R Superior Temporal Gyrus		
			-60	-40	-10	L Middle Temporal Gyrus		
	.173	55	-62	-32	-6			
			62	-32	-6	R Middle Temporal Gyrus		
R sdACC 4	<.001	176	ns	14	-4	56	L Superior Medial Gyrus	
			ns	18	-4	24	48	L Posterior Medial Gyrus
			16	32	46	R Superior Frontal Gyrus		
			20	40	52			
			22	24	42			

	ns	51	-68	-32	-4	L Middle Temporal Gyrus
			-62	-34	-10	
	ns	48	60	-32	-8	R Middle Temporal Gyrus
	ns	50	38	10	50	R Middle Frontal Gyrus
			42	16	38	
			46	12	54	
R sdACC 5	ns	5	-62	-32	-8	L Middle Temporal Gyrus
	ns	22	-8	48	46	L Superior Medial Gyrus

3.3.6. Sex differences were present only in the FC of the gyri seeds

There were no sex differences for correlation slopes between alexithymia and sulci and gyri ACC FC maps towards frontal or temporal regions. However, unexpectedly, a consistent difference for both L and R gyri ACC seeds between sexes was found towards R Putamen, where men displayed higher FC between regions (Figure 3.2, Table S3. 3.).

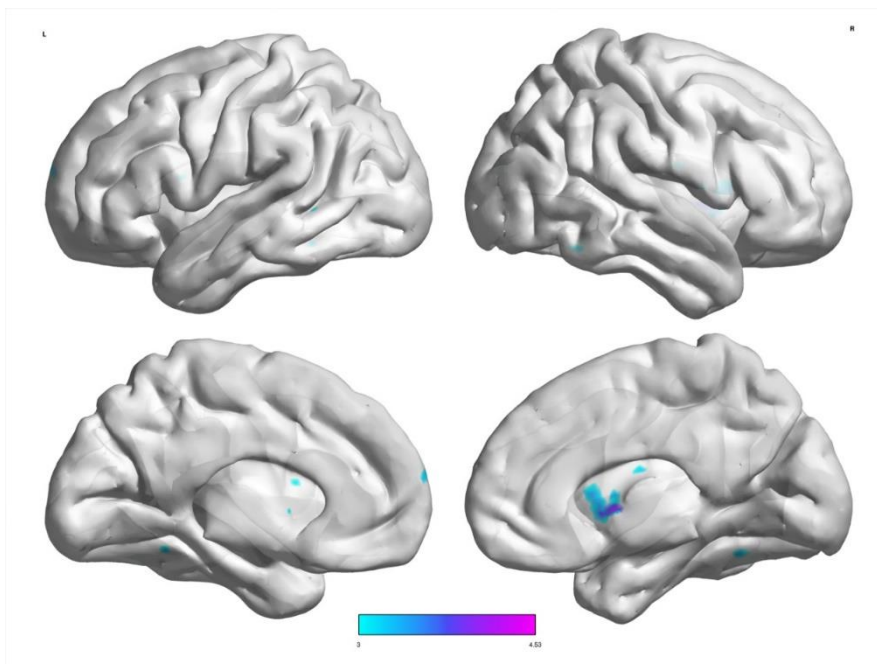


Figure 3.2. Differences in correlations of TAS-20 and FC of mid cingulate seeds between men and women.

Representative cluster in R Putamen of the difference between correlation slopes of TAS-20 and L & R gyri dACC/MCC seeds for men > women. Cluster size differed between 8 and 82 voxels.

3.4. Discussion of Study 1

Both 3T and 7T study showed that the ACC is associated with the level of alexithymia. However, it was also clear that subregions contribute to different features of alexithymia, given their respective functional profile. Moreover, some findings were shared between the sexes, but discernible regional sex-specificities were exhibited.

3.4.1. Demographic properties

Commonly, German TAS-20 test shows similar factor reliability compared to the original English version (Bach *et al.*, 1996; Müller, Bühner and Ellgring, 2003; Franz *et al.*, 2008). In both studies, TAS-20 showed good internal consistency and inter-item correlation except for the subscale EOTS, especially in men (Table 3.1). Subscales DDF and DIF could be clustered together because differentiation and verbalization of feelings are interconnected (Kooiman, Spinhoven and Trijsburg, 2002). The distinctiveness of EOTS in terms of the inter-scale correlation and the correlation to metabolite markers, points out that alexithymia is multidimensional (Müller, Bühner and Ellgring, 2003) and probably encompasses functional change in more than one brain region.

Previous population studies suggest that age is positively associated with alexithymia (Moriguchi *et al.*, 2007b). In both studies, there was no significant correlation between alexithymia and age. The age distribution in the samples was however quite homogenous, so it could be that to see an age effect a wider age range is needed.

3.4.2. 3T metabolite study

Metabolite mapping revealed that the NAA/tCr, a sensitive marker of neuronal integrity, correlated negatively with the alexithymia scores across sexes in the pgACC (Table 3.2.). In women, a robust negative correlation was found for the Glx/NAA in the PCC, while in men in the dACC Glx/NAA exerted an additional positive correlation with the TAS-20, on an uncorrected level. These correlations were not related to cortical thickness.

The pgACC is frequently placed within the DMN which has been connected to various self-referential processes, *i.e.*, affect processing, planning and rumination (Raichle *et al.*, 2001; Fox *et al.*, 2005; Laird *et al.*, 2009; Andrews-Hanna *et al.*, 2010). Moreover, it has been associated with mood regulation and identification of affective internal states (Lane *et al.*, 1998; Medford and Critchley, 2010; Sturm *et al.*, 2012).

During visual emotional processes a reduced activation of the pgACC was observed in alexithymic individuals (Moriguchi and Komaki, 2013). Earlier MRS study has reported a correlation of TAS-20 and GABA/tCr in the pgACC. GABA mediates neuronal inhibition, so higher GABA levels might decrease local activity. Unfortunately, in this study, GABA was not measured due to the technical limitations of the multiple voxel measures. Nevertheless, both findings point to a reduced activity either by neurotransmitter mediation or by the diminished neuronal integrity in the pgACC. The previous study did not find changes in the NAA in the pgACC, which stands in contrast to the herein robust correlation, across sexes and subscale (Table 3.2., Table 3.4.) Methodological aspects between the studies might have contributed to that discrepancy. In this study a smaller voxel was used, that was placed in an anatomically defined subregion, namely Brodmann areas (BA) 24a-d, while the J-PRESS assessment used by Ernst et al. (Ernst *et al.*, 2013) had to integrate signals from ACC and large parts of adjacent BA1. Further on, confounding factors such as age, gray matter voxel composition and potential influence of local cortical thickness were controlled for in this study. Incorporating inter-individual variations of voxel tissue composition corrects against potentially spurious correlations and can increase detection of true associations as it denoises the metabolite levels from variations attributed to varying gray matter content, due to voxel positioning and anatomical variability.

NAA is connected to neuronal integrity (Lin *et al.*, 2005; Kalra *et al.*, 2006; Oz *et al.*, 2014), and is considered to be a neuronal marker (Moffett *et al.*, 2007). Decrease in the NAA levels was reported for affective and metabolite disorders (Sassi *et al.*, 2005; Shinno *et al.*, 2007) and in aging (Schuff *et al.*, 2001; Kaiser *et al.*, 2005). Following, the results indicate lower neuronal integrity of the pgACC with higher TAS-20 score. Curiously, there was no converging conformation for a substrate-based macroscopic changes measured via cortical thickness.

This could mark a very subtle effect in a generally healthy young population. Scanning clinical populations or using higher spatial resolution could resolve the conundrum of whether the association with a putative marker of neuronal integrity is independent from the structural changes or if the subtle regional alterations can be first observed on this metabolite marker. Voxel based morphometric studies have reported decreased gray matter volume in the ACC of alexithymic participants (Borsci *et al.*, 2009; Ihme *et al.*, 2013; Goerlich-Dobre *et al.*, 2014). One reason to negative

observation in this study population could be the intermediate scores, while the above-mentioned studies used alexithymic individuals with values over 50 on the TAS-20 total scale.

The results are also the first evidence of sex specific extension of regional abnormalities towards either the default mode network or the SN. In women, in the PCC there was a strong negative correlation between Glx/NAA with TAS-20, which was significantly stronger than in men, while in the dACC men showed positive correlation of the Glx/NAA, although on an uncorrected trend level. The Glx/NAA ratio can be used as a measure of the dynamics of neuronal and glial processes (Savic *et al.*, 2000) indicating an activation related state of the measured regions.

The PCC has been associated with the DMN and was connected to self-relevant mental processes including autobiographical memory and internally directed attention (Vogt, Vogt and Laureys, 2006; Leech and Sharp, 2014). Negative association to Glx/NAA might mark a lower activity of that region with higher TAS-2. Congruently, a fMRI study showed a decreased activation during an imagery task in the PCC in alexithymic participants (Mantani *et al.*, 2005). Review studies have pointed out that women are characterized by higher self-focus and attention towards their own emotions via processes such as introspection and rumination (McRae *et al.*, 2008; Moriguchi *et al.*, 2014). This behavioral tendency might be then reflected by stronger correlations in women of TAS-20 with the microstructural deficits (measured by NAA/tCr in the pgACC) and lower metabolite activity (measured by Glx/NAA in the PCC) in the DMN.

The positive correlation with the Glx/NAA in the dACC was found in men. Even though the findings were not on a corrected statistical level, they could point to a regional hyper activation of the dACC in those participants. The dACC and Anterior Insula compose the SN that monitors external and internal cues and appropriates attention to the most relevant stimuli (Taylor, Seminowicz and Davis, 2009; Menon and Uddin, 2010). It has been also implicated in the cognitive control of the affective state (Lane *et al.*, 1998; Lane, 2008) and a differential activation for men and women has been shown for this area (McRae *et al.*, 2008). Increase in the dACC volume with alexithymia was found, supporting the idea of the enhanced activity of this region in alexithymia (Gundel, 2004; Goerlich-Dobre *et al.*, 2014). The presumed hyperactivity might be the consequence of a compensation mechanism of the general unspecific arousal in alexithymia (Lane *et al.*, 2000; Medford and Critchley, 2010), or of an

emotion regulatory mechanism of suppression (Ochsner and Gross, 2005; Swart, Kortekaas and Aleman, 2009).

Together, the sex-specific network differences of the neurobiological correlates of alexithymia could be a consequence of sex differences in emotional processing (Koch *et al.*, 2007; McRae *et al.*, 2008; Moriguchi *et al.*, 2014).

Essentially though, the results should be viewed as general, sex independent effects in a region crucial for the establishment of mood states, the pgACC. Decrease in the neuronal integrity could be a starting point of the observed alexithymia difficulties (Sturm and Levenson, 2011). Sex-specific regulations strategies might then correlate with the regional patterns of activation and consequentially explain the network specific variation of the metabolite markers.

There were no metabolite correlates between left dlPFC and TAS-20. Following, one could speculate that alexithymia manifests primarily as a construct of difficulties in the cognitive evaluation of feelings (SN) or at the level of introspection (DMN) and less on the level of attention to external stimuli or executive control functions. This needs to be taken with caution. The localization of the dlPFC was less stringent due to anatomical position, and therefore had an increased inter-individual variability. It is possible that the exact location was not captured in all participants with the same level of anatomical preciseness.

In the exploratory analysis, two subscales DDD and DIF showed the same pattern as of metabolite correlations as the total TAS-20 score (although on a differential statistical threshold) (Table 3.4.). The subscale EOTS also replicated the correlation pattern to a lesser extent, thus supporting the previous notion that it might be a distinct item of the TAS-20 scale (Kooiman, Spinhoven and Trijsburg, 2002). The lack of significance in one subscale nevertheless supplies only indirect evidence for a difference in the underlying constructs and necessitates follow-up testing.

3.4.3.7T connectivity study

The most prominent finding of the FC analyses were the positive correlations between TAS-20 and FC of both gyri and sulci mid-cingulate ROIs bilaterally towards large areas of the Medial Frontal Gyrus- also known as the dorsomedial Prefrontal Cortex (dmPFC), and to R Superior Frontal Gyrus (Table 3.5.). Moreover, the sulci ROIs showed a positive correlation to L Temporal regions with TAS-20. Lastly, a sex-specific correlation was found, where men displayed stronger positive correlation

between gyri ROIs and R Caudate region, which was however on a marginal statistical level (Table S3. 3.).

It has been previously described that the dmPFC is involved in affect generation and regulation (Banks *et al.*, 2007; Ochsner *et al.*, 2009; Etkin, Egner and Kalisch, 2011), and has been considered as an interface region of emotion and attention (Ochsner *et al.*, 2004; Morris, Leclerc and Kensinger, 2013; Satpute *et al.*, 2013). Curiously, the mid-cingulate and the dmPFC are not part of a described empathy circuit (Engen and Singer, 2013) and are representative of the social cognitive context and attribution of affect (Frith and Frith, 2007; Bernhardt *et al.*, 2014). Further on, dmPFC was associated with mentalizing in the social context of the non-similar other (Mitchell, Macrae and Banaji, 2006). FMRI studies of alexithymia have reported both higher and lower activity to emotional stimuli in the larger mid-cingulate area and frontal cortices depending on the valence of the stimuli: positive stimuli induced higher activation in alexithymic compared to control participants whereas negative a lower one (Berthoz *et al.*, 2002; Deng, Ma and Tang, 2013). Higher baseline FC between the two areas with higher TAS-20 score might influence (de)activation of both regions during a task (Kellermann *et al.*, 2012). In the case of self-related processes that would include activation of the DMN and deactivation of the frontal emotional - cognitive areas such as dmPFC and SFG (Fox *et al.*, 2005). In the case of heightened baseline connectivity, dmPFC thus might not properly deactivate during such task. Another rs-fMRI study of alexithymia using independent component analysis (ICA) found increased right sided medial prefrontal connectivity, congruent to the here presented results (Liemburg *et al.*, 2012).

The results can be moreover placed in the context of a theory that postulates functional difference between mid-cingulate gyrus and sulcus in terms of the other-versus the self- reference. According to findings from animal electrophysiological and human fMRI studies, gyrus is involved in the predictions of the social context, and sulcus in the self-referenced updates (Lockwood *et al.*, 2015, 2018; Apps, Rushworth and Chang, 2016). Intriguingly, the histological hallmark of the ACC, the spindle neurons, are found in the gyrus, and not sulcus, which is moreover considered as a transition area towards prefrontal cortex (Devinsky, Morrell and Vogt, 1995). The spindle neurons have been also connected to the social mentalization capabilities (Allman *et al.*, 2011). Both gyri and sulci ROIs showed heightened connectivity to dmPFC, implying problems both in the context of self (Sturm *et al.*, 2006; Satpute *et*

al., 2013) and evaluating other people (Mitchell, Banaji and Macrae, 2005; Mitchell, Macrae and Banaji, 2006; Radke *et al.*, 2011). In other words, higher FC with higher TAS-20 might mean that the self-affect is also placed in the context of other which would align with the EOTS dimension of alexithymia. If the engagement of the whole mid-cingulate and the dmPFC is somewhat atypical, one could imagine having difficulties in appraising emotions or having appropriate behavioral response in social situations (Chester and DeWall, 2014).

One of the most commonly described dimensions of alexithymia is “difficulty in describing feelings”. L Middle Temporal Gyrus is involved in the explicit evaluation of speech prosody (Wildgruber *et al.*, 2006), semantic inference and control (Whitney *et al.*, 2011; Visser *et al.*, 2012) and works as a multimodal association cortex (Binder *et al.*, 2009). Previous research has also reported different activation patterns (Velde *et al.*, 2013) and lower volume of the L MTG in highly alexithymic individuals (Ihme *et al.*, 2013). Correlation of TAS-20 and FC between the mid-cingulate sulci ROIs and the L MTG could represent the inability to differentiate language representation. One study reported a reduced effective connectivity in autism spectrum disorder participants between the left temporal area to the dACC and medial prefrontal parts during task integration of faces and voices (Hoffmann *et al.*, 2016). At a first glance this is contradictory to our findings. However, it can be imagined that a hyper connectivity at rest could translate to lower ability to effectively (de)activate during task execution. Only the ROIs in the sulcus showed an association with temporal areas, in contrast to the association towards medial frontal areas (Table 3.5.). Consequently, it can be argued that the deficits of contextualizing own feelings are mirrored in the connectivity between the mid-cingulate sulcus and semantic association cortex. In addition, posterior part of the L MTG has been associated with mentalizing processes of attribution and identification of states, co-activating with the medial frontal cortex (Spunt and Lieberman, 2012).

Finally, men displayed higher connectivity between gyri nodes and R Caudate with higher TAS-20 (Figure 3.2., Table S3. 3.). Both healthy and depressive disorder patients with alexithymia show less activation in R Caudate during automatic emotional faces processing (Lee *et al.*, 2011; Ihme *et al.*, 2014; Suslow *et al.*, 2016). Moreover, one study has connected higher levels of alexithymia with increased activation in R Caudate during emotion-based decision-making gambling task, and the authors concluded that alexithymic individuals might not internalize signals

during such tasks (Kano, Ito and Fukudo, 2011; Kano and Fukudo, 2013). The higher FC with gyri ROIs (other- related ACC part) could thus again indicate heightened reliance to external stimuli and/or problems in other's emotion processing, even more so in men. Nevertheless, this difference could also be the consequence of general sex differences in fiber connections (Lei *et al.*, 2016) or of a later maturation of cortico-striatal circuits in men (Gennatas *et al.*, 2017; Kaczurkin, Raznahan and Satterthwaite, 2018).

3.4.4. Alexithymia and disorders of affect regulation: an unspecific cross-relationship

Alexithymia comes in a high comorbidity with affective disorders (Honkalampi *et al.*, 2000). However, it is also present in other psychiatric disorders (O'Driscoll, Laing and Mason, 2014) or medical conditions (Sturm *et al.*, 2006; Shibata *et al.*, 2014), underscoring that affect regulation deficiencies are part of symptomatology of many psychiatric and neurological conditions.

The dmPFC, for example, shows distinct functional profile in the MDD (Grimm *et al.*, 2009; Sheline *et al.*, 2010), reflecting the shared region of deficits in affective processing with alexithymia. However, in the MDD these deficits are related to heightened self-focus and self-related negative bias (Disner *et al.*, 2011). Therefore, one should be careful not to infer the disease state based merely on a regional convergence.

The difference in metabolic and connectivity profiles between sexes could have a clinical application. The findings indicate that DMN and SN might contribute differentially and in opposite directions to the overall identification of own emotional states in men and women. Notably, men and women show not only different prevalence patterns to affective disorders, but also treatment response, e.g. in depression (Addis, 2008). It has been also suggested that comorbidity between the depression and alexithymia could affect treatment outcomes (Carpenter and Addis, 2000). Thus, future research could benefit from a sex-specific approach to better understand the development of dysfunction in affect regulation (Hauwel-Fantini and Pardinielli, 2008).

3.5. Limitations of Study 1

The sample size was moderate for the 3T study. Furthermore, the voxels were placed across both hemispheres to maximize gray matter coverage. Previous studies have

shown different levels of metabolite markers between the hemispheres (Nagae-Poetscher *et al.*, 2004; Hjelmervik *et al.*, 2018). Although there was no specific hypothesis on the ACC lateralization effects, this needs to be confirmed in future studies.

In the 7T connectivity study, 26 ROI were used to calculate the respective FC maps. Although the dACC/MCC seeds seem to show great similarity in their connectivity at rest, one could consider applying a higher significance threshold. The consistency of results bounded to a mid-cingulate subregion, however, gives certitude that the results are not random or a consequence of an fMRI artefact.

Additionally, there were no correlations between the TAS-20 and FC of SN towards nodes of the DMN that were hypothesized, possibly due to the preprocessing strategy. Steps of the fMRI data analysis did not include global signal regression (GSR) (paragraph 2.3.4). GSR is thought to artificially introduce anti-correlation in the FC analysis (Murphy *et al.*, 2009; Saad *et al.*, 2013), but there are also opposite opinions stating it reveals the true biological brain organization (Chai *et al.*, 2012; Yang *et al.*, 2014). Accordingly, it must be considered that non-applying GSR is “masking” possible baseline negative correlations between the SN and DMN.

The discrepancy of regional sex convergence between the 3T (pgACC) and 7T (wider MCC) might come from field strength, resolution differences and signal-to-noise (SNR) aspect. Moreover, the 3T metabolite study had a modest number of participants (3T $n = 36$, versus 7T $n = 59$), thus a robust replication sample is needed to make final conclusions. Ultimately, it might be that the metabolite levels and connectivity patterns are tapping into different aspects of affective phenotypes and might be thus considered as distinct imaging markers.

Menstrual cycle was not accounted for in both studies. Phase of the menstrual cycle might impact the MRS measures (Hjelmervik *et al.*, 2018). However, it is not likely that cycle would give rise to a spurious correlation in the PCC, or in the FC connectivity, since it presupposes similar fluctuations in alexithymia levels along the normal cycle.

Finally, neither study included participants with sub-clinical or clinical levels of alexithymia (52-60 or >61 on TAS-20). This might explain the absence of an association with the cortical thickness, and along the same lines, the minimal cluster sizes in the FC analysis.

3.6. Conclusions of Study 1

For the 3T study, a convergent, sex independent negative correlation between TAS-20 and the marker of neuronal integrity (NAA/tCr) in the pgACC was found, that could be the neuronal substrate for the deficits in processing of feelings in alexithymia. There were moreover sex-specific association of TAS-20 and the Glx/NAA in distinct networks indicating differential compensation or activation of the affect modulating pathways in men and women. A functional conclusion of the results could take the differences between men and women as a suggestion that women experience alexithymia predominantly as a function of a reduced internal appraisal processes mediated by the DMN, while men employ affect conflict suppression mediated by the SN. This would consequentially suggest sex-specific routes of the development of affective impairments.

For the 7T study, a convergent sex-independent difference in the association to TAS-20 between gyri and sulci mid cingulate ROIs was found. The gyri ROIs showed changes in connectivity towards the medial PFC parts involved in the cognitive social processing, while the sulci ROIs additionally displayed connectivity changes to L Middle Temporal gyrus involved in the semantic processing. Together, the correlations between TAS-20 and FC towards these regions reflects two sides of alexithymia, one that includes inability to engage with others and recognition of affective states, and the other that includes inability to express verbally self-affect. The distinction between gyri and sulci could also show a functional specificity that follows the anatomical one and might corroborate earlier assumptions.

The sex-specific changes were seen too, where men displayed a more positive correlation between TAS-20 and FC of gyri nodes to R Caudate. The enhanced connectivity could represent mechanisms of affect regulation between social reward and salience regions. Alternatively, it might be a consequence of the maturation differences between young-adult men and women.

Chapter 4. Study 2: Genetic and sex effects of anxiety-related endophenotypes in the pgACC

This study aimed at looking at genetic variation of an anxiety-related phenotype in controls. Genetic variations in the GABA synthesizing enzyme glutamate decarboxylase (GAD) were examined based on previous animal and human research. Anxiety disorders, common and debilitating psychiatric disorders, are also more prevalent in women. Therefore, sex was viewed as an additional moderating factor.

The following study was first published in:

Colic, L., Li, M., Demenescu, L. R., Li, S., Müller, I., Richter, A., ... & Walter, M. (2018). GAD65 promoter polymorphism rs2236418 modulates harm avoidance in women via inhibition/excitation balance in the rostral ACC. *Journal of Neuroscience*, 1985-17.

4.1. Introduction to Study 2

Anxiety endophenotypes are significant parameters for development of affective psychopathologies, including anxiety disorders (Mathews and Macleod, 2005). Importantly, as with majority of affective disorders, there is a considerable female bias for anxiety disorders during different age groups (McLean *et al.*, 2011; Donner and Lowry, 2013). Investigating neurobiological substrate of anxiety endophenotypes and their sex specificity is of uttermost importance for the development of effective new treatment strategies. So far, research on neurobiological mechanisms of anxiety development and symptoms have stressed the role of cortico-limbic circuits, which contain amygdala, ventromedial prefrontal cortex and ACC (Dörfel *et al.*, 2014).

To elucidate the role of the ACC in anxiety endophenotypes, one must keep in mind its well-characterized rostro-caudal division (Vogt, Finch and Olson, 1992; Bush, Luu and Posner, 2000; Palomero-Gallagher, Vogt, *et al.*, 2009); see paragraph 1.2.1. for more details). In short, the dorsal ACC or the anterior mid-cingulate (aMCC) is part of the salience detection and cognition system (Menon and Uddin, 2010), while the pgACC is part of the affect processing networks (Raichle *et al.*, 2001). PgACC is involved in down-regulation of amygdala activity, thereby modulating automatic affect regulation and the formation of fear memory (Etkin, Egner and Kalisch, 2011; Giustino and Maren, 2015).

At the neurotransmitter level, affect regulation in the cortico-limbic circuit, and control regions such as pgACC, depends on the on the coordinated and dynamic balance of gamma-aminobutyric acid (GABA) and glutamate (Glu). Inhibition/excitation balance controls neural excitability, plasticity and network stability (Cline, 2005) and is often in disequilibrium in affective disorders. Crucial role of GABAergic system in anxiety phenotypes and disorders has been shown in pre-clinical and clinical studies (Nuss, 2015; Goddard, 2016). For example, dysregulation of metabolites in the pgACC was shown in clinical populations (Phan *et al.*, 2005; Long *et al.*, 2013). Even in healthy populations, association between GABA and anxiety is present; in the pgACC, which shows an adaptive response to anticipatory anxiety (Straube *et al.*, 2009), acute stress leads to decreased GABA availability as assessed with in vivo ^1H MRS (Hasler *et al.*, 2010). Further on, a combined fMRI-MRS study that detected correlation between the pgACC deactivation during emotion processing and GABA concentrations in the same region (Northoff *et al.*, 2007) indicating a role of local pgACC GABA levels in general affect regulation.

GABA is synthesized by glutamic acid decarboxylase (GAD), which exists in two isoforms GAD65 (encoded by *GAD2* gene) and GAD67 (encoded by *GAD1* gene) (Erlander *et al.*, 1991; Feldblum, Erlander and Tobin, 1993; Esclapez *et al.*, 1994). GAD65 and GAD67 differ in their function, location, role in development and activity-dependent regulation (Esclapez *et al.*, 1994). GAD67 is spread throughout neurons, and provides intracellular cytoplasmic GABA pool, important for metabolite stability (Pinal and Tobin, 1998; Soghomonian and Martin, 1998; Patel *et al.*, 2006), whereas GAD65 synthesizes GABA for neurotransmission and is found mostly in the nerve terminals of interneurons with active phasic firing (Feldblum, Erlander and Tobin, 1993). Importantly, GAD65 activity is coupled to neuronal activity (Patel *et al.*, 2006; Stagg, Bachtiar and Johansen-Berg, 2011), which can be investigated indirectly via BOLD response in rs-fMRI. Following, a genetic effect on the inhibition/excitation balance in the pgACC, that would further mediate its role in anxiety, was hypothesized.

To follow-up on this hypothesis, an A>G single nucleotide polymorphism (SNP) in the 5'-flanking promoter region of *GAD2* (chromosome 10p, position -243, NCBI accession number rs2236418) was chosen. Boutin *et al.* (Boutin *et al.*, 2003) showed a 6-fold increase in promoter activity in the presence of the rs2236418 SNP,

suggesting that this polymorphism actively influences GABA levels in vitro. Genetic variation in both *GAD1* and *GAD2* show connection to affective disorders in genetic association studies (Hettema *et al.*, 2006). Moreover, one genetic association study has identified several *GAD2* SNP, not including rs2236418, as potential risk factors for anxiety disorders specifically (Unschuld *et al.*, 2009), but the functional or metabolite consequences of genetically mediated variability of *GAD2* in humans are thus far unknown.

The SNP effects on the inhibition/excitation balance in the ACC subregions were studied with high-field (7T) multi-voxel ¹H MRS via GABA/Glu ratio. Brain activity was measured using resting state fMRI (rs-fMRI) indices, amplitudes of low-frequency fluctuations (ALFF) and regional homogeneity (ReHo). Based on the differential functional role of ACC subregions, a regional specificity of genetic effects was assumed for the pgACC, given its distinguished role in affect processing. As a behavioural measure, individual proneness to anxiety was tested with harm avoidance scale of the Temperament and Character Inventory (TCI; Cloninger, Przybeck and Svrakic, 1994), a scale which correlates with other self-reported measures of anxiety-related traits (Ludwig *et al.*, 2015).

Given the epidemiological observation that anxiety disorders are considerably more prevalent in women (McLean *et al.*, 2011; Schuch *et al.*, 2014), it is noteworthy that the GABAergic system is participant to sex differences and its activity is modulated by circulating gonadal hormones (Davis *et al.*, 1999; McCarthy, Auger and Perrot-Sinal, 2002; Seney *et al.*, 2013). Promotor region of the *GAD2* gene has been identified as a target for oestrogen receptors as transcriptional factors (Hudgens *et al.*, 2009), and oestrogens modulate both *GAD65* and *GAD67* mRNA levels, but often in opposite directions and in a regionally specific manner (McCarthy *et al.*, 1995; Ikeda, Makino and Yamada, 2015). Therefore, sex-driven effect was expected and investigated for in all analyses.

Lastly, to validate the specificity of the *GAD2* rs2236418, additional candidate SNPs in the GABAergic and glutamatergic pathway were tested: i) in the *GAD2* gene (position 26211729 in the intron region, rs10508715 A>G), polymorphism in promoter region associated with neurotic phenotype (Unschuld *et al.*, 2009), to test in-gene polymorphism specificity; ii) in the sister gene *GAD1* (chromosome 2, position 170851590 in the intron region, rs3791850 C>T), from an association study for anxiety disorders (Hettema *et al.*, 2006), and *GAD1* (position 170836945 in the

intron region, rs769390, A>C), which showed effects on GABA levels in dACC (Marenco *et al.*, 2010), to test enzyme form specificity; iii) in the glutaminase gene (*GLS* chromosome 2, position 190964627, rs13035504 A>G) associated with increased risk for suicidality (Yin *et al.*, 2016), to test for metabolite specificity.

4.2. Specific materials and methods of Study 2

4.2.1. Participants

Study sample was 105 healthy participants (age= 27.09± 6.72, 44 women), included in three studies, with the same measurement protocol which included: genotyping, rs-fMRI and ¹H MRS at ultra-high-field strength 7T. Studies employed identical protocols for recruitment, and the scan order of the MRS voxels and rs-fMRI was the same during the measurements. Participants in two studies were used as control participants for patient studies, so after MRS and rs-fMRI scan they performed additional fMRI tasks which differed according to the respective patient study, but this fMRI task did not affect prior measurements. Participants were in good physical condition and medication free as confirmed by medical history. Medical history was approved by a study physician. Participants were questioned about previous hospitalization (including psychotherapy), medical conditions and medication, where medication for neurological diseases (e.g. epilepsy), diabetes and hypo/hyperthyroidism were considered as an exclusion criterion. Psychiatric disorders according to DSM-IV were excluded using the German Version 5.0 of the M.I.N.I. Mini International Neuropsychiatric Interview (Sheehan *et al.*, 1998; Ackenheil *et al.*, 1999). Additional exclusion criteria were left-handedness as assessed with the short form (10 items) of the Edinburgh Handedness Inventory (Oldfield, 1971) and MRI contraindications. The study was approved by the Institutional Review Board of Otto von Guericke University of Magdeburg, Faculty of Medicine. The study was conducted in accordance with the Declaration of Helsinki (World Medical Association, 2002) and all participants gave written informed consent.

4.2.2. Genotyping

Genotyping was done in collaboration with the lab Imaging Genetics (Leibniz Institute for Neurobiology Magdeburg) and was performed by G.B. Whole-blood samples were collected in EDTA-coated tubes (BD Vacutainer, K3E, 7.2 mg. REF 368884) and stored at 4 °C until further processing. Using GeneMole® automated system (Mole Genetics AS, Lysaker, Norway), genomic DNA was extracted from

blood leukocytes. Genotyping for all SNPs was done with polymerase chain reaction (PCR), followed by an allele-specific restriction analysis. Below is a brief description for all SNPs.

GAD2 rs2236418: The DNA fragment on chromosome 10p12.1 containing the *GAD2* c.-243A>G polymorphism (NCBI accession number: rs2236418) was amplified using the primers *GAD2*-F: 5'-CGA AAG ACC AAA AGC CAG AG-3' and *GAD2*-B: 5'-TTC TAC CAA GGC GCT GAA AT-3' and standard Taq polymerase (Qiagen). The resulting PCR products were digested with *Dra*I (Thermo Scientific # ER0221), yielding two fragments (279+ 575bp) for the A allele or a single fragment (854bp) for the G allele. DNA fragments were separated on a 1% agarose gel stained with Midori Green (Biozym Scientific, Hessisch Oldendorf, Germany) and visualized under UV light.

GAD2 rs10508715: The DNA fragment on chromosome 10p12.1 containing *GAD2* n.4828-114A>G polymorphism (NCBI accession number: rs10508715) was amplified using the primers *GAD2*-F: 5'- CCC TCT GCT CCT CAG CTT AGA GGA G -3' and *GAD2*-B: 5'- CTC CTC CTC CTT CTC GGG GCT CTC -3' and standard Taq polymerase (Qiagen). The resulting PCR products were digested with *Dde*I (Thermo Scientific #ER1881), yielding three fragments (80+154+16bp) for the G allele or two fragments (234+16bp) for the A allele. DNA fragments were separated on a 3-3.5% agarose gel stained with Midori Green (Biozym Scientific, Hessisch Oldendorf, Germany) and visualized under UV light.

GAD1 rs3791850: The DNA fragment on chromosome 2p31.1 containing the *GAD1* c.1185-1124C>T polymorphism (NCBI accession number rs3791850) was amplified using primers *GAD1*-F: 5'- GTG AAG GAT CTT TTC CCC CAG ATA GAG C -3' and *GAD1*-B: 5'- CAC TGA AGG GAA AAG TTC TTC AGA CC -3' and standard Taq polymerase (Qiagen). The resulting PCR products were digested with *Dra*I (Thermo Scientific # ER0221), yielding two fragments (63+138bp) for the C allele or a single fragment (201bp) for the T allele. DNA fragments were separated on a 3.5-4% agarose gel stained with Midori Green (Biozym Scientific, Hessisch Oldendorf, Germany) and visualized under UV light.

GAD1 rs769390: The DNA fragment on chromosome 2p31.1 containing the *GAD1* c.638+62A>C polymorphism (NCBI accession number rs769390) was amplified using primers *GAD1*-F: 5'- CCA CTG GAT TGG ATA TTA TTG GCC -3' and *GAD1*-B: 5'- GTT AGA GTT ATT ATT TCT CAT GAC CAT GC -3' and standard Taq polymerase

(Qiagen). The resulting PCR products were digested with DraI (Thermo Scientific # ER0221), yielding two fragments (123+169bp) for the A allele or a single fragment (292bp) for the C allele. DNA fragments were separated on a 3.0% agarose gel stained with Midori Green (Biozym Scientific, Hessisch Oldendorf, Germany) and visualized under UV light.

GLS rs13035504 The DNA fragment on chromosome 2p32.2 containing the GLS1 c.*1641 A>G polymorphism (NCBI accession number rs13035504) was amplified using primers GLS-F: 5'- GCT TTC ATT TTC ACT TCC AGT CTA AGC C -3' and GLS-B: 5'- GCG GGC TGC TCT TTG AAT AAA GTT ATC -3' and standard Taq polymerase (Qiagen). The resulting PCR products were digested with HpaII (Thermo Scientific # ER0511), yielding two fragments (113+200bp) for the G allele or a single fragment (313bp) for the A allele. DNA fragments were separated on a 3.0% agarose gel stained with Midori Green (Biozym Scientific, Hessisch Oldendorf, Germany) and visualized under UV light.

4.2.3. Personality questionnaire

To assess levels of harm avoidance, the corresponding scale from the self-reported Temperament and Character Inventory (TCI) (Cloninger, Przybeck and Svrakic, 1994) was used. TCI was constructed as a questionnaire to describe and predict clinical phenotypes both in healthy and patient populations. It was designed on a psychobiological model of personality based on temperaments- heritable and stable dimensions of “involuntary emotional processes” and characters- dimensions developed later in life of “voluntary rational processes”.

Harm avoidance, a temperament, was associated with cognitive symptoms of anxiety (Cloninger, 1987). It consists of four subscales, which reflect different aspects of anxious tendencies: Anticipatory worry, Fear of uncertainty, Shyness with strangers and Fatigability and asthenia (weakness). Harm avoidances correlates with other personality scales, for example strongly positively with Neuroticism and negatively with Extraversion from the NEO Personality Inventory and Eysenck personality dimensions (Stallings *et al.*, 1996; De Fruyt, Van De Wiele and Van Heeringen, 2000), thereby indicating it mirrors individual anxiety-like trait. TCI has as long-term (Josefsson *et al.*, 2013) and cross-cultural stability (Miettunen *et al.*, 2006). Moreover, German version of the questionnaire and scale show high internal consistency and factor structure (Richter, Eisemann and Richter, 2000), as the

original too (Cloninger, Przybeck and Svrakic, 1994). These features indicated transferability of underlying biological and environmental determinants of differences in healthy populations.

In the present study, seventy-two participants filled out the questionnaire. Internal consistency of Harm avoidance was considered good (Cronbach's $\alpha = .9$ for thirty-five items; for sixty-nine participants item by item scores were available).

4.2.4.7T MRS and rs-fMRI acquisition

The data were obtained on the 7T scanner. Details of the acquisition and preprocessing can be found in paragraphs 2.1.2., 2.1.3., 2.2.6. and 2.3.4.

In short, rs-fMRI data were preprocessed and indices of baseline neuronal activity, ALFF and ReHo, were used for further statistical analysis.

MRS was obtained with the STEAM sequence in two voxels, the pgACC and the aMCC. GABA, Glu and tCr were quantified with the LCModel. GABA/Glu, GABA/tCr and Glu/tCr ratios were residualized for gray matter volume proportion. The gray matter partial volume of the individual voxel was calculated as the segmented gray matter divided by the total volume within voxels.

4.2.5. Statistical analysis

Demographic characteristics (age, sex, BMI, smoking, alcohol consumption or contraception use) for the full set between genotype groups of *GAD2* rs2236418 were tested. Variables were checked with Kolmogorov-Smirnov test for normality ($p < .05$) and Mann-Whitney's *U* tests or χ^2 tests were conducted (Table 4.1.). Datasets for subsequent analyses varied due to: scanner artifacts or excessive head movement during scanning (27 participants excluded), insufficient MRS quality (aMCC= 28; pgACC= 14; both= 37 participants excluded), or incomplete questionnaires (33 participants excluded), and each analysis was done with the maximum number of participants available for the modality or combination of them. To control for the possible confounding effects, demographic difference between the groups were checked again.

To determine the genotype and sex effects on the local intrinsic neuronal activity, ALLF and ReHo were compared with an ANOVA within the boundaries of the ACC subregions. ACC mask was created with a 50% threshold for overlap of individual aMCC and pgACC voxels. ANOVA was done in SPM12 with genotype and sex as

independent between- participant factors (46 AA, 22 women; 29 G carriers, 14 women), with age as nuisance covariate. Statistical significance was set at $p < .05$, peak level family-wise error (FWE) corrected for the search volume.

Following, further regional specificity was tested with an ANCOVA model. A model with region (pgACC vs. aMCC), *GAD2* rs2236418 genotype, sex (45 AA, 22 women; 21 G carriers, 6 women) and their interaction on the GABA/Glu ratio was set. Furthermore, to find specificity of genotype effects, additional SNPs were tested with the same model, with a statistical threshold $p < .01$ (equal to a Bonferroni-corrected $p < .05$). Additional SNPs included: *GAD2*, rs10508715; *GAD1*, rs3791850 & rs769390; and *GLS*, rs13035504. Significant main effects or interactions were investigated with *post hoc* Student's *t*- or Mann-Whitney's *U*- tests.

To demonstrate metabolite specificity of significant interactions on the GABA/Glu ratio, supplementary ANCOVA models were done for the GABA/tCr and Glu/tCr, with an exploratory threshold of $p < .05$. ANCOVA models had region as the within-participant factor, and genotype and sex as between- participant factors, with age as a covariate. Computations were done with SPSS (IBM SPSS Statistics for Windows, Version 24., Armonk, NY, USA)

Behavioral relevance of the pgACC GABA/Glu in regard to anxiety-related trait was tested next. A non-parametric correlation of GABA/Glu ratio and harm avoidance scores was computed, controlling for age. Considering sex differences, the correlation was computed separately for men and women (35 men, 27 women), with a $p < .025$, two-tailed, Bonferroni-corrected. Correlation coefficients were then compared for a significant difference with the Fischer's *Z*-test, with a statistical threshold set at $Z > 1.96$ (equivalent to a $p < .05$, two-sided), using VassarStats (Website for statistical computation, Poughkeepsie, NY, USA). Direct sex differences were tested with Mann-Whitney's *U*-tests for harm avoidance and pgACC GABA/Glu ratio.

Finally, to examine the effects of the baseline neuronal activity or the pgACC GABA/Glu ratio on the genotype-related prediction of harm avoidance, mediation analyses using the SPSS extension PROCESS v2.15 (Preacher and Hayes, 2004; Hayes, 2013) were done. Mediation models are used to examine direct influence of a predictor on the dependent variable, as well as the indirect underlying influence which is accounted only through an interaction of the predictor with a third-mediator variable. Model was set with *GAD2* rs2236418 genotype as a predictor, harm

avoidance as an outcome and age as a nuisance covariate. First, models that considered two mediator variables independently, as well as their additive effect (GABA/Glu pgACC with ALFF or ReHo β estimate) were calculated ($n= 41$ participants, Model 6 in the PROCESS extension). Then, each mediator variable was estimated in a separate model ($n= 48$ for ALFF and ReHo; $n= 62$ participants for GABA/Glu pgACC). Here, sex was added as a moderating factor to account for any sex-specific effects (Model 59 in the PROCESS extension). In all calculations, heteroscedasticity-consistent standard errors were set, and 95% CI were estimated via bootstrap resampling with 1000 repetitions.

4.3. Results of Study 2

4.3.1. Demographic data

For the target SNP *GAD2* rs2236418 participants were grouped into AA homozygotes ($n= 65$, age= 27.58 ± 7.25 , 28 women) and G allele carriers (G carriers) (31 AG and 9 GG: $n= 40$, age= 26.28 ± 5.73 , 16 women). There were no demographic differences between the groups (Table 4.1.). Linkage between the target and other SNPs was also checked, and *GAD2* rs10508715 was the only one significantly linked to the target SNP. Further analysis-specific differences of subgroups are listed in Table 4.2. Overall, there were no significant differences between genotype groups for other SNPs as well (Table 4.3.).

Table 4.1 Study sample demographics for the GAD2 rs2236418.

Mann-Whitney test was conducted to test for difference in age and BMI (mean± SD), and χ^2 test of independence to test for distribution of genotype by sex, smoking status, alcohol consumption or contraception use. All values were $p > .05$, two-sided. Allele frequencies of the whole data set ($n = 105$) were within the Hardy-Weinberg equilibrium.

Variable	AA	G carriers	Statistical test
Whole sample	65 participants	40 participants	$\chi^2(1) = 3.208, p = .073$ #
Age	27.58± 7.25	26.28± 5.73	$U = 1102, p = .189$
Sex	28 women	16 women	$\chi^2(1) = .096, p = .756$
BMI * (59/36)	23.49±2.88	24.46± 3.20	$U = 887, p = .179$
Smoking status * (62/38)	21 yes	10 yes	$\chi^2(1) = .629, p = .428$
Alcohol consumption * ¹ (56/33)	39 yes	20 yes	$\chi^2(1) = .759, p = .384$
Contraceptive use * (27/16)	13 yes	9 yes	$\chi^2(1) = .264, p = .607$
GAD2 rs10508715	58 AA	6 AA	$\chi^2(1) = 59.404, p < .001$
GAD1 rs3791850	37 CC	20 CC	$\chi^2(1) = .359, p = .549$
GAD1 rs769390	35 AA	17 AA	$\chi^2(1) = .945, p = .331$
GLS rs13035504	48 AA	33 AA	$\chi^2(1) = .580, p = .446$

* The data were not available for all participants; total number is written in brackets for the respective genotype group; ¹ yes= at least one drink per week-daily; no= rarely-never;

.1 > $p > .05$

Table 4.2. Analyses sample characteristics for the *GAD2* rs2236418.

For each analysis number of participants differed; showed are genotype groups with age (mean± SD) and sex frequencies. Mann-Whitney test was conducted to test for difference in age, and χ^2 test of independence to test for distribution of genotype by sex. All values are $p > .05$, two-sided.

Analysis	Groups	<i>n</i>	Age	Mann-Whitney test	Sex, <i>n</i>	Interaction genotype* sex
Local intrinsic activity	AA	46	28.07± 7.53	$U = 474,$ $p = .035 *$	22 women	$\chi^2(1) = .001,$ $p = .970$
	G carriers	29	24.86± 3.92		14 women	
Inhibition/ excitation balance	AA	45	27.87± 7.59	$U = 403,$ $p = .136$	17 women	$\chi^2(1) = 3.267,$ $p = .071 \#$
	G carriers	23	25.30± 4.48		6 women	
Behavioral correlates	Men	35	26.91± 6.44	$U = 441,$ $p = .653$		
	Women	27	26.63± 6.69			
Mediation model 6 (M= pgACC GABA/Glu & ALFF/ReHo β estimate)	AA	20	29.20± 9.29	$U = 140,$ $p = .066 \#$	12 women	$\chi^2(1) = .631,$ $p = .427$
	G carriers	21	24.52± 4.09		10 women	
Mediation model 59 (M=ALFF/ReHo β estimates)	AA	26	28.62± 8.29	$U = 19.5,$ $p = .047 *$	15 women	$\chi^2(1) = .284,$ $p = .594$
	G carriers	22	24.77± 4.16		11 women	
Mediation model 59 (M= pgACC GABA/Glu)	AA	36	27.89± 7.45	$U = 347,$ $p = .083 \#$	16 women	$\chi^2(1) = .028,$ $p = .867$
	G carriers	26	25.27± 4.61		11 women	

* $p < .05$; # $.1 > p > .05$

Table 4.3. Study sample characteristics for additional polymorphisms.

Mann-Whitney test was conducted to test for difference in age (mean \pm SD), and χ^2 test of independence to test for distribution of genotype by sex. All values were $p > .05$, two-sided.

Polymorphism	Groups	Age	Mann-Whitney test	Sex, <i>n</i>	Interaction genotype * sex
GAD2 rs2236418	AA	27.58 \pm 7.25	$U = 1102, p = .19$	28 women	$\chi^2(1) = .1,$ $p = .76$
	G Carriers	26.28 \pm 5.73		16 women	
GAD2 rs10508715	AA	27.36 \pm 7.02	$U = 1073, p = .43$	22 women	$\chi^2(1) = 2.80,$ $p = .094 \#$
	G Carriers	26.65 \pm 6.31		19 women	
GAD1 rs3791850	CC	27.09 \pm 6.17	$U = 1162, p = .53$	21 women	$\chi^2(1) = 1.21,$ $p = .27$
	T Carriers	27.14 \pm 7.48		21 women	
GAD1 rs769390	AA	27.19 \pm 6.91	$U = 1250, p = .74$	25 women	$\chi^2(1) = 2.09,$ $p = .15$
	C Carriers	26.92 \pm 6.60		17 women	
GLS rs13035504	AA	27.11 \pm 6.53	$U = 795, p = .44$	32 women	$\chi^2(1) = .25,$ $p = .62$
	G Carriers	26.41 \pm 6.80		10 women	

.1 > $p > .05$

4.3.2. Genotype differences in the local neuronal activity

ALFF and ReHo Fischer transformed maps were calculated to determine the effects of genotype and sex on the intrinsic activity within the search area of ACC subregions. There was a main effect of genotype on both metrics with peak activation in the pgACC (Figure 4.1.). G carriers exhibited a trend towards a decrease in the intrinsic neuronal activity measured with ALFF ($[-4 \ 42 \ -2], t(70) = 3.67, p = .059$, FWE peak level corrected) (Figure 4.1A) and significantly lower ReHo indices at the same

location ($[-2\ 42\ -2]$, $t(70)= 3.80$, $p= .026$, FWE peak level corrected) (Figure 4.1B), compared to AA homozygotes. There was no significant genotype by sex interaction for either metric. A main effect of sex was however present, significantly for ALFF in the pgACC ($[6\ 38\ -2]$, $t(70)= 4.62$, $p= .004$, FWE peak level corrected), as well as marginally for ReHo in the aMCC ($[-6\ 24\ 24]$, $t(70)= 3.43$, $p= .069$, FWE peak level corrected). For both metrics' women had lower baseline activity.

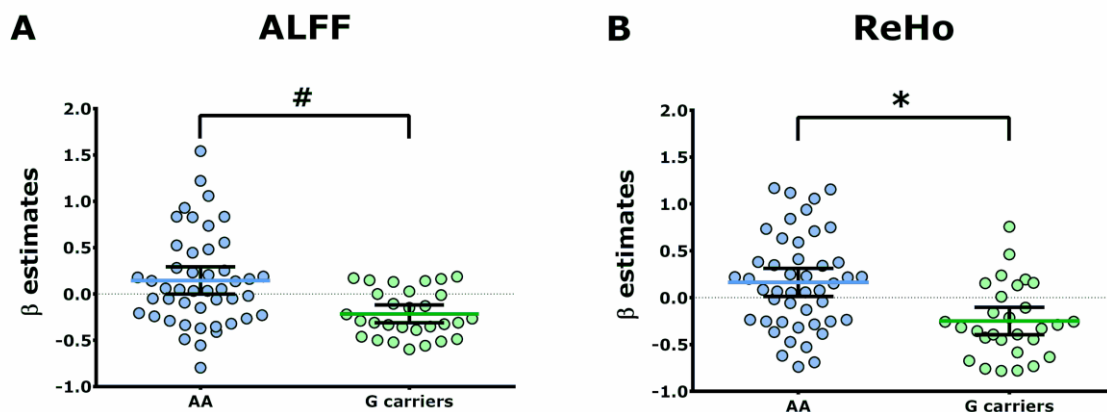


Figure 4.1. Difference in the resting-state fMRI indices for the *GAD2* rs2236418.

A ALFF, peak $[-4\ 42\ -2]$; B ReHo, peak $[-2\ 42\ -2]$. AA homozygotes (pale blue) and G carriers (pale green), * $p < .05$, # $.1 > p > .05$. Data is presented in mean \pm 95% CI.

4.3.3. *GAD2* polymorphism rs2236418 and sex show effect on the GABA/Glu ratio in the pgACC

ANCOVA models were run to test for potential effects of region, genotype polymorphism in the *GAD2* rs2236418 and sex on the on the inhibition/excitation balance in the ACC subregions. ANCOVA model revealed a Bonferroni corrected significant two-way interaction of region and *GAD2* rs2236418 genotype for GABA/Glu ratios ($F(1, 63)= 7.53$, $p= .008$, $\eta^2= .11$) and a three-way interaction (region by genotype by sex; $F(1, 63)= 8.66$, $p= .005$, $\eta^2= .12$) (Figure 4.2, Table 4.4.). *Post hoc* comparisons showed that female G Carriers had significantly higher GABA/Glu levels in the pgACC ($t(36)= -2.19$, $p= .035$). Even though there were no significant interactions for the additional SNPs, confirmatory comparisons of the pgACC GABA/Glu for women between other genotypes were done. Again, only the target SNP *GAD2* rs2236418 showed significant differences between the AA homozygotes and G Carriers (Table S4. 1.).

Table 4.4. Analyses of the GABA/Glu levels within the ACC subregions for the five investigated SNPs.

Region was a within- participant factor, genotype and sex between- participant factors, and age nuisance covariate.

Polymorphism	Effect	GABA/Glu
GAD2 rs2236418	Region x Genotype	$F(1, 63) = 7.53, p = .008, \eta^2 = .11$ **
	Region x Sex	$F(1, 63) = .52, p = .47, \eta^2 = .008$
	Region x Genotype x Sex	$F(1, 63) = 8.66, p = .005, \eta^2 = .12$ **
GAD2 rs10508715	Region x Genotype	$F(1, 61) = .25, p = .62, \eta^2 = .004$
	Region x Sex	$F(1, 61) = .29, p = .60, \eta^2 = .005$
	Region x Genotype x Sex	$F(1, 61) = .81, p = .37, \eta^2 = .013$
GAD1 rs3791850	Region x Genotype	$F(1, 60) = .01, p = .93, \eta^2 < .001$
	Region x Sex	$F(1, 60) = .48, p = .49, \eta^2 = .008$
	Region x Genotype x Sex	$F(1, 60) = .82, p = .37, \eta^2 = .013$
GAD1 rs769390	Region x Genotype	$F(1, 61) = 1.71, p = .19, \eta^2 = .027$
	Region x Sex	$F(1, 61) = .38, p = .54, \eta^2 = .006$
	Region x Genotype x Sex	$F(1, 61) = .15, p = .69, \eta^2 = .002$
GLS rs13035504	Region x Genotype	$F(1, 62) = .17, p = .66, \eta^2 = .003$
	Region x Sex	$F(1, 62) = 1.41, p = .20, \eta^2 = .027$
	Region x Genotype x Sex	$F(1, 62) = .78, p = .38, \eta^2 = .012$

Bonferroni corrected threshold equal to ** $p < .01$

In a follow-up analysis, for target *GAD2* rs2236418, region by genotype by sex interaction was shown for GABA/tCr ($F(1, 63) = 4.92, p = .03, \eta^2 = .072$), and a trend level for region by genotype ($F(1, 63) = 3.57, p = .063, \eta^2 = .054$). This was not seen for Glu/tCr ratio (Table 4.6.) suggesting GABA-levels are the driving force for the main interaction effect.

From other analyzed SNPs, only *GLS* rs13035504 displayed a significant region by genotype by sex interaction for Glu/tCr ($F(1, 68) = 4.18, p = .016, \eta^2 = .082$) and a trend-level region by genotype by sex interaction for GABA/tCr ($F(1, 62) = 3.56, p = .064, \eta^2 = .054$) (Table 4.6.).

Table 4.5. Post hoc analyses of the GABA/Glu levels within the ACC subregions.

Student’s t-test or Mann-Whitney’s U-test (two-sided), were conducted to assess directionality for the significant ANCOVA interactions, region by *GAD2* rs2236418 by sex for the GABA/Glu ratios.

Region	Sex	AA/ G carriers	n	Statistics
aMCC	Men	27 / 18	27	$U= 211, p= .458$
	Women	24/ 8	24	$U= 82, p= .564$
pgACC	Men	30/ 23	30	$U= 317, p= .615$
	Women	24/ 11	24	$t(36)= -2.19, p= .035 *$

* $p < .05$

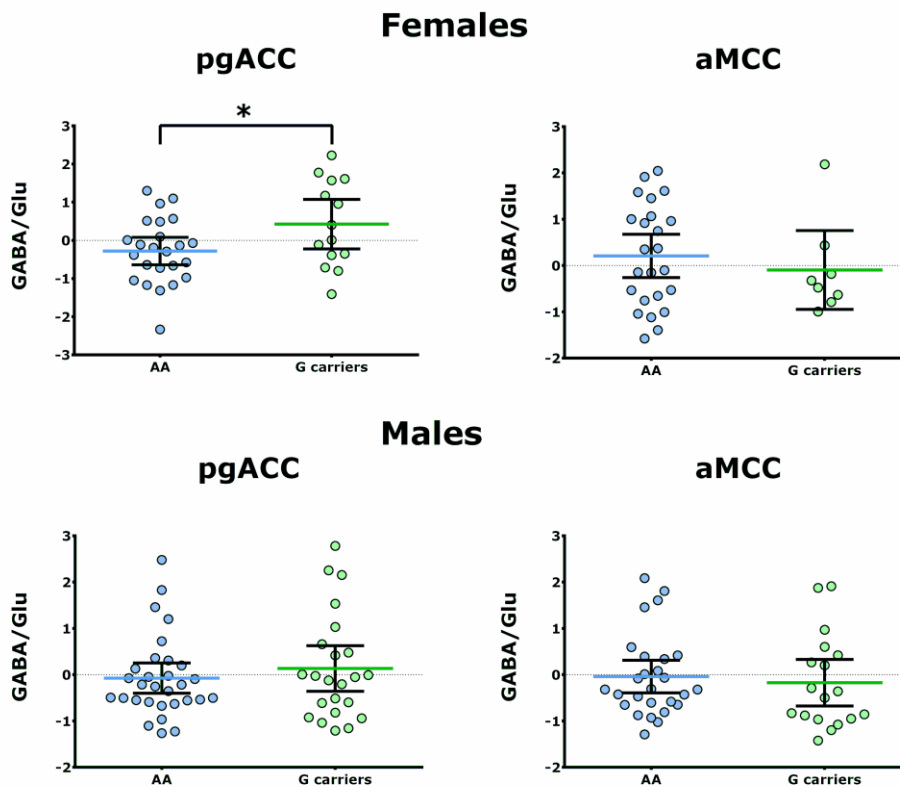


Figure 4.2. Differences in the GABA/Glu ratio for the *GAD2* rs2236418.

Post hoc results for the significant interaction of region by *GAD2* rs2236418 by sex: in the pgACC, for women, G carriers showed significantly increased GABA/Glu ($t(36)= -2.19, p= .035$). AA homozygotes (pale blue) and G carriers (pale green), * $p < .05$. Data is presented in mean± 95% CI.

Table 4.6. Exploratory ANCOVAs for GABA/tCr and Glu/tCr levels within the ACC subregions.

In the ANCOVA model region was a within- participant factor, genotype and sex between-participant factors, and age nuisance covariate. Statistical threshold was set at $p < .05$.

Polymorphism	Effect	Glu/tCr	GABA/tCr
GAD2 rs2236418	Region x Genotype	$F(1, 69) = .51, p = .48, \eta^2 = .007$	$F(1, 63) = 3.57, p = .063, \eta^2 = .054^{\#}$
	Region x Genotype x Sex	$F(1, 69) = .002, p = .97, \eta^2 < .001$	$F(1, 63) = 4.92, p = .03, \eta^2 = .072^*$
GAD2 rs10508715	Region x Genotype	$F(1, 67) = 2.50, p = .12, \eta^2 = .036$	$F(1, 61) = .001, p = .98, \eta^2 < .001$
	Region x Genotype x Sex	$F(1, 67) = 1.55, p = .22, \eta^2 = .023$	$F(1, 61) = .09, p = .76, \eta^2 = .002$
GAD1 rs3791850	Region x Genotype	$F(1, 66) = .44, p = .51, \eta^2 = .007$	$F(1, 60) = .27, p = .61, \eta^2 = .004$
	Region x Genotype x Sex	$F(1, 66) = .99, p = .32, \eta^2 = .015$	$F(1, 60) = .20, p = .66, \eta^2 = .003$
GAD1 rs769390	Region x Genotype	$F(1, 67) = .009, p = .93, \eta^2 < .001$	$F(1, 61) = 2.06, p = .16, \eta^2 = .033$
	Region x Genotype x Sex	$F(1, 67) = .84, p = .36, \eta^2 = .012$	$F(1, 61) = .57, p = .45, \eta^2 = .009$
GLS rs13035504	Region x Genotype	$F(1, 68) = 2.29, p = .14, \eta^2 = .033$	$F(1, 62) = .89, p = .35, \eta^2 = .014$
	Region x Genotype x Sex	$F(1, 68) = 4.18, p = .016, \eta^2 = .082^*$	$F(1, 62) = 3.56, p = .064, \eta^2 = .054^{\#}$

* $p < .05$; # $.1 > p > .05$

4.3.4. In women GABA/Glu ratio correlates negatively with harm avoidance

To assess the functional relevance of the pgACC inhibition/excitation balance for the anxiety-related traits, a non-parametric partial correlation of the pgACC GABA/Glu ratios and harm avoidance was computed, separately in male and female participants. In women, a significant negative correlation between the pgACC GABA/Glu ratio and harm avoidance was observed ($\rho(24) = -.549, p = .004, 95\% \text{ CI} = [-.768, -.214]$), which was not seen in men ($\rho(32) = .048, p = .79, 95\% \text{ CI} = [-.289, .375]$). Moreover, Fischer's Z test confirmed a significant difference between the correlation slopes ($Z = 2.46$, equivalent to $p = .014$) (Figure 4.3.). Women also displayed higher harm

avoidance scores ($U = 327.5, p = .039$), but there was no difference between the sexes for the pgACC GABA/Glu ratio ($U = 450, p = .75$).

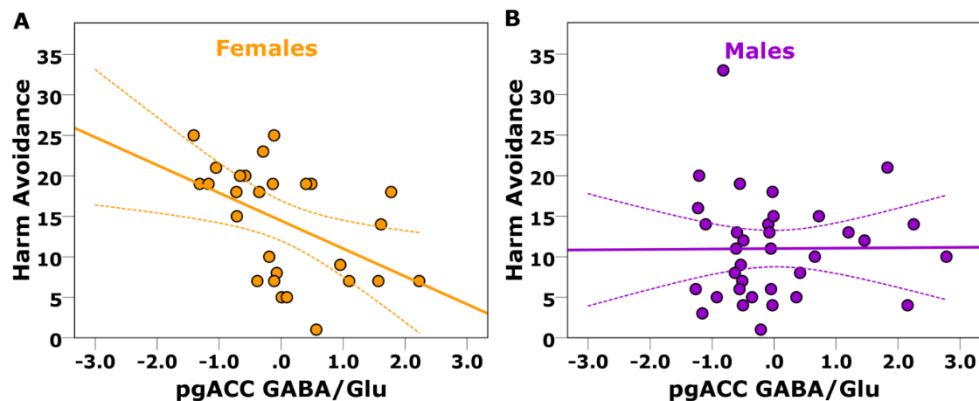


Figure 4.3. Correlation slopes of harm avoidance and pgACC GABA/Glu residuals.

Slopes differed significantly ($p = .014$) between women ($\rho(24) = -.549, p = .004$) (orange) and men ($\rho(32) = .048, p = .79$) (purple). CI is 95% of the mean.

4.3.5. PgACC GABA/Glu mediates relationship between *GAD2* rs2236418 genotype and harm avoidance but only in women

To clarify the relationship between *GAD2* rs2236418 genotype, pgACC GABA/Glu ratio, baseline neuronal activity and harm avoidance, mediation and moderated mediation models were computed. Genotype was set as a predictor, harm avoidance as an outcome, pgACC GABA/Glu and/or ALFF/ReHo as mediator variables, and sex as a moderator variable.

The analyses showed a significant effect only for the fully moderated model in which the pgACC GABA/Glu was the mediator variable (index = -3.147 , bootstrapped 95% CI = $[-9.929, -.478]$). In detail, a pgACC GABA/Glu ratio-dependent influence of genotype on harm avoidance was present in women ($b = -3.088$, boot 95% CI = $[-9.896, -.502]$), but not in men ($b = .059$, boot 95% CI = $[-.334, 1.451]$). A direct effect of genotype on harm avoidance was not significant in either sex (women: $b = 4.926$, boot 95% CI = $[-.831, 1.684]$; men: $b = 1.726$, boot 95% CI = $[-3.026, 6.478]$) (Figure 4.4.).

Other models did not show any significant effects. In short, the results are: additive mediation model with pgACC GABA/Glu and ALFF (total indirect effects: $b = -.641$, boot 95% CI = $[-3.656, 1.563]$; direct effect: $b = -.903$, boot 95% CI = $[-6.258, 4.452]$), additive mediation model with pgACC GABA/Glu and ReHo (total indirect effects: $b =$

.114, boot 95% CI= [-1.966, 2.319]; direct effect: $b = -1.658$, boot 95% CI= [-6.991, 3.676]), moderated mediation model with ALFF (moderated mediation index= -1.291, boot 95% CI= [-5.369, 1.493]) and moderated mediation model with ReHo as mediator variable (moderated mediation index= .946, boot 95% CI= [-1.612, 4.937]) (Figure S4. 1. - Figure S4. 4.).

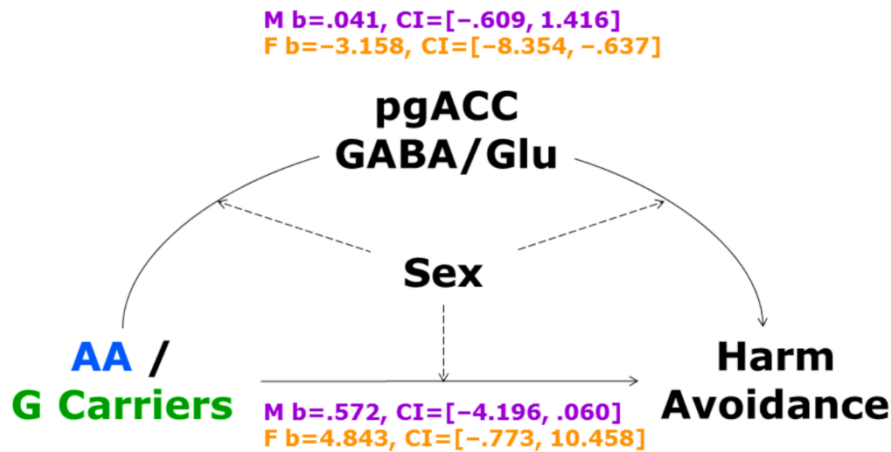


Figure 4.4. Mediation model moderated by sex.

Index= -3.147, bootstrapped 95% CI= [-9.929, -.478]. In both sexes the direct effect of GAD65 genotype on harm avoidance was not significant. For the indirect effect, the GABA/Glu ratio (curved arrow), in the pgACC significantly mediated the relationship between *GAD2* and harm avoidance in women ($b = -3.088$, boot 95% CI= [-9.896, -.502]), but not in men; M = men (purple), F = women (orange), b = effect.

4.4. Discussion of Study 2

The pivotal role of the GABAergic system for anxiety endophenotypes, intermediate phenotypes and anxiety disorders, and their women biased occurrence is well established in research (Nuss, 2015; Goddard, 2016). This study showed a role of a polymorphism rs2236418 in the promoter region of *GAD2* on GABA/Glu ratio in the pgACC, and its association to anxiety proneness, only in women.

There were reduced levels of both rs-fMRI indices ALFF and ReHo in G carriers localized in the pgACC (Figure 4.1.), indicating lower intrinsic resting state activity. GABA/Glu differences were detected in the same region, with G carriers showing higher ratio, indicating a change in the inhibition/excitation balance (Figure 4.2.). The genetic differences of GABA/Glu ratio were moreover metabolite (compared to *GLS*) and isoform specific (compared to *GAD1*), as well as polymorphism specific (rs10508715 in *GAD2*).

Observed polymorphism specificity may be due to transcription factor binding differences between two SNPs, a speculation which needs further conformation in cell culture investigations. Looking at neurometabolites, the *GAD2* rs2236418 differences were driven by the GABA/tCr ratio compared to Glu/tCr (Table 4.6.), however with a smaller effect size. GABA is synthesized from Glu via GAD enzyme isoforms, and thusly GABA and Glu share the same metabolite pathway. However, Glu is the more abundant molecule in the brain tissue and the proportion of GABA synthesis and energetic rates is around only one fourth of total neurotransmitter cycling (Patel *et al.*, 2005; Hyder *et al.*, 2006). Hence, the hypothesized effect of the *GAD2* rs2236418 on synthesis rates could have negligible effects on the total Glu concentration, while affecting GABA-levels. Nevertheless, the gene effect was more significant when the entire metabolite milieu is considered implying that at least in healthy controls at rest, inhibition/excitation balance is functionally relevant. It would be interesting then to follow-up on the genetic effects in populations that are in metabolite disequilibrium, such as for manifested anxiety disorder or aging.

The results are congruent with previous research showing that pgACC has highest levels of GABA/Glu to other mid and caudal ACC subregions (Dou *et al.*, 2013). Receptor density of GABA-B is also high in this region (Palomero-Gallagher, Vogt, *et al.*, 2009) indicating high inhibitory potential of the region. Together these findings predict a relevance of GABAergic transmission for activity regulation in this subregion of the ACC and hence a potential vulnerability to genetic alterations in GABA metabolism.

Next to the receptor fingerprint, there is also behavioural relevance of the regional specificity; the pgACC is node region of automatic affect processing and its hypo- and hyperactivation have been related to affective pathologies (Etkin, Egner and Kalisch, 2011). Increased ALFF was reported in anxious depression (Liu *et al.*, 2015) and both ALFF and ReHo were positively correlated to trait anxiety (Tian *et al.*, 2016). During an emotional task a higher BOLD in the pgACC was also observed in patients with generalized anxiety disorder (Zhao *et al.*, 2007). Following the same region-specific pattern, elevated Glu and diminished GABA levels were found in social anxiety disorder and panic disorder (Phan *et al.*, 2005; Long *et al.*, 2013), proposing a shift in the inhibition/excitation axis in various anxiety profiles. The regional specificity of anxiety phenotypes was also evident for healthy participants: during anticipation of shock there was a connection between higher anxiety score and lower levels of GABA

measured with MRS (Hasler *et al.*, 2010). The inter-individual variability in the metabolite fluctuation to acute stressor illustrates necessity of dynamic neurotransmitter response for successful affect regulation, which could have a genetic component and predispose to anxiety phenotypes.

In accordance with our convergent finding of fMRI and MRS correlates of the GAD65 genotype, GABA levels in the pgACC have been previously associated with negative BOLD signal in the pgACC during emotional processing (Northoff *et al.*, 2007) suggesting a modulation of local neural responses by metabolite measures of inhibition/excitation ratio. Higher negative BOLD response of regions implicated in inwardly directed cognition, such as pgACC, during task execution corresponded to a better control over emotion processing. In the current study, we used resting state fMRI considering that the degree of resting state activity has also been shown to be modulated by local GABA concentrations (Kapogiannis *et al.*, 2013). The relationship between GAD65 genotype and task-induced BOLD signal fluctuations in the pgACC is yet to be determined. Particularly it needs to be shown in future studies, if the higher activity and lower GABA/Glu ratio at rest seen in the AA homozygotes causes a reduced negative BOLD signal in the pgACC during emotional tasks, which is crucial for successful emotion regulation (Grimm *et al.*, 2009). Responsiveness of the inhibition/excitation balance is important not only for the momentary behavioural actions but also for learning (Jocham *et al.*, 2012; Heba *et al.*, 2016). Higher levels of inhibition/excitation balance in the G carriers could thus provide better local regulatory abilities and, given the role of the pgACC, a finer control over limbic inputs.

Based on the regional profiles, no genetic effect was expected or seen in the aMCC, region associated to salience detection and cognitive control rather than affect regulation (Braver *et al.*, 2001; Menon and Uddin, 2010; Hoffstaedter *et al.*, 2014). PgACC and aMCC differ in cortical layer composition with cell types (as outlined in paragraph 1.2.1.) (Vogt *et al.*, 1995; Vogt and Palomero-Gallagher, 2012). Further on, although both GAD65 and GAD67 are expressed in majority of GABAergic neurons, they differ in expression levels and regulation (Esclapez *et al.*, 1994). Hence, the GAD2 rs2236418 is likely to express in a subregion and cell-type specific manner. In fact, GAD65 transcription regulation by BDNF and CREB as well as histone acetylation has been described (Sánchez-Huertas and Rico, 2011; Zhang *et al.*, 2011). The previously reported 6-fold change of GAD65 expression levels for the GAD2

rs2236418 was done in a pancreatic cell line (Boutin *et al.*, 2003), and it needs to be further investigated how this SNP affects gene expression in particular cell types in the pgACC.

In this line, there was no effect of *GAD1* rs769390 on GABA/Glu or GABA/tCr levels despite previous reports of GABA differences in larger mid cingulate area (Marenco *et al.*, 2010). The size and positioning of voxels between the two studies differs, and composition of included cortical layer therefore has significant effects on metabolite levels, at least for GABA.

The importance *GAD65* gene activity for anxiety and stress processing is well documented in animal research (Müller *et al.*, 2014). *GAD65* deficient mice display higher anxiety in behaviour tests and lower levels of GABA in cortico-limbic structures (Stork *et al.*, 2000). These mice are also more vulnerable to develop post-traumatic stress disorder - like behaviour after stress induction (Bergado-Acosta *et al.*, 2008; Sangha *et al.*, 2009). By contrast, heterozygous mice show increased resilience to early life stress due to later maturation of the same circuits (Müller, Çalışkan and Stork, 2015).

Genotype-dependent difference was evident in women (Figure 4.2., Table 4.5.), implying that sex hormones might interact with rs2236418 polymorphism in the promoter region thereby affecting *GAD65* expression (Hudgens *et al.*, 2009), and consequentially levels of GABA. This assumption is in line with previous research on sex and hormonal effects on the GABAergic system (Donner and Lowry, 2013; Seney *et al.*, 2013; Barth, Villringer and Sacher, 2015). It is therefore tempting to imagine that the interaction between the sex hormones and the GABAergic system is the underlying mechanism of higher prevalence rates of anxiety disorders in women (Schuch *et al.*, 2014). In support of this idea, a study connected SNPs in the *GAD1* gene (coding for the second *GAD67* isoform) to panic disorder only in women (Weber *et al.*, 2012). Further evidence for interaction between sex hormones and GABAergic system come from studies on menstrual cycle (De Bondt *et al.*, 2015) or puerperal women (Epperson *et al.*, 2002, 2005), where varying levels of GABA were found dependent on the hormonal status. The sex-related variance of affective disorders and endophenotypes in both preclinical and human research (Blanchard, Griebel and Blanchard, 1995; Zakiniaez *et al.*, 2016) is thus of critical interest, also in terms of genetic polymorphisms. In addition to biological characteristics, it should be considered that women and men employ different emotion strategies, with women

being more internally focused (Moriguchi *et al.*, 2014). In that manner, metabolite profiles of the pgACC, as a region involved in internal evaluation, could be more relevant for women (Colic *et al.*, 2015).

Further, correlation between GABA/Glu ratio and harm avoidance was found also only in women (Figure 4.3). Harm avoidance is closely related to anxiety proneness (Cloninger, Przybeck and Svrakic, 1994) and for healthy populations indicates an endophenotype that might develop to disease phenotype in patient populations (Zohar *et al.*, 2003). Based on the negative correlation, at least for women, higher GABA/Glu ratio could indicate protective mechanisms towards increased anxiety proneness.

The relationship of *GAD2* rs2236418 and behaviour in this study is best accounted for with a mediation model: in women the effect of gene variation on harm avoidance becomes evident only when GABA/Glu is considered (Figure 4.4). This was specific for GABA/Glu since rs-fMRI indices ALFF and ReHo did not significantly mediate the relationship. In the mediation model, it was displayed that that female G carriers potentially have higher harm avoidance scores within the same GABA/Glu levels. This model unravels a complex interplay between genes encoding components of the GABAergic system and sex hormones in anxiety intermediate endophenotypes.

The functional consequences of genetic polymorphisms on behaviour or personality traits should be viewed in terms of their modulatory potential, which can be either protective or disadvantageous contingent on the environment. Following, female G carriers might be less prone to anxiety phenotypes in healthy young participants, which might not hold true for other cases, for example during childhood stress or trauma. It will be interesting to investigate how *GAD65* genotypes differ for clinically relevant changes in affect regulation, including trauma resilience or vulnerability.

4.5. Limitations of Study 2

This multimodal 7T study has some constraints that need to be considered. Due to strict quality examination and exclusion criteria and incomplete behavioural measurements, some genotype/ sex subgroups have modest number of participants. This should be however viewed in the light of a previous meta-analysis of the *COMT* Val108/158Met polymorphism which showed that neuroimaging phenotypes are more strongly associated with gene variants compared to behavioural or disease phenotypes (Mier, Kirsch and Meyer-Lindenberg, 2010). The authors proposed that

this was due to the neural activity and the resulting BOLD response being more closely coupled to the cellular effects of genetic variations. Correspondingly, metabolites might associate to genotype differences even more, whereas the baseline BOLD response might be compensated by other factors such as vascular responsiveness in healthy young participants. The use of high-field 7T made possible to analyse high-resolution data (2 mm acquisition voxel and 4 mm smoothing kernel) and implement a custom MRS sequence to obtain both GABA and Glu (paragraph 2.2.6.) in two voxels, leading to neurochemical measures that should be sufficiently close to the immediate biological genotype effects. Unfortunately, this limited to scanning at a single scanner in Magdeburg, which had requested technical support, instead of using sequence protocols which would allow multisite scanning with replication cohorts. Therefore, the results warrant replication, ideally with genotype groups big enough to detect differences at behavioural level.

Another important consideration is that menstrual cycle of female participants was not controlled for. Functional association between *GAD2* rs2236418, GABA/Glu and harm avoidance was present only in women, which implies modulation of gene activity either through transcription activity or through hormones (Seney *et al.*, 2013). Menstrual cycle can also influence MRS levels (Epperson *et al.*, 2002). Thus, the effect of cycle on GABA/Glu ratio can't be excluded, but a similar distribution of menstrual phases between genotypes in randomly picked sample is presupposed.

4.6. Conclusions of Study 2

The *GAD2* rs2236418 SNP-by-sex interaction modulates GABAergic system in the pgACC and its association to anxiety related trait. The results provide insight to region-specific GABAergic system, and the intermediate phenotypes in women which is relevant for the development of affective pathologies.

Chapter 5. Study 3: Glutamatergic disbalance in pgACC depends on symptom severity in major depressive disorder

This Study investigated glutamatergic markers related to a pathological affective condition- the major depressive disorder (MDD). Relationship to clinical dimensions, symptom severity and anhedonia was tested with moderation models. Medication status in patients was additionally examined.

The following study was first submitted to:

Colic, L., von Duering, F., Denzel, D., Demenescu, L.R., Lord, A., Martens, L., ... & Walter, M. (2018). Rostral anterior cingulate glutamatergic disbalance in major depressive disorder depends on symptom severity. *Submitted to Biological Psychiatry: Cognitive Neuroscience and Neuroimaging.*

5.1. Introduction to Study 3

Major depressive disorder (MDD) is a prevalent and serious affective disorder. Based on evidence from animal models and post-mortem studies, the hypothesis of serotonergic-driven pathology of MDD has been complemented with indications for glutamatergic deficits in depression (Krystal *et al.*, 2002; Sanacora, Treccani and Popoli, 2012; see also paragraph 1.4.). This instigated development of new generation of glutamatergic-based antidepressants. However, part of the patients does not go into remission after glutamate-modulating medication. Thus, proper glutamatergic biomarkers of the MDD disease status connected to treatment response has yet to be confirmed

To resolve neurobiological components of glutamatergic deficits, the glutamatergic system in the MDD was often investigated with MRS. Most of the spectroscopic studies have been conducted with 1.5 or 3T scanners, thus in most of the cases, only the Glx (a joint measure of predominantly glutamate (Glu) and Glutamine (Gln)) (Govindaraju, Young and Maudsley, 2000) was reported. Glx represents total glutamatergic pool that is available both in neurons and astrocytes (Rothman *et al.*, 2003; Patel *et al.*, 2005). In the anterior cingulate cortex (ACC), reduced levels of Glx were found time after time, as illustrated in several meta-analyses (Luykx *et al.*, 2012;

Taylor, 2014; Moriguchi *et al.*, 2018). Yet, some investigations have also found no change of the Glx levels (Taylor, Godlewska, *et al.*, 2012). Using Glx as a measure of glutamatergic system is however inconclusive, since it does not allow for a separate evaluation of Glu and Gln, which may change in opposing directions in pathological conditions (Ramadan, Lin and Stanwell, 2014).

Only few MRS studies examined Glu and Gln levels separately, and the results were so far ambiguous. One meta-analysis recorded Glu decrease in the ACC in MDD, but with a smaller effect size in comparison to the Glx decrease (Luykx *et al.*, 2012). In contrast, other meta-analyses found no changes in the Glu levels (Arnone *et al.*, 2012; Moriguchi *et al.*, 2018). The reviews differed in the methodology and number of included studies, but they nevertheless emphasized that the central finding of the decreased Glx in the MDD might not solely reflect decreased Glu, but also changes in Gln. Using ultra high-field measurements at 7T with an optimized sequence provide chance to investigate separate Glu and Gln levels in the same measurement (Dou *et al.*, 2015) and may help to discern contributions of Glu and Gln to the deviant Glx levels.

When we examine these metabolites separately, the Gln-Glu cycling can be additionally considered. The Gln-Glu cycling between neurons and astrocytes is a dynamic and metabolically costly process, which consumes approximately 70-80% of the total cerebral energy consumption (Pellerin and Magistretti, 1994; Magistretti *et al.*, 1999; Shulman *et al.*, 2004). Shortly described, Glu is released from neurons during synaptic activity to the synaptic cleft. Afterwards, astrocytes uptake the majority of Glu, and to a much smaller extent presynaptic neurons, both through excitatory amino acid transporters (EAAT). Concentration of extracellular Glu is supposed to be low to maintain proper Glu- receptors functioning, as well as to avoid excitotoxicity (Bak, Schousboe and Waagepetersen, 2006). In astrocytes, Glu is converted to Gln by the glutamine synthetase. Gln is a non-neuroactive intermediary of the neurotransmitters recycling (Schousboe *et al.*, 1997; Waagepetersen, Sonnewald and Schousboe, 2003; Bak, Schousboe and Waagepetersen, 2006), and is shuttled back into the excitatory and the inhibitory neurons. There, it is re-converted to Glu via phosphate-activated glutaminase (Bak, Schousboe and Waagepetersen, 2006; Rothman *et al.*, 2011; Hertz, 2013). Glu is approximately twice more abundant than Gln in the human brain (Govindaraju, Young and Maudsley, 2000). Glu is synthesized from Gln and bound to the Gln-Glu cycle (around 80-85%), while the rest

undergoes oxidation process and is replenished by *de novo* synthesis in astrocytes (Shen *et al.*, 1999; Hertz, 2013). Next to neurotransmitter activity, Glu is also part of the cellular metabolism, the tricarboxylic acid cycle, (TCA cycle) (Shen, 2006, 2013; Magistretti and Allaman, 2015), so changes in the glutamatergic transmission might not unequivocally reflect in the overall Glu levels estimated with the ^1H MRS. On the other hand, almost all Gln is limited to the Gln-Glu cycle (Maddock and Buonocore, 2011). The Gln/Glu ratio has been hence suggested as a better index for the cycling process and glutamatergic neurotransmission than either metabolite individually (Théberge *et al.*, 2002, 2003; Öngür *et al.*, 2008; Soeiro-de-Souza *et al.*, 2015).

The equilibrium of cycling and neuron-astroglia interaction is essential for stable brain functioning (Ramadan, Lin and Stanwell, 2013), and some authors have postulated that the Gln-Glu cycle is disbalanced in the MDD (Brennan *et al.*, 2010; Yüksel and Öngür, 2010). Animal models of depression have indeed proved that the metabolite activity and cycling is reduced in the prefrontal cortex (Veeraiah *et al.*, 2014). The source of the disbalance, and consequentially of depressive symptoms and behavior, has been attributed to mechanisms related to both neurons and astrocytes (Duman *et al.*, 2016). Animal models of chronic stress paradigms that lead to depressive-like behavior, show loss in dendritic branching, synaptic strength and general neuronal atrophy in the PFC and hippocampus (Krishnan and Nestler, 2008; Popoli *et al.*, 2012; Duman *et al.*, 2016). Post-mortem studies in MDD patients have also found reduction in glutamatergic neuronal size (Rajkowska *et al.*, 1999) and synaptic markers (Duric *et al.*, 2013).

Coextending, the glutamatergic changes have been also traced to deficits in astroglia (Rajkowska and Stockmeier, 2013). MR studies have recorded prefrontal volume loss in depression, which was accompanied with normal levels of NAA, a neuronal integrity marker, indirectly hinting at astroglia loss (Maddock and Buonocore, 2011). In animal models, toxic glial ablation induced depressive-like behavior, and this, in contrast, was not induced by toxic neuronal ablation (Banasr and Duman, 2008). In human post-mortem studies, reductions in astrocyte number and density (Rajkowska, 2003; Stockmeier and Rajkowska, 2004; Rajkowska and Stockmeier, 2013) have been found. This has been paralleled with reduced levels of astroglia markers (Si *et al.*, 2004), such as mRNA levels of Glu transporters (Choudary *et al.*, 2005), or cingulate glutamine-synthetase positive astrocytes (Bernstein *et al.*, 2015). In sum, these findings have hinted towards astrocyte-related reductions in Glu

uptake and conversion of Glu to Gln, which may eventually lead to downstream Glu reduction (Rajkowska, 2000; Rajkowska and Stockmeier, 2013).

Pharmacological modulation of glutamatergic levels in MDD patients could be ideally used as an indicator of treatment response to medication targeting glutamatergic receptors (Murrrough, Abdallah and Mathew, 2017). For instance, NMDAR antagonist ketamine has induced increase in the Gln/Glu ratio in the pregenual anterior cingulate cortex (pgACC) 24 h after infusion in controls (Li *et al.*, 2017). This increase coincided with the maximal antidepressant response found in patients (Caddy *et al.*, 2014; McGirr *et al.*, 2015). In another earlier study, baseline Glx/Glu (denoting Gln levels) predicted reduction in symptoms severity in patients after ketamine infusion (Salvadore *et al.*, 2012). Moreover, riluzole, another glutamate-modulating medication, increased levels of Gln/Glu ratio also in the pgACC (Brennan *et al.*, 2010). These pharmacological findings in junction with literature, lead to the hypothesis that ketamine and similar medication normalize reduced Gln-Glu cycling in patients, which is reflected in reduced Gln/Glu ratio (Walter, Li and Demenescu, 2014). Notwithstanding, it has not yet been proven that MDD patients in fact have reduced Gln/Glu. This reduction would be particularly expected in a region that is functionally important for MDD deficits, and ideally, ketamine's brain response.

In this study levels of glutamatergic metabolites- Glu and Gln, and Gln/Glu ratio as a surrogate for cycling in MDD were therefore assessed. Based on previous studies, lower levels of Gln/Glu, and, to a potentially different degree, Gln and Glu were expected. The MRS was measured in the pgACC, following anatomically and anatomically defined subregion. This region was involved prominently in hedonic processing (Walter *et al.*, 2008), and differences between MDD and controls in functional (Grimm *et al.*, 2009) or connectivity profiles (Horn *et al.*, 2010; Sheline *et al.*, 2010; Sambataro *et al.*, 2014).

Comprehensive trial of treatment response and remission, Sequenced Treatment Alternatives to Relieve Depression (STAR*D), has shown that baseline clinical features, such as high baseline symptom severity, influence remission rates after selective serotonin reuptake inhibitors (SSRI) treatment (McGrath *et al.*, 2008). Curiously, patients with high baseline severity have also shown stronger differentiation between active treatment and placebo compared to mild and moderate levels (Fournier and DeRubeis, 2010). Therefore, associating baseline neurometabolite levels with clinical features might advance endeavors in determining

best treatment choice, based on the neurobiological and symptomatologic levels. So far, two clinical dimensions of the MDD, severity and anhedonia, have been attributed to different glutamatergic status. For severely depressed groups lower Glx and Glu have been found (Auer *et al.*, 2000; Horn *et al.*, 2010; van Tol *et al.*, 2013), although a direct linear relationship between severity scores on depression questionnaires and Glu has not been meta-analytically confirmed (Yüksel and Öngür, 2010; Moriguchi *et al.*, 2018). Contrary, anhedonia has been connected to Gln, where highly anhedonic patients had lower Gln and no changes in Glu levels (Walter *et al.*, 2009). Thus, to inspect the diversity of the metabolite associations to clinical dimensions, the relationship between glutamatergic metabolites and both the severity and anhedonia levels was evaluated with moderation models, with respective high- and low- symptom severity or anhedonia subgroups.

Lastly, in longitudinal studies, SSRI medication has induced differences in GABA and Glx/tCr levels, in a voxel placed in the occipital cortex (Sanacora *et al.*, 2002; Taylor *et al.*, 2008). Recently, another study has reported an acute increase of GABA, but not Gln/Glu in the pgACC after SSRI medication (Brennan *et al.*, 2017). In addition to pharmacological interventions, an increase of Glx in the frontal cortex after electroconvulsive therapy (Pfleiderer *et al.*, 2003), and a decrease in occipital Glu after cognitive behavioral therapy (Abdallah *et al.*, 2014) have been also noted, but only in the responder subgroups. Therefore, an influence of the medication status on the levels of relevant metabolites in the pgACC was tested. The study included only one, baseline scan, hence only the state influence of the medication intake could be taken into account.

5.2. Study 3 specific materials and methods

5.2.1. Participants

Thirty-two patients with an acute major depressive episode and sex-and-age matched controls were used in the following study. Patients were recruited from the inpatient and outpatient clinic of Psychiatry and Psychotherapy department, Otto von Guericke University Magdeburg (OVGU), Department of Psychosomatics and Psychotherapy, OVGU and Psychiatry and Psychosomatics, AWO Fachkrankenhaus Jerichow. MDD patients were clinically diagnosed according to the ICD-10-criteria (Dilling *et al.*, 2011). Exclusion criteria for MDD patients were neurological conditions (e.g. epilepsy) or other major medical illness. Other exclusion criteria were also any other

psychiatric disorder and a history of substance abuse or dependence. MDD patients were furthermore evaluated with clinical questionnaires. German version of the 17-item Hamilton depression scale (HAMD) was used to measure symptom severity (Hamilton, 1960), and German version of the Snaith-Hamilton pleasure scale (SHAPS) (Snaith, Hamilton, Morley, Humayan, 1995; Franz *et al.*, 1998) was used to determine the level of anhedonia. Twenty-three patients were under medication during the study. Full medication list (based on the Neuroscience based Nomenclature (NbN) app) is in Table S5. 1.

Healthy controls were recruited via public advertisement. Exclusion criteria for controls were any prior neurological diseases or major illness. Controls were moreover medication free (excluding contraception pills). Controls were evaluated with the German Version 5.0 of the M.I.N.I. Mini International Neuropsychiatric Interview (Sheehan *et al.*, 1998; Ackenheil *et al.*, 1999), to ensure the absence of psychiatric conditions according to DSM-IV. Thirty-two participants were included in statistical analysis matching the MDD patient group for sex (19 women) and age (33.09 ± 8.24).

Further exclusion criteria for both groups were MRI contraindications like metallic implants. Handedness was measured with the short form of the Edinburgh Handedness Inventory (Oldfield, 1971). All participants were right-handed, except one MDD patient. Medical history and examination were done and confirmed by the study physician. The study was approved by the Institutional Review Board of Otto von Guericke University of Magdeburg, Faculty of Medicine. The study was conducted in accordance with the Declaration of Helsinki (World Medical Association, 2002) and all participants gave written informed consent.

5.2.2. 7T MRS and rs-fMRI acquisition

The MRS data were obtained on the 7T scanner with a 32-channel head array coil (Siemens Healthineers, Erlangen, Germany). Details of the acquisition and preprocessing can be found in General methods 2.1.2., 2.1.3., 2.2.6. and 2.3.4.

In short, MRS was obtained with the STEAM sequence within a voxel placed in the pgACC. Gln, Glu, GABA and tCr were quantified with the LCModel. Gln/Glu, Gln/tCr, Glu/tCr and GABA/tCr were used for the analyses. Moreover, the gray matter partial volume of the individual voxel was calculated as the segmented gray matter divided by the total volume within voxels and was used as a co-variate in the analyses.

5.2.3. Statistical analyses

Due to the exclusion criteria and availability of data for the clinical questionnaires, number of participants per metabolite or MDD subgroups differed between analyses.

All variables were checked for normality with the Kolmogorov-Smirnov test ($p > .05$). Additionally, MRS data outliers were excluded based on the 1.5 interquartile range thresholds.

First, equality of variances for each metabolite ratio was measured using robust Levene's non-parametric test.

Group differences were calculated for Gln/Glu, Gln/tCr, Glu/tCr and GABA/tCr. Analysis of co-variance was used, with gray matter volume partial volume as co-variate. The effective individual significance threshold was adjusted for interdependence of metabolites across groups (joint mean $|r = .390|$), and was thus set at $\alpha < .0215$, to reach a family wise correction (FWE) for a target $\alpha < .05$ by four tests (Sankoh, Huque and Dubey, 1997).

Afterwards, the metabolites that showed difference to the healthy control group were assessed in their relation to clinical dimensions severity and anhedonia. Moderation analyses were conducted with Gln/Glu ratio as a predictor variable, HAMD or SHAPS as outcome variables, and subgroups as moderator variables. Patient subgroups were defined as moderate-severe and mild depression using HAMD 17-item scale with a clinical cutoff of ≥ 18 HAMD (Zimmerman, Posternak and Chelminski, 2002). For SHAPS there is no clinical cutoff to distinguish highly anhedonic patients, so to equalize the number of participants for each subgroup, a cutoff of ≥ 4 was applied. Gray matter partial volume was used as a covariate. Statistical threshold was set at $p < .025$, FWE corrected. HAMD and SHAPS did not correlate significantly for this sample ($\rho(26) = .03$, $p = .87$), and the subgroups did not overlap in participant composition ($\chi^2(1) = .49$, $p = .48$). Follow-up moderation analyses were done for the Gln/tCr and Glu/tCr to dissociate metabolite specificity for clinical dimensions.

Ensuing the moderation analysis for severity, MDD patients were furthermore divided to incorporate several intermediate severity subgroups based on APA's Handbook of Psychiatric Measures (Rush *et al.*, 2006; Fournier and DeRubeis, 2010). Subgroups were mild depression (8-13; $n = 10$), moderate (14-18; $n = 14$) and severe & very severe depression (> 19 ; $n = 8$, three patients were very severe ≥ 23). Four patients had score < 8 and were added to the mild depression subgroup.

Subgroup differences to controls were tested also with an ANCOVA, with a FWE corrected $p < .05$, resulting in a $p < .0297$ (mean r across groups $| = .347|$).

Finally, medication status was tested with an ANCOVA for the levels of Gln/Glu, Gln/tCr and Glu/tCr. Same FWE corrected threshold $p < .0297$ was applied.

Tests were done with SPSS (IBM SPSS Statistics for Windows, Version 24. Armonk, NY, USA). SPSS extension PROCESS v2.15 (Preacher and Hayes, 2004; Hayes, 2013) was used to calculate moderations. Graphs were created with Prism 6 (GraphPad Software Inc., La Jolla, USA).

5.3. Results Study 3

5.3.1. Demographics

There were no significant group differences with respect to demographic variables. Age was however trend-wise increased in the MDD. As expected, MDD and healthy control group differed in clinical questionnaires HAMD and SHAPS (Table 5.1.)

Table 5.1. Demographic and clinical properties of MDD and control participants.

Data is presented in frequencies or mean \pm SD.

	MDD	Controls	Statistics
Sex (F/M)	19/ 13	19/ 13	
Age	4.88 \pm 13.66	33.09 \pm 8.24	$U = 383.5, p = .084^{\#}$
BMI (n= 29/29)	25.33 \pm 5.49	23.38 \pm 2.80	$U = 358, p = .33$
Smoking (no/yes/quitted)	13 / 11 / 6	11 / 13 / 8	$\chi^2(2) = .56, p = .76$
HAMD (n= 32/31)	14.97 \pm 6.21	.55 \pm .81	$U = 8.5, p < .001 ***$
SHAPS (n= 30/28)	4.57 \pm 3.81	.37 \pm .81	$U = 97.5, p < .001 ***$
pgACC gm (%) (n= 29/32)	.601 \pm .077	.596 \pm .078	$t(59) = -.25, p = .81$

Nu of participants with available data is shown in brackets: *** $p < .001$, # $.1 > p > .05$

5.3.2. Variance of the pgACC metabolites is equal between the MDD and the healthy control group

There were no significant differences between the MDD and the healthy control group in the variance of the pgACC metabolites. The results were: Gln/Glu, $Welch(1,5.895) = .62$, $p = .43$; Gln/tCr, $Welch(1, 47.351) = 1.65$, $p = .21$; Glu/tCr, $Welch(1,53.755) = .47$, $p = .50$; GABA/tCr, $Welch(1, 46.846) < .001$, $p = .98$.

5.3.3. Gln/Glu ratio was increased in the MDD

MDD patients had higher levels of Gln/Glu ($F(2, 47) = 11.19$, $p = .002$, $\eta^2 = .199$) (Figure 5.1.). Higher Gln/tCr levels ($F(2, 48) = 5.85$, $p = .02$, $\eta^2 = .113$) and lower Glu/tCr ($F(2,53) = 4.78$, $p = .033$, $\eta^2 = .086$) in MDD patients were also found. The Glu/tCr decrease however was not significant on a corrected threshold ($p < .0215$). There were no differences in GABA/tCr levels ($F(2,45) = .97$, $p = .33$, $\eta^2 = .022$).

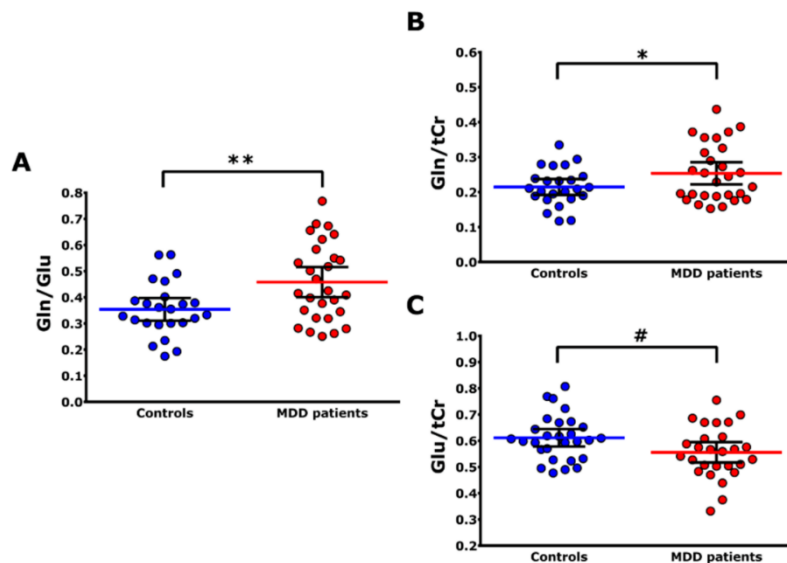


Figure 5.1. Main effect of the MDD on glutamatergic metabolites.

A Gln/Glu ** $p < .01$; **B** Gln/tCr * $p < .05$; **C** Glu/tCr # $.1 < p < .05$, adjusted FWE corrected. Data points are not corrected for gray matter partial volume and are presented as mean \pm 95% CI.

5.3.4. Severity displays a moderated relationship with Gln/Glu levels in the pgACC

HAMD subgroups differed in age (Table S5. 2.). Primary moderation analysis for the relationship between Gln/Glu and HAMD values showed a significant interaction effect on a corrected threshold (total model summary: $R^2 = .646$, $F(4,21) = 8.29$, $p = .0004$; R^2 increase = $.063$, $F(1,21) = 6.38$, $p = .020$). Conditional effects were trend level for the subgroup $HAMD < 18$ ($t = -1.86$, $p = .077$) and non-significant for the $HAMD > 18$ ($t = 1.64$, $p = .12$) (Figure 5.2.A).

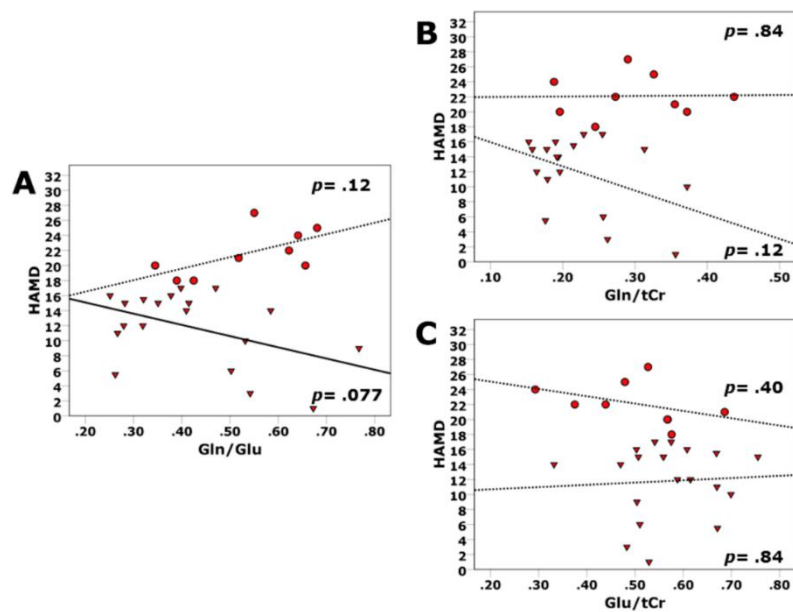


Figure 5.2. Moderation by HAMD groups between HAMD scores and metabolites.

Moderation was most observable for Gln/Glu (interaction is $* p < .025$); B follow-up interaction effect for Gln/tCr and C for Glu/tCr was not significant $^{ns} p > .1$. Values for conditional effects are written on the slopes. Data points are not corrected for gray matter partial volume and are presented as mean \pm 95% CI.

Follow-up moderations revealed that the interaction pattern was partially reflected for the Gln/tCr levels, but the interaction or conditional effects were not significant (total model summary: $R^2 = .659$, $F(4,20) = 7.85$, $p = .006$; interaction R^2 increase = $.042$, $F(1,20) = 1.58$, $p = .22$; conditional $HAMD < 18$ $t = -1.63$, $p = .12$, conditional $HAMD > 18$ $t = .21$, $p = .84$) (Figure 5.2.B). The moderation was also not significant for the Glu/tCr (total model summary: $R^2 = .568$, $F(4,21) = 9.27$, $p = .0002$; interaction R^2 increase = $.006$, $F(1,21) = .64$, $p = .43$; conditional $HAMD < 18$ $t = .21$, $p = .84$, conditional $HAMD > 18$ $t = -.86$, $p = .40$) (Figure 5.2.C). The subsequent analyses

displayed a main effect of group for Gln/Glu ($F(4,46)= 7.81, p < .001, \eta^2 = .358$), with a *post hoc* differences between controls and mild ($p = .03$) and severe subgroups ($p = .002$). There were also differences between the moderate and severe ($p = .012$) (Figure 5.3.A). The pattern was mirrored in the Gln/tCr levels (main effect $F(4,48)= 7.11, p = .001, \eta^2 = .327$), with the distinction between the severe subgroup and controls ($p = .001$) and between the severe and moderate subgroups ($p = .003$) (Figure 5.3.B). For the Glu/tCr the effect was not presented on a corrected threshold (main effect $F(4,51)= 2.60, p = .063, \eta^2 = .142$). Moreover, it had a more gradual linear pattern which was underscored with a trend wise difference between the severe subgroup and controls only ($p = .087$) (Figure 5.3.C).

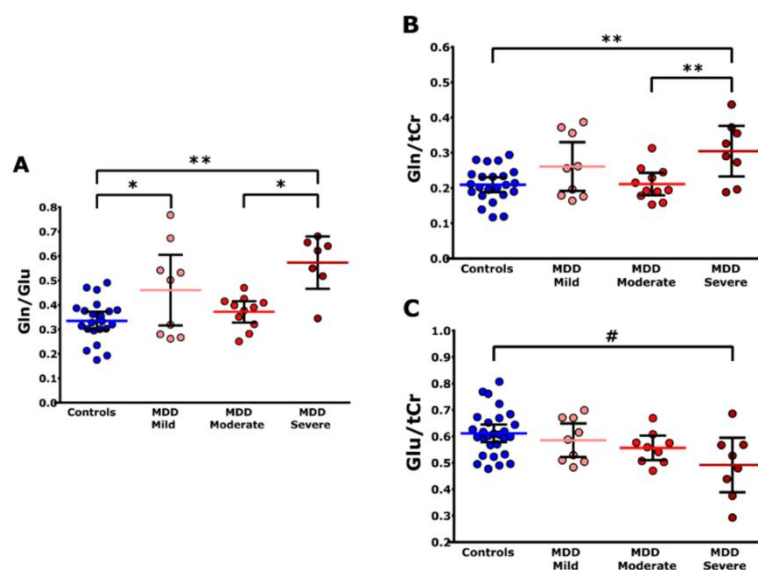


Figure 5.3. Influence of the MDD intermediate severity groups.

A Gln/Glu moderate subgroup differed from severe cases as well as for B Gln/tCr; C Glu/tCr only severe cases differed from controls; ** $p < .01$, * $p < .05$, # $.1 < p < .05$, *post hoc* FWE corrected. Data points are not corrected for gray matter partial volume and are presented as mean \pm 95% CI.

5.3.5. Glutamine levels drive the metabolite associations to anhedonia

There were no differences in demographic properties between SHAPS subgroups (Table S5. 3.). On an uncorrected threshold, main moderation analysis showed a significant interaction effect for Gln/Glu (total model summary: $R^2 = .866, F(4,18)= 15.67, p < .001$; interaction R^2 increase = $.070, F(1,18)= 5.66, p = .029$). The conditional effect was trend wise significant for the subgroup $SHAPS < 4$ ($t = -1.95, p = .068$), but not for $SHAPS > 4$ ($t = 1.38, p = .19$) (Figure 5.4.A). Similar uncorrected

values were present for the Gln/tCr (total model summary: $R^2 = .884$, $F(4,17) = 16.62$, $p < .001$; interaction R^2 increase = $.090$, $F(1, 17) = 5.13$, $p = .04$; trend wise conditional effect for the SHAPS < 4, $t = -2.06$, $p = .055$; but not significant for the SHAPS > 4 $t = 1.31$, $p = .21$) (Figure 5.4.B). In contrast, there were no significant effects for the Glu/tCr (total model summary: $R^2 = .795$, $F(4,16) = 11.67$, $p = .0001$, interaction R^2 increase < $.001$, $F(1, 16) < .001$, $p = .99$; conditional effect for the SHAPS < 4, $t = -.15$, $p = .88$, conditional effect for the SHAPS > 4, $t = -.20$, $p = .84$) (Figure 5.4.C).

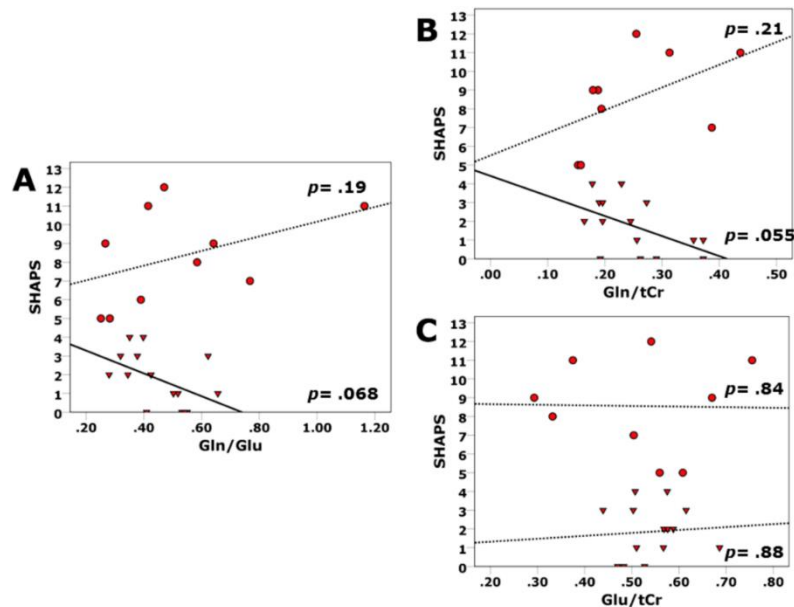


Figure 5.4. Moderation by SHAPS groups between SHAPS scores and metabolites.

It was observable in A Gln/Glu (interaction is * $p < .05$); B and Gln/tCr (interaction is * $p < .05$); C but not for Glu/tCr ns $p > .5$. Values for conditional effects are written on the slopes. Data points are not corrected for gray matter partial volume and are presented as mean \pm 95% CI.

5.3.6. Medication use does not affect metabolite levels in the pgACC

Medication groups displayed some demographic differences, for example in BMI ($U = 24$, $p = .002$) (Table S5. 4.).

Again, a significant main effect of group was observed for the Gln/Glu ratio ($F(3,47) = 6.51$, $p = .003$, $\eta^2 = .228$), for which both medication groups showed difference to the healthy control group (no medication to controls $p = .006$, yes medication to controls $p = .047$), but not between themselves ($p = .62$, all *post hoc* tests are Bonferroni corrected, Figure 5.5.A). Gln/tCr and Glu/tCr did were not significantly different on a

corrected threshold (Gln/tCr: main effect of the group, $F(3,48) = 3.32, p = .045, \eta^2 = .128$, no medication to controls $p = .075$, yes medication to controls $p = .24$, no medication to yes medication $p > .99$, Figure 5.5.B; Glu/tCr: main effect of the group, $F(3,53) = 2.34, p = .11, \eta^2 = .086$, no medication to controls $p = .46$, yes medication to controls $p = .17$, no medication to yes medication $p > .99$, Figure 5.5.C).

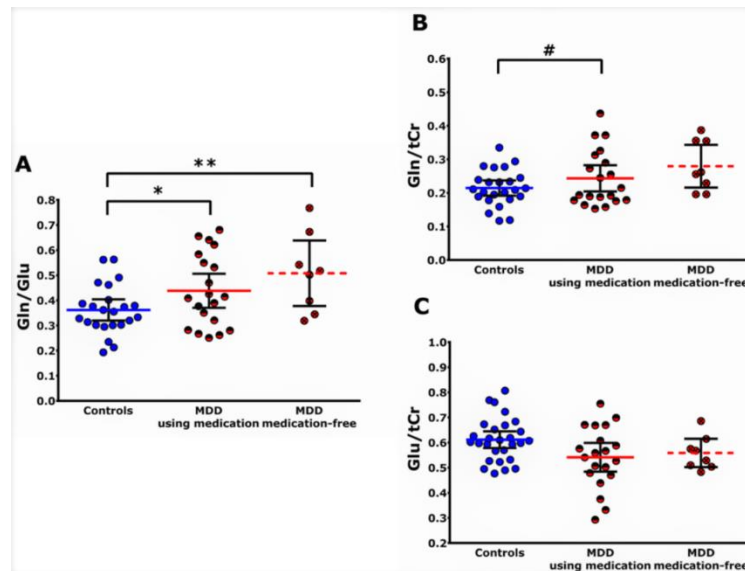


Figure 5.5. Effect of the medication on glutamatergic metabolites.

There was a main effect of group for the A Gln/Glu ratio ($p = .003$), with a difference between controls and both no medication and medication, but there was no difference between medication status groups. B main group effect was not significant on a corrected threshold for B Gln/tCr ($p = .045$); and C for Glu/tCr ($p = .11$); *Post hoc* ** $p < .01$, * $p < .05$, # $.1 > p > .05$. Data points are not corrected for gray matter partial volume and are presented as mean \pm 95% CI.

5.4. Discussion Study 3 MDD

In an age and sex matched sample, there was a general increase in the pgACC Gln/Glu ratio in MDD patients. This increase was driven by higher Gln/tCr and marginally lower Glu/tCr (Figure 5.1.). The MDD group showed a variation between Gln/Glu and symptom severity, measured with HAMD (Figure 5.2., Figure 5.3.). Moreover, on an uncorrected level, SHAPS subgroups moderated relationship between the Gln/Glu levels and anhedonia, which was driven solely by the Gln/tCr (Figure 5.4.). Lastly, medication intake did not significantly affect glutamatergic status in the pgACC (Figure 5.5.).

The increase in the Gln/Glu ratio, and Gln/tCr was unexpected, since literature postulated lower glutamatergic pool (reflected via Glx) and reduced conversion rates (reflected via Gln/Glu ratio) (Yüksel and Öngür, 2010; Arnone *et al.*, 2012; Luykx *et al.*, 2012; Moriguchi *et al.*, 2018). In addition to these results, recently another 7T study also reported an increase, instead of a decrease, in Gln levels in the MDD patients, significantly in putamen and trend-wise in the ACC (Godlewska *et al.*, 2017).

Previous studies have indicated that riluzole and ketamine infusions increase Gln or Gln/Glu in controls in the ventral ACC (Rowland *et al.*, 2005; Brennan *et al.*, 2010; Li *et al.*, 2017; Abdallah *et al.*, 2018), and consequentially it was thought that the antidepressant effect observed in patients comes from correcting deviant baseline Gln/Glu levels. The presented results however contradict the assumptions of favorable properties of glutamate-modulating antidepressant medication. In support of a more complex mechanisms, recent study in a large patient cohort indicated that ketamine might not affect glutamatergic levels in MDD in ventral part of the ACC after all (Evans, Lally, *et al.*, 2018).

The glutamatergic deficits in MDD have been attributed to astrocyte deficits (Rajkowska and Stockmeier, 2013). Post-mortem studies of human brain samples have reported reduced astrocyte density (Miguel-Hidalgo and Rajkowska, 2003; Si *et al.*, 2004; Khundakar and Thomas, 2009), sometimes with an increase in astrocyte size. Moreover, reduced levels of mRNA of proteins involved in Glu astrocyte uptake (Choudary *et al.*, 2005) and other astrocyte-related protein markers have been also found. Authors discussed their observation to primarily represent an adaptation to a lower level of synaptic glutamate although the sequential order of deficits remains to be proven. Importantly, reduced density of Gln synthetase-positive astrocytes has been detected in the ACC in unipolar depression (Bernstein *et al.*, 2015), confirming regional coupling of spectroscopy and fMRI findings with pathological ones.

The increased Gln/Glu can be viewed as an indicator of shifted Gln-Glu cycling following a different pathomechanism than previously thought. As a speculative interpretation, we can think that marginal decrease in Glu/tCr might mirror slow decrease in integrity of glutamatergic synapses and neuronal atrophy usually seen in animal models of depression (Popoli *et al.*, 2012; Duman *et al.*, 2016). This might lead to glial hypertrophy (Rajkowska *et al.*, 2005) and compensatory mechanism of increase in Gln to Glu astrocyte conversion and Gln/tCr (Soeiro-de-Souza *et al.*, 2015).

Alternative speculation for the glutamatergic disbalance in the MDD would be by the cause of metabolite activity. Glutamatergic system and energy metabolism in the brain are coupled via astrocyte-mediate functions (Bak, Schousboe and Waagepetersen, 2006; Shen, 2013). Moreover, Gln-Glu cycle is energetically demanding (Magistretti *et al.*, 1999), and disturbances in it could be an outcome of a shifted energy metabolism (Magistretti and Allaman, 2015). PET studies have demonstrated that MDD patients have lower glucose metabolism in the PFC-ACC brain areas (Mayberg, 1997; Drevets, 2000). In the case of decreased glucose metabolism, Glu would be used as an energy (Shen, 2013). For example, a study investigated short-term consequences of fasting in healthy participants has found a decrease in Glx levels (Ding *et al.*, 2018). Notably, the level of decrease was region specific, where the frontal lobe underwent the most dramatic changes. This highlights that the medial and frontal lobe are vulnerable to even short-term energetic stress. Studies measuring energetic capacity in MDD via ¹³P MRS have found a decrease in metabolite measures in the occipital (Abdallah *et al.*, 2014) and prefrontal cortex (Volz *et al.*, 1998), as well as in the PFC of animal models of depression (Veeraiah *et al.*, 2014). Moreover, increased levels of lactate, metabolite indicating a shift to anaerobic metabolism, have been found in the ventral ACC (Ernst *et al.*, 2017). Lactate levels furthermore correlated to symptom severity (Ernst *et al.*, 2017). In sum, these results indicate that there are general metabolite shifts in the MDD, which are more prominent in regions directly related to the disease manifestation and the functional response.

Symptom severity subgroups showed differential neurometabolite profile compared to controls; severe and mild subgroup showed increased Gln/Glu, while moderate cases were similar to controls. The moderation results might also explain heterogeneity of Glx and Glu reports, and their relationship to symptom severity or other clinical measures. Depending on the inclusion range of a study, one would then expect, *i.e.* for Gln/tCr no changes for the case of moderate depression or an increase for the severe cases. The exact pathological mechanisms of glutamatergic differentiation of symptom severity need to be further tested, ideally with larger, matched subgroups. Nevertheless, differential metabolite patterns can be seen already between mild and severe cases. Both subgroups show an increase in Gln/Glu ratio, but, compared to controls, only the severe subgroup shows individually an increase in Gln/tCr and a decrease in Glu/tCr, which has been furthermore identified

for chronic disease states (Auer *et al.*, 2000; Théberge *et al.*, 2003; Portella *et al.*, 2011). Occipital Glu levels have been also correlated negatively with number of episodes (Abdallah *et al.*, 2014) supporting the idea that duration of the disease influences magnitude of Glu deficits. Moreover, the severe subgroup was also older (Table S5. 2.) and more medicated (Table S5. 4.). The results would thus match earlier suggestion of the MDD disease progression (Rajkowska, 2000; Rajkowska and Stockmeier, 2013); in the younger participants astroglia or cycling deficits are noticeable, but only in the older, chronically diseased participants we see neuronal atrophy and prominent lower Glu. Only in older participants, this is paired with, possibly medication induced, astroglia overcompensation (Rajkowska, 2000).

In this sample there was no correlation between HAMD and SHAPS or participant overlap between subgroups. Notwithstanding, the ratio Gln/Glu seems to reflect both clinical dimensions (Figure 5.2A, Figure 5.4A). However, in anhedonia, the interaction was driven by the Gln/tCr and more strongly for the low-anhedonia group (Figure 5.4B), while there was no relationship to Glu/tCr at all (Figure 5.4C). This diverges to symptoms severity, where Gln/tCr and Glu/tCr contributed to a similar extent (Figure 5.2B& C). Relationship between anhedonia and Gln has been previously suggested though in an opposite direction. Reduced levels of Gln/tCr were found only in highly anhedonic subgroup of patients, which also had no changes in Glu levels (Walter *et al.*, 2009). Here, conversely, low-anhedonia subgroup showed a trend level negative relationship between Gln/tCr and SHAPS, and a non-significant positive slope for the clinically relevant subgroup (>4) in the moderation analysis. Important differences between the two studies is the use of different anhedonia questionnaires (BDI items versus SHAPS), which tap into distinctive disease categories (amotivation versus true anhedonia) (Ballard *et al.*, 2018). Another possible source for discrepancy is different voxel size and position; Walter *et al.*, (Walter *et al.*, 2009) voxel was 17.5 mL and spanned histoarchitectonically different regions: pgACC and larger ventromedial prefrontal cortex (vmPFC) (Brodmann areas 24 and 32). In comparison, voxel size in this investigation was 4 mL and was placed in a histoarchitectonically defined subregion of the ACC, based on the notion that pgACC and adjacent prefrontal cortical area show distinct histological and connectivity profiles (Palomero-Gallagher *et al.*, 2018).

Early spectroscopic studies with modest number of participants have shown GABA differences in unipolar depression in occipital cortex (Sanacora *et al.*, 2002; Price *et*

al., 2009), as well as an increase in GABA levels after SSRI treatment (Sanacora *et al.*, 2002). On the contrary and in agreement with our results, most studies of MDD have reported no change in the GABA levels in frontal brain regions (for meta-analysis see Romeo *et al.*, 2018). This might hint that the ACC GABA-related deficits in MDD are less prominent than for other conditions like premenstrual dysphoria disorder (Liu *et al.*, 2015) or anxiety (Ham *et al.*, 2007), or traits such as harm avoidance from Study 2 (Colic *et al.*, 2018).

Medication status did not significantly influence levels of glutamatergic metabolites, speaking for a disease marker which is not strongly affected by current medication intake, at least in the pgACC. The non-medicated group had however slightly higher levels of Gln/Glu than the medicated group. This importantly shows that the results are not an artefact of medication use. In this case, medication could be even minimizing group differences. Additionally, medicated patients had higher HAMD and SHAPS scores (Table S5. 4.). Therefore, a reduction of the group difference in glutamatergic metabolites cannot be directly interpreted in terms of successfully counteracting depressive symptoms at the time of investigation.

5.5. Limitations of Study 3

The main limitation of the study is related to study design which led to different subgroup sizes depending on the respective clinical scale. Thus, the results of the moderation by the severity subgroups should be interpreted with caution and replicated in an ideally large sample with equal group sizes for the respective cut-offs. There was a difference in BMI between medicated versus un-medicated patients and controls, but it is unlikely that BMI is driving the metabolite differences, since the values of the healthy control group are in the middle range for BMI but are lowest for Gln/Glu (Table S5. 4., Figure 5.5.).

5.6. Conclusions of Study 3

Results confirm earlier accounts of disbalance in the glutamatergic system in a key region of MDD. In contrast to earlier predictions of general MDD pathological changes, the Gln/Glu ratio was increased, with a following increase in Gln/tCr and a slight decrease in Glu/tCr. They moreover conflict with previous hypotheses on mode of action of new glutamatergic antidepressants like ketamine. Imperatively, we must acknowledge that different pathomechanisms are in play for different patient subgroups characterized by symptom severity. This follows the earlier descriptions of

the STAR*D trial, which already hinted that symptom severity might predicts differential treatment response, rotted probably in neurobiological substrate. Further on, the lack of group difference to controls for the moderate subgroup could help to interpret former conflicting results and should be taken into account during stratification of future patient samples.

Chapter 6. Study 4: Ketamine infusion in healthy participants induces delayed changes in glutamatergic levels in the pgACC, peripheral blood markers and long-term safety outcomes

In this last study, an experimental pharmacological intervention was applied to examine multilevel neuro-biological response. Ketamine was chosen as a pharmacological agent. Since the exact mechanisms of antidepressant action are still unclear, the study population was healthy young participants, and acute, delayed, and long-term safety parameters were measured.

First, using MRS, glutamatergic levels were assessed in the pgACC. Secondly, there is a growing necessity to develop workable peripheral biomarkers that reflect changes in the CNS and can be further used for personalized treatment strategies. This motivated to examine peripheral biomarkers of synaptic plasticity, namely Acetyl-Tubulin in connection to glutamatergic changes. Thirdly, ketamine is still considered as an experimental drug. Therefore, it necessitates to be validated for safety parameters, both acute, such as blood pressure and dissociation, and sustained, for example blood parameters.

Parts of the following study were first published in:

Colic, L., Woelfer, M., Colic, M., Leutritz, A. L., Liebe, T., Fensky, L., ... & Isermann, B. (2018). Delayed increase of thrombocyte levels after a single sub-anesthetic dose of ketamine-A randomized trial. *European Neuropsychopharmacology*.

&

Colic, L., McDonnell, C., Li, M., Woelfer, M., Liebe, T., Kretschmar, M., Speck, O., ...& Walter, M. (2018). Neuronal glutamatergic changes and peripheral markers of cytoskeleton dynamics change synchronically 24h after sub-anaesthetic dose of ketamine in healthy participants. *Accepted in Behavioural Brain Research*

Other relevant publication for this chapter is:

Li, M., Demenescu, L. R., Colic, L., Metzger, C. D., Heinze, H. J., Steiner, J., ... & Walter, M. (2017). Temporal dynamics of antidepressant ketamine effects on glutamine cycling follow regional fingerprints of AMPAR and NMDAR densities. *Neuropsychopharmacology*, 42(6), 1201.

6.1. Introduction

Treatment with single sub-anaesthetic doses of ketamine elicits rapid and robust antidepressant effects in research and clinical settings (Caddy *et al.*, 2014; Zarate and Machado-Vieira, 2017) and improves depression - like behavioural measures in preclinical animal models (Krystal, Sanacora and Duman, 2013; Saland, Duclot and Kabbaj, 2017). Ketamine is considered in cases where antidepressant treatments targeting serotonin, norepinephrine or dopamine pathway do not show efficacy or in critical moments such as for acute suicidality (Bartoli *et al.*, 2017).

Ketamine's mechanisms of action are not fully grasped, but they involve modulation of the glutamatergic system and improvement in synaptic plasticity, specifically in regions important for affect regulation (Serafini *et al.*, 2014; Murrough, Abdallah and Mathew, 2017). In short, ketamine blocks the NMDAR, but at the same time, paradoxically, upregulates other type of glutamate receptors, AMPAR. Recently, a spectroscopy study has detected a regional and temporal specific increase in the Gln/Glu ratio; it was found in the pgACC, the subregion that is rich in AMPAR (Palomero-Gallagher *et al.*, 2009), while no effects were found in the aMCC (Li *et al.*, 2017). The temporal specificity of significant glutamatergic changes also overlaps with the peak clinical effect in the MDD (Caddy *et al.*, 2014), as the increase was found 24 h but not 1 h after infusion.

Glutamatergic changes are thought to activate downstream neuronal machinery and promotes synaptic plasticity (Abdallah, Sanacora, *et al.*, 2018). Enhancement of synaptic plasticity comprises of synaptic activation and remodeling, done in part via microtubule reorganization (Conde and Cáceres, 2009; Hoogenraad and Bradke, 2009). Microtubules are polymers of α - and β -tubulin, and they form structural, but highly dynamic part of the cytoskeleton (Desai and Mitchison, 1997). Regulation of microtubule activity is measured with post-translational modifications (PTMs) of α -tubulin (Janke and Bulinski, 2011). There are several forms of alpha-tubulin, and acetylated α -tubulin (Acet-Tub) is a PTM which associates to less dynamic microtubules (Janke and Kneussel, 2010; Song and Brady, 2015). Increase in Acet-

Tub negatively impact the neurite and growth cone formation in vitro (Dent and Gertler, 2003). In animal models of depression, increased levels of hippocampal Acet-Tub were found pointing towards decreased microtubule dynamics and possible dysfunctions in synaptic plasticity (Bianchi, Hagan and Heidebreder, 2005; Yang *et al.*, 2009; Bianchi and Baulieu, 2012). Function of microtubules was recovered by administration of antidepressant medication, SSRI (Bianchi *et al.*, 2009).

Microtubular dynamics, namely levels of Acet-Tub measured peripherally in patients (in blood or CSF) may be considered as a potential disease biomarker (O'Driscolle, Bianchi, unpublished data). Moreover, total expression of α -tubulin in rat plasma was modulated by neurotoxic agents such as acrylamide (Yi *et al.*, 2006). The variation in peripheral tubulin dynamics was thus presumed to reflect CNS changes. The peripheral readout of microtubular dynamics might then also indicate propensity of plasticity, especially if it is connected to CNS measures, and serve as a pharmacological marker.

Importantly, it must be noted that ketamine infusions also affect blood cells and protein markers as shown in animal models (Clarke *et al.*, 2017) and human samples (Kiraly *et al.*, 2017). PMTs of α -tubulin are also involved in peripheral cell activation and signal transduction after stimulation of leukocytes (Robinson and Vandr e, 1995) and thrombocytes (Aslan *et al.*, 2013). Therefore, any observed changes could also stand for dynamics of peripheral cells.

The acute side effects, which are measured during or shortly after infusion, have been, for the most part, thoroughly screened. The prominent ones are the increase in blood pressure and heart rate (Liebe *et al.*, 2017), general health condition (nausea, dizziness, fatigue) and dissociative and psychomimetic symptoms (for a review see Short *et al.*, 2018).

Ketamine antidepressant effect is rapid, but lasts only up to a week, so clinical future implies repeated infusions or intranasal administration. So far only a handful of studies investigated repeated infusion in MDD patients (for review see Iadarola *et al.*, 2015). Therefore, longer-term acute side effects and safety of ketamine treatment are not yet established (Short *et al.*, 2018).

In higher doses ketamine is also used as a recreational drug, and some long term medical and psychological consequences of such (ab)use can guide possible outcomes also in repeated clinical administration. These changes include: cortical thickness

changes (Liao *et al.*, 2011; Wang *et al.*, 2013), cognitive decline and lower well-being (Morgan, Muetzelfeldt and Curran, 2010) and renal and urinary tract problems (Chu *et al.*, 2008; Selby *et al.*, 2008). A case study of ketamine abusers in emergency department reported changes in haematological parameters (Ng *et al.*, 2010). These prolonged effects, although probably confounded with factors such multiple drug use, still provide valuable insight to possible safety risks which should be monitored during multiple ketamine infusions, especially in patients with previous medical conditions, such as coronary diseases or stroke.

Another line of evidence of ketamine active interaction with peripheral system comes from veterinary sciences. Studies in non-human primates have revealed modifications in haematological parameters after ketamine: an acute drop in leukocyte and thrombocyte number immediately after infusion (Ündar *et al.*, 2004; Roviroso-Hernández *et al.*, 2011), but an increase in thrombocytes after repeated anaesthesia with ketamine (Lugo-Roman *et al.*, 2010). Curiously, ketamine analogues were proposed as a treatment for thrombocytopenia (Kogan and Somers, 1993).

Studies in human patients are unfortunately scarce and limited in size. Moreover, they are often confounded with factors such as such as comorbidities, and medication. Thus, to thoroughly investigate modes of action of active doses of ketamine investigations in healthy participants are necessary. Further on, these investigations provide opportunity to detect peripheral biomarkers, which could be subsequently used for stratifying treatment options. Finally, assessment of safety parameters is required for the standardized clinical practice. Therefore, the following hypothesis were generated for several levels of investigation;

To investigate the individual variations and homogeneity of a healthy study population, a linear regression analysis of demographic factors on baseline measurements was conducted. For example, age and sex differences were reported for transferrin, with women having higher levels baseline levels (Ritchie *et al.*, 2004). Moreover, blood measures such as erythrocyte and thrombocyte were also shown to differ between sexes. These parameters were then hypothesized to display the same effect in our healthy cohort. For Glu/tCr and Acet-Tub (/TRF) so far there were no observations of sex specificity thus we did not expect significant effects. Considering reported behavioral and molecular differences between male and female animals (Saland, Duclot and Kabbaj, 2017) and humans (Zarate *et al.*, 2012), sex was added as

a co-variate of interest, which was further corroborated by the results from baseline regression analysis.

To measure central glutamatergic system, changes in the Glu/tCr levels were assessed in the pgACC 24 h after infusion. Time point and region were targeted based on the previous accounts of Li *et al.*, (Li *et al.*, 2017), which included a subsample of the participants analyzed here. Glu/tCr seems to fall below the baseline 24 h after the infusion, which is in stark contrast to a hyper-acute glutamatergic surge (Stone *et al.*, 2012; Chowdhury *et al.*, 2017).

In parallel, changes in peripheral marker of microtubule dynamics, namely Acet-Tub/TRF in plasma, were also tested. In the context of previous findings of increased Acet-Tub levels in rodent models of depression (Bianchi, Hagan and Heidbreder, 2005) and reductions following antidepressant treatment (Bianchi *et al.*, 2009), a decrease of peripheral Acet-Tub/TRF was hypothesized. Although transferrin has been extensively used as a loading control protein in human plasma and serum analysis, there are also indications of transferrin level change during systemic physiological response (e.g. during infusion) (Gabay and Kushner, 1999) or after pharmacological interventions (Bianchi, unpublished observations). Consequentially, absolute quantities of Acet-Tub and Transferrin were separately analyzed in an exploratory manner.

The relative ratio of Glu/tCr and Acet-Tub/TRF was then correlated to specify relationship between central and peripheral markers of plasticity. Based on the hypothesis on their absolute changes after ketamine, glutamatergic decrease was presumed to be largest for cases of strongest Acet-Tub decreases, *i.e.* a positive correlation of changes in peripheral and brain markers was expected.

To investigate relevant safety risks, aftereffects were analyzed on blood parameters 14 days after infusion. To that end, hematology parameters, hemoglobin, and number of leukocytes, thrombocytes, and erythrocytes, and levels of sodium, calcium, and potassium were determined during safety laboratory (Figure 6.1.). No specific hypothesis was generated since previous clinical trials did not report any changes. However, based on the findings from non-human primate research and increases in peripheral serum and plasma BDNF levels, an increase in thrombocyte counts was plausible, also given that thrombocytes are major pools of peripheral BDNF (Chacón-Fernández *et al.*, 2016).

Previous research has indicated certain demographic parameters, such as BMI (Niciu *et al.*, 2014) or history of alcoholism in family (Phelps *et al.*, 2009) affect ketamine efficacy. So, a regression analysis of demographic parameters on the magnitude of changes of central and peripheral markers and safety parameters which displayed a change after ketamine was conducted. Next to sex, which was marked as a co-variate of interest in rmANOVAs, prediction by age, BMI, smoking, alcohol or drug use, and contraception was tested.

Clinical trials have stated that early dissociative symptoms, usually measured with the Clinician-Administered Dissociative States (CADSS; Bremner *et al.*, 1998), predict the level of antidepressant response in patients (Luckenbaugh *et al.*, 2014; Niciu *et al.*, 2018), so, as a final exploratory analysis, participants in the ketamine group were divided based on their experience of dissociation, and magnitude of changes of central and peripheral markers and safety parameters that showed change after ketamine, were compared between the groups.

6.2. Study 4 specific materials and methods

6.2.1. Study design

The presented studies were embedded in a large trial, which aimed to decipher neurobiological mechanisms of action of single intravenous infusion of sub-anesthetic dose of racemic ketamine in healthy participants. Moreover, the trial also measured peripheral markers and controlled for safety parameters. To that end, a randomized, double-blind, placebo-controlled, parallel-design investigation was carried out. The study was registered as a clinical trial (under EudraCT number 2010-023414-31, the EU Clinical Trials Register). The study was approved by the Institutional Review Board of Otto von Guericke University of Magdeburg, Faculty of Medicine. The study was conducted in accordance with the Declaration of Helsinki (World Medical Association, 2002) and all participants gave written informed consent.

Number of participants and design were adjusted to fulfil the primary outcome of the clinical trial, which was to investigate temporal and regional specificity of glutamatergic changes after ketamine infusion (Li *et al.*, 2017). For this purpose, sample size was calculated based on the effect sizes and dropout rates from previous studies, which reported significant effects on glutamatergic changes after ketamine infusion in cohorts with average 11 participants: $n = 13$, dropout rate = 63% (Stone *et*

al., 2012); $n = 10$, dropout rate = 20% (Rowland *et al.*, 2005); $n = 11$, dropout rate = 27% (Milak *et al.*, 2016). To have at least 11 participants per group with good data quality in 6 independent measurements (two regions and three time points), with dropout rate = 15%, a total study $n > 58$ was calculated ($= (2 \times 11) / [(1 - 15\%)^6] =$). In the end $n = 80$ (40 per group) were included in the trial.

Participants were stratified by sex and age and allocated to treatment groups with RITA randomization software (Evidat, Sereetz, Germany). Participants, research staff and study physicians were blinded to treatment assignment. Study was carried out between August 2012 and April 2016.

6.2.2. Participants

Healthy participants were recruited via public advertisement. participants were screened for 7T MR compatibility (e.g. absence of metal implants, tinnitus, and claustrophobia). Next, they underwent extensive medical examination which included: medical history, current use of medication, blood laboratory tests, toxicology examination, physical examination, electrocardiography, and ophthalmic examination to exclude ocular hypertension. Further exclusion criteria included current drug abuse or dependence, regular medication, and excessive caffeine intake. Moreover, to exclude ICD-10 psychiatric disorders, participants completed German version of the Mini-International Neuropsychiatric Interview (M.I.N.I.) (Sheehan *et al.*, 1998; Ackenheil *et al.*, 1999) and interview with the study physician. participants that fulfilled inclusion criteria received detailed written information sheets about the study and gave written informed consent to take part.

6.2.3. Study Medication

Study 4 followed the most frequent administration protocol (Caddy *et al.*, 2014). participants received 50 ml of either 0.5 mg/kg body weight of ketamine +/- racemate (Ketamine-ratiopharm® 500 mg/10 ml; Ratiopharm GmbH, Ulm, Germany) or 0.9% saline solution (NaCl .9%; Berlin-Chemie AG, Berlin, Germany). The medication was supplied by the hospital pharmacy in prefilled identical 50 ml syringes. It was administered via an infusion pump (Injectomat 2000, Fresenius Kabi GmbH, Langenhagen, Germany) in a continuous rate over 40 min.

6.2.4. Study procedure

The study was composed of several days and measurements: screening day (medical examination, safety blood test and clinical questionnaires), day 1 baseline

measurement (MRI, blood markers and clinical questionnaires), day 1 post-infusion measurement (MRI, blood markers and clinical questionnaires), day 2, 24 h post-infusion measurement (MRI, blood markers and clinical questionnaires) and a follow-up visit (medical examination, safety blood test, blood markers and clinical questionnaires) (Figure 6.1.). Infusions and MRS scans were performed between 12.00 and 18.00 to control for the potential diurnal variations.

After passing screening procedure, participants underwent two experimental days. On day one, a baseline MRI scan was acquired, which included structural scan, MRS measurement, resting state and emotional face matching task. Baseline blood marker samples were taken before or immediately after scan. After intravenous catheter was placed, participants went to a resting supine position and infusion was started. During infusion systolic/diastolic arterial blood pressure (RR) and heart rate (HR) were automatically measured every 5 minutes for 40 minutes (Saegeling Invivo MAGNITUDE 3150). After the end of infusion, participants completed clinical questionnaires, including Clinician-Administered Dissociative States Scale (CADSS) (Bremner *et al.*, 1998), as a measure of behavioral response to the treatment. The participant then underwent second post-infusion MR scan and blood marker sampling. The same set of measurements was done the following day, approximately 24 h after the end of the infusion. participants came for a final follow-up visit to check their health and safety blood markers.

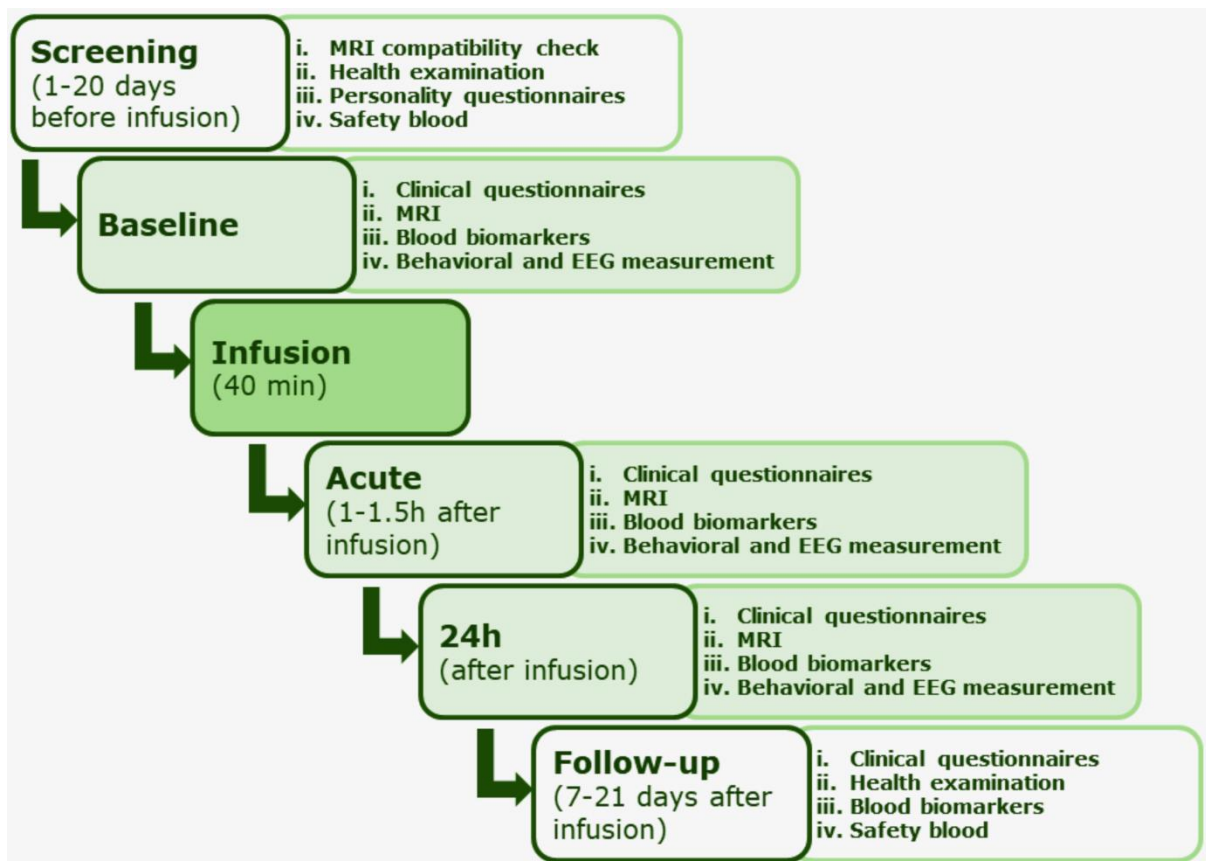


Figure 6.1. Ketamine study schema.

Study included several days with peripheral blood measurements, MRI, questionnaires and EEG& and behavioral tasks. Screening questionnaires included: ATF, MINI, Medication, HAMD, HAMA, BPRS, YMRS; Clinical questionnaires included: HAMD, SSI, MADRAS, SHAPS, CADSS, General Condition; Personality questionnaires included: TCI, BFPE, AIM, ECR-R, STAI, ABI, TAS-20, CTQ, RFQ, SEE and OPD; MRI entailed structural MPRAGE, magnetic resonance spectroscopy (MRS), resting state fMRI (rs-fMRI), and emotional face matching task; Blood biomarkers, Acet-Tub/TRF and BDNF, were measured in plasma or/and serum samples; EEG was measured during a reversal learning with a retrieval memory task; Behavioral measurement was a Flanker task (cognitive inhibition task).

6.2.5. MR measurements

Structural and magnetic resonance spectroscopy scan were obtained with the protocol described in the general methods, paragraphs 2.1.2., 2.1.3. and 2.2.6.

In short, glutamate (Glu) and creatine (Cr) levels were obtained with STEAM sequence in the pgACC (Figure 2.4.). The gray matter partial volume of the individual voxel was calculated as the segmented gray matter divided by the total volume within

voxels. Ratio Glu/tCr residualized for the gm partial volume was used in following analyses.

6.2.6. Blood marker measurement and analysis

Participants gave blood samples in a sitting position between 12.00 pm and 6.00 pm for four time points (baseline, 1 h, 24 h and follow-up) and serum (BD Vacutainer SST II Advance REF 367953) and heparin tubes (BD Vacutainer LH 68 I.U. REF 368884) were collected. Tubes were transported on ice. Heparin tubes were centrifuged within 10 min after sampling at 20 °C, 2000 RcF for 15 min, and serum tubes within 30 min after sampling with the same procedure. The plasma and serum supernatant were aliquoted to 300 µl Eppendorf tubes and stored in -80 °C.

For the Acetyl- Tubulin analysis baseline and 24 h plasma samples were taken and 2% (v/v) protease inhibitor cocktail (Sigma) was added to ensure protein stability. Western blott analyses were done in collaboration with Transpharmation Ireland (Trinity College, Ireland), and were performed by C.M.

Protein quantification was determined using Bradford Colorimetric Assay (Sigma). Samples were adjusted to total protein concentration of 6 µg per 1 µl with v/v Laemmli buffer 2X (Sigma). To obtain final total protein concentration of 60 µg, 10 µl of samples was loaded to gels. Electrophoresis was done in 26-well 10% Bisacrylamide/ Trisacrylamide gels (NuPAGE, Invitrogen), running at constant 200 V. To assure correct location of the proteins based on their molecular weight, 3 µl of an infrared molecular size marker (250-10 kDa range; Li-Cor) was loaded on the gel. Proteins were then transferred to a polyvinylidene fluoride (PVDF) membrane (Millipore) using the dry Iblot2 transfer unit (Invitrogen). Membranes were blocked for one hour in a 1:1 Phosphate-buffered saline (PBS): Odyssey Blocking Buffer (Li-Cor) solution at room temperature. Membranes were incubated overnight with the primary antibodies at 4 °C. Next day, membranes underwent six 10 min washes with a PBS-.05% Tween 20 solution before one-hour incubation with the secondary antibodies' solution. After the secondary antibody incubation, membranes again underwent a six 10 min washing period with PBS-.01% Tween 20 solution and were finally stored in PBS at 4 °C. Multi-plexed IFWB to detect on the same blot Acet-Tub and TRF was performed with primary monoclonal antibodies against Acet-Tub (clone 6-11B-1, Sigma) diluted 1:500 and TRF (polyclonal, Abcam) diluted 1:333,333. Membranes were incubated with secondary antibodies anti-mouse IRDye 680 (LiCor,

ScienceTec) and anti-rabbit IRDye 800 (LiCor) both diluted 1:100. The infrared signal was detected and quantified using the Odyssey scanner and software (LiCor) (Figure 6.2.). Gels were run in duplicate. Infrared signal was expressed as raw optical density (OD) and data from the duplicates were averaged. Ratio between Acet-Tub and TRF was used in the main analysis and OD data of separate proteins were used in the exploratory analyses. When appropriate data were natural logarithm transformed for statistical analysis.



Figure 6.2. Example of an Infrared Western Blot for Acet-Tub/TRF.

Western blot holds samples from both treatment groups and time points (baseline & 24 h).

6.2.7. Safety blood measurement and analysis

During screening and follow-up visit whole blood biochemistry was measured. Venous blood was collected via butterfly system, in a sitting position between 10 am and 6 pm, 1-20 days prior and 10-20 days after the infusion in standard tubes: serum (BD Vacutainer SST II Advance REF 367953), EDTA (BD Vacutainer K3E 7.2 mg REF 368884), heparin (BD Vacutainer LH PST II REF 367378) and Sodium-Citrate (BD Vacutainer 0.129 M buffered Sodium-Citrate (= 3.8 %) REF 367704-9NC). Samples were brought to the Medical Biochemistry lab within 60 min after collection for processing and analyses. The analyses were done in collaboration with J.H.

Blood collected to EDTA tubes was used to analyze hematological parameters. The samples were analyzed on an ADVIA2120 Hematology Analyzer (Siemens Healthineers GmbH, Erlangen, Germany). Number of erythrocytes, leukocytes, and thrombocytes was determined using flow cytometry. The levels of hemoglobin were measured colorimetrically. Blood levels of sodium, potassium, and calcium were analyzed in blood serum and plasma on Roche Modular Systems (Roche Diagnostics Deutschland GmbH, Mannheim, Germany) from the beginning of the study until January 2015 and Roche Cobas Systems (Roche Diagnostics Deutschland GmbH, Mannheim, Germany) from January 2015 until the end of the study. Sodium and potassium were analyzed using ion selective electrodes, and calcium was measured photometrically. Coagulation parameters were analyzed using samples from Sodium-

Citrate tubes. Reference range for the investigated metabolites can be found in Table S6. 1.

6.2.8. Statistical analyses

Each analysis was done with the maximum available number for the modality or combination of modalities. All variables were checked for normality with Kolmogorov-Smirnov test ($p < .05$), and appropriate tests were applied. Statistical tests were done in IBM SPSS Version 24 (IBM Corp., Armonk, NY, USA). Graphs were done in GraphPad 6 (GraphPad Software Inc., San Diego, CA, USA). Statistical threshold was generally set at $p < .05$.

Baseline regression analysis

First, for variables of interest, linear regression (enter-method) were run to test which demographic variables affect baseline values. Age, sex, body-mass-index (BMI), smoking status (yes/no), quantitative alcohol consumption (more than 1 drink per week) and drug usage (ever used any kind of drugs) were added. Regressions were also calculated separately for women, with contraception as an additional predictor variable. Glu/tCr (res), Acet-Tub/TRF, absolute Acet-Tub, absolute TRF and safety blood parameters (erythrocytes, leukocytes, thrombocytes, hemoglobin, sodium, potassium, and calcium) were tested.

Treatment effects

To test the treatment effects repeated measures analyses of variance (rmANOVA) were done for the residualized Glu/tCr, Acet-Tub/TRF (plus exploratory analysis of the absolute Acet-Tub & TRF levels) and safety blood parameters. Factor time point was within, while group and sex were between- participants' factors. *Post hoc* paired *t*-test/Wilcoxon signed ranked test or Students *t*-/ Mann-Whitney *U* tests were conducted for significant interactions.

Based on the reviewer and statisticians (A.L.) suggestions for the publication Colic et al., (Colic, Woelfer, *et al.*, 2018), slightly different statistical analysis was conducted as described below;

Outliers were detected ($< 3 \cdot iq3 <$) and excluded from the analyses. Repeated measures analyses of co-variance (rmANCOVA) were done for the number of erythrocytes, leukocytes, thrombocytes, and the levels of hemoglobin, sodium, calcium, and potassium, with the within- participants factor time point (baseline and

follow-up) and between- participants factor group. Age, body mass index (BMI) and sex were used as covariates of nuisance. To confirm specificity of ketamine effects on coagulation parameters partial thromboplastin time (PTT) and international normalized ratio of prothrombin time (INR) were additionally tested. Frequency of participants exceeding the reference range was checked for the baseline and the follow-up measurement.

Correlation of central and peripheral markers 24 h after infusion

Relative ratio (24 h-baseline/baseline) was calculated for Glu/tCr and Acet-Tub/TRF. Two variables were correlated with Pearson or Spearman test for ketamine and placebo group separately, with sex as a covariate. The same was done for absolute Acet-Tub and TRF on an exploratory level.

Factors influencing treatment effects

Linear regressions (enter-method) were conducted to check if basic demographic factors are predictive of the level of change of the relative ratio of the investigated variables. Same predictor variables were used as for the baseline measurement regression analysis.

Lastly, to determine if the hyper-acute dissociative symptoms are associated with the level of changes in the relevant parameters, ketamine group was further dichotomized to two subgroups based on the CADSS total score, measured immediately after the end of the infusion. participants were divided to ones that did not experience dissociative symptoms, with total score smaller than 4, and participant who did, total score equal or bigger than 5 (Bremner *et al.*, 1998). Univariate ANOVA was conducted on the relative increases of the residualized Glu/tCr, Acet-Tub/TRF (plus exploratory analysis of the absolute Acet-Tub & TRF levels) and thrombocytes, with factors group and sex.

6.3. Results Study 4 Ketamine

6.3.1. Demographics

One hundred participants were assessed for eligibility. From those, forty-one received ketamine infusion, and forty saline infusions. One participant in the ketamine group did not finish the follow-up measurement; hence study groups were the same. For some measurements blood sampling was not possible. Moreover, some participants were excluded based on the quality of the data. Details on the participant enrollment,

and specific *n* for each analysis can be found in the flow-chart following the CONSORT guidelines (Figure 6.3.). Ketamine and saline groups did not differ in demographic variables, except for the hyper-acute dissociative symptoms (CADSS total score >5, $\chi^2(1) = 32.28, p < .001^{***}$) (Table 6.1.)

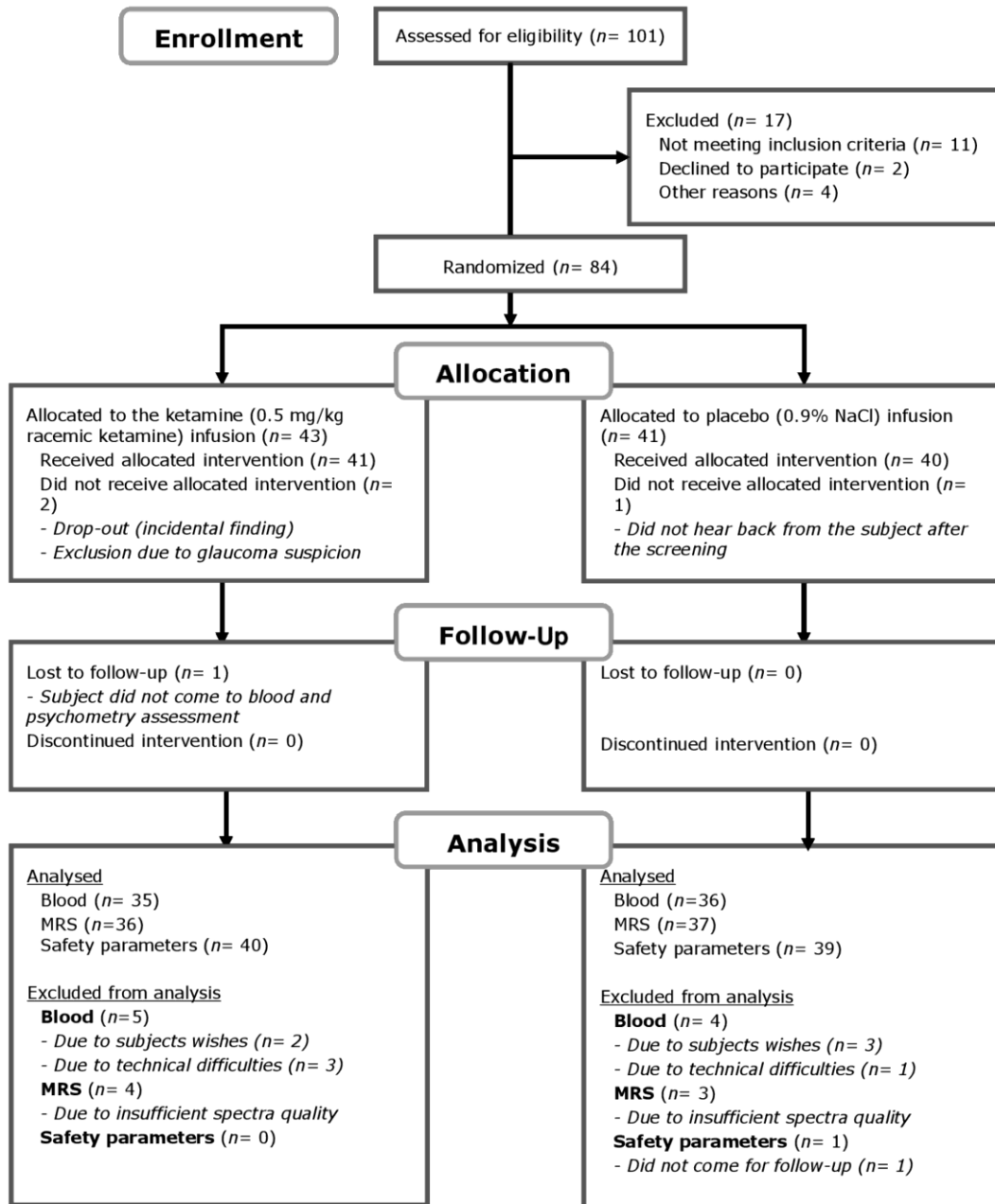


Figure 6.3. Diagram of the trial based on the CONSORT 2010 recommendations.

Table 6.1. Demographic data of the trial.

There were no differences between the groups, except for the acute dissociative symptoms. Data is presented in mean± S.D or frequencies.

	Ketamine (N= 40)	Placebo (N= 40)	Mann-Whitney U-test or χ^2 interaction test
Age	25.95± 5.65	25.83± 4.98	$U= 794.0, p= .95$
Sex	16 women	17 women	$\chi^2(1)= .05, p= .82$
BMI	23.81± 3.07	23.76± 2.94	$U= 793.5, p= .95$
Smoking yes	11	15	$\chi^2(1)= .91, p= .34$
Alcohol usage ^A	23	27	$\chi^2(1)= .85, p= .36$
Drugs yes ^B	13	15	$\chi^2(1)= .22, p= .64$
Contraceptive pill yes ^C	10	8	$\chi^2(1)= .79, df= 1, p= .37$
CADSS > 5 ^D	0	23	$\chi^2(1)= 32.28, p< .001^{***}$
Days baseline ^E	5± 2	5± 3	$U= 776.5, p= .80$
Days follow-up ^E	14± 1	14± 2	$U= 704.5, p= .44$

^A Frequency of 1-3 drinks per week; ^B Ever consumed drugs; ^C Only for women; ^D *n* of participants marks those who had total CADSS score higher than 5; ^E Days baseline marks days between baseline blood collection and infusion, and follow-up days between infusion and follow-up blood collection.

6.3.2. Sex predicts baseline levels of Acet-Tub/TRF, their absolute levels, haemoglobin and number of erythrocytes and thrombocytes

For the baseline Glu/tCr levels only age was a trend-wise significant predictor (Table S6. 2.).

Sex was a strong predictor of the baseline levels of Acet-Tub/TRF ($t(68)= 5.578, p< .001$), where men had higher Acet-Tub/TRF than women (Figure S6. 1., Table S6. 2.B). This was also observed in the exploratory analysis for absolute Acet-Tub ($t(68)= -6.307, p< .001$) and TRF ($t(68)= -1.523, p< .001$), for which women had higher levels for both proteins (Figure S6. 1., Table S6. 2.C&D). Other parameters were not predictive of the baseline ratio expression or absolute values except age for absolute TRF ($t(68)= -2.168, p= .034$) (Table S6. 2.D). Additionally, in women, use of contraceptives was a significant factor for Acet-Tub/TRF ($t(28)= -2.918, p= .007$) and

TRF ($t(28)= 2.334, p= .027$) (Table S6. 2.B&D). *Post hoc* Student's t-tests showed that the sex difference was not driven by the contraceptive group in both Acet-Tub/TRF or TRF as the non-contraceptive group also had different values than men (Acet-Tub/TRF: men vs women taking contraceptives $t(59)= -7.784, p< .001$, men vs women not using contraceptives $t(57)= -3.540, p= .001$, Figure S6. 1.A; TRF: men vs women taking contraceptives $U> .99, p< .001$, men vs women not using contraceptives $t(57)= 9.201, p< .001$, Figure S6. 1.C).

For blood measurements sex was a significant predictor for erythrocytes ($t(73)= 5.314, p< .001$, Table S6. 2.F), thrombocytes ($t(73)= -2.592, p= .012$, Table S6. 2.G) and haemoglobin ($t(73)= 8.347, p< .001$, Table S6. 2.H). Men had higher number of erythrocytes and haemoglobin; whereas women had higher number of thrombocytes. Other significant predictors for blood variables can be found in Table S6. 2.E-K.

6.3.3. Glutamate levels in the pgACC change 24 h after ketamine infusion

There was a significant time by treatment interaction ($F(1,69)= 4.137, p= .047, \eta^2= .056$), but not time by treatment by sex ($F(1,69)= 1.013, p= .253, \eta^2= .019$) (Table 6.2.). *Post hoc* analysis indicated that the interaction effect was driven by a trend difference between groups at 24 h (baseline: $t(73)= .488, p= .627$; 24 h: $U(77)= 565, p= .073$) (Figure 6.4.).

Table 6.2. Results of the rmANOVA for Glu/tCr residualized for gray matter partial volume.

Effect	Glu/tCr
Within- participants	
Time point	$F(1, 69) < .001, p = .989, \eta^2 < .001$
Time point by sex	$F(1, 69) = .374, p = .543, \eta^2 = .005$
Time point by treatment	$F(1, 69) = 4.084, p = .047, \eta^2 = .056 *$
Time point by treatment by sex	$F(1, 69) = 1.330, p = .253, \eta^2 = .019$
Between- participants	
Sex	$F(1, 69) = .273, p = .603, \eta^2 = .004$
Treatment	$F(1, 69) = 1.513, p = .223, \eta^2 = .021$
Treatment by Sex	$F(1, 69) = .050, p = .823, \eta^2 = .001$

* $p < .05$

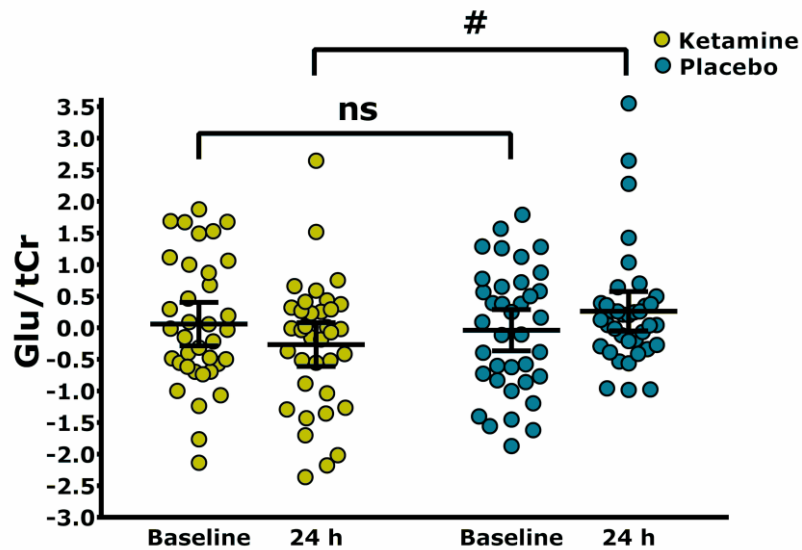


Figure 6.4. Significant interaction of time points and group for the Glu/tCr residuals measured in the pgACC.

(* $F(1,69)= 4.137, p= .047, \eta^2= .056$). There was a trend-wise difference at 24 h (# $U(77)= 565, p= .073$) but not at baseline (ns $t(73)= .488, p= .627$). Data is presented in mean \pm 95% CI.

6.3.4. Change of Acet-Tub/TRF levels after ketamine is sex specific

There was a significant interaction of time point by treatment by sex ($F(1,67)= 5.131, p= .027, \eta^2= .071$) for Acet-Tub/TRF (Table 6.3.). *Post hoc* analysis showed a significant difference in women for the relative change of Acet-Tub/TRF between the treatment groups ($t(25)= 2.618, p= .015$), which was driven by an increase in the ketamine group (ketamine: $t(12)= -2.329, p= .038$; placebo: $t(13)= 1.535, p= .149$) (Table 6.3., Figure 6.5.). In men there was no difference between ketamine and placebo group for the relative increase ($t(42)= -.683, p= .527$).

Exploratory analysis of absolute levels showed a significant time point by treatment ($F(1, 67)= 4.555, p= .036, \eta^2= .064$) and trend-wise significant time point by treatment by sex interaction ($F(1, 67)= 3.108, p= .082, \eta^2= .044$) for TRF levels (Figure 6.5C, Table S6. 3.B). This was again driven by the difference between treatment groups in the relative change in women ($t(25)= -2.805, p= .010$) (Figure S6. 2.B). There were no significant interactions for the absolute Acet-Tub levels (Figure 6.5B, Table S6. 3.A).

Table 6.3. Results of the rmANOVA for Acet-Tub/TRF levels.

Effect	Acet-Tub/ TRF
Within- participants	
Time point	$F(1,67) = 13.725, p < .001, \eta^2 = .170$ ***
Time point by sex	$F(1,67) = 9.829, p = .003, \eta^2 = .128$ **
Time point by treatment	$F(1,67) = 2.689, p = .106, \eta^2 = .039$
Time point by treatment by sex	$F(1,67) = 5.131, p = .027, \eta^2 = .071$ *
Between- participants	
Sex	$F(1,67) = 58.501, p < .001, \eta^2 = .466$ ***
Treatment	$F(1,67) = .077, p = .783, \eta^2 = .001$
Treatment by Sex	$F(1,67) = .173, p = .679, \eta^2 = .003$

*** $p < .001$; ** $p < .01$; * $p < .05$

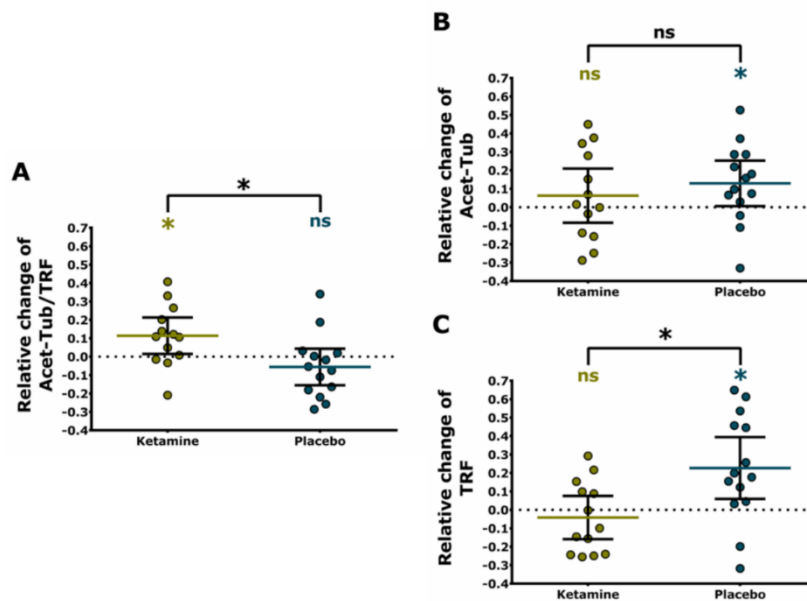


Figure 6.5. Relative increase for Acet-Tub/TRF and absolute values in women.

For women, there was a significant difference of the relative ratio Acet-Tub/TRF between groups (* $t(25) = 2.618, p = .015$), driven by an increase in the ketamine group (* $t(12) = -2.329, p = .038$) which was not observable in the placebo group (ns $t(13) = 2.535, p = .149$). Data is presented in mean \pm 95% CI.

6.3.5. Relative changes of Acet-Tub/TRF and Glu/tCr correlate negatively after ketamine infusion

In the ketamine group, Glu/tCr relative change was negatively correlated with the Acet-Tub/TRF change ($r(28) = -.464, p = .010$) (Figure 6.6A). The correlation was significant in women (women: $r(9) = -.618, p = .043$), and not in men ($r(18) = -.374, p = .104$) (Figure 6.6B&C). This correlation was not observed in the placebo group ($\rho(30) = .123, p = .503$). Exploratory analysis showed that the Glu/tCr relative change was correlated with the change in absolute TRF ($\rho(28) = .397, p = .030$), but not absolute Acet-Tub expression ($r(28) = .123, p = .518$) (Figure S6. 2.).

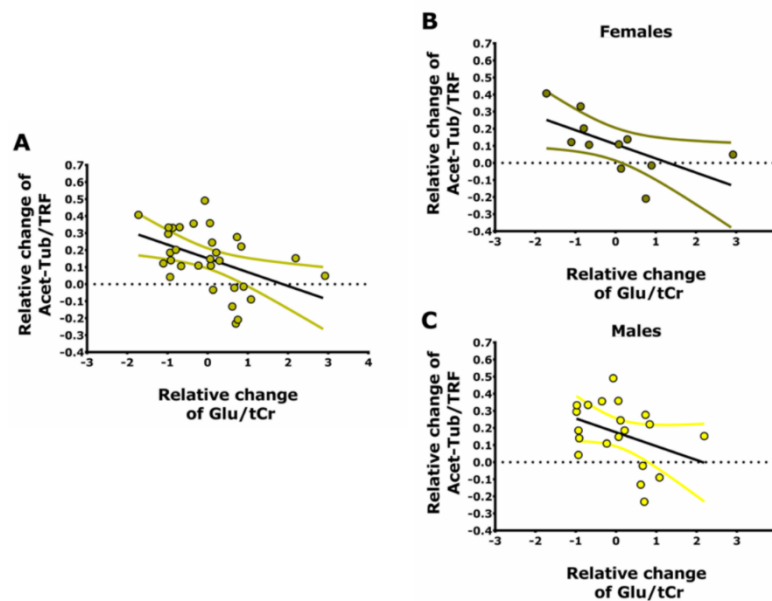


Figure 6.6. Correlation between relative change of Glu/tCr and Acet-Tub/TRF.

A Correlation of the relative changes of Acet-Tub/TRF and Glu/tCr for the whole ketamine group ($r(28) = -.464, p = .010$); **B** correlation was statistically significant for women ($r(9) = -.618, p = .043$), **C** but not men ($r(18) = -.374, p = .10$).

6.3.6. Thrombocyte number increases 14 days after ketamine infusion

Analysis revealed a Bonferroni corrected significant time point by treatment interaction for thrombocyte levels ($F(1,75) = 12.66, p = .001, \eta^2 = .144$). The increase was sex unspecific since time point by treatment by sex was not significant ($F(1,75) = .034, p = .854, \eta^2 < .001$) (Table 6.4.C). The interaction was marked by a difference in the follow-up measurement (baseline: $t(77) = .13, p = .90$; follow-up: $t(77) = 2.20, p = .03$), and an increase in the ketamine group (ketamine: $t(38) = -3.51, p = .001$;

placebo: $t(39) = 1.47, p = .15$) (Figure 6.7.). Other blood parameters did not display significant effects on a corrected threshold (Table 6.4.).

Furthermore, *post hoc* ANOVA tests showed that this effect was specific for thrombocyte number, since other coagulation parameters, partial thromboplastin time (PTT) and international normalized ratio (INR), did not have significant time point by treatment interaction (PTT: $F(1,71) = .02, p = .89, \eta^2 < .001$; INR: $F(1,71) = 1.68, p = .20, \eta^2 = .023$) or significant time point by treatment by sex interaction (PTT: $F(1,71) = 1.31, p = .26, \eta^2 = .018$; INR: $F(1,71) = .02, p = .90, \eta^2 < .001$).

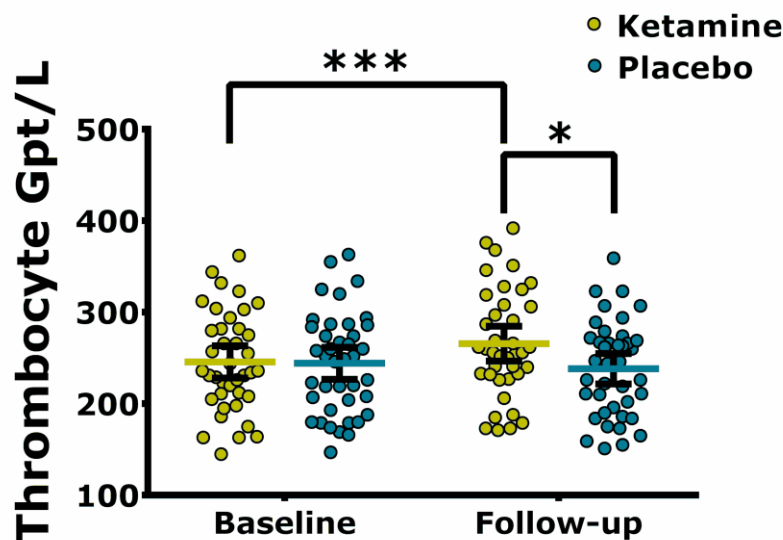


Figure 6.7. Results of the rmANOVA for the thrombocyte levels.

Post hoc test show group difference for the follow-up (Student's t-test, $t(77) = 2.20, p = .03^*$) and difference between baseline and follow-up within the ketamine group (paired t-test $t(38) = -3.51, p = .001^{***}$). There was no difference between groups (Student's t-test, $t(77) = .13, p = .90$) at baseline, and no difference between baseline and follow-up within the placebo group (paired t-test, $t(39) = 1.47, p = .15$). Data is presented in mean \pm 95% CI, *** $p < .001$, ** $p < .01$, * $p < .05$.

Table 6.4. Results of the rmANOVAs for safety parameters.

For **A** Leukocytes; **B** Erythrocytes; **C** Thrombocytes; **D** Haemoglobin; **E** Sodium; **F** Potassium and **G** Calcium

Effect	Erythrocytes	B Leukocytes	C Thrombocytes	D Haemoglobin	E Sodium	F Potassium	G Calcium
Within- participants							
Time point	$F(1,75) = 1.885, p = .174, \eta^2 = .025$	$F(1,75) = 3.547, p = .064, \eta^2 = .045 \#$	$F(1,75) = 2.957, p = .09, \eta^2 = .038$	$F(1,75) = 5.685, p = .020, \eta^2 = .070$	$F(1,75) = .421, p = .518, \eta^2 = .006$	$F(1,74) = .369, p = .545, \eta^2 = .005$	$F(1,75) = .738, p = .393, \eta^2 = .010$
Time point by sex	$F(1,75) = .401, p = .529, \eta^2 = .005$	$F(1,75) = .109, p = .742, \eta^2 = .001$	$F(1,75) = 1.573, p = .214, \eta^2 = .021$	$F(1,75) = .600, p = .441, \eta^2 = .008$	$F(1,75) = 1.196, p = .278, \eta^2 = .016$	$F(1,74) = .877, p = .352, \eta^2 = .012$	$F(1,75) = .149, p = .701, \eta^2 = .002$
Time point by treatment	$F(1,75) = .157, p = .693, \eta^2 = .002$	$F(1,75) = .141, p = .708, \eta^2 = .002$	$F(1,75) = 12.658, p = .001, \eta^2 = .144$	$F(1,75) < .001, p = .990, \eta^2 < .001$	$F(1,75) = .012, p = .915, \eta^2 = < .001$	$F(1,74) = .184, p = .669, \eta^2 = .002$	$F(1,75) = .142, p = .707, \eta^2 = .002$
Time point by treatment by sex	$F(1,75) = 3.893, p = .052, \eta^2 = .049 \#$	$F(1,75) = .146, p = .703, \eta^2 = .002$	$F(1,75) = .034, p = .854, \eta^2 < .001$	$F(1,75) = 1.530, p = .220, \eta^2 = .020$	$F(1,75) = .114, p = .737, \eta^2 = .002$	$F(1,74) = .001, p = .969, \eta^2 < .001$	$F(1,75) = 1.961, p = .161, \eta^2 = .025$
Between- participants							
Sex	$F(1,75) = 44.440, p < .001, \eta^2 = .372$ ***	$F(1,75) = .003, p = .955, \eta^2 < .001$	$F(1,75) = 5.410, p = .023, \eta^2 = .067$	$F(1,75) = 119.170, p < .001, \eta^2 = .614$	$F(1,75) = 4.845, p = .031, \eta^2 = .061$	$F(1,74) = .613, p = .436, \eta^2 = .008$	$F(1,75) = 1.541, p = .218, \eta^2 = .020$
Treatment	$F(1,75) = .183, p = .670, \eta^2 = .002$	$F(1,75) = 1.665, p = .201, \eta^2 = .022$	$F(1,75) = 1.359, p = .247, \eta^2 = .018$	$F(1,75) = .019, p = .892, \eta^2 < .001$	$F(1,75) = .046, p = .831, \eta^2 = .001$	$F(1,74) = .264, p = .609, \eta^2 = .004$	$F(1,75) < .001, p = .987, \eta^2 < .001$
Treatment by sex	$F(1,75) = .927, p = .339, \eta^2 = .012$	$F(1,75) = 2.690, p = .105, \eta^2 = .035$	$F(1,75) = .714, p = .401, \eta^2 = .009$	$F(1,75) = .052, p = .820, \eta^2 = .001$	$F(1,75) = .059, p = .809, \eta^2 = .001$	$F(1,74) = 1.898, p = .172, \eta^2 = .025$	$F(1,75) = 1.541, p = .218, \eta^2 = .020$
Corrected threshold $p < .007$; *** $p < .001$; * $p < .05$; # $.1 < p < .05$							

Auxiliary analysis of blood safety parameters with ANCOVA-s yielded similar results, with only thrombocyte numbers showing significant effect of treatment ($F(1, 74)=13.54, p < .001, \eta^2 = .155$) (Table S6. 4).

Compared to the baseline measurement, in which two participants were exceeding reference range (Table S6. 1.) in the whole study population, for the follow-up measurement three participants in the ketamine group were above the reference range, while none in the placebo group (Figure S6. 3.).

6.3.7. Demographic factors do not predict relative increase of investigated parameters

Demographic factors (age, sex, BMI, smoking, alcohol consumption, drug use and contraception in women) did not significantly predict relative increase of residualized Glu/tCr, Acet-Tub/TRF, absolute Acet-Tub and TRF or thrombocyte number in the ketamine group (Table S6. 5.).

6.3.8. Acute Dissociative symptoms do not associate to the magnitude of changes within the ketamine group

Participants were split to participants that did not experience dissociative symptoms, CADSS < 4 (n= 16) and those who did, CADSS > 5 (n= 24). CADSS groups did not differ between each other and compared to placebo for demographic variables (Table S6. 6.). There was also no differentiation between the two CADSS groups for the relative increase of investigated variables, which previously showed treatment effect, as presented in Table 6.5.

Table 6.5. Results of the univariate ANOVA between CADSS groups and placebo.

A Glu/tCr relative increase (residualized for gray matter partial volume); B Acet-Tub/TRF relative increase; C thrombocytes relative increase.

Effect	A Glu/tCr	B Acet-Tub/ TRF	C Thrombocytes
Between- participants			
Group	$F(5,70)= 1.569, p = .216, \eta^2 = .046$	$F(5,70)= 1.742, p = .183, \eta^2 = .051$	$F(5,78)= 6.969, p = .002, \eta^2 = .160^{**}$
Sex	$F(5,70)= .083, p = .774, \eta^2 = .001$	$F(5,70)= 3.550, p = .064, \eta^2 = .052 \#$	$F(5,78)= 1.819, p = .182, \eta^2 = .024$
Group by sex	$F(5,70)= .382, p = .684, \eta^2 = .012$	$F(5,70)= 3.151, p = .049, \eta^2 = .088^*$	$F(5,78)= .237, p = .790, \eta^2 = .006$

Post hoc group comparison (Bonferroni corrected)

CADSS < 4 to Placebo	$p = .337$	$p > .999$	$p = .003^{**}$
CADSS > 5 to Placebo	$p = .803$	$p = .201$	$p = .011^*$
CADSS < 4 to CADSS > 5	$p > .999$	$p = .758$	$p > .999$

** $p < .01$; * $p < .05$; # $.1 < p < .05$

6.4. Discussion Study 4 Ketamine

6.4.1. Baseline sex differences

The Study 4 showed that baseline plasma Acet-Tub/TRF ratios and Acet-Tub absolute quantities differ between healthy male and female volunteers. This unexpected observation demonstrates the need to consider the contributions of basic demographic factors in pharmacological studies. One reason for this sex-dependent variability could be sex differences in thrombocyte (Daly, 2011) or leukocyte numbers (Chen *et al.*, 2016) or reactivity. Steroids have been also shown to be involved in the modulation of microtubule dynamics (Ferreira and Caceres, 1991; Bianchi, Hagan and Heidbreder, 2005; Bianchi and Baulieu, 2012), and this can also be considered as another source of sex differences based on the distinction in circulating sexual steroids between men and women. Additional studies will be required to further elucidate the underlying mechanisms of this interesting sex difference in peripheral Acet-Tub. Furthermore, previously reported higher baseline levels of TRF in women (Ritchie *et al.*, 2004) were replicated in our study. Our data also support controlling for use of contraceptives, given the general influence of contraceptives on plasma proteins (Laurell and Rannevik, 1979).

6.4.2. Ketamine-induced effects are general for Glu/tCr change, but sex specific for Acet-Tub/TRF change

Ketamine is known to influence glutamatergic system function in the prefrontal cortex. Previous studies have reported acute increase in Glx (Milak *et al.*, 2016) and Glu (Stone *et al.*, 2012) after ketamine administration. Peak antidepressant response was, however, measured 24 h after the infusion (Berman *et al.*, 2000; Caddy *et al.*, 2014). We speculate that former MRS studies measured a transient glutamatergic

surge, which is followed by a sustained neural remodeling leading to a reduction in depressive symptoms (Walter, Li and Demenescu, 2014; Abdallah, Sanacora, *et al.*, 2018). In this study, we saw a decrease of Glu/tCr within the pgACC 24 h after ketamine infusion in healthy volunteers (Figure 6.4.). Li *et al.*, (Li *et al.*, 2017) described the temporal (24 h) and regional (pgACC) specificity of the ketamine effects, with regard to glutamate receptor densities. Moreover, animal studies have also shown a decrease in Glu levels 24 h after ketamine (Chowdhury *et al.*, 2017) or phencyclidine, -an NMDAR antagonist- (Iltis *et al.*, 2009) administration. Thus, the time window of increase in Glu might be restricted to immediately post infusion, while 24 h later downregulated or normal Glu levels are observed.

The modulation of the glutamatergic system by ketamine has been suggested to activate intracellular pathways such as mTOR signalling (Li *et al.*, 2010) and eEF2K (Monteggia, Gideons and Kavalali, 2013), and downstream BDNF (Björkholm and Monteggia, 2016). All of those pathways end up modulating microtubule dynamics, with potential to affect neuronal plasticity, including synaptic remodelling and synaptogenesis (Bianchi, Hagan and Heidbreder, 2005). And indeed, animal and cell culture experiments show an increase in spine density after treatment with ketamine (Phoumthippavong *et al.*, 2016).

The relative change of Acet-Tub/TRF in response to ketamine was observed only in women (Table 6.3.) and was in the opposite direction than expected. Although associated with a more stable form of microtubules, Acet-Tub has recently been implicated in other processes of neuronal plasticity and remodelling such as dendrite extensions and arborisation (Creppe *et al.*, 2009). The exact mechanism of ketamine action on peripheral Acet-Tub / TRF is not known. Ketamine does, however, stimulate leukocytes and thrombocytes via NMDA type glutamate receptors and voltage-gated ion channels (Nakagawa *et al.*, 2002; Chang *et al.*, 2004; Kahlfuß *et al.*, 2014). Importantly, Acet-Tub can be detected in human leukocytes (Carta *et al.*, 2006) and thrombocytes (Bianchi, unpublished data). For example, Acet-Tub in peripheral macrophages has been suggested to exert anti-inflammatory effects by amplifying p38 kinase signalling following LPS challenge (Wang *et al.*, 2014). Furthermore, changes in leukocyte markers have been reported in MDD patients, acutely and 24 h after ketamine infusion (Park *et al.*, 2016; Kiraly *et al.*, 2017). Moreover, delayed increase in thrombocyte numbers after ketamine infusion has recently been described (Colic, Woelfer, *et al.*, 2018), providing another possible

source of Acet-Tub change. On the other hand, the pathway of ketamine interaction with TRF is more covert. Transferrin and its receptors are highly connected to liver function (Fleming, Anton and Spies, 2004; Kawabata, 2018). Since ketamine is metabolized primarily in the liver (Hijazi and Boulieu, 2002), this presents one possible mechanism of differential ketamine action on TRF levels.

Considering absolute levels, both Acet-Tub and TRF showed significant increases in the female placebo group, while the female ketamine group showed a slight, non-significant increase in Acet-Tub and slight, non-significant, decrease in TRF (Figure 6.5.). Importantly, our results do not provide conclusive evidence for an isolated effect on either Acet-Tub or TRF under ketamine, which is, next to the non-significance of ketamine-induced changes, related to the necessity to control for varying protein content per observation.

The negative correlation between central glutamatergic changes and peripheral markers of microtubule dynamics represents parallel and temporally aligned consequences of ketamine infusion (Figure 6.6.). The peripheral Acet-Tub/TRF ratio can be regarded as an illustration of cytoskeleton modulation in neurons, although certainly not a final conclusion on ketamine induced dynamics of neuronal Acet-Tub.

We should note that the reported sex differences to ketamine infusion had small effect size, especially when compared to the basal levels, and Acet-Tub/TRF and Glu/tCr correlation slopes did not differ between the male and female ketamine groups. This indicates subtle differences between sexes in their physiological response to ketamine, possibly as a consequence of differences in their immune responses (Klein and Flanagan, 2016), pharmacodynamics (Soldin and Mattison, 2009), liver enzymes function (Choi, Koh and Jeong, 2013) or via oestrogen-mediated mechanisms (Dossat *et al.*, 2018; Ho *et al.*, 2018).

6.4.3. Safety considerations

Number of thrombocytes was a single parameter from the safety panel affected by ketamine infusion (Table 6.4.). Furthermore, it did not differ between sexes and was not predicted by any of the demographic factors (Table S6. 5.). The 10% increase in thrombocyte count was also evident in an increase in the number of participants exceeding the normal reference (140-360 Gp/L; Table S6. 1.), from 2.5% at baseline to 7.7% at follow-up (Figure S6. 3.). The increase in the ketamine group did not cause any complications, so in healthy participants this can be labelled as clinically non-

significant. This might not be the case for psychiatric populations with pre-existing risk factors, where additive effects with medication and state during cardiovascular diseases and coagulation disorders should be surveyed. In contrast, all other blood parameters were not affected long-term by the ketamine infusion.

Mechanism of peripheral interaction

So far effects of ketamine on thrombocytes have not been actively pursued. Even for high doses administered during anaesthesia, nothing has been reported, either as an oversight or it was attribute to trauma or surgery causing an acute phase reaction.

Nevertheless, one retrospective study of ketamine abusers in an emergency department (up to 48 h after use) has reported leukocytosis (above reference range, $> 10 = 89\%$) and thrombocytosis (above reference range, $> 360 = 14.3\%$) in one-third of participants (Ng *et al.*, 2010). The increase in thrombocyte count might thus start early after ketamine administration. The study did not include repeated measures of blood parameters, so it is not possible to say if the increase was observed in all participants after ketamine abuse but passed reference values only in one-third due to the interindividual basal levels, as shown here. Another indication that the change in thrombocyte-related system starts early comes from a study which investigated broad immune and growth factor panel in TDR patients after ketamine. They found a decrease in platelet derived growth factor (PDGF) 24 h after infusion (Kiraly *et al.*, 2017). In this study an increase in leukocyte number was not seen. Change in leukocytes number or composition is probably present shortly after infusion, as it was illustrated for cytokine levels.

Studies in rodents and primates are the other available source of information. In primates after anaesthesia, an acute drop in activation and thrombocyte number shortly after ketamine infusion (Ündar *et al.*, 2004; Rovirosa-Hernández *et al.*, 2011) was seen, but an increase with repeated application (Lugo-Roman *et al.*, 2010). Further on, an acute drop in aggregation of thrombocytes was detected after ketamine application in cell culture (Atkinson, Taylor and Chetty, 1985; Dwyer and Meyers, 1986; Nakagawa *et al.*, 2002). In support, examination of another NMDA antagonist, phencyclidine also found an inhibition of thrombocyte aggregation and secretion of 5-HT after activation with adrenalin, but not after α -thrombin activation (Jamieson *et al.*, 1992). This demonstrated that the exact binding site and

mechanisms of ketamine and other NMDA antagonists remain unclear (Nakagawa *et al.*, 2002; Chang *et al.*, 2004).

One speculation of time activity would be that ketamine induces acute decrease in aggregation and thrombocyte levels. This might trigger thrombopoietin production and subsequent megakaryocytopoiesis, the maturation of bone marrow cells that are responsible for thrombocyte production (Patel, Hartwig and Italiano, 2005; Kaushansky, 2006). Coincidentally, thrombopoietic stimulation leads to a transient increment in thrombocyte numbers, with peak around 12-15 days, and returns to basal levels within a month (Harker *et al.*, 2000; Jenkins *et al.*, 2008) which corresponds to the time of the follow-up measurement in this study.

The delayed increase, a consequence of transient activation of thrombopoietic system, is in direct contrast to here proposed acute side-effect. NMDARs on mature megakaryocytes are one possible interaction sites of acute activation immediately after infusion (Hitchcock *et al.*, 2003; Karolczak, Pieniazek and Watala, 2017). NMDARs were found to play a substantial role in the regulation of platelet activation and aggregation, and NMDAR antagonists such as ketamine seem to attenuate thrombus formation (Kalev-Zylinska *et al.*, 2014). In support, in a case report a patient treated with another NMDAR antagonist (memantine) had bleeding complications connected to the memantine-medication (Scharf, Parikh and Dillon, 2005). Notably, in this study, other coagulation parameters INR and PTT did not show any prolonged changes, which might reflect the nature of the proposed biphasic response, where the coagulation parameters would show a drop as a consequence of modulation of thrombocyte aggregation properties but would normalize shortly after. The study used only single infusion, so for repeated infusions one can therefore imagine counteracting mechanisms of the acute and delayed responses, but also accumulated effects. The assumed model however needs to be tested with measures during several time points.

Alternative pathway of thrombocyte fluctuation might be through the sympathetic nervous system. Ketamine has affinity for norepinephrine transporters (NET), blocks the reuptake of norepinephrine in the periphery and consequentially affects the sympathetic nervous system (Tweed, Minuck and Mymin, 1972). During the infusion and shortly after, the sympathetic nervous system is activated, which is visible with the increase in the systolic blood pressure and heart rate (Liebe *et al.*, 2017). The sympathetic efferent nerves innervate, among other organs, bone marrow (Mignini,

Streccioni and Amenta, 2003). This interaction might thus cause activation of megakaryocytes (Mignini, Streccioni and Amenta, 2003) or potentiate platelet numbers (Dwyer and Meyers, 1986).

Clinical implications of safety findings

Pathologies in platelet count are related with higher risk of vascular complications (Banach *et al.*, 2017; Falchi *et al.*, 2017). In patients, high thrombocyte levels in reference range were found to be associated with the manifestation of thrombotic events (Fenaux *et al.*, 1990; Regev *et al.*, 1997), although the literature is inconclusive (van der Bom *et al.*, 2009). Thrombotic complications typically occur in patients with other risk factors, such as in postoperative setting or with underlying malignancy (Bleeker and Hogan, 2011). This is essential since in palliative care mood disorders have prevalence of around 30% (Mitchell *et al.*, 2011), and ketamine has already been proposed as a potential treatment option for depressive symptoms and chronic pain (Loveday and Sindt, 2015; Faisal and Jacques, 2017). There are several other situations where ketamine might interfere with existing pathologies and medical drugs. Thrombocytes are also involved in tumour progress (Nash *et al.*, 2002; Sierko and Wojtukiewicz, 2007). Cardiovascular risk factors like hypertension, hypercholesterolemia or smoking could also potentiate thrombotic events (Previtali *et al.*, 2011). In women, use of contraceptives in conjunction with smoking increases general risk for thrombosis (Pomp, Rosendaal and Doggen, 2008). All of these factors are to be encountered since patients with mental illness show 53% higher risk for cardiovascular diseases than general population (Correll *et al.*, 2017) and prevalence rates of depression are higher in women (Kessler, 2003).

Next to clinical setting, other important consideration is interaction with other medication. Ketamine target population are patients with treatment resistant depression, who are more likely to receive polypharmacy, not just because of the need for add-on treatments for depression but also because of psychiatric and physical comorbidities (Al-Harbi, 2012; Rizvi *et al.*, 2014).

Majority of psychotropic agents lead to thrombocytopenia, with the exception of lithium, a mood regulator, which is known to cause benign thrombocytosis (Flanagan and Dunk, 2008). As lithium is also used often in treatment resistant depression as an add-on therapy (Jollant, 2015), there is high probability that some patients will receive both. The potential pharmacokinetic drug interactions are dependent on

cytochrome P450 enzymes (Hijazi and Boulieu, 2002). Plasma levels of ketamine might be increased by enzyme inhibitors of CYP3A4 or CYP2C9, for example by protease inhibitors, some antibiotics, antiarrhythmic and psychotropic agents (Pelkonen *et al.*, 2008; Peltoniemi *et al.*, 2016). In contrast, ketamine metabolism might be enhanced by enzyme inducers for example by barbiturates and rifampicin (Pelkonen *et al.*, 2008). Another determinant which should be take into account is chirality, since S(+) isoform has higher clearance rates, and might thus invoke lower sanguine side effects. Notwithstanding, since the mechanism of ketamine induced delayed thrombocytosis is not known, it is also possible that plasma availability of ketamine does not directly relate to its thrombocytosis inducing effect.

Biomarker potential

As discussed, the necessity of cheap and reliable markers of ketamine efficacy is indispensable, and thrombocyte dynamics should be additionally evaluated. For example peripheral blood levels of brain-derived neurotrophic factor (BDNF), a biomarker of mood disorders and synaptic plasticity (Panja and Bramham, 2014; Polyakova *et al.*, 2015; Nuernberg *et al.*, 2016), were connected to levels of symptom improvement (Haile *et al.*, 2014) and brain plasticity measures (Duncan *et al.*, 2013). In humans, thrombocytes store peripheral BDNF and megakaryocytes show BDNF gene expression (Lommatzsch *et al.*, 2005; Chacón-Fernández *et al.*, 2016). The proposed biphasic pattern of thrombocyte fluctuations could then be the source of the previously reported BDNF increase after ketamine administration (Chacón-Fernández *et al.*, 2016).

Depression disorder was previously associated with increased thrombocytes activity, and serotonin-based antidepressant medication decreases thrombocyte count (Ataoglu and Canan, 2009; Morel-Kopp *et al.*, 2009; Song *et al.*, 2012). This supports the idea that thrombocytes can serve as markers of the disease's course.

Demographic parameters are not predicating thrombocyte increase

In the context of safety parameters, there was no sex difference in the delayed thrombocyte increase in the ketamine group (Table 6.4.). Even when the groups were split by sex, in both cases the effect was significant (women: $F(1, 28) = 4.23, p = .049, \eta^2 = .131$; men: $F(1, 43) = 9.20, p = .004, \eta^2 = .176$). The inter-sex difference might be a

consequence of hormonal fluctuations during menstrual cycle in women, which was unfortunately not controlled for in the trial.

Moreover, other demographic parameters did not also predict relative increase of thrombocytes (Table S6. 5.). On one hand this attest again for a population-unspecific drug effect, but on the other hand it should be recalled that the study population is not representative of “general population” for variables such as age and BMI.

6.4.4. Hyper-acute dissociative symptoms

In an acute state ketamine induces dissociative and psychomimetic symptoms which resemble schizophrenia-like symptoms (Krystal *et al.*, 1994). Therefore, ketamine is readily used as an agent to mimic such states. CADSS is thought to capture part of these symptoms, although the scale itself was primarily developed to measure dissociative symptoms within post-traumatic stress disorders (Bremner *et al.*, 1998). In patients, CADSS score was positively correlated to symptoms improvement acutely and 7 days, but not 24 h after ketamine infusion (Luckenbaugh *et al.*, 2014). Moreover, the sub scale depersonalization was the most positively correlated one (Niciu *et al.*, 2018). The underlying mode of action for manifestation of the hyper acute symptoms is thought to be via NMDA blockage (Anticevic *et al.*, 2015) and glutamate surge. Correspondingly, the authors interpreted that higher hyper acute glutamate release translates both to heightened symptoms and to higher delayed synaptic strength and antidepressant effect (Luckenbaugh *et al.*, 2014; Scheidegger *et al.*, 2016).

Here, the exploratory results for CADSS subgroups did not show any difference in Glu/tCr after 24 h (Table 6.5.). Previous studies have described a correlation of CADSS with Glu/Gln ratio in prefrontal cortex during infusion (Abdallah *et al.*, 2018), but no correlation to mGlu5 binding potential during and 24 h after infusion (Esterlis *et al.*, 2018). One can thus speculate that the discrepancy might come from the time points of the measured glutamate release or receptor specificity (NMDAR versus mGlu5), and that the hyper acute dissociation is indeed only correlated to the hyper acute release.

In addition to modulating glutamatergic system, ketamine also stimulates acute dopamine release in striatal and medial PFC regions in rodents (Moghaddam *et al.*, 1997), although human findings are inconclusive (for a review see Kokkinou, Ashok

and Howes, 2017). The increase of dopamine might also associate to dissociative and/or psychotomimetic symptoms, given the role of dopamine system in schizophrenia-related diseases (Kesby, 2018). Therefore, it could be that the concordance of dissociation and antidepressant response also comes from off-target parallel activations.

Surprisingly, there was a marginal interaction effect for CADSS groups by sex on the Acet-Tub/TRF, where in women, an incremental increase in Acet-Tub/TRF was observed with higher CADSS scores (Table 6.5.). Given the small n size, and confound of the leading control, this result needs to be taken with a caution. The inferential mechanisms are to be determined in animal or cell culture experiments, given the probable additional interaction with sex hormones.

Lastly, there was also no difference between CADSS groups for the thrombocyte increase (Table 6.5.). This outcome seems plausible, since CADSS did not correlate to other peripheral physiological measures, for example event to hyper acute changes in blood pressure and heart rate (Luckenbaugh *et al.*, 2014). It might be that majority of peripheral measures is a consequence of either ketamine's interaction with the sympathetic system via blockage of NET (Liebe *et al.*, 2017; Liebe *et al.*, 2018), or direct interaction with the NMDAR on thrombocytes and leukocytes, which might follow a different receptor pharmacodynamics than the ones on neurons.

6.5. Limitations Study 4 Ketamine

The limitations of Study 4 primarily stem from the notion that these analyses were secondary and secondary-exploratory of a clinical trial. The primary outcome was set to investigate temporal and regional specificity of glutamatergic changes after ketamine infusion (Li *et al.*, 2017). Consequentially, the experimental design and collection time points were not optimized in some cases (for example safety parameters). They however reflect the idea to make most efficient and economic use of resources from the already obtained datasets. In connection, correction for number of secondary analyses was not applied. Below are listed specific limitations for each of the analysis points.

Glutamatergic and peripheral measures 24 h after infusion

Effect sizes of the individual changes of central and peripheral markers were small to medium, and thus results are limited for far-reaching inferences with respect to the

contributing mechanisms of action, or treatment effects. They thus warrant a replication, ideally accounting for menstrual cycle in women.

Follow-up studies should consider using different loading controls for quantification of Acet-Tub, which was limited in this study. The most reasonable control would be to use total Tub, or Tub with other PMTs, which would additionally allow inspecting the origin and directionality of changes.

Lastly, the development of other more cost-effective biomarkers addressing plasticity changes can be motivated by our findings, including sex differences and general effect sizes of changes in peripheral markers.

Safety analysis

Baseline measurements of safety lab were done before the infusion day to affirm the health status of the participants to include them in the trial. In theory, it could introduce variance due to the different time span between the baseline and follow-up blood collection, but groups did not differ in their baseline levels of thrombocytes or number of days between the baseline to the infusion, and the infusion to the follow-up (Table 6.1.). Although it was not the primary end point of the safety lab, in the context of these results and literature, it would have been compelling to sample blood at other time points, *i.e.* 1 h, 24 h and 30 days after infusion, in conjunction with thrombocyte reactivity. It would enable to test the proposed biphasic model and to monitor in which timeframe normalization would be reached.

6.6. Conclusion Study 4 Ketamine

Glutamatergic and peripheral markers of ketamine action

There was a significant negative correlation between changes in Acet-Tub/TRF ratio in plasma, a marker of microtubule dynamics in the brain with the glutamatergic system in the pgACC, and it was particularly pronounced in women. In the pgACC the Glu/tCr was decreased 24 h after infusion, which was sex-independent effect. In contrasts, the increase in Acet-Tub/TRF was significant only in women. The results suggest that both Glu/tCr and microtubular proteins such as Acet-Tub/TRF have ketamine-related biomarker potential. However, patient studies connecting clinical outcomes to these imaging and molecular measures are needed for future validation and development.

Safety analysis

After a single sub-anaesthetic dose of ketamine healthy participants showed a sex-independent increase in number of thrombocytes, while other blood safety lab parameters were unchanged two weeks after infusion. These results suggest monitoring of patients with pre-existing conditions, for example ones with history of coagulation or coronary diseases (Biffi, Scotti and Corrao, 2017). Moreover, the potential aftereffects of repeated doses need to be investigated, especially in conjunction with other drugs. Lastly, proposed thrombocyte dynamics after ketamine may explain the previously observed BDNF changes to depend on thrombocyte variation.

Prediction of peripheral and imaging measures

In controls, demographic factors did not predict the magnitude of the relative changes of any of the measured variables. Moreover, total acute dissociative score did not also associate to any of the investigated variables, except marginally with the Acet-Tub/TRF in women.

Chapter 7. General conclusion & Critical outlook

7.1. Summary

Studies 1 & 2 sought to examine imaging markers of vulnerability traits and endophenotype of affect-related disorders in controls, in the cingulate cortex, with an emphasis on the pgACC. Measure of alexithymia, a personality construct of deficiencies in affect recognition, was correlated to neuronal metabolite markers in a sex-independent (in the pgACC), and sex-dependent (in the PCC and the dACC) manner. The inhibition/excitation balance in the pgACC mediated the relationship between a SNP in a GABAergic-related gene, *GAD2*, but only in women. Study 3 showed glutamatergic changes in the pgACC in the MDD patients, which was moreover symptom dependent. Finally, Study 4 showed changes in the glutamate in the pgACC 24 h after ketamine challenge, which were correlated to peripheral blood markers, again more significantly for women.

Taken together, results from these multilevel, multimodal investigations corroborate critical role of the pgACC in affect-related measures. However, there are certain aspects which should be taken into account when considering application of imaging markers.

7.2. Regional and metabolite convergence

The regional convergence of deviations in Study 1, 2 & 3 confirmed the importance of the pgACC in affect-related processing, even though the measures were covering different aspects of the latter: alexithymia, with deficits in processing of self& other feelings, harm avoidance, a measure of anxiety-related phenotype, and MDD, a complex disorder with, for example, deficits in valence processing and ruminative thoughts.

The role of the pgACC in affect-related and other psychiatric disorders is very well recorded. Results from structural (Ellison-Wright and Bullmore, 2010), connectivity (Anand *et al.*, 2009), spectroscopy (Yüksel and Öngür, 2010), task fMRI (Victor *et al.*, 2013) and PET studies (Cannon *et al.*, 2007) all point towards aberrant functioning of this frontal brain hub. Nevertheless, the directionality, or the emergence of the aberrant functioning differs between disorders (for example between unipolar and bipolar depression) (Anand *et al.*, 2009; Taylor, 2014) or even within a disorder

(Etkin and Wager, 2007). This speaks for a general regional vulnerability, which depending on the genetic composition and environmental exposures, externalizes with a distinct pathological affective phenotype. As a speculation, we can imagine that the individual pathological affective phenotype develops as compensation to a particular stressor, such as childhood trauma (Birn *et al.*, 2014).

The vulnerability and the plasticity of the pgACC to life-stressors is compelling and comparable to the one of hippocampus, the most investigated region in animal models of depression (Krishnan and Nestler, 2008). This might be due to its position as a 'gate region' between limbic and cortical areas (Kupfer, Frank and Phillips, 2012), which on one hand makes it susceptible to any aberrant inputs, but on the other, a good candidate marker for detecting pathological changes, wherever they might originate from.

The regional convergence was however not confirmed with specific metabolite confluence. In Study 1 the sex-unspecific finding was a negative correlation of TAS-20 and NAA/tCr, which was interpreted as a signature of neuronal integrity decrease which has not yet reached macroscopic level observable with cortical thickness. Glutamatergic-related findings were associated with other areas of the cingulate cortex and were sex specific; in women TAS-20 negatively correlated to the PCC Glx/NAA, and in men positively with the dACC/aMCC Glx/NAA. Further on, in Study 2, GABA/Glu mediated the association between HA and polymorphism in a GABA synthesizing enzyme, GAD65, but only in women. Lastly, in Study 3, MDD patients showed increased Gln/Glu ratio and Gln/tCr, and marginally decreased Glu/tCr, that was furthermore dependent on symptom severity. The results speak for astrocyte affiliated Gln-Glu cycling aberrations.

The association of GABAergic system to variety of anxiety-related disorders is well documented (Nuss, 2015), but it seems generally absent for the MDD (Romeo *et al.*, 2018). The results from Study 2 and 3 could thus be evaluated as biomarkers of specific phenotipology that could relate to treatment success of pharamcoagents, related to their respective target receptors. As an illustration, patients with comorbid MDD and anxiety have displayed lower remission rates after SSRI intake (Rush *et al.*, 2006; Chekroud *et al.*, 2016).

On the other hand, the results of Study 1 show certain overlap with both Study 2& 3. The NAA/tCr is an indicator of lower neuronal integrity, which can have multiple

origins. Complementing, in a more recent study from our lab, a positive correlation between the pgACC Glu/GABA ratio and TAS-20 was found in a robust sample (Widmann, Kuhnel, 2018, *in submission*). Authors interpreted that the Glu/GABA ratio reflects facets of affect processing, automatic (Glu) and cognitive (GABA). Nevertheless, alexithymia, which subsumes both aspects of self- and other- affect identification deficits, is represented best with regional excitation/inhibition and neuronal integrity.

In sum, the lack of metabolite convergence, and its modulation by sex, or clinical status, is a sobering fact that spectroscopic measures are not independent continuous variables with a clear cut-off point for a pathological change. Rather, they should be considered in the context of other markers, like genetic predispositions.

7.3. Demographic diversity as an asset and not a confound

There is an increasing recognition that part of the failure of translation of mechanistic psychiatric research to clinical realm comes from a demographic bias, where young, fit, men with European descent, or male animals are predominantly recruited. For example, recent account of polygenic risk score for schizophrenia showed a clear ancestry component (Curtis, 2018). Given that most of the GWAS studies are done on participants with European ancestry, the wider applicability was put in question. Other fields of biomedicine are also trying to move forward with inclusion of relevant demographic characteristics, which will have also improved treatment success.

Here, Studies 1& 2 have demonstrated that a minimal correction with including sex as a moderating factor, might have differential result on the assumed markers of affective behavior. Major limitation of both Studies 1&2 was lack of information on the menstrual cycle, which might have explained further variance. In the light of higher prevalence of affective disorders (anxiety and MDD in particular) in women, it is pressing to understand causal mechanisms of such sex-driven discrepancies. In Study 2 GABA/Glu levels were related the gene polymorphism and HA only in women, consequentially implying a sex-hormone modulation of gene activity. However, differences in metabolites might also come as consequences of different socialization patterns (Study 1), and not necessarily as a biological ground truth.

Therefore, it is imperative not to make causal conclusions without substantiated data, on the biological predispositions following any demographic parameter, since that can lead to cases of neuroracism, neurosexism, etc. Fulfilling societal responsibility of

proper research use, the wider participants' inclusion will nevertheless enhance translational efforts.

7.4. Clinical heterogeneity

An important limitation of the high-field imaging of a patient population are inclusion criteria and psychiatric and other medical comorbidities, so the final patient group was significantly more modest when compared to control population from Study 1, 2 & 4. Moreover, the clinical heterogeneity of affective disorder patients, even in small samples, is inevitable. Additionally, moderation of symptom severity and glutamatergic levels displayed that a relationship between clinical dimensions and underlying metabolites does not necessarily needs to be linear, probably was a consequence of compensation mechanisms.

Consequentially, some researchers have considered moving from classical diagnostic criteria (such as ICD-10 or DSM) towards dimensional categorization (e.g. focusing on anxiety symptoms across disorders), as proposed by the Research Domain Criteria (RDoC) (Insel *et al.*, 2010). Recently, within the framework of RDoC, studies have employed endophenotypes at intermediate levels (molecular, cellular, circuitry, physiology), which are ultimately related to dimensional pathophysiological phenotypes instead of diagnostic, categorical ones (Miller and Rockstroh, 2013). Further on, this approach proposes to connect the dimensional phenotype in patients with a similar one in controls (e.g. trait anxiety), which would then indeed provide a continuum of measurable intermediate endophenotypes (Preisig, Merikangas and Angst, 2001). This reliable intermediate endophenotypes would ideally in future pertain to diagnostic tests battery, but the clinical utility in terms of treatment selection has yet to be tested and proven (Alexopoulos and Areean, 2014). The problematics of comorbidity or symptom fluidity however stays, even when we move to dimensional categorization. It is easy to imagine a patient that has more than one “dimensional phenotype”; which one is the more reliable or important one for diagnosis or treatment selection?

An idealistic approach would acknowledge individual clinical heterogeneity, in an alliance with well-established surrogate markers that are also sensitive to treatment response.

Finally, majority of research of affective disorders does not enforce the standardized definition of an endophenotype, or intermediate phenotype, specifically the

heritability or segregation from other psychiatric disorders (Hasler *et al.*, 2004). This is rooted in the reality that most of the endophenotypes for affective disorders and disorders themselves are polygenic, and that a genetic polymorphism does not necessarily corresponds one-to-one to a complex behavioural phenotype (Glazier, Nadeau and Aitman, 2002; Daskalakis *et al.*, 2013). However, this should not prevent from harmonizing the terminology across research domains.

7.5. Ketamine mechanisms of action and future applications

In sum, Study 4 observed a general decrease in Glu/tCr 24 h after infusion that was correlated with an increase in Acet-Tub/TRF increase, significantly only in women.

Major limitation of Study 4 was inclusion of only healthy controls. MDD might respond to the treatment differentially than controls, as a function of baseline or shifted homeostasis, especially in the Gln-Glu cycling or brain energetics. Even so, several studies have found very similar imaging readouts across modalities in both groups (Esterlis *et al.*, 2017; Evans, Szczepanik, *et al.*, 2018) suggesting investigations in controls might be useful in determining proper biomarkers of drug reactivity.

In connection to the decrease of Glu/tCr reported here, an increase in Gln/Glu 24 h after infusion in controls was previously found in our lab (Li *et al.*, 2017). Together these results are in direct opposition with data from Study 3, and the assumed antidepressant mechanisms of glutamate-modulating medication. The primary hypothesis of restorative properties of ketamine by increasing cycling of glutamatergic system in MDD by ketamine, has yet remained to be proven (Evans, Lally, *et al.*, 2018). What was additionally discernable from the results of Study 3, is that clinical heterogeneity connects to the underlying metabolite substrate. It might be then that only certain severity population will profit from ketamine. In support, a recent study has noted that clinical features such as suicide ideation correlate to treatment response (Ballard *et al.*, 2018).

The outcome of presuming different glutamatergic pathomechanisms across symptom severity subgroups would be to expect differences also on the level of treatment success of glutamate-based medication. Unfortunately, neither clinical differences in antidepressant efficacy nor metabolite changes have been reported for ketamine across severity subgroups.

Evidence of other neurotransmitter systems (like norepinephrine) acting in parallel to directly targeted glutamatergic system have been brought forward. In addition,

some studies have focused on alternative pathways of mechanisms of action, including via sex-steroids (Dossat *et al.*, 2018; Ho *et al.*, 2018), anti-inflammation or astroglia (Ardalan *et al.*, 2017).

Notwithstanding, the prevailing theory of ketamine's mode of action remains the increase of synaptic potentiation (Cornwell *et al.*, 2012; Abdallah, Sanacora, *et al.*, 2018). Using ketamine as an augmentation to other medication, and most importantly therapy, will have increase the chances of restoring biases in affect processing via creating new neuronal pathways (Walter, Li and Demenescu, 2014).

So far, there has been a lack of a clear peripheral biomarker in connection to either drug activity or efficacy. Majority of research efforts has been put on BDNF, with mixed success (Duncan *et al.*, 2013; Haile *et al.*, 2014). The reasons are two-fold, there is not a not a distinct validated biomarker for MDD (Hasler *et al.*, 2004), and the influence of diurnal variation and demographic properties on the parameters, such as BDNF (Bus *et al.*, 2011) is not accounted for in majority of studies. The Acet-Tub/TRF was also influenced, mainly by sex and contraception use. Moreover, the increase was present only in women, limiting its universality. Future research might focus on cheaper options, such as basic blood parameters, leukocytes or thrombocytes, which have been shown to change after ketamine infusion (Kiraly *et al.*, 2017; Colic *et al.*, 2018). The fact that there was a change in transferrin and that it was more prominent in women hints that the impact of hepatic metabolism on markers of ketamine activity is substantial and should be further investigated.

Alternative approach would be to investigate drug related markers of cellular and circuit mechanisms which are more closely related to the genetic architecture of MDD. For example, two complementary studies from our lab have demonstrated that the same SNP for the NET affects magnitude of hyper-acute blood pressure change (Liebe *et al.*, 2017), as well as acute FC of the Locus Coeruleus (LC) (Liebe *et al.*, 2018). From a clinical perspective, it may be that patients with one gene variant will respond faster to the treatment, or regarding safety parameters, should receive different care during ketamine infusions.

The imaging or the peripheral markers of activity and efficacy of ketamine's antidepressant mechanisms are still inadequate for clinical usage. Although some imaging markers like functional connectivity reconfiguration, have been replicated (Scheidegger *et al.*, 2012; Evans, Szczepanik, *et al.*, 2018; Li *et al.*, 2018), more

applicable and robust (with bigger effect size) biomarkers, especially ones reflecting synaptic potentiation need to still be validated.

7.6. Methodological considerations

Employing high-field MRS to separate similar spectral signals of Glu, Gln and GABA proved to be crucial, especially in Study 3, where unexpected finding of increased Gln/tCr in MDD was found (Godlewska *et al.*, 2017). Such studies strengthen or correct previous hypothesis. Based on the results, future studies can than scan at lower field strengths with sequences optimized for the metabolite in question.

Nevertheless, using SVS spectroscopy might bias the report considering that putative effects were tested only in the *a priori* chosen voxels. This is particularly important for Study 4, since ketamine-related changes in glutamate levels might also occur in other brain regions like the dmPFC or the hippocampus (Salvadore *et al.*, 2012; Kraguljac *et al.*, 2017), especially during hyper-acute phase (glutamatergic surge). This would be resolved by applying MRSI during infusion, but such technically advanced experiment was not available during this study. This would allow prospective trials, to confirm the overall regional specificity of the ventral ACC, also considering modest effect sizes of Glu/tCr change 24 h after infusion.

References

- Abdallah, C. G. *et al.* (2014) 'Decreased occipital cortical glutamate levels in response to successful cognitive-behavioral therapy and pharmacotherapy for major depressive disorder', *Psychotherapy and Psychosomatics*, 83(5), pp. 298–307. doi: 10.1159/000361078.
- Abdallah, C. G., De Feyter, H. M., *et al.* (2018) 'The effects of ketamine on prefrontal glutamate neurotransmission in healthy and depressed subjects', *Neuropsychopharmacology*. Springer US, 43(10), pp. 2154–2160. doi: 10.1038/s41386-018-0136-3.
- Abdallah, C. G., Sanacora, G., *et al.* (2018) 'The neurobiology of depression, ketamine and rapid-acting antidepressants: Is it glutamate inhibition or activation?', *Pharmacology and Therapeutics*. Elsevier Inc., 190(June), pp. 148–158. doi: 10.1016/j.pharmthera.2018.05.010.
- Abler, B. *et al.* (2011) 'Neural correlates of antidepressant-related sexual dysfunction: a placebo-controlled fMRI study on healthy males under subchronic paroxetine and bupropion', *Neuropsychopharmacology*. Nature Publishing Group, 36(9), p. 1837.
- Ackenheil, M. *et al.* (1999) 'MINI mini international neuropsychiatric interview, German version 5.0. o DSM IV', *Psychiatrische Universitätsklinik München, Germany*.
- Addis, M. E. (2008) 'Gender and depression in men', *Clinical Psychology: Science and Practice*, 15(3), pp. 153–168. doi: 10.1111/j.1468-2850.2008.00125.x.
- Aiello, M. *et al.* (2015) 'Relationship between simultaneously acquired resting-state regional cerebral glucose metabolism and functional MRI: A PET/MR hybrid scanner study', *NeuroImage*. Elsevier Inc., 113, pp. 111–121. doi: 10.1016/j.neuroimage.2015.03.017.
- Al-Harbi, K. S. (2012) 'Treatment-resistant depression: Therapeutic trends, challenges, and future directions', *Patient Preference and Adherence*, 6, pp. 369–388. doi: 10.2147/PPA.S29716.
- Alexopoulos, G. S. and Arean, P. (2014) 'A model for streamlining psychotherapy in the RDoC era: the example of "Engage"', *Molecular psychiatry*. Nature Publishing Group, 19(1), p. 14.
- Allen, A. P. *et al.* (2015) 'Serum BDNF as a peripheral biomarker of treatment-resistant depression and the rapid antidepressant response: A comparison of ketamine and ECT', *Journal of Affective Disorders*. Elsevier, 186, pp. 306–311. doi: 10.1016/j.jad.2015.06.033.
- Allman, J. *et al.* (2001) 'The Anterior Cingulate Cortex', *Annals of the New York Academy of Sciences*, 935(1), pp. 107–117. doi: 10.1111/j.1749-6632.2001.tb03476.x.
- Allman, J. M. *et al.* (2011) 'The von Economo neurons in the fronto-insular and anterior cingulate cortex', *Annals of the New York Academy of Sciences*, 1225(1), pp. 59–71. doi: 10.1111/j.1749-6632.2011.06011.x.
- Anand, A. *et al.* (2009) 'Resting state corticolimbic connectivity abnormalities in unmedicated bipolar disorder and unipolar depression.', *Psychiatry research*. Elsevier Ireland Ltd, 171(3), pp. 189–98. doi: 10.1016/j.psychres.2008.03.012.
- Andrews-Hanna, J. R. *et al.* (2010) 'Functional-anatomic fractionation of the brain's default network.', *Neuron*. Elsevier Ltd, 65(4), pp. 550–62. doi: 10.1016/j.neuron.2010.02.005.
- Anticevic, A. *et al.* (2015) 'N-methyl-D-aspartate receptor antagonist effects on prefrontal cortical connectivity better model early than chronic schizophrenia', *Biological Psychiatry*, 77(6), pp. 569–580. doi: 10.1016/j.biopsych.2014.07.022.
- Apps, M. A. J., Rushworth, M. F. S. and Chang, S. W. C. (2016) 'The Anterior Cingulate Gyrus and Social Cognition: Tracking the Motivation of Others', *Neuron*. The Authors, 90(4), pp. 692–707. doi: 10.1016/j.neuron.2016.04.018.
- Ardalan, M. *et al.* (2017) 'Rapid antidepressant effect of ketamine correlates with astroglial plasticity in the hippocampus', *British Journal of Pharmacology*, 174(6), pp. 483–492. doi: 10.1111/bph.13714.
- Arnone, D. *et al.* (2012) 'Magnetic resonance imaging studies in unipolar depression: Systematic review and meta-regression analyses', *European Neuropsychopharmacology*. Elsevier B.V., 22(1), pp. 1–16. doi: 10.1016/j.euroneuro.2011.05.003.
- Aslan, J. E. *et al.* (2013) 'Histone deacetylase 6-mediated deacetylation of α -tubulin coordinates cytoskeletal and signaling events during platelet activation', *American Journal of Physiology-Cell Physiology*, 305(12), pp. C1230–C1239. doi: 10.1152/ajpcell.00309.2013.
- Ataoglu, A. and Canan, F. (2009) 'Mean Platelet Volume in Patients With Major Depression Effect of Escitalopram Treatment', *J Clin Psychopharmacol*, 29(4), pp. 368–371. doi: 10.1097/JCP.0b013e3181abdf7.
- Atkinson, P. M., Taylor, D. I. and Chetty, N. (1985) 'Inhibition of platelet aggregation by ketamine hydrochloride', *Thrombosis*

- Research*, 40(2), pp. 227–234.
- Auer, D. P. *et al.* (2000) 'Reduced glutamate in the anterior cingulate cortex in depression: an in vivo proton magnetic resonance spectroscopy study.', *Biological psychiatry*, 47(4), pp. 305–13. Available at: <http://www.ncbi.nlm.nih.gov/pubmed/10686265>.
- Autry, A. E. *et al.* (2011) 'NMDA receptor blockade at rest triggers rapid behavioural antidepressant responses.', *Nature*. Nature Publishing Group, 475(7354), pp. 91–95. doi: 10.1038/nature10130.
- Azevedo, R. T. *et al.* (2017) 'Cardiac afferent activity modulates the expression of racial stereotypes', *Nature Communications*. Nature Publishing Group, 8, pp. 1–9. doi: 10.1038/ncomms13854.
- Bach, M. *et al.* (1996) 'Validation of the German version of the 20-item Toronto Alexithymia Scale in normal persons and psychiatric patients', *Psychotherapie, Psychosomatik, Medizinische Psychologie*, 46(1), pp. 23–28.
- Bagby, R. M., Parker, J. D. A. and Taylor, G. J. (1994) 'The twenty-item Toronto Alexithymia Scale—I. Item selection and cross-validation of the factor structure', *Journal of psychosomatic research*. Elsevier, 38(1), pp. 23–32.
- Bagby, R. M., Taylor, G. J. and Parker, J. D. A. (1994) 'The twenty-item Toronto Alexithymia Scale—II. Convergent, discriminant, and concurrent validity', *Journal of psychosomatic research*. Elsevier, 38(1), pp. 33–40.
- Bak, L. K., Schousboe, A. and Waagepetersen, H. S. (2006) 'The glutamate/GABA-glutamine cycle: Aspects of transport, neurotransmitter homeostasis and ammonia transfer', *Journal of Neurochemistry*, 98(3), pp. 641–653. doi: 10.1111/j.1471-4159.2006.03913.x.
- Ballard, Elizabeth D *et al.* (2018) 'Characterizing the course of suicidal ideation response to ketamine', *Journal of affective disorders*. Elsevier, 241, pp. 86–93.
- Ballard, Elizabeth D. *et al.* (2018) 'Parsing the heterogeneity of depression: An exploratory factor analysis across commonly used depression rating scales', *Journal of Affective Disorders*. Elsevier B.V., 231(August 2017), pp. 51–57. doi: 10.1016/j.jad.2018.01.027.
- Banach, M. *et al.* (2017) 'Etiology and clinical relevance of elevated platelet count in ICU patients', *Medizinische Klinik - Intensivmedizin und Notfallmedizin*, pp. 1–7. doi: 10.1007/s00063-017-0276-y.
- Banasr, M. and Duman, R. S. (2008) 'Glial Loss in the Prefrontal Cortex Is Sufficient to Induce Depressive-like Behaviors', *Biol Psychiatry*, 64(10), pp. 863–870. doi: 10.1016/j.biopsych.2008.06.008.
- Banks, S. J. *et al.* (2007) 'Amygdala-frontal connectivity during emotion regulation', *Social Cognitive and Affective Neuroscience*, 2(4), pp. 303–312. doi: 10.1093/scan/nsm029.
- Barth, C., Villringer, A. and Sacher, J. (2015) 'Sex hormones affect neurotransmitters and shape the adult female brain during hormonal transition periods.', *Frontiers in neuroscience*, 9(37). doi: 10.3389/fnins.2015.00037.
- Bartoli, F. *et al.* (2017) 'Ketamine as a rapid-acting agent for suicidal ideation: A meta-analysis', *Neuroscience and Biobehavioral Reviews*. Elsevier Ltd, 77, pp. 232–236. doi: 10.1016/j.neubiorev.2017.03.010.
- Beauchaine, T. P. (2009) 'Role of biomarkers and endophenotypes in prevention and treatment of psychopathological disorders'. *Future Medicine*.
- Bergado-Acosta, J. R. *et al.* (2008) 'Critical role of the 65-kDa isoform of glutamic acid decarboxylase in consolidation and generalization of Pavlovian fear memory', *Learning & Memory*, 15(3), pp. 163–171. doi: 10.1101/lm.705408.during.
- Berman, R. M. *et al.* (2000) 'Antidepressant effects of ketamine in depressed patients.', *Biological psychiatry*, 47(4), pp. 351–4. Available at: <http://www.ncbi.nlm.nih.gov/pubmed/10686270>.
- Bermond, B., Vorst, H. C. M. and Moorman, P. P. (2006) 'Cognitive neuropsychology of alexithymia: implications for personality typology.', *Cognitive neuropsychiatry*, 11(3), pp. 332–360. doi: 10.1080/13546800500368607.
- Berpohl, F. *et al.* (2009) 'Attentional modulation of emotional stimulus processing in patients with major depression—Alterations in prefrontal cortical regions', *Neuroscience Letters*, 463(2), pp. 108–113. doi: 10.1016/j.neulet.2009.07.061.
- Bernhardt, B. C. *et al.* (2014) 'Selective disruption of sociocognitive structural brain networks in autism and alexithymia', *Cerebral Cortex*, 24(12), pp. 3258–3267. doi: 10.1093/cercor/bht182.
- Bernstein, H.-G. *et al.* (2015) 'Reduced density of glutamine synthetase immunoreactive astrocytes in different cortical areas in major depression but not in bipolar I disorder', *Frontiers in Cellular Neuroscience*, 9(August), pp. 1–12. doi: 10.3389/fncel.2015.00273.
- Berthoz, S. *et al.* (2002) 'Effect of impaired recognition and expression of emotions on frontocingulate cortices: an fMRI study of men with alexithymia.', *The American journal of psychiatry*, 159(6), pp. 961–7. Available at: <http://www.ncbi.nlm.nih.gov/pubmed/12042184>.
- Beurel, E., Song, L. and Joep, R. S. (2011) 'Inhibition of glycogen synthase kinase-3 is necessary for the rapid antidepressant effect of ketamine in mice', *Molecular Psychiatry*, 16(11), pp. 1068–1070. doi: 10.1038/mp.2011.47.

- Bianchi *et al.* (2009) 'Chronic fluoxetine differentially modulates the hippocampal microtubular and serotonergic system in grouped and isolation reared rats', *European Neuropsychopharmacology*. Elsevier B.V., 19(11), pp. 778–790. doi: 10.1016/j.euroneuro.2009.06.005.
- Bianchi, Hagan, J. J. and Heidbreder, C. a (2005) 'Neuronal plasticity, stress and depression: involvement of the cytoskeletal microtubular system?', *Current drug targets. CNS and neurological disorders*, 4(5), pp. 597–611. doi: 10.2174/156800705774322012.
- Bianchi, M. and Baulieu, E.-E. (2012) '3-Methoxy-pregnenolone (MAP4343) as an innovative therapeutic approach for depressive disorders', *Proceedings of the National Academy of Sciences*, 109(5), pp. 1713–1718. doi: 10.1073/pnas.1121485109.
- Bienvenu, O. J. *et al.* (2004) 'Anxiety and depressive disorders and the five-factor model of personality: A higher-and lower-order personality trait investigation in a community sample', *Depression and anxiety*. Wiley Online Library, 20(2), pp. 92–97.
- Biffi, A., Scotti, L. and Corrao, G. (2017) 'Use of antidepressants and the risk of cardiovascular and cerebrovascular disease: a meta-analysis of observational studies', *European Journal of Clinical Pharmacology*, pp. 1–11. doi: 10.1007/s00228-016-2187-x.
- Binder, J. R. *et al.* (2009) 'Where is the semantic system? A critical review and meta-analysis of 120 functional neuroimaging studies', *Cerebral Cortex*, 19(12), pp. 2767–2796. doi: 10.1093/cercor/bhp055.
- Bird, G. *et al.* (2010) 'Empathic brain responses in insula are modulated by levels of alexithymia but not autism', *Brain*. Oxford University Press, 133(5), pp. 1515–1525.
- Birn, R. M. *et al.* (2014) 'Childhood maltreatment and combat posttraumatic stress differentially predict fear-related fronto-subcortical connectivity', *Depression and anxiety*. Wiley Online Library, 31(10), pp. 880–892.
- Biswal, B. *et al.* (1995) 'Functional connectivity in the motor cortex of resting human brain using echo-planar MRI', *Magnetic resonance in medicine*. Wiley Online Library, 34(4), pp. 537–541.
- Biswal, B. B. *et al.* (2010) 'Toward discovery science of human brain function.', *Proceedings of the National Academy of Sciences of the United States of America*, 107(10), pp. 4734–4739. doi: 10.1073/pnas.0911855107.
- Björkholm, C. and Monteggia, L. M. (2016) 'BDNF - A key transducer of antidepressant effects', *Neuropharmacology*, 102(2016), pp. 72–79. doi: 10.1016/j.neuropharm.2015.10.034.
- Blanchard, D. C., Griebel, G. and Blanchard, R. J. (1995) 'Gender bias in the preclinical psychopharmacology of anxiety: male models for (predominantly) female disorders', *Journal of Psychopharmacology*, 9(2), pp. 79–82. doi: 10.1177/026988119500900201.
- Bleeker, J. S. and Hogan, W. J. (2011) 'Thrombocytosis: Diagnostic Evaluation, Thrombotic Risk Stratification, and Risk-Based Management Strategies', *Thrombosis*, 2011, pp. 1–16. doi: 10.1155/2011/536062.
- Boly, M. *et al.* (2008) 'Intrinsic brain activity in altered states of consciousness: How conscious is the default mode of brain function?', *Annals of the New York Academy of Sciences*, 1129, pp. 119–129. doi: 10.1196/annals.1417.015.
- van der Bom, J. G. *et al.* (2009) 'Platelet count and the risk for thrombosis and death in the elderly', *Journal of Thrombosis and Haemostasis*, 7(3), pp. 399–405. doi: 10.1111/j.1538-7836.2008.03267.x.
- De Bondt, T. *et al.* (2015) 'Stability of resting state networks in the female brain during hormonal changes and their relation to premenstrual symptoms', *Brain Research*. Elsevier, 1624, pp. 275–285. doi: 10.1016/j.brainres.2015.07.045.
- Borsci, G. *et al.* (2009) 'Alexithymia in healthy women: A brain morphology study', *Journal of Affective Disorders*. Elsevier B.V., 114(1–3), pp. 208–215. doi: 10.1016/j.jad.2008.07.013.
- Bottomley, P. A. (1987) 'Spatial localization in NMR spectroscopy in vivo', *Annals of the New York Academy of Sciences*. Wiley Online Library, 508(1), pp. 333–348.
- Botvinick, M. M., Cohen, J. D. and Carter, C. S. (2004) 'Conflict monitoring and anterior cingulate cortex: An update', *Trends in Cognitive Sciences*, 8(12), pp. 539–546. doi: 10.1016/j.tics.2004.10.003.
- Boutin, P. *et al.* (2003) 'GAD2 on chromosome 10p12 is a candidate gene for human obesity', *PLoS Biology*, 1(3), pp. 361–371. doi: 10.1371/journal.pbio.0000068.
- Brandão, L. A. and Domingues, R. C. (2004) *MR Spectroscopy of the Brain*. Lippincott Williams & Wilkins.
- Braver, T. S. *et al.* (2001) 'Anterior cingulate cortex and response conflict: Effects of frequency, inhibition and errors', *Cerebral Cortex*, 11(9), pp. 825–36. doi: 10.1093/cercor/11.9.825.
- Bremner, J. D. *et al.* (1998) 'Measurement of dissociative states with the', *Clinician Administered Dissociative States Scale (CADSS)*. *J Trauma Stress*, 11(1), pp. 125–36.
- Brennan, B. P. *et al.* (2010) 'Rapid enhancement of glutamatergic neurotransmission in bipolar depression following treatment

- with riluzole', *Neuropsychopharmacology*, 35(3), pp. 834–846. doi: 10.1038/npp.2009.191.
- Brennan, B. P. *et al.* (2017) 'Acute change in anterior cingulate cortex GABA, but not glutamine/glutamate, mediates antidepressant response to citalopram', *Psychiatry Research - Neuroimaging*. Elsevier Ireland Ltd, 269(July), pp. 9–16. doi: 10.1016/j.psychres.2017.08.009.
- Bright, M. G. and Murphy, K. (2015) 'Is fMRI "noise" really noise? Resting state nuisance regressors remove variance with network structure', *NeuroImage*. Elsevier B.V., 114, pp. 158–169. doi: 10.1016/j.neuroimage.2015.03.070.
- Brown, T. R. (2007) 'Chemical shift imaging', *eMagRes*. Wiley Online Library.
- Brown, T. R., Kincaid, B. M. and Ugurbil, K. (1982) 'NMR chemical shift imaging in three dimensions', *Proceedings of the National Academy of Sciences*. National Acad Sciences, 79(11), pp. 3523–3526.
- Buckner, R. L., Andrews-Hanna, J. R. and Schacter, D. L. (2008) 'The brain's default network: Anatomy, function, and relevance to disease', *Annals of the New York Academy of Sciences*, 1124, pp. 1–38. doi: 10.1196/annals.1440.011.
- Burke, H. M. *et al.* (2005) 'Depression and cortisol responses to psychological stress: a meta-analysis', *Psychoneuroendocrinology*. Elsevier, 30(9), pp. 846–856.
- Bus, B. A. *et al.* (2011) 'Determinants of serum brain-derived neurotrophic factor', *Psychoneuroendocrinology*. Elsevier Ltd, 36(2), pp. 228–239. doi: 10.1016/j.psyneuen.2010.07.013.
- Bush, G. *et al.* (2002) 'Dorsal anterior cingulate cortex: A role in reward-based decision making', *Proceedings of the National Academy of Sciences*, 99(1), pp. 523–528. doi: 10.1073/pnas.012470999.
- Bush, G., Luu, P. and Posner, M. (2000) 'Cognitive and emotional influences in anterior cingulate cortex.', *Trends Cogn. Sci.*, 4(6), pp. 215–222. doi: 10.1016/S1364-6613(00)01483-2.
- Caddy, C. *et al.* (2014) 'Ketamine as the prototype glutamatergic antidepressant: pharmacodynamic actions, and a systematic review and meta-analysis of efficacy', *Therapeutic Advances in Psychopharmacology*, 4(2), pp. 75–99. doi: 10.1177/2045125313507739.
- Cannon, D. M. *et al.* (2007) 'Elevated Serotonin Transporter Binding in Major Depressive Disorder Assessed Using Positron Emission Tomography and [¹¹C]DASB; Comparison with Bipolar Disorder', *Biological Psychiatry*, 62(8), pp. 870–877. doi: 10.1016/j.biopsych.2007.03.016.
- Cao, Q. *et al.* (2006) 'Abnormal neural activity in children with attention deficit hyperactivity disorder: A resting-state functional magnetic resonance imaging study', *NeuroReport*, 17(10), pp. 1033–1036. doi: 10.1097/01.wnr.0000224769.92454.5d.
- Carlson, P. J. *et al.* (2013) 'Neural correlates of rapid antidepressant response to ketamine in treatment-resistant unipolar depression: A preliminary positron emission tomography study', *Biological Psychiatry*. Elsevier, 73(12), pp. 1213–1221. doi: 10.1016/j.biopsych.2013.02.008.
- Carpenter, K. M. and Addis, M. E. (2000) 'Alexithymia, gender, and responses to depressive symptoms', *Sex Roles*, 43(9/10), pp. 629–644. doi: 10.1023/A:1007100523844.
- Carspecken, C. W. *et al.* (2018) 'Ketamine Anesthesia Does Not Improve Depression Scores in Electroconvulsive Therapy: A Randomized Clinical Trial.', *Journal of neurosurgical anesthesiology*.
- Carta, S. *et al.* (2006) 'Histone deacetylase inhibitors prevent exocytosis of interleukin-1beta-containing secretory lysosomes: role of microtubules.', *Blood*, 108(5), pp. 1618–26. doi: 10.1182/blood-2006-03-014126.
- Casoni, D., Spadavecchia, C. and Adami, C. (2015) 'S-ketamine versus racemic ketamine in dogs: Their relative potency as induction agents', *Veterinary Anaesthesia and Analgesia*. Association of Veterinary Anaesthetists and the American College of Veterinary Anesthesia and Analgesia, 42(3), pp. 250–259. doi: 10.1111/vaa.12200.
- Caspi, A. *et al.* (2003) 'Influence of life stress on depression: moderation by a polymorphism in the 5-HTT gene', *Science*. American Association for the Advancement of Science, 301(5631), pp. 386–389.
- Cavassila, S. *et al.* (2001) 'Cramér–Rao bounds: an evaluation tool for quantitation', *NMR in Biomedicine: An International Journal Devoted to the Development and Application of Magnetic Resonance In Vivo*. Wiley Online Library, 14(4), pp. 278–283.
- Cem Gabay, M. D. and Irving Kushner, M. D. (1999) 'Acute-Phase Proteins and Other Systemic Responses to Inflammation', *The New England journal of medicine*, 340(6), pp. 448–454. doi: 10.1056/NEJM199902113400607.
- Chacón-Fernández, P. *et al.* (2016) 'Brain-derived neurotrophic factor in megakaryocytes', *Journal of Biological Chemistry*, 291(19), pp. 9872–9881. doi: 10.1074/jbc.M116.720029.
- Chai, X. J. *et al.* (2012) 'Anticorrelations in resting state networks without global signal regression', *NeuroImage*, 59(2), pp. 1420–1428. doi: 10.1016/j.neuroimage.2011.08.048.
- Chang, Y. *et al.* (2004) 'Mechanisms involved in the antiplatelet activity of ketamine in human platelets', *Journal of Biomedical*

- Science*, 11(6), pp. 764–772. doi: 10.1159/000081823.
- Chao-Gan, Y. and Yu-Feng, Z. (2010) 'DPARSF: A MATLAB Toolbox for "Pipeline" Data Analysis of Resting-State fMRI.', *Frontiers in systems neuroscience*, 4(May), p. 13. doi: 10.3389/fnsys.2010.00013.
- Chekroud, A. M. *et al.* (2016) 'Cross-trial prediction of treatment outcome in depression: A machine learning approach', *The Lancet Psychiatry*. Elsevier Ltd, 3(3), pp. 243–250. doi: 10.1016/S2215-0366(15)00471-X.
- Chen, A. C. *et al.* (2013) 'Causal interactions between fronto-parietal central executive and default-mode networks in humans', *Proceedings of the National Academy of Sciences*, 110(49), pp. 19944–19949. doi: 10.1073/pnas.1311772110.
- Chen, Y. *et al.* (2016) 'Difference in Leukocyte composition between women before and after menopausal age, and distinct sexual dimorphism', *PLoS ONE*, 11(9), pp. 1–10. doi: 10.1371/journal.pone.0162953.
- Chester, D. S. and DeWall, C. N. (2014) 'Prefrontal recruitment during social rejection predicts greater subsequent self-regulatory imbalance and impairment: Neural and longitudinal evidence', *NeuroImage*. Elsevier Inc., 101, pp. 485–493. doi: 10.1016/j.neuroimage.2014.07.054.
- Choi, S. Y., Koh, K. H. and Jeong, H. (2013) 'Isoform-specific regulation of cytochromes P450 expression by estradiol and progesterone', *Drug Metabolism and Disposition*, 41(2), pp. 263–269. doi: 10.1124/dmd.112.046276.
- Choudary, P. V. *et al.* (2005) 'Altered cortical glutamatergic and GABAergic signal transmission with glial involvement in depression', 102(43).
- Chowdhury, G. M. I. *et al.* (2017) 'Transiently increased glutamate cycling in rat PFC is associated with rapid onset of antidepressant-like effects.', *Mol Psychiatry*, 22(1), pp. 120–126. doi: 10.1038/mp.2016.34.
- Chu, P. S. K. *et al.* (2008) 'The destruction of the lower urinary tract by ketamine abuse: A new syndrome?', *BJU International*, 102(11), pp. 1616–1622. doi: 10.1111/j.1464-410X.2008.07920.x.
- Chung, J. Y. *et al.* (2011) 'An improved PSF mapping method for EPI distortion correction in human brain at ultra high field (7T)', *Magnetic Resonance Materials in Physics, Biology and Medicine*, 24(3), pp. 179–190. doi: 10.1007/s10334-011-0251-1.
- Cieslik, E. C. *et al.* (2013) 'Is there "one" DLPFC in cognitive action control? Evidence for heterogeneity from co-activation-based parcellation.', *Cerebral cortex (New York, N.Y. : 1991)*, 23(11), pp. 2677–89. doi: 10.1093/cercor/bhs256.
- Clarke, M. *et al.* (2017) 'Ketamine modulates hippocampal neurogenesis and pro-inflammatory cytokines but not stressor induced neurochemical changes', *Neuropharmacology*. Elsevier Ltd, 112(2017), pp. 210–220. doi: 10.1016/j.neuropharm.2016.04.021.
- Cline, H. (2005) 'Synaptogenesis : A Balancing Act', *Current Biology*, 2(6), pp. 203–205. doi: 10.1016/j.cub.2005.03.010.
- Cloninger, C. R. (1987) 'A Systematic Method for Clinical Description and Classification of Personality Variants', *Archives of General Psychiatry*, 44(6), p. 573. doi: 10.1001/archpsyc.1987.01800180093014.
- Cloninger, C. R., Przybeck, T. R. and Svrakic, D. M. (1994) *The Temperament and Character Inventory (TCI): A guide to its development and use*. St. Louis, MO: Center fo Psychobiology of Personality, Washington University.
- Colic, L. *et al.* (2015) 'Metabolic mapping reveals sex-dependent involvement of default mode and salience network in alexithymia', *Social Cognitive and Affective Neuroscience*, 11(2), pp. 289–298. doi: 10.1093/scan/nsv110.
- Colic, L. *et al.* (2018) 'Delayed increase of thrombocyte levels after a single sub-anesthetic dose of ketamine – A randomized trial', *European Neuropsychopharmacology*. doi: 10.1016/j.euroneuro.2018.03.014.
- Colic, Lejla, Li, M., *et al.* (2018) 'GAD65 promoter polymorphism rs2236418 modulates harm avoidance in women via inhibition/excitation balance in the rostral ACC', *Journal of Neuroscience*. Soc Neuroscience, 38(22), pp. 5067–5077.
- Conde, C. and Cáceres, A. (2009) 'Microtubule assembly, organization and dynamics in axons and dendrites.', *Nature reviews. Neuroscience*, 10(5), pp. 319–332. doi: 10.1038/nrn2631.
- Conrad, R. *et al.* (2009) 'Alexithymia, temperament and character as predictors of psychopathology in patients with major depression', *Psychiatry Research*. Elsevier Ireland Ltd, 165(1–2), pp. 137–144. doi: 10.1016/j.psychres.2007.10.013.
- Cornwell, B. R. *et al.* (2012) 'Synaptic potentiation is critical for rapid antidepressant response to ketamine in treatment-resistant major depression', *Biological psychiatry*. Elsevier, 72(7), pp. 555–561.
- Correll, C. U. *et al.* (2017) 'Prevalence , incidence and mortality from cardiovascular disease in patients with pooled and specific severe mental illness : a large-scale meta-analysis of 3 , 211 , 768 patients and 113 , 383 , 368 controls', *World Psychiatry*, 16(2), pp. 163–180. doi: 10.1002/wps.20420.
- Creppe, C. *et al.* (2009) 'Elongator Controls the Migration and Differentiation of Cortical Neurons through Acetylation of α -Tubulin', *Cell*. Elsevier Inc., 136(3), pp. 551–564. doi: 10.1016/j.cell.2008.11.043.
- Critchley, H. D. *et al.* (2003) 'Human cingulate cortex and autonomic control: converging neuroimaging and clinical evidence', *Brain*. Oxford University Press, 126(10), pp. 2139–2152.

- Critchley, H. D. *et al.* (2005) 'Anterior cingulate activity during error and autonomic response', *NeuroImage*, 27(4), pp. 885–895. doi: 10.1016/j.neuroimage.2005.05.047.
- Curtis, D. (2018) 'Polygenic risk score for schizophrenia is more strongly associated with ancestry than with schizophrenia', *bioRxiv*. Cold Spring Harbor Laboratory, p. 287136.
- Dalgleish, T. (2004) 'The emotional brain', *Nature Reviews Neuroscience*. Nature Publishing Group, 5, p. 583. Available at: <https://doi.org/10.1038/nrn1432>.
- Daly, E. J. *et al.* (2018) 'Efficacy and safety of intranasal esketamine adjunctive to oral antidepressant therapy in treatment-resistant depression: A randomized clinical trial', *JAMA Psychiatry*, 75(2), pp. 139–148. doi: 10.1001/jamapsychiatry.2017.3739.
- Daly, M. E. (2011) 'Determinants of platelet count in humans', *Haematologica*, 96(1), pp. 10–13. doi: 10.3324/haematol.2010.035287.
- Daskalakis, N. P. *et al.* (2013) 'The three-hit concept of vulnerability and resilience: Toward understanding adaptation to early-life adversity outcome', *Psychoneuroendocrinology*. Elsevier Ltd, 38(9), pp. 1858–1873. doi: 10.1016/j.psyneuen.2013.06.008.
- Davey, C. G., Pujol, J. and Harrison, B. J. (2016) 'Mapping the self in the brain's default mode network', *Neuroimage*. Elsevier, 132, pp. 390–397.
- Davis, A. M. *et al.* (1999) 'Developmental sex differences in amino acid neurotransmitter levels in hypothalamic and limbic areas of rat brain', *Neuroscience*, 90(4), pp. 1471–1482. doi: 10.1016/S0306-4522(98)00511-9.
- Demenescu, L. R. *et al.* (2017) 'A spectroscopic approach toward depression diagnosis: local metabolism meets functional connectivity', *European Archives of Psychiatry and Clinical Neuroscience*, 267(2). doi: 10.1007/s00406-016-0726-1.
- Deng, Y., Ma, X. and Tang, Q. (2013) 'Brain response during visual emotional processing: an fMRI study of alexithymia.', *Psychiatry research*. Elsevier, 213(3), pp. 225–9. doi: 10.1016/j.pychresns.2013.03.007.
- Dent, E. W. and Gertler, F. B. (2003) 'Cytoskeletal Dynamics and Review Transport in Growth Cone Motility and Axon Guidance', *Neuron*, 40(2), pp. 209–227. doi: 10.1016/S0896-6273(03)00633-0.
- Desai, A. and Mitchison, T. J. (1997) 'Microtubule polymerization dynamics', *Annual review of cell and developmental biology*. Annual Reviews 4139 El Camino Way, PO Box 10139, Palo Alto, CA 94303-0139, USA, 13(1), pp. 83–117.
- Devinsky, O., Morrell, M. J. and Vogt, B. a (1995) 'Contributions of anterior cingulate cortex to behaviour', *Brain : a journal of neurology*, 118 (Pt 1(March)), pp. 279–306. doi: 10.1093/brain/118.1.279.
- van Dijk, K. R. A., Sabuncu, M. R. and Buckner, R. L. (2012) 'The influence of head motion on intrinsic functional connectivity MRI', *NeuroImage*. Elsevier Inc., 59(1), pp. 431–438. doi: 10.1016/j.neuroimage.2011.07.044.
- Dilling, H. *et al.* (2011) 'Diagnostische Kriterien für Forschung und Praxis [International classification of mental disorders. ICD-10 Chapter V (F). Diagnostic criteria for research and practice]', *Bern: Huber*.
- Ding, X. Q. *et al.* (2018) 'Effects of a 72 hours fasting on brain metabolism in healthy women studied in vivo with magnetic resonance spectroscopic imaging', *Journal of Cerebral Blood Flow and Metabolism*, 38(3), pp. 469–478. doi: 10.1177/0271678X17697721.
- Dinis-Oliveira, R. J. (2017) 'Metabolism and metabolomics of ketamine: a toxicological approach', *Forensic Sciences Research*. Taylor & Francis, 2(1), pp. 2–10. doi: 10.1080/20961790.2017.1285219.
- Disner, S. G. *et al.* (2011) 'Neural mechanisms of the cognitive model of depression.', *Nature reviews. Neuroscience*, 12(8), pp. 467–77. doi: 10.1038/nrn3027.
- Domschke, K. *et al.* (2008) 'Cannabinoid receptor 1 (CNR1) gene: impact on antidepressant treatment response and emotion processing in major depression', *European Neuropsychopharmacology*. Elsevier, 18(10), pp. 751–759.
- Donner, N. C. and Lowry, C. A. (2013) 'Sex differences in anxiety and emotional behavior', *Pflugers Archiv European Journal of Physiology*, 465(5), pp. 601–626. doi: 10.1007/s00424-013-1271-7.
- Dörfel, D. *et al.* (2014) 'Common and differential neural networks of emotion regulation by detachment, reinterpretation, distraction, and expressive suppression: A comparative fMRI investigation', *NeuroImage*. Elsevier Inc., 101, pp. 298–309. doi: 10.1016/j.neuroimage.2014.06.051.
- Dossat, A. M. *et al.* (2018) 'Behavioral and biochemical sensitivity to low doses of ketamine: Influence of estrous cycle in C57BL/6 mice', *Neuropharmacology*. Elsevier Ltd, 130(2018), pp. 30–41. doi: 10.1016/j.neuropharm.2017.11.022.
- Dou, W. *et al.* (2013) 'Systematic regional variations of GABA, glutamine, and glutamate concentrations follow receptor fingerprints of human cingulate cortex.', *The Journal of neuroscience : the official journal of the Society for Neuroscience*, 33(31), pp. 12698–704. doi: 10.1523/JNEUROSCI.1758-13.2013.
- Dou, W. *et al.* (2015) 'The separation of Gln and Glu in STEAM: a comparison study using short and long TEs/TMs at 3 and 7 T',

- Magnetic Resonance Materials in Physics, Biology and Medicine*. Springer, 28(4), pp. 395–405.
- Drevets, W. C. (2000) 'Neuroimaging studies of mood disorders', *Biological Psychiatry*, 48(8), pp. 813–829. doi: 10.1016/S0006-3223(00)01020-9.
- Drevets, W. C. (2001) 'Neuroimaging and neuropathological studies of depression: Implications for the cognitive-emotional features of mood disorders', *Current Opinion in Neurobiology*, 11(2), pp. 240–249. doi: 10.1016/S0959-4388(00)00203-8.
- Duman, R. S. *et al.* (2016) 'Synaptic plasticity and depression: new insights from stress and rapid-acting antidepressants', *Nature Medicine*. Nature Publishing Group, 22(3), pp. 238–249. doi: 10.1038/nm.4050.
- Duncan, N. W. *et al.* (2013) 'How to investigate neuro-biochemical relationships on a regional level in humans? Methodological considerations for combining functional with biochemical imaging.', *Journal of neuroscience methods*, 221, pp. 183–188. doi: 10.1016/j.jneumeth.2013.10.011.
- Duncan, N. W. *et al.* (2013) 'Concomitant BDNF and sleep slow wave changes indicate ketamine-induced plasticity in major depressive disorder', pp. 301–311. doi: 10.1017/S1461145712000545.
- Duric, V. *et al.* (2013) 'Altered expression of synapse and glutamate related genes in post-mortem hippocampus of depressed subjects', *International Journal of Neuropsychopharmacology*. Cambridge University Press Cambridge, UK, 16(1), pp. 69–82.
- Dwyer, S. D. and Meyers, K. M. (1986) 'Anesthetics and anticoagulants used in the preparation of rat-platelet-rich plasma alter rat platelet aggregation', *Thrombosis Research*, 42(2), pp. 139–151.
- von Economo, C. F. and Koskinas, G. N. (1925) *Die cytoarchitektonik der hirnrinde des erwachsenen menschen*. J. Springer.
- Eid, P. and Boucher, S. (2012) 'Alexithymia and dyadic adjustment in intimate relationships: Analyses using the Actor Partner Interdependence Model.', *Journal of Social and Clinical Psychology*, 31(10), pp. 1095–1111. doi: 10.1521/jscp.2012.31.10.1095.
- Elia, N. and Tramèr, M. R. (2005) 'Ketamine and postoperative pain - A quantitative systematic review of randomised trials', *Pain*, 113(1–2), pp. 61–70. doi: 10.1016/j.pain.2004.09.036.
- Ellison-Wright, I. and Bullmore, E. (2010) 'Anatomy of bipolar disorder and schizophrenia: A meta-analysis', *Schizophrenia Research*. Elsevier B.V., 117(1), pp. 1–12. doi: 10.1016/j.schres.2009.12.022.
- Elywa, M. *et al.* (2012) 'Proton magnetic resonance spectroscopy in deep human brain structures at 7 T', *Journal of Applied Spectroscopy*. Springer, 79(1), pp. 120–125.
- Ende, G. (2015) 'Proton Magnetic Resonance Spectroscopy: Relevance of Glutamate and GABA to Neuropsychology', *Neuropsychology Review*, 25(3), pp. 315–325. doi: 10.1007/s11065-015-9295-8.
- Engen, H. G. and Singer, T. (2013) 'Empathy circuits', *Current Opinion in Neurobiology*. Elsevier Ltd, 23(2), pp. 275–282. doi: 10.1016/j.conb.2012.11.003.
- Epperson, C. N. *et al.* (2002) 'Cortical γ -Aminobutyric Acid Levels Across the Menstrual Cycle in Healthy Women and Those With Premenstrual Dysphoric Disorder', *Archives of General Psychiatry*, 59(9), p. 851. doi: 10.1001/archpsyc.59.9.851.
- Epperson, C. N. *et al.* (2005) 'Sex, GABA, and nicotine: The impact of smoking on cortical GABA levels across the menstrual cycle as measured with proton magnetic resonance spectroscopy', *Biological Psychiatry*, 57(1), pp. 44–48. doi: 10.1016/j.biopsych.2004.09.021.
- Erlander, M. G. *et al.* (1991) 'Two genes encode distinct glutamate decarboxylases.', *Neuron*, 7(1), pp. 91–100. doi: 10.1016/0896-6273(91)90077-D.
- Ernst, J. *et al.* (2013) 'The association of interoceptive awareness and alexithymia with neurotransmitter concentrations in insula and anterior cingulate.', *Social cognitive and affective neuroscience*. doi: 10.1093/scan/nst058.
- Ernst, J. *et al.* (2017) 'Increased pregenual anterior cingulate glucose and lactate concentrations in major depressive disorder', *Molecular psychiatry*. Nature Publishing Group, 22(1), p. 113.
- Esclapez, M. *et al.* (1994) 'Comparative localization of two forms of glutamic acid decarboxylase and their mRNAs in rat brain supports the concept of functional differences between the forms.', *The Journal of neuroscience : the official journal of the Society for Neuroscience*, 14(3), pp. 1834–1855.
- Esterlis, I. *et al.* (2017) 'Ketamine-induced reduction in mGluR5 availability is associated with an antidepressant response: an [11C]ABP688 and PET imaging study in depression', *Molecular Psychiatry*. Nature Publishing Group, (November 2016), pp. 1–9. doi: 10.1038/mp.2017.58.
- Etkin, A. *et al.* (2006) 'Resolving Emotional Conflict: A Role for the Rostral Anterior Cingulate Cortex in Modulating Activity in the Amygdala', *Neuron*, 51(6), pp. 871–882. doi: 10.1016/j.neuron.2006.07.029.
- Etkin, A., Egner, T. and Kalisch, R. (2011) 'Emotional processing in anterior cingulate and medial prefrontal', *Trends in cognitive*

- sciences, 15(2), pp. 85–93. doi: 10.1016/j.tics.2010.11.004.Emotional.
- Etkin, A., Egner, T. and Kalisch, R. (2011) 'Emotional processing in anterior cingulate and medial prefrontal cortex.', *Trends in cognitive sciences*. Elsevier Ltd, 15(2), pp. 85–93. doi: 10.1016/j.tics.2010.11.004.
- Etkin, A. and Wager, T. D. (2007) 'Functional neuroimaging of anxiety: a meta-analysis of emotional processing in PTSD, social anxiety disorder, and specific phobia', *American Journal of Psychiatry*. Am Psychiatric Assoc, 164(10), pp. 1476–1488.
- Evans, J. W., Lally, N., et al. (2018) '7T 1H-MRS in Major Depressive Disorder : A Ketamine Treatment Study 7T 1 H-MRS in Major Depressive Disorder: a Ketamine Treatment Study', *Neuropharmacology*, 1(November 2017). doi: 10.1038/s41386-018-0057-1.
- Evans, J. W., Szczepanik, J., et al. (2018) 'Default mode connectivity in major depressive disorder measured up to 10 days after ketamine administration', *Biological psychiatry*. Elsevier.
- Faisal, W. and Jacques, J. (2017) 'Role of Ketamine and Methadone as Adjunctive Therapy in Complex Pain Management: A Case Report and Literature Review', *Indian J Palliat Care.*, 23(1), pp. 100–103. doi: 10.4103/0973-1075.197956.
- Falchi, L. et al. (2017) 'Approach to patients with essential thrombocythaemia and very high platelet counts: what is the evidence for treatment?', *British Journal of Haematology*, 176(3), pp. 352–364. doi: 10.1111/bjh.14443.
- Fan, Y. et al. (2018) 'Dorsal and ventral PCC switch network assignment via changes in relative functional connectivity strength to non-canonical networks', *Brain connectivity*, (ja).
- Feldblum, S., Erlander, M. G. and Tobin, A. J. (1993) 'Different distributions of GAD65 and GAD67 mRNAs suggest that the two glutamate decarboxylases play distinctive functional roles', *Journal of Neuroscience Research*, 34(6), pp. 689–706. doi: 10.1002/jnr.490340612.
- Fenaux, P. et al. (1990) 'Clinical course of essential thrombocythemia in 147 cases', *Cancer*, 66(3), pp. 549–556. doi: 10.1002/1097-0142(19900801)66:3<549::AID-CNCR2820660324>3.0.CO;2-6.
- Ferrari, A. J. et al. (2013) 'Burden of Depressive Disorders by Country , Sex , Age , and Year : Findings from the Global Burden of Disease Study 2010', 10(11). doi: 10.1371/journal.pmed.1001547.
- Ferreira, A. and Caceres, A. (1991) 'Estrogen-enhanced neurite growth: evidence for a selective induction of Tau and stable microtubules.', *Journal of Neuroscience*, 11(2), pp. 392–400. doi: 10.1002/pmhc.200600974.
- Flanagan, R. J. and Dunk, L. (2008) 'Haematological toxicity of drugs used in psychiatry', *Human Psychopharmacology*, 23, pp. 27–41. doi: 0.1002/hup.917.
- Fleming, M. F., Anton, R. F. and Spies, C. D. (2004) 'A review of genetic, biological, pharmacological, and clinical factors that affect carbohydrate-deficient transferrin levels.', *Alcoholism, clinical and experimental research*, 28(9), pp. 1347–1355. doi: 10.1097/01.ALC.0000139815.89794.BE.
- Flint, J. and Munafò, M. R. (2007) 'The endophenotype concept in psychiatric genetics', *Psychological medicine*. Cambridge University Press, 37(2), pp. 163–180.
- Fournier, J. and DeRubeis, R. (2010) 'Antidepressant drug effects and depression severity', *JAMA: The Journal of ...*, 303(1), pp. 47–53. doi: 10.1016/j.tips.2009.02.003.
- Fox, M. D. et al. (2005) 'The human brain is intrinsically organized into dynamic, anticorrelated functional networks.', *Proceedings of the National Academy of Sciences of the United States of America*, 102(27), pp. 9673–8. doi: 10.1073/pnas.0504136102.
- Fox, M. D. et al. (2012) 'Efficacy of transcranial magnetic stimulation targets for depression is related to intrinsic functional connectivity with the subgenual cingulate', *Biological Psychiatry*. Elsevier Inc., 72(7), pp. 595–603. doi: 10.1016/j.biopsych.2012.04.028.
- Fox, M. D. and Raichle, M. E. (2007) 'Spontaneous fluctuations in brain activity observed with functional magnetic resonance imaging.', *Nature reviews. Neuroscience*, 8(9), pp. 700–11. doi: 10.1038/nrn2201.
- Frahm, J. al et al. (1989) 'Localized high-resolution proton NMR spectroscopy using stimulated echoes: initial applications to human brain in vivo', *Magnetic Resonance in Medicine*. Wiley Online Library, 9(1), pp. 79–93.
- Fransson, P. (2006) 'How default is the default mode of brain function?: Further evidence from intrinsic BOLD signal fluctuations', *Neuropsychologia*. Elsevier, 44(14), pp. 2836–2845.
- Fransson, P. and Marrelec, G. (2008) 'The precuneus/posterior cingulate cortex plays a pivotal role in the default mode network: Evidence from a partial correlation network analysis', *NeuroImage*, 42(3), pp. 1178–1184. doi: 10.1016/j.neuroimage.2008.05.059.
- Franz, M. et al. (1998) 'Deutsche Version der Snaith-Hamilton-Pleasure-Scale (SHAPS-D)', *Fortschritte der Neurologie-Psychiatrie*. © Georg Thieme Verlag KG Stuttgart· New York, 66(09), pp. 407–413.
- Franz, M. et al. (2008) 'Alexithymia in the German general population.', *Social psychiatry and psychiatric epidemiology*, 43(1),

- pp. 54–62. doi: 10.1007/s00127-007-0265-1.
- Friston, K. *et al.* (1996) 'Movement-Related Effects in {fMRI} Time-Series', 35(0181), pp. 346–355. Available at: /spm/doc/papers/fMRI_1/welcome.html.
- Frith, C. D. and Frith, U. (2007) 'Social cognition in humans', *Current Biology*. Elsevier, 17(16), pp. R724–R732.
- De Fruyt, F., Van De Wiele, L. and Van Heeringen, C. (2000) 'Cloninger's Psychobiological Model of Temperament and Character and the Five-Factor Model of Personality', *Personality and Individual Differences*, 29(3), pp. 441–452. doi: 10.1016/S0191-8869(99)00204-4.
- Fuchs, P. N. *et al.* (2014) 'The anterior cingulate cortex and pain processing', *Frontiers in integrative neuroscience*. Frontiers, 8, p. 35.
- Gaynes, B. N. *et al.* (2009) 'What did STAR* D teach us? Results from a large-scale, practical, clinical trial for patients with depression', *Psychiatric services*. Am Psychiatric Assoc, 60(11), pp. 1439–1445.
- Gennatas, E. D. *et al.* (2017) 'Age-Related Effects and Sex Differences in Gray Matter Density, Volume, Mass, and Cortical Thickness from Childhood to Young Adulthood', *The Journal of Neuroscience*, 37(20), pp. 5065–5073. doi: 10.1523/JNEUROSCI.3550-16.2017.
- Giustino, T. F. and Maren, S. (2015) 'The Role of the Medial Prefrontal Cortex in the Conditioning and Extinction of Fear.', *Frontiers in behavioral neuroscience*, 9(November), p. 298. doi: 10.3389/fnbeh.2015.00298.
- Glahn, D. C. *et al.* (2016) 'Chapter 31 - Conceptualizing Major Depression: From Genes to Neuroanatomy to Epidemiology', in Lehner, T., Miller, B. L., and State Circuits, and Pathways in Clinical Neuropsychiatry, M. W. B. T.-G. (eds). San Diego: Academic Press, pp. 487–501. doi: <https://doi.org/10.1016/B978-0-12-800105-9.00031-7>.
- Glazier, A. M., Nadeau, J. H. and Aitman, T. J. (2002) 'Finding genes that underlie complex traits', *Science*. American Association for the Advancement of Science, 298(5602), pp. 2345–2349.
- Glue, P. *et al.* (2011) 'Dose- and Exposure-Response to Ketamine in Depression', *Biological Psychiatry*, 70(4), pp. e9–e10. doi: 10.1016/j.biopsych.2010.11.031.
- Goddard, A. W. (2016) 'Cortical and subcortical gamma amino acid butyric acid deficits in anxiety and stress disorders: Clinical implications', *World J Psychiatry*, 6(1), pp. 43–53. doi: 10.5498/wjpv.6.i1.43.
- Godlewska, Beata R *et al.* (2017) 'Brain glutamate in medication-free depressed patients: a proton MRS study at 7 Tesla.', *Psychological medicine*, pp. 1–7. doi: 10.1017/S0033291717003373.
- Godlewska, Beata R. *et al.* (2017) 'Ultra-high-field magnetic resonance spectroscopy in psychiatry', *Frontiers in Psychiatry*, 8(JUL), pp. 1–9. doi: 10.3389/fpsyt.2017.00123.
- Goerlich-Dobre, K. S. *et al.* (2014) 'Distinct associations of insula and cingulate volume with the cognitive and affective dimensions of alexithymia.', *Neuropsychologia*. Elsevier, 53, pp. 284–92. doi: 10.1016/j.neuropsychologia.2013.12.006.
- Gottesman, I. I. and Gould, T. D. (2003) 'The endophenotype concept in psychiatry: etymology and strategic intentions', *American Journal of Psychiatry*. Am Psychiatric Assoc, 160(4), pp. 636–645.
- Govindaraju, V., Young, K. and Maudsley, A. A. (2000) 'Proton NMR chemical shifts and coupling constants for brain metabolites', pp. 129–153.
- Greicius, M. D. *et al.* (2007) 'Resting-state functional connectivity in major depression: abnormally increased contributions from subgenual cingulate cortex and thalamus.', *Biological psychiatry*, 62(5), pp. 429–37. doi: 10.1016/j.biopsych.2006.09.020.
- Greicius, M. D. *et al.* (2009) 'Resting-state functional connectivity reflects structural connectivity in the default mode network.', *Cerebral cortex (New York, N.Y. : 1991)*, 19(1), pp. 72–8. doi: 10.1093/cercor/bhn059.
- Grimm, O. *et al.* (2014) 'Striatal response to reward anticipation evidence for a systems-level intermediate phenotype for schizophrenia', *JAMA Psychiatry*, 71(5), pp. 531–539. doi: 10.1001/jamapsychiatry.2014.9.
- Grimm, S. *et al.* (2006) 'Segregated neural representation of distinct emotion dimensions in the prefrontal cortex—an fMRI study', *Neuroimage*. Elsevier, 30(1), pp. 325–340.
- Grimm, S. *et al.* (2009) 'Altered negative BOLD responses in the default-mode network during emotion processing in depressed subjects.', *Neuropsychopharmacology : official publication of the American College of Neuropsychopharmacology*, 34(4), pp. 932–843. doi: 10.1038/npp.2008.81.
- Grimm, S. *et al.* (2012) 'Prefrontal cortex glutamate and extraversion.', *Social cognitive and affective neuroscience*, 7(7), pp. 811–8. doi: 10.1093/scan/nsr056.
- Groenewold, N. A. *et al.* (2013) 'Emotional valence modulates brain functional abnormalities in depression: evidence from a meta-analysis of fMRI studies', *Neuroscience & Biobehavioral Reviews*. Elsevier, 37(2), pp. 152–163.
- Group, B. D. W. *et al.* (2001) 'Biomarkers and surrogate endpoints: preferred definitions and conceptual framework', *Clinical*

- Pharmacology & Therapeutics*. Wiley Online Library, 69(3), pp. 89–95.
- Grynberg, D. *et al.* (2010) 'Alexithymia in the interpersonal domain : A general deficit of empathy?', *Personality and Individual Differences*. Elsevier Ltd, 49(8), pp. 845–850. doi: 10.1016/j.paid.2010.07.013.
- Gundel, H. (2004) 'Alexithymia Correlates With the Size of the Right Anterior Cingulate', *Psychosomatic Medicine*, 66(1), pp. 132–140. doi: 10.1097/01.PSY.0000097348.45087.96.
- Gyurak, A., Gross, J. and Etkin, A. (2011) 'Explicit and implicit emotion regulation: A dual process framework', *Cognition & Emotion*, 25(3), pp. 400–412. doi: 10.1080/02699931.2010.544160.Explicit.
- Haase, A. *et al.* (1985) '1H NMR chemical shift selective (CHESS) imaging', *Physics in Medicine & Biology*. IOP Publishing, 30(4), p. 341.
- Haile, C. N. *et al.* (2014) 'Plasma brain derived neurotrophic factor (BDNF) and response to ketamine in treatment-resistant depression', *International Journal of Neuropsychopharmacology*, 17(2), pp. 331–336. doi: 10.1017/S1461145713001119.
- Ham, B. J. *et al.* (2007) 'Decreased GABA levels in anterior cingulate and basal ganglia in medicated subjects with panic disorder: A proton magnetic resonance spectroscopy (1H-MRS) study', *Progress in Neuro-Psychopharmacology and Biological Psychiatry*, 31(2), pp. 403–411. doi: 10.1016/j.pnpbp.2006.10.011.
- Hamilton, M. (1960) 'A rating scale for depression', *Journal of neurology, neurosurgery, and psychiatry*. BMJ Publishing Group, 23(1), p. 56.
- Hampson, M. *et al.* (2006) 'Brain connectivity related to working memory performance', *Journal of Neuroscience*. Soc Neuroscience, 26(51), pp. 13338–13343.
- Harker, L. A. *et al.* (2000) 'Effects of megakaryocyte growth and development factor on platelet production, platelet life span, and platelet function in healthy human volunteers', *Blood*, 95(8), pp. 2514–22. Available at: <http://www.ncbi.nlm.nih.gov/pubmed/8695799>.
- Hasler, G. *et al.* (2004) 'Discovering Endophenotypes for Major Depression', pp. 1765–1781. doi: 10.1038/sj.npp.1300506.
- Hasler, G. *et al.* (2010) 'Effect of Acute Psychological Stress on Prefrontal GABA Concentration Determined by Proton Magnetic Resonance Spectroscopy', *Am J Psychiatry*, 167(October), pp. 1226–1231. doi: 10.1176/appi.ajp.2010.09070994.
- Hasler, G. and Northoff, G. (2011) 'Discovering imaging endophenotypes for major depression', *Molecular psychiatry*. Nature Publishing Group, 16(6), p. 604.
- Hauwel-Fantini, C. and Pedinielli, J. L. (2008) 'De la non-expression ?? la surexpression des ??motions ou comment l'exp??rience ??motionnelle repose la question des liens entre sexe, alexithymie et r??pression', *Annales Medico-Psychologiques*, 166(4), pp. 277–284. doi: 10.1016/j.amp.2006.11.003.
- Hayes, A. F. (2013) 'SPSS Process Models', p. 2015.
- Heba, S. *et al.* (2016) 'Local GABA Concentration Predicts Perceptual Improvements after Repetitive Sensory Stimulation in Humans', *Cerebral Cortex*, 26(3), pp. 1295–1301. doi: 10.1093/cercor/bhv296.
- Heinzel, A. *et al.* (2012) 'Alexithymia in healthy young men: a voxel-based morphometric study.', *Journal of affective disorders*. Elsevier B.V., 136(3), pp. 1252–6. doi: 10.1016/j.jad.2011.06.012.
- Hertz, L. (2013) 'The glutamate-glutamine (GABA) cycle: Importance of late postnatal development and potential reciprocal interactions between biosynthesis and degradation', *Frontiers in Endocrinology*, 4(MAY), pp. 1–16. doi: 10.3389/fendo.2013.00059.
- Hettema, J. M. *et al.* (2006) 'Association between glutamic acid decarboxylase genes and anxiety disorders, major depression, and neuroticism.', *Molecular psychiatry*, 11(8), pp. 752–762. doi: 10.1038/sj.mp.4001858.
- Hijazi, Y. and Bouliou, R. (2002) 'Contribution of CYP3A4, CYP2B6, and CYP2C9 isoforms to N-demethylation of ketamine in human liver microsomes', *Drug Metabolism and Disposition*, 30(7), pp. 853–858. doi: 10.1124/dmd.30.7.853.
- Hintikka, J. *et al.* (2001) 'Are alexithymia and depression distinct or overlapping constructs?: A study in a general population', *Comprehensive Psychiatry*, 42(3), pp. 234–239. doi: 10.1053/comp.2001.23147.
- Hitchcock, I. S. *et al.* (2003) 'NMDA receptor – mediated regulation of human megakaryocytopoiesis', *Blood*, 102(4), pp. 1254–1259. doi: 10.1182/blood-2002-11-3553.
- Hjelmervik, H. *et al.* (2018) 'Sex-and sex hormone-related variations in energy-metabolic frontal brain asymmetries: A magnetic resonance spectroscopy study', *NeuroImage*. Elsevier, 172, pp. 817–825.
- Ho, M.-F. *et al.* (2018) 'Ketamine and Ketamine Metabolites as Novel Estrogen Receptor Ligands: Induction of Cytochrome P450 and AMPA Glutamate Receptor Gene Expression', *Biochemical Pharmacology*. Elsevier Inc. doi: 10.1016/j.bcp.2018.03.032.
- Ho, N. S. P., Wong, M. M. C. and Lee, T. M. C. (2016) 'Neural connectivity of alexithymia : Specific association with major depressive disorder', 193, pp. 362–372. doi: 10.1016/j.jad.2015.12.057.

- Hoffmann, E. *et al.* (2016) 'Reduced functional connectivity to the frontal cortex during processing of social cues in autism spectrum disorder.', *Journal of neural transmission (Vienna, Austria : 1996)*. doi: 10.1007/s00702-016-1544-3.
- Hoffstaedter, F. *et al.* (2014) 'The role of anterior midcingulate cortex in cognitive motor control: Evidence from functional connectivity analyses', *Human Brain Mapping*, 35(6), pp. 2741–2753. doi: 10.1002/hbm.22363.
- Honkalampi, K. *et al.* (2000) 'Depression is strongly associated with alexithymia in the general population.', *Journal of psychosomatic research*, 48(1), pp. 99–104. Available at: <http://www.ncbi.nlm.nih.gov/pubmed/10750635>.
- Honkalampi, K. *et al.* (2001) 'Alexithymia and Depression: A Prospective Study of Patients With Major Depressive Disorder', *Psychosomatics*, 42(3), pp. 229–234. doi: 10.1176/appi.psy.42.3.229.
- Honkalampi, K. *et al.* (2010) 'Is alexithymia a risk factor for major depression, personality disorder, or alcohol use disorders? A prospective population-based study', *Journal of psychosomatic research*. Elsevier, 68(3), pp. 269–273.
- Hoogenraad, C. C. and Bradke, F. (2009) 'Control of neuronal polarity and plasticity - a renaissance for microtubules?', *Trends in Cell Biology*, 19(12), pp. 669–676. doi: 10.1016/j.tcb.2009.08.006.
- Horn, D. I., Yu, C., Steiner, J., Buchmann, J., Kaufmann, J., Osoba, A., *et al.* (2010) 'Glutamatergic and resting-state functional connectivity correlates of severity in major depression - the role of pregenual anterior cingulate cortex and anterior insula.', *Frontiers in systems neuroscience*, 4(July), pp. 1–10. doi: 10.3389/fnsys.2010.00033.
- Hu, S. *et al.* (2014) 'Changes in cerebral morphometry and amplitude of low-frequency fluctuations of BOLD signals during healthy aging: Correlation with inhibitory control', *Brain Structure and Function*, 219(3), pp. 983–994. doi: 10.1007/s00429-013-0548-0.
- Hudgens, E. D. *et al.* (2009) 'The gad2 promoter is a transcriptional target of estrogen receptor α (ER α) and ER β : A unifying hypothesis to explain diverse effects of estradiol', *J Neurosci*, 29(27), pp. 8790–8797. doi: 10.1523/JNEUROSCI.1289-09.2009.The.
- Hyder, F. *et al.* (2006) 'Neuronal-glia glucose oxidation and glutamatergic-GABAergic function', *Journal of Cerebral Blood Flow and Metabolism*, 26(7), pp. 865–877. doi: 10.1038/sj.jcbfm.9600263.
- Iadarola, N. D. *et al.* (2015) 'Ketamine and other N-methyl-D-aspartate receptor antagonists in the treatment of depression: a perspective review', *Therapeutic advances in chronic disease*. SAGE Publications Sage UK: London, England, 6(3), pp. 97–114.
- Ihme, K. *et al.* (2013) 'Alexithymia is related to differences in gray matter volume: a voxel-based morphometry study.', *Brain research*. Elsevier, 1491, pp. 60–7. doi: 10.1016/j.brainres.2012.10.044.
- Ihme, K. *et al.* (2014) 'Alexithymia and the labeling of facial emotions: Response slowing and increased motor and somatosensory processing', *BMC Neuroscience*, 15, pp. 1–10. doi: 10.1186/1471-2202-15-40.
- Ikeda, T., Makino, Y. and Yamada, M. K. (2015) '17 α -Estradiol is generated locally in the male rat brain and can regulate GAD65 expression and anxiety', *Neuropharmacology*. Elsevier Ltd, 90, pp. 9–14. doi: 10.1016/j.neuropharm.2014.10.019.
- Iltis, I. *et al.* (2009) 'Neurochemical changes in the rat prefrontal cortex following acute phencyclidine treatment: an in vivo localized 1H MRS study', *NMR in Biomedicine: An International Journal Devoted to the Development and Application of Magnetic Resonance In vivo*. Wiley Online Library, 22(7), pp. 737–744.
- In, M. H. and Speck, O. (2012) 'Highly accelerated PSF-mapping for EPI distortion correction with improved fidelity', *Magnetic Resonance Materials in Physics, Biology and Medicine*, 25(3), pp. 183–192. doi: 10.1007/s10334-011-0275-6.
- Insel, T. *et al.* (2010) 'Research domain criteria (RDoC): toward a new classification framework for research on mental disorders'. Am Psychiatric Assoc.
- Jamieson, G. a. *et al.* (1992) 'Phencyclidine binds to blood platelets with high affinity and specifically inhibits their activation by adrenaline', *Biochemical Journal*, 285(1), pp. 35–39. doi: 10.1042/bj2850035.
- Janke, C. and Bulinski, J. C. (2011) 'Post-translational regulation of the microtubule cytoskeleton: mechanisms and functions', *Nature Publishing Group*, (November), pp. 1–14. doi: 10.1038/nrm3227.
- Janke, C. and Kneussel, M. (2010) 'Tubulin post-translational modifications: Encoding functions on the neuronal microtubule cytoskeleton', *Trends in Neurosciences*. Elsevier Ltd, 33(8), pp. 362–372. doi: 10.1016/j.tins.2010.05.001.
- Jansen, J. F. A. *et al.* (2006) 'H MR Spectroscopy of the Brain : Absolute Quantification of', 240(2).
- Jenkins, J. M. *et al.* (2008) 'thrombopoietin receptor agonist Brief report Phase 1 clinical study of eltrombopag , an oral , nonpeptide thrombopoietin receptor agonist', *Blood*, 109(11), pp. 4739–4741. doi: 10.1182/blood-2006-11-057968.
- Jenkinson, M. *et al.* (2002) 'Improved optimization for the robust and accurate linear registration and motion correction of brain images', *NeuroImage*, 17(2), pp. 825–841. doi: 10.1016/S1053-8119(02)91132-8.
- Jocham, G. *et al.* (2012) 'A mechanism for value- guided choice based on the excitation-inhibition balance in prefrontal cortex',

- Nature Neuroscience*. Nature Publishing Group, 15(7), pp. 960–961. doi: 10.1038/nn.3140.
- John, B. and Lewis, K. R. (1966) 'Chromosome variability and geographic distribution in insects', *Science*. JSTOR, 152(3723), pp. 711–721.
- John Rush, A. *et al.* (2006) 'STAR-D (2006; AjPsych) Tiered approach for depression', *Am J Psychiatry*, 163(11)(November), pp. 1905–1917. doi: 10.1176/ajp.2006.163.11.1905.
- Jollant, F. (2015) 'Add-on lithium for the treatment of unipolar depression: Too often forgotten?', *Journal of Psychiatry & Neuroscience*, 40(1), pp. E23–E24. doi: 10.1503/jpn.140162.
- Josefsson, K. *et al.* (2013) 'Maturity and change in personality: Developmental trends of temperament and character in adulthood', *Development and Psychopathology*, 25(03), pp. 713–727. doi: 10.1017/S0954579413000126.
- Kaczurkin, A. N., Raznahan, A. and Satterthwaite, T. D. (2018) 'Sex differences in the developing brain: insights from multimodal neuroimaging', *Neuropsychopharmacology*. Springer US, (May), pp. 1–15. doi: 10.1038/s41386-018-0111-z.
- Kahlfuß, S. *et al.* (2014) 'Immunosuppression by N-methyl-D-aspartate receptor antagonists is mediated through inhibition of Kv1.3 and KCa3.1 channels in T cells.', *Molecular and cellular biology*, 34(5), pp. 820–31. doi: 10.1128/MCB.01273-13.
- Kaiser, L. G. *et al.* (2005) 'Age-related glutamate and glutamine concentration changes in normal human brain: 1H MR spectroscopy study at 4 T', *Neurobiology of Aging*, 26(5), pp. 665–672. doi: 10.1016/j.neurobiolaging.2004.07.001.
- Kalev-Zylinska, M. L. *et al.* (2014) 'N-methyl-d-aspartate receptors amplify activation and aggregation of human platelets', *Thrombosis Research*, 133(5), pp. 837–847. doi: 10.1016/j.thromres.2014.02.011.
- Kalra, S. *et al.* (2006) 'Rapid improvement in cortical neuronal integrity in amyotrophic lateral sclerosis detected by proton magnetic resonance spectroscopic imaging.', *Journal of neurology*, 253(8), pp. 1060–3. doi: 10.1007/s00415-006-0162-7.
- Kang, H. J. *et al.* (2012) 'Decreased expression of synapse-related genes and loss of synapses in major depressive disorder', *Nature Medicine*, 18(9), pp. 1413–1417. doi: 10.1038/nm.2886.
- Kano, M. and Fukudo, S. (2013) 'The alexithymic brain: The neural pathways linking alexithymia to physical disorders', *BioPsychoSocial Medicine*, 7(1), pp. 1–9. doi: 10.1186/1751-0759-7-1.
- Kano, M., Ito, M. and Fukudo, S. (2011) 'Neural Substrates of Decision Making as Measured With the Iowa Gambling Task in Men With Alexithymia', *Psychosomatic Medicine*, 73(7).
- Kapogiannis, D. *et al.* (2013) 'Posteromedial cortex glutamate and GABA predict intrinsic functional connectivity of the default mode network', *NeuroImage*. Elsevier B.V., 64(1), pp. 112–119. doi: 10.1016/j.neuroimage.2012.09.029.
- Kapur, S. and Seeman, P. (2002) 'NMDA receptor antagonists ketamine and PCP have direct effects on the dopamine D 2 and serotonin 5-HT 2 receptors—implications for models of schizophrenia', *Molecular psychiatry*. Nature Publishing Group, 7(8), p. 837.
- Karolczak, K., Pieniżek, A. and Watala, C. (2017) 'Inhibition of glutamate receptors reduces the homocysteine-induced whole blood platelet aggregation but does not affect superoxide anion generation or platelet membrane fluidization', *Platelets*, 28(1), pp. 90–98. doi: 10.1080/09537104.2016.1204438.
- Kaushansky, K. (2006) 'Lineage-specific hematopoietic growth factors', *The New England journal of medicine*, 354(19), pp. 2034–2045. doi: 10.1056/NEJMra052706.
- Kavalali, E. T. and Monteggia, L. M. (2012) 'Synaptic mechanisms underlying rapid antidepressant action of ketamine', *American Journal of Psychiatry*, 169(11), pp. 1150–1156. doi: 10.1176/appi.ajp.2012.12040531.
- Kawabata, H. (2018) 'Transferrin and transferrin receptors update', *Free Radical Biology and Medicine*. Elsevier B.V., (June), pp. 1–9. doi: 10.1016/j.freeradbiomed.2018.06.037.
- Kellermann, T. S. *et al.* (2012) 'Modulating the processing of emotional stimuli by cognitive demand', *Social Cognitive and Affective Neuroscience*, 7(3), pp. 263–273. doi: 10.1093/scan/nsq104.
- Kelly, a. M. C. *et al.* (2009) 'Development of anterior cingulate functional connectivity from late childhood to early adulthood', *Cerebral Cortex*, 19(3), pp. 640–657. doi: 10.1093/cercor/bhn117.
- Kendall, M. and Gibbons, J. D. R. (1990) 'Correlation methods'. Oxford: Oxford University Press.
- Kesby, J. P. (2018) 'Dopamine , psychosis and schizophrenia : the widening gap between basic and clinical neuroscience', *Translational Psychiatry*. Springer US. doi: 10.1038/s41398-017-0071-9.
- Kessler, R. C. (2003) 'Epidemiology of women and depression', *Journal of Affective Disorders*, 74(1), pp. 5–13. doi: 10.1016/S0165-0327(02)00426-3.
- Kessler, R. C. (2012) 'The costs of depression', *Psychiatric Clinics*. Elsevier, 35(1), pp. 1–14.
- Kharasch, E. D. and Labroo, R. (1992) 'Metabolism of Ketamine Stereoisomers by Human Liver Microsomes', *Anesthesiology*, 77(6), pp. 1201–1207.

- Khundakar, A. A. and Thomas, A. J. (2009) 'Morphometric changes in early- and late-life major depressive disorder: Evidence from postmortem studies', *International Psychogeriatrics*, 21(5), pp. 844–854. doi: 10.1017/S104161020999007X.
- Kim, H. J. *et al.* (2009) 'Associations between anterior cingulate cortex glutamate and gamma-aminobutyric acid concentrations and the harm avoidance temperament.', *Neuroscience letters*, 464(2), pp. 103–7. doi: 10.1016/j.neulet.2009.07.087.
- Kim, Y. (2018) 'The role of neuroinflammation and neurovascular dysfunction in major depressive disorder', pp. 179–192.
- Kiraly, D. D. *et al.* (2017) 'Altered peripheral immune profiles in treatment-resistant depression: response to ketamine and prediction of treatment outcome', *Translational Psychiatry*. Nature Publishing Group, 7(3), p. e1065. doi: 10.1038/tp.2017.31.
- Klein, S. L. and Flanagan, K. L. (2016) 'Sex differences in immune responses', *Nature Reviews Immunology*. Nature Publishing Group, 16(10), pp. 626–638. doi: 10.1038/nri.2016.90.
- Klose, U. (1990) 'In vivo proton spectroscopy in presence of eddy currents', *Magnetic resonance in medicine*. Wiley Online Library, 14(1), pp. 26–30.
- Kober, H. *et al.* (2008) 'Functional grouping and cortical-subcortical interactions in emotion: A meta-analysis of neuroimaging studies', *NeuroImage*, 42(2), pp. 998–1031. doi: 10.1016/j.neuroimage.2008.03.059.
- Koch, K. *et al.* (2007) 'Gender differences in the cognitive control of emotion: An fMRI study', *Neuropsychologia*, 45(12), pp. 2744–2754. doi: 10.1016/j.neuropsychologia.2007.04.012.
- Kogan, T. P. and Somers, T. C. (1993) 'Ketamine analogues for treatment of thrombocytopenia'. USA: United States Patent.
- Kokkinou, M., Ashok, A. H. and Howes, O. D. (2017) 'The effects of ketamine on dopaminergic function : meta-analysis and review of the implications for neuropsychiatric disorders', *Nature Publishing Group*. Nature Publishing Group, (February), pp. 1–11. doi: 10.1038/mp.2017.190.
- Kooiman, C. G., Spinhoven, P. and Trijsburg, R. W. (2002) 'The assessment of alexithymia A critical review of the literature and a psychometric study of the Toronto Alexithymia Scale-20', 53, pp. 1083–1090.
- Kool, W. *et al.* (2010) 'Decision making and the avoidance of cognitive demand.', *Journal of experimental psychology. General*, 139(4), pp. 665–82. doi: 10.1037/a0020198.
- Kraguljac, N. V. *et al.* (2017) 'Ketamine modulates hippocampal neurochemistry and functional connectivity: a combined magnetic resonance spectroscopy and resting-state fMRI study in healthy volunteers', *Molecular psychiatry*. Nature Publishing Group, 22(4), p. 562.
- Krishnan, V. and Nestler, E. J. (2008) 'The molecular neurobiology of depression.', *Nature*, 455(7215), pp. 894–902. doi: 10.1038/nature07455.
- Krystal, J. H. *et al.* (1994) 'Subanesthetic effects of the noncompetitive NMDA antagonist, ketamine, in humans: psychotomimetic, perceptual, cognitive, and neuroendocrine responses', *Archives of general psychiatry*. American Medical Association, 51(3), pp. 199–214.
- Krystal, J. H. *et al.* (2002) 'Glutamate and GABA systems as targets for novel antidepressant and mood-stabilizing treatments', *Molecular Psychiatry*, 7, pp. S71–S80. doi: 10.1038/sj.mp.4001021.
- Krystal, J. H., Sanacora, G. and Duman, R. S. (2013) 'Rapid-acting glutamatergic antidepressants: The path to ketamine and beyond', *Biological Psychiatry*. Elsevier, 73(12), pp. 1133–1141. doi: 10.1016/j.biopsych.2013.03.026.
- Kupfer, D. J., Frank, E. and Phillips, M. L. (2012) 'Major depressive disorder: New clinical, neurobiological, and treatment perspectives', *The Lancet*. Elsevier Ltd, 379(9820), pp. 1045–1055. doi: 10.1016/S0140-6736(11)60602-8.
- Laird, A. R. *et al.* (2009) 'Investigating the functional heterogeneity of the default mode network using coordinate-based meta-analytic modeling', *Journal of Neuroscience*. Soc Neuroscience, 29(46), pp. 14496–14505.
- Lane, R. D. *et al.* (1998) 'Neural correlates of levels of emotional awareness. Evidence of an interaction between emotion and attention in the anterior cingulate cortex.', *Journal of cognitive neuroscience*, 10(4), pp. 525–35. Available at: <http://www.ncbi.nlm.nih.gov/pubmed/9712681>.
- Lane, R. D. *et al.* (2000) 'Pervasive emotion recognition deficit common to alexithymia and the repressive coping style.', *Psychosomatic medicine*, 62(4), pp. 492–501. Available at: <http://www.ncbi.nlm.nih.gov/pubmed/10949094>.
- Lane, R. D. (2008) 'Neural substrates of implicit and explicit emotional processes: a unifying framework for psychosomatic medicine.', *Psychosomatic medicine*, 70(2), pp. 214–31. doi: 10.1097/PSY.0b013e3181647e44.
- Laurell, C. B. and Rannevik, G. (1979) 'A comparison of plasma protein changes induced by danazol, pregnancy, and estrogens.', *The Journal of clinical endocrinology and metabolism*, 49(5), pp. 719–725. doi: 10.1210/jcem-49-5-719.
- Lee, B. *et al.* (2011) 'Neural Substrates of Affective Face Recognition in Alexithymia : A Functional', pp. 119–124. doi: 10.1159/000318086.
- Lee, C. R., Goldstein, J. a. and Pieper, J. a. (2002) 'Cytochrome P450 2C9 polymorphisms: A comprehensive review of the in-

- vitro and human data', *Pharmacogenetics*, 12(3), pp. 251–263. doi: 10.1097/00008571-200204000-00010.
- Leech, R. and Sharp, D. J. (2014) 'The role of the posterior cingulate cortex in cognition and disease', *Brain*, 137(1), pp. 12–32. doi: 10.1093/brain/awt162.
- Lei, X. *et al.* (2016) 'Sex Differences in Fiber Connection between the Striatum and Subcortical and Cortical Regions', *Frontiers in Computational Neuroscience*, 10(September). doi: 10.3389/fncom.2016.00100.
- Lekman, M. *et al.* (2008) 'The FKBP5-gene in depression and treatment response—an association study in the Sequenced Treatment Alternatives to Relieve Depression (STAR* D) Cohort', *Biological psychiatry*. Elsevier, 63(12), pp. 1103–1110.
- Lener, M. S. *et al.* (2017) 'Glutamate and Gamma-Aminobutyric Acid Systems in the Pathophysiology of Major Depression and Antidepressant Response to Ketamine', *Biological Psychiatry*. Elsevier, 81(10), pp. 886–897. doi: 10.1016/j.biopsych.2016.05.005.
- Lener, M. S. and Iosifescu, D. V. (2015) 'In pursuit of neuroimaging biomarkers to guide treatment selection in major depressive disorder: A review of the literature', *Annals of the New York Academy of Sciences*, 1344(1), pp. 50–65. doi: 10.1111/nyas.12759.
- Lenzenweger, M. F. (2013) 'Thinking clearly about the endophenotype–intermediate phenotype–biomarker distinctions in developmental psychopathology research', *Development and psychopathology*. Cambridge University Press, 25(4pt2), pp. 1347–1357.
- Levant, R. F. *et al.* (2003) 'A multicultural investigation of masculinity ideology and alexithymia.', *Psychology of Men & Masculinity*. Educational Publishing Foundation, 4(2), p. 91.
- Levant, R. F. *et al.* (2009) 'Gender differences in alexithymia.', *Psychology of Men & Masculinity*, 10(3), pp. 190–203. doi: 10.1037/a0015652.
- Leweke, F. *et al.* (2004) 'Patterns of neuronal activity related to emotional stimulation in alexithymia', *Psychotherapie, Psychosomatik, medizinische Psychologie*, 54(12), pp. 437–444.
- Leweke, F. *et al.* (2012) 'Is alexithymia associated with specific mental disorders', *Psychopathology*. Karger Publishers, 45(1), pp. 22–28.
- Lewis, L. D. *et al.* (2016) 'Fast fMRI can detect oscillatory neural activity in humans', *Proceedings of the National Academy of Sciences*, 113(43), pp. E6679–E6685. doi: 10.1073/pnas.1608117113.
- Li, C.-T. *et al.* (2016) 'The effects of low-dose ketamine on the prefrontal cortex and amygdala in treatment-resistant depression: A randomized controlled study', *Human Brain Mapping*, 37(3), pp. 1080–1090. doi: 10.1002/hbm.23085.
- Li, M. *et al.* (2014) 'Dissociation of glutamate and cortical thickness is restricted to regions subserving trait but not state markers in major depressive disorder.', *Journal of affective disorders*. Elsevier, 169C, pp. 91–100. doi: 10.1016/j.jad.2014.08.001.
- Li, M. *et al.* (2017) 'Temporal Dynamics of Antidepressant Ketamine Effects on Glutamine Cycling Follow Regional Fingerprints of AMPA and NMDA Receptor Densities', *Neuropsychopharmacology*, 42(6). doi: 10.1038/npp.2016.184.
- Li, M. *et al.* (2018) 'Default mode network connectivity change corresponds to ketamine's delayed glutamatergic effects', *European Archives of Psychiatry and Clinical Neuroscience*. Springer, pp. 1–10.
- Li, N. *et al.* (2010) 'mTOR-Dependent Synapse Formation Underlies the Rapid Antidepressant Effects of NMDA Antagonists', *Science*, 329(5994), pp. 959–964. doi: 10.1126/science.1190287.
- Li, Y. *et al.* (2013) 'The CYP2B6* 6 allele significantly alters the N-demethylation of ketamine enantiomers in vitro.', *Drug Metabolism and Disposition*. ASPET, p. dmd-113.
- Li, Y. *et al.* (2015) 'CYP2B6* 6 allele and age substantially reduce steady-state ketamine clearance in chronic pain patients: impact on adverse effects', *British journal of clinical pharmacology*. Wiley Online Library, 80(2), pp. 276–284.
- Liao, Y. *et al.* (2011) 'Reduced dorsal prefrontal gray matter after chronic ketamine use', *Biological Psychiatry*, 69(1), pp. 42–48. doi: 10.1016/j.biopsych.2010.08.030.
- Licinio, J., Dong, C. and Wong, M.-L. (2009) 'Novel sequence variations in the brain-derived neurotrophic factor gene and association with major depression and antidepressant treatment response', *Archives of general psychiatry*. American Medical Association, 66(5), pp. 488–496.
- Liebe, Thomas *et al.* (2017) 'Factors Influencing the Cardiovascular Response to Subanesthetic Ketamine: A Randomized, Placebo-Controlled Trial', *International Journal of Neuropsychopharmacology*, 20, pp. 909–918. doi: 10.1093/ijnp/pyx055.
- Liebe, T. *et al.* (2018) 'Ketamine influences the locus coeruleus norepinephrine network, with a dependency on norepinephrine transporter genotype—a placebo controlled fMRI study', *NeuroImage: Clinical*. Elsevier, 20, pp. 715–723.
- Liemburg, E. J. *et al.* (2012) 'Altered resting state connectivity of the default mode network in alexithymia.', *Social cognitive and*

- affective neuroscience*, 7(6), pp. 660–6. doi: 10.1093/scan/nss048.
- Lin, A.-L. *et al.* (2010) 'Nonlinear coupling between cerebral blood flow, oxygen consumption, and ATP production in human visual cortex', *Proceedings of the National Academy of Sciences*. National Acad Sciences, 107(18), pp. 8446–8451.
- Lin, A. *et al.* (2005) 'Efficacy of proton magnetic resonance spectroscopy in neurological diagnosis and neurotherapeutic decision making.', *NeuroRx : the journal of the American Society for Experimental NeuroTherapeutics*, 2(2), pp. 197–214. doi: 10.1602/neurorx.2.2.197.
- Liu, B. *et al.* (2015) 'Psychiatry Research : Neuroimaging Alterations of GABA and glutamate – glutamine levels in premenstrual dysphoric disorder : A 3T proton magnetic resonance spectroscopy study', *Psychiatry Research: Neuroimaging*. Elsevier, 231(1), pp. 64–70. doi: 10.1016/j.psychresns.2014.10.020.
- Liu, C. H. *et al.* (2015) 'Abnormal spontaneous neural activity in the anterior insular and anterior cingulate cortices in anxious depression', *Behavioural Brain Research*. Elsevier B.V., 281, pp. 339–347. doi: 10.1016/j.bbr.2014.11.047.
- Lockwood, P. L. *et al.* (2015) 'Encoding of Vicarious Reward Prediction in Anterior Cingulate Cortex and Relationship with Trait Empathy.', *The Journal of neuroscience : the official journal of the Society for Neuroscience*, 35(40), pp. 13720–7. doi: 10.1523/JNEUROSCI.1703-15.2015.
- Lockwood, P. L. *et al.* (2018) 'Neural mechanisms for learning self and other ownership', *Nature Communications*. Springer US, 9(1), p. 4747. doi: 10.1038/s41467-018-07231-9.
- Lommatzsch, M. *et al.* (2005) 'The impact of age, weight and gender on BDNF levels in human platelets and plasma', *Neurobiology of Aging*, 26(1), pp. 115–123. doi: 10.1016/j.neurobiolaging.2004.03.002.
- Long, X. Y. *et al.* (2008) 'Default mode network as revealed with multiple methods for resting-state functional MRI analysis', *Journal of Neuroscience Methods*, 171(2), pp. 349–355. doi: 10.1016/j.jneumeth.2008.03.021.
- Long, Z. *et al.* (2013) 'Decreased GABA levels in anterior cingulate cortex / medial prefrontal cortex in panic disorder', *Progress in Neuropsychopharmacology & Biological Psychiatry*. Elsevier Inc., 44, pp. 131–135. doi: 10.1016/j.pnpbp.2013.01.020.
- Loveday, B. A. and Sindt, J. (2015) 'Ketamine Protocol for Palliative Care in Cancer Patients With Refractory Pain', *Journal of the Advanced Practitioner in Oncology*, 6(6), pp. 555–561. doi: 10.6004/jadpro.6.6.4.
- Luckenbaugh, D. A. *et al.* (2014) 'Do the dissociative side effects of ketamine mediate its antidepressant effects?', *Journal of affective disorders*, 159, pp. 56–61. doi: 10.1016/j.jad.2014.02.017.
- Ludwig, V. U. *et al.* (2015) 'Delay discounting without decision-making: medial prefrontal cortex and amygdala activations reflect immediacy processing and correlate with impulsivity and anxious-depressive traits.', *Frontiers in behavioral neuroscience*, 9(280), pp. 1–15. doi: 10.3389/fnbeh.2015.00280.
- Lugo-Roman, L. A. *et al.* (2010) 'Effects of serial anesthesia using ketamine or ketamine/medetomidine on hematology and serum biochemistry values in rhesus macaques (*Macaca Mulatta*)', *Journal of Medical Primatology*, 39(1), pp. 41–49. doi: 10.1111/j.1600-0684.2009.00394.x.
- Luu, P. and Posner, M. I. (2003) 'Anterior cingulate cortex regulation of sympathetic activity'. Oxford University Press.
- Luykx, J. J. *et al.* (2012) 'Region and state specific glutamate downregulation in major depressive disorder: a meta-analysis of (1)H-MRS findings.', *Neuroscience and biobehavioral reviews*. Elsevier Ltd, 36(1), pp. 198–205. doi: 10.1016/j.neubiorev.2011.05.014.
- Maalouf, F. T. *et al.* (2011) 'Neurocognitive impairment in adolescent major depressive disorder: state vs. trait illness markers', *Journal of Affective Disorders*. Elsevier, 133(3), pp. 625–632.
- Maddock, R. J. and Buonocore, M. H. (2011) 'MR spectroscopic studies of the brain in psychiatric disorders', in *Brain imaging in behavioral neuroscience*. Springer, pp. 199–251.
- Maddock, R. J., Garrett, a. S. and Buonocore, M. H. (2001) 'Remembering familiar people: The posterior cingulate cortex and autobiographical memory retrieval', *Neuroscience*, 104(3), pp. 667–676. doi: 10.1016/S0306-4522(01)00108-7.
- Mader, I. *et al.* (2002) 'Proton magnetic resonance spectroscopy with metabolite nulling reveals regional differences of macromolecules in normal human brain', *Journal of Magnetic Resonance Imaging*, 16(5), pp. 538–546. doi: 10.1002/jmri.10190.
- Maeng, S. *et al.* (2008) 'Cellular Mechanisms Underlying the Antidepressant Effects of Ketamine: Role of α -Amino-3-Hydroxy-5-Methylisoxazole-4-Propionic Acid Receptors', *Biological Psychiatry*, 63(4), pp. 349–352. doi: 10.1016/j.biopsych.2007.05.028.
- Magistretti, P. J. *et al.* (1999) 'Energy on demand', *Science*. American Association for the Advancement of Science, 283(5401), pp. 496–497.
- Magistretti, P. J. and Allaman, I. (2015) 'A cellular perspective on brain energy metabolism and functional imaging', *Neuron*.

- Elsevier, 86(4), pp. 883–901.
- Majós, C. *et al.* (2004) 'Brain tumor classification by proton MR spectroscopy: comparison of diagnostic accuracy at short and long TE', *American Journal of Neuroradiology*. Am Soc Neuroradiology, 25(10), pp. 1696–1704.
- Mantani, T. *et al.* (2005) 'Reduced activation of posterior cingulate cortex during imagery in subjects with high degrees of alexithymia: a functional magnetic resonance imaging study.', *Biological psychiatry*, 57(9), pp. 982–90. doi: 10.1016/j.biopsych.2005.01.047.
- Marenco, S. *et al.* (2010) 'Genetic Modulation of GABA Levels in the Anterior Cingulate Cortex by GAD1 and COMT', *Neuropsychopharmacology*. Nature Publishing Group, 35(8), pp. 1708–1717. doi: 10.1038/npp.2010.35.
- Margulies, D. S. *et al.* (2007) 'Mapping the functional connectivity of anterior cingulate cortex.', *NeuroImage*, 37(2), pp. 579–88. doi: 10.1016/j.neuroimage.2007.05.019.
- Martin, E. I. *et al.* (2009) 'The neurobiology of anxiety disorders: brain imaging, genetics, and psychoneuroendocrinology', *Psychiatric Clinics*. Elsevier, 32(3), pp. 549–575.
- Marusak, H. A. *et al.* (2016) 'You say 'prefrontal cortex' and I say "anterior cingulate": meta-analysis of spatial overlap in amygdala-to-prefrontal connectivity and internalizing symptomology', *Translational psychiatry*. Nature Publishing Group, 6(11), p. e944.
- Mathews, A. and Macleod, C. (2005) 'Cognitive vulnerability to emotional disorders.', *Annual review of clinical psychology*, 1, pp. 167–95. doi: 10.1146/annurev.clinpsy.1.102803.143916.
- Mattila, A. K. *et al.* (2006) 'Age is strongly associated with alexithymia in the general population.', *Journal of psychosomatic research*, 61(5), pp. 629–35. doi: 10.1016/j.jpsychores.2006.04.013.
- Mayberg, H. S. (1997) 'Limbic-cortical dysregulation: a proposed model of depression', *J Neuropsychiatry Clin Neurosci*, 9(3), pp. 471–481. doi: 10.1176/jnp.9.3.471.
- McCarthy, M. M. *et al.* (1995) 'Estrogen modulation of mRNA levels for the two forms of glutamic acid decarboxylase (GAD) in female rat brain', *Journal of Comparative Neurology*, 360(4), pp. 685–697. doi: 10.1002/cne.903600412.
- McCarthy, M. M., Auger, A. P. and Perrot-Sinal, T. S. (2002) 'Getting excited about GABA and sex differences in the brain', *Trends in Neurosciences*, 25(6), pp. 307–312. doi: 10.1016/S0166-2236(02)02182-3.
- McGirr, A. *et al.* (2015) 'A systematic review and meta-analysis of randomized, double-blind, placebo-controlled trials of ketamine in the rapid treatment of major depressive episodes', *Psychological Medicine*, 45(4), pp. 693–704. doi: 10.1017/S0033291714001603.
- McGrath, P. J. *et al.* (2008) 'Response to a selective serotonin reuptake inhibitor (citalopram) in major depressive disorder with melancholic features: a STAR* D report.', *The Journal of clinical psychiatry*, 69(12), pp. 1847–1855.
- McLean, C. P. *et al.* (2011) 'Gender Differences in Anxiety Disorders: Prevalence, Course of Illness, Comorbidity and Burden of Illness', *Journal of psychiatric research*, 45(8), pp. 1027–1035. doi: 10.1016/j.jpsychires.2011.03.006.Gender.
- McRae, Kateri *et al.* (2008) 'Association between trait emotional awareness and dorsal anterior cingulate activity during emotion is arousal-dependent', *NeuroImage*, 41(2), pp. 648–655. doi: 10.1016/j.neuroimage.2008.02.030.
- McRae, K. *et al.* (2008) 'Gender Differences in Emotion Regulation: An fMRI Study of Cognitive Reappraisal', *Group Processes & Intergroup Relations*, 11(2), pp. 143–162. doi: 10.1177/1368430207088035.
- Meda, S. A. *et al.* (2012) 'Differences in resting-state functional magnetic resonance imaging functional network connectivity between schizophrenia and psychotic bipolar probands and their unaffected first-degree relatives', *Biological Psychiatry*. Elsevier Inc., 71(10), pp. 881–889. doi: 10.1016/j.biopsych.2012.01.025.
- Medford, N. and Critchley, H. D. (2010) 'Conjoint activity of anterior insular and anterior cingulate cortex: awareness and response.', *Brain structure & function*, 214(5–6), pp. 535–49. doi: 10.1007/s00429-010-0265-x.
- Menon, V. and Uddin, L. Q. (2010) 'Saliency, switching, attention and control: a network model of insula function.', *Brain structure & function*, 214(5–6), pp. 655–67. doi: 10.1007/s00429-010-0262-0.
- Meyer-Lindenberg, A. and Weinberger, D. R. (2006) 'Intermediate phenotypes and genetic mechanisms of psychiatric disorders', *Nat Rev Neurosci*, 7(10), pp. 818–827. doi: 10.1038/nrn1993.
- Mier, D., Kirsch, P. and Meyer-Lindenberg, A. (2010) 'Neural substrates of pleiotropic action of genetic variation in COMT: A meta-analysis', *Molecular Psychiatry*. Nature Publishing Group, 15(9), pp. 918–927. doi: 10.1038/mp.2009.36.
- Miettunen, J. *et al.* (2006) 'International comparison of Cloninger's temperament dimensions', *Personality and Individual Differences*, 41(8), pp. 1515–1526. doi: 10.1016/j.paid.2006.06.006.
- Mignini, F., Streccioni, V. and Amenta, F. (2003) 'Autonomic innervation of immune organs and neuroimmune modulation', *Autonomic and Autacoid Pharmacology*, 23(1), pp. 1–25. doi: 10.1046/j.1474-8673.2003.00280.x.
- Miguel-Hidalgo, J. J. and Rajkowska, G. (2003) 'Comparison of prefrontal cell pathology between depression and alcohol

- dependence', *Journal of Psychiatric Research*, 37(5), pp. 411–420. doi: 10.1016/S0022-3956(03)00049-9.
- Milak, M. S. *et al.* (2016) 'A Pilot In Vivo Proton Magnetic Resonance Spectroscopy Study of Amino Acid Neurotransmitter Response to Ketamine Treatment of Major Depressive Disorder HHS Public Access', *Mol Psychiatry*, 21(3), pp. 320–327. doi: 10.1038/mp.2015.83.
- Miller, G. A. and Rockstroh, B. (2013) 'Endophenotypes in psychopathology research: where do we stand?', *Annual review of clinical psychology*. Annual Reviews, 9, pp. 177–213.
- Mitchell, A. J. *et al.* (2011) 'Prevalence of depression, anxiety, and adjustment disorder in oncological, haematological, and palliative-care settings: A meta-analysis of 94 interview-based studies', *The Lancet Oncology*, 12(2), pp. 160–174. doi: 10.1016/S1470-2045(11)70002-X.
- Mitchell, J. P., Banaji, M. R. and Macrae, C. N. (2005) 'The link between social cognition and self-referential thought in the medial prefrontal cortex.', *Journal of cognitive neuroscience*, 17(8), pp. 1306–1315. doi: 10.1162/0898929055002418.
- Mitchell, J. P., Macrae, C. N. and Banaji, M. R. (2006) 'Dissociable Medial Prefrontal Contributions to Judgments of Similar and Dissimilar Others', *Neuron*, 50(4), pp. 655–663. doi: 10.1016/j.neuron.2006.03.040.
- Moffett, J. R. *et al.* (2007) 'N-Acetylaspartate in the CNS: from neurodiagnostics to neurobiology', *Progress in neurobiology*. Elsevier, 81(2), pp. 89–131.
- Moghaddam, B. *et al.* (1997) 'Activation of glutamatergic neurotransmission by ketamine: a novel step in the pathway from NMDA receptor blockade to dopaminergic and cognitive disruptions associated with the prefrontal cortex.', *The Journal of neuroscience : the official journal of the Society for Neuroscience*, 17(8), pp. 2921–2927.
- Monteggia, L. M., Gideons, E. and Kavalali, E. T. (2013) 'The role of eukaryotic elongation factor 2 kinase in rapid antidepressant action of ketamine', *Biological Psychiatry*. Elsevier, 73(12), pp. 1199–1203. doi: 10.1016/j.biopsych.2012.09.006.
- Morel-Kopp, M. C. *et al.* (2009) 'The association of depression with platelet activation: Evidence for a treatment effect', *Journal of Thrombosis and Haemostasis*, 7(4), pp. 573–581. doi: 10.1111/j.1538-7836.2009.03278.x.
- Morgan, C. J. a, Muetzelfeldt, L. and Curran, H. V. (2010) 'Consequences of chronic ketamine self-administration upon neurocognitive function and psychological wellbeing: A 1-year longitudinal study', *Addiction*, 105(1), pp. 121–133. doi: 10.1111/j.1360-0443.2009.02761.x.
- Moriguchi, S. *et al.* (2018) 'Glutamatergic neurometabolite levels in major depressive disorder: a systematic review and meta-analysis of proton magnetic resonance spectroscopy studies.', *Molecular Psychiatry*, 1. doi: 10.1038/s41380-018-0252-9.
- Moriguchi, Y. *et al.* (2007a) 'Age and gender effect on alexithymia in large, Japanese community and clinical samples: a cross-validation study of the Toronto Alexithymia Scale (TAS-20).', *BioPsychoSocial medicine*, 1, p. 7. doi: 10.1186/1751-0759-1-7.
- Moriguchi, Y. *et al.* (2007b) 'Age and gender effect on alexithymia in large, Japanese community and clinical samples: a cross-validation study of the Toronto Alexithymia Scale (TAS-20).', *BioPsychoSocial medicine*, 1, p. 7. doi: 10.1186/1751-0759-1-7.
- Moriguchi, Y. *et al.* (2014) 'Sex differences in the neural correlates of affective experience.', *Social cognitive and affective neuroscience*, 9(5), pp. 591–600. doi: 10.1093/scan/nst030.
- Moriguchi, Y. and Komaki, G. (2013) 'Neuroimaging studies of alexithymia: physical, affective, and social perspectives.', *BioPsychoSocial medicine*. BioPsychoSocial Medicine, 7(1), p. 8. doi: 10.1186/1751-0759-7-8.
- Morris, J. a., Leclerc, C. M. and Kensinger, E. a. (2013) 'Effects of valence and divided attention on cognitive reappraisal processes', *Social Cognitive and Affective Neuroscience*, 9(12), pp. 1952–1961. doi: 10.1093/scan/nsu004.
- Müller, I. *et al.* (2014) 'GAD65 haplodeficiency conveys resilience in animal models of stress-induced psychopathology.', *Frontiers in behavioral neuroscience*, 8(August), p. 265. doi: 10.3389/fnbeh.2014.00265.
- Müller, I., Çalışkan, G. and Stork, O. (2015) 'The GAD65 knock out mouse - A model for GABAergic processes in fear- and stress-induced psychopathology', *Genes, Brain and Behavior*, 14(1), pp. 37–45. doi: 10.1111/gbb.12188.
- Müller, J., Bühner, M. and Ellgring, H. (2003) 'Is there a reliable factorial structure in the 20-item Toronto Alexithymia Scale?', *Journal of Psychosomatic Research*, 55(6), pp. 561–568. doi: 10.1016/S0022-3999(03)00033-3.
- Murphy-Royal, C. *et al.* (2017) 'Astroglial glutamate transporters in the brain: regulating neurotransmitter homeostasis and synaptic transmission', *Journal of neuroscience research*. Wiley Online Library, 95(11), pp. 2140–2151.
- Murphy, K. *et al.* (2009) 'The impact of global signal regression on resting state correlations: Are anti-correlated networks introduced?', *NeuroImage*. Elsevier B.V., 44(3), pp. 893–905. doi: 10.1016/j.neuroimage.2008.09.036.
- Murphy, K. and Fox, M. D. (2017) 'Towards a consensus regarding global signal regression for resting state functional

- connectivity MRI', *NeuroImage*. Elsevier, 154(November), pp. 169–173. doi: 10.1016/j.neuroimage.2016.11.052.
- Murrough, J. W. *et al.* (2013) 'Antidepressant efficacy of ketamine in treatment-resistant major depression: A two-site randomized controlled trial', *American Journal of Psychiatry*, 170(10), pp. 1134–1142. doi: 10.1176/appi.ajp.2013.13030392.
- Murrough, J. W., Abdallah, C. G. and Mathew, S. J. (2017) 'Targeting glutamate signalling in depression: progress and prospects', *Nature Reviews Drug Discovery*. Nature Publishing Group, (Mdd). doi: 10.1038/nrd.2017.16.
- Nagae-Poetscher, L. M. *et al.* (2004) 'Asymmetry and gender effect in functionally lateralized cortical regions: a proton MRS imaging study.', *Journal of magnetic resonance imaging : JMRI*, 19(1), pp. 27–33. doi: 10.1002/jmri.10429.
- Nakagawa, T. *et al.* (2002) 'Ketamine Suppresses Platelet Aggregation Possibly by Suppressed Inositol Triphosphate Formation and Subsequent Suppression of Cytosolic Calcium Increase', *Anesthesiology*, 96(5), pp. 1147–52. doi: 0000542-200205000-00018 [pii].
- Nash, G. F. *et al.* (2002) 'Platelets and cancer', *Lancet Oncology*, 3(7), pp. 425–430. doi: 10.1016/S1470-2045(02)00789-1.
- Le Nedelec, M. *et al.* (2018) 'Acute low-dose ketamine produces a rapid and robust increase in plasma BDNF without altering brain BDNF concentrations.', *Drug delivery and translational research*. Drug Delivery and Translational Research. doi: 10.1007/s13346-017-0476-2.
- Nelson, S. J., Vigneron, D. B. and Dillon, W. P. (1999) 'Serial evaluation of patients with brain tumors using volume MRI and 3D 1H MRSI', *NMR in Biomedicine: An International Journal Devoted to the Development and Application of Magnetic Resonance In Vivo*. Wiley Online Library, 12(3), pp. 123–138.
- Nemeroff, C. B. (2007) 'Prevalence and management of treatment-resistant depression', *Journal of Clinical Psychiatry*. Physicians Postgraduate Press; 1999, 68(8), p. 17.
- Nemiah, J. C. and Sifneos, P. E. (1970) 'Psychosomatic illness: a problem in communication', *Psychotherapy and Psychosomatics*. Karger Publishers, 18(1–6), pp. 154–160.
- Ng, S. H. *et al.* (2010) 'Emergency department presentation of ketamine abusers in Hong Kong: A review of 233 cases', *Hong Kong Medical Journal*, 16(1), pp. 6–11.
- Niciu, M. J. *et al.* (2014) 'Clinical Predictors of Ketamine Response in Treatment-Resistant Major Depression', *The Journal of clinical psychiatry*, 75(5), pp. e417–e423. doi: 10.4088/JCP.13m08698.
- Niciu, M. J. *et al.* (2018) 'Features of dissociation differentially predict antidepressant response to ketamine in treatment-resistant depression', *Journal of Affective Disorders*. Elsevier B.V., 232(January), pp. 310–315. doi: 10.1016/j.jad.2018.02.049.
- Nimchinsky, E. a *et al.* (1999) 'A neuronal morphologic type unique to humans and great apes.', *Proceedings of the National Academy of Sciences of the United States of America*, 96(9), pp. 5268–5273. doi: 10.1073/pnas.96.9.5268.
- Nordstokke, D. W. and Zumbo, B. D. (2010) 'A new nonparametric Levene test for equal variances.', *Psicologica: International Journal of Methodology and Experimental Psychology*. ERIC, 31(2), pp. 401–430.
- Northoff, G. *et al.* (2006) 'Self-referential processing in our brain-A meta-analysis of imaging studies on the self', *NeuroImage*, 31(1), pp. 440–457. doi: 10.1016/j.neuroimage.2005.12.002.
- Northoff, G. *et al.* (2007) 'GABA concentrations in the human anterior cingulate cortex predict negative BOLD responses in fMRI', *Nature Neuroscience*, 10(12), pp. 1515–1517. doi: 10.1038/nn2001.
- Nuernberg, G. L. *et al.* (2016) 'Brain-derived neurotrophic factor increase during treatment in severe mental illness inpatients', *Translational Psychiatry*, 6(12), p. e985. doi: 10.1038/tp.2016.227.
- Nugent, A. C. *et al.* (2015) 'The relationship between glucose metabolism, resting-state fMRI BOLD signal, and GABA A -binding potential: A preliminary study in healthy subjects and those with temporal lobe epilepsy', *Journal of Cerebral Blood Flow and Metabolism*, 35(October 2014), pp. 583–591. doi: 10.1038/jcbfm.2014.228.
- Nuss, P. (2015) 'Anxiety disorders and GABA neurotransmission: A disturbance of modulation', *Neuropsychiatric Disease and Treatment*, 11, pp. 165–175. doi: 10.2147/NDT.S58841.
- O'Driscoll, C., Laing, J. and Mason, O. (2014) 'Cognitive emotion regulation strategies, alexithymia and dissociation in schizophrenia, a review and meta-analysis', *Clinical Psychology Review*. Elsevier, 34(6), pp. 482–495.
- Ochsner, K. N. *et al.* (2004) 'Reflecting upon feelings: an fMRI study of neural systems supporting the attribution of emotion to self and other.', *Journal of cognitive neuroscience*, 16(10), pp. 1746–1772. doi: 10.1162/0898929042947829.
- Ochsner, K. N. *et al.* (2009) 'Bottom up and top down processes in emotion generation: common and distinct neural mechanisms', *Psychol Sci*, 20(11), pp. 1322–1331. doi: 10.1111/j.1467-9280.2009.02459.x.Bottom-Up.
- Ochsner, K. N. and Gross, J. J. (2005) 'The cognitive control of emotion.', *Trends in cognitive sciences*, 9(5), pp. 242–9. doi: 10.1016/j.tics.2005.03.010.

- Ogawa, S. *et al.* (1990) 'Oxygenation-sensitive contrast in magnetic resonance image of rodent brain at high magnetic fields', *Magnetic resonance in medicine*. Wiley Online Library, 14(1), pp. 68–78.
- Oldfield, R. C. (1971) 'The Assessment and Analysis of Handedness: The Edinburgh Inventory', *Neuropsychologia*, 9, pp. 97–113.
- Öngür, D. *et al.* (2008) 'Abnormal glutamatergic neurotransmission and neuronal-glia interactions in acute mania', *Biological psychiatry*. Elsevier, 64(8), pp. 718–726.
- Ordidge, R. J. and Gordon, R. E. (1985) 'Methods and apparatus of obtaining NMR spectra'. Google Patents.
- Orser, B. A., Pennefather, P. S. and MacDonald, J. F. (1997) 'Multiple mechanisms of ketamine blockade of N-methyl-D-aspartate receptors', *Anesthesiology: The Journal of the American Society of Anesthesiologists*. The American Society of Anesthesiologists, 86(4), pp. 903–917.
- Oz, G. *et al.* (2014) 'Clinical proton MR spectroscopy in central nervous system disorders.', *Radiology*, 270(3), pp. 658–79. doi: 10.1148/radiol.13130531.
- Palomero-Gallagher, N., *et al.* (2009) 'Receptor architecture of human cingulate cortex: evaluation of the four-region neurobiological model.', *Human brain mapping*, 30(8), pp. 2336–55. doi: 10.1002/hbm.20667.
- Palomero-Gallagher, N. *et al.* (2018) 'Human Pregenual Anterior Cingulate Cortex: Structural, Functional, and Connectional Heterogeneity', *Cerebral Cortex*, (June), pp. 1–23. doi: 10.1093/cercor/bhy124.
- Palomero-Gallagher, N. *et al.* (2008) 'Cytology and receptor architecture of human anterior cingulate cortex', *Journal of Comparative Neurology*. Wiley Online Library, 508(6), pp. 906–926.
- Panja, D. and Bramham, C. R. (2014) 'BDNF mechanisms in late LTP formation: A synthesis and breakdown', *Neuropharmacology*. Elsevier Ltd, 76(PART C), pp. 664–676. doi: 10.1016/j.neuropharm.2013.06.024.
- Pardo, J. V. *et al.* (1990) 'The anterior cingulate cortex mediates processing selection in the Stroop attentional conflict paradigm', *Proceedings of the National Academy of Sciences*. National Acad Sciences, 87(1), pp. 256–259.
- Park, M. *et al.* (2016) 'Change in cytokine levels is not associated with rapid antidepressant response to ketamine in treatment-resistant depression.', *Journal of psychiatric research*. Elsevier Ltd, 84, pp. 113–118. doi: 10.1016/j.jpsychires.2016.09.025.
- Parker, J. D. ., Taylor, G. J. and Bagby, R. M. (2003) 'The 20-Item Toronto Alexithymia Scale', *Journal of Psychosomatic Research*, 55(3), pp. 269–275. doi: 10.1016/S0022-3999(02)00578-0.
- Patel, A. B. *et al.* (2005) 'The contribution of GABA to glutamate/glutamine cycling and energy metabolism in the rat cortex in vivo.', *Proceedings of the National Academy of Sciences of the United States of America*, 102(15), pp. 5588–5593. doi: 10.1073/pnas.0501703102.
- Patel, A. B. *et al.* (2006) 'Evidence that GAD65 mediates increased GABA synthesis during intense neuronal activity in vivo', *Journal of Neurochemistry*, 97(2), pp. 385–396. doi: 10.1111/j.1471-4159.2006.03741.x.
- Patel, S. R., Hartwig, J. H. and Italiano, J. E. J. (2005) 'The biogenesis of platelets from megakaryocyte proplatelets', *The journal of clinical investigation*, 115(12). doi: 10.1172/JCI26891.3348.
- Paul, R. K. *et al.* (2014) 'Target of Rapamycin Function', *Anesthesiology*, 121(1), pp. 149–159.
- Pelkonen, O. *et al.* (2008) 'Inhibition and induction of human cytochrome P450 enzymes: Current status', *Archives of Toxicology*, 82(10), pp. 667–715. doi: 10.1007/s00204-008-0332-8.
- Pellerin, L. and Magistretti, P. J. (1994) 'Glutamate uptake into astrocytes stimulates aerobic glycolysis: a mechanism coupling neuronal activity to glucose utilization', *Proceedings of the National Academy of Sciences*. National Acad Sciences, 91(22), pp. 10625–10629.
- Peltoniemi, M. a. *et al.* (2016) 'Ketamine: A Review of Clinical Pharmacokinetics and Pharmacodynamics in Anesthesia and Pain Therapy', *Clinical Pharmacokinetics*. Springer International Publishing, 55(9), pp. 1059–1077. doi: 10.1007/s40262-016-0383-6.
- Perkovic, M. N. *et al.* (2018) 'Biomarkers of Depression: Potential Diagnostic Tools', in *Understanding Depression*. Springer, pp. 35–51.
- Pérusse, F., Boucher, S. and Fernet, M. (2012) 'Observation of couple interactions: Alexithymia and communication behaviors', *Personality and Individual Differences*. Elsevier Ltd, 53(8), pp. 1017–1022. doi: 10.1016/j.paid.2012.07.022.
- Pfleiderer, B. *et al.* (2003) 'Effective electroconvulsive therapy reverses glutamate/glutamine deficit in the left anterior cingulum of unipolar depressed patients', *Psychiatry Research - Neuroimaging*, 122(3), pp. 185–192. doi: 10.1016/S0925-4927(03)00003-9.
- Phan, K. L. *et al.* (2005) 'Neural substrates for voluntary suppression of negative affect: A functional magnetic resonance imaging study', *Biological Psychiatry*, 57(3), pp. 210–219. doi: 10.1016/j.biopsych.2004.10.030.

- Phelps, L. E. *et al.* (2009) 'Family history of alcohol dependence and initial antidepressant response to an N-methyl-D-aspartate antagonist', *Biological psychiatry*. Elsevier, 65(2), pp. 181–184.
- Phoumthippavong, V. *et al.* (2016) 'Longitudinal Effects of Ketamine on Dendritic Architecture In Vivo in the Mouse Medial Frontal Cortex', *Eneuro*, 3(2), pp. 91–95. doi: 10.1523/eneuro.0133-15.2016.
- Pinal, C. S. and Tobin, A. J. (1998) 'Uniqueness and redundancy in GABA production.', *Perspectives on developmental neurobiology*, 5(December), pp. 109–118.
- Pinna, F., Sanna, L. and Carpiniello, B. (2014) 'Alexithymia in eating disorders: Therapeutic implications', *Psychology Research and Behavior Management*, 8, pp. 1–15. doi: 10.2147/PRBM.S52656.
- Polyakova, M. *et al.* (2015) 'BDNF as a biomarker for successful treatment of mood disorders: A systematic & quantitative meta-analysis', *Journal of Affective Disorders*, 174, pp. 432–440. doi: 10.1016/j.jad.2014.11.044.
- Pomp, E. R., Rosendaal, F. R. and Doggen, C. J. (2008) 'Smoking increases the risk of venous thrombosis and acts synergistically with oral contraceptive use', *American journal of hematology*, 83(2), pp. 97–102. doi: 10.1002/ajh.
- Popoli, M. *et al.* (2012) 'The stressed synapse: The impact of stress and glucocorticoids on glutamate transmission', *Nature Reviews Neuroscience*. Nature Publishing Group, 13(1), pp. 22–37. doi: 10.1038/nrn3138.
- Porcelli, S. *et al.* (2011) 'Genetic polymorphisms of cytochrome P450 enzymes and antidepressant metabolism', *Expert opinion on drug metabolism & toxicology*. Taylor & Francis, 7(9), pp. 1101–1115.
- Portella, M. J. *et al.* (2011) 'Ventromedial prefrontal spectroscopic abnormalities over the course of depression: a comparison among first episode, remitted recurrent and chronic patients', *Journal of psychiatric research*. Elsevier, 45(4), pp. 427–434.
- Power, J. D., Schlaggar, B. L. and Petersen, S. E. (2015) 'Recent progress and outstanding issues in motion correction in resting state fMRI', *NeuroImage*. Elsevier Inc., 105(2015), pp. 536–551. doi: 10.1016/j.neuroimage.2014.10.044.
- Preacher, K. J. and Hayes, A. F. (2004) 'SPSS and SAS procedures for estimating indirect effects in simple mediation models', *Behavior research methods, instruments, & computers*, 36(4), pp. 717–731. doi: 10.3758/BF03206553.
- Preisig, M., Merikangas, K. R. and Angst, J. (2001) 'Clinical significance and comorbidity of subthreshold depression and anxiety in the community', *Acta Psychiatrica Scandinavica*. Wiley Online Library, 104(2), pp. 96–103.
- Previtali, E. *et al.* (2011) 'Risk factors for venous and arterial thrombosis', *Blood Transfusion*, 9(2), pp. 120–138. doi: 10.2450/2010.0066-10.
- Price, J. L. and Drevets, W. C. (2012) 'Neural circuits underlying the pathophysiology of mood disorders', *Trends in Cognitive Sciences*, 16(1), pp. 61–71. doi: 10.1016/j.tics.2011.12.011.
- Price, R. B. *et al.* (2009) 'Amino acid neurotransmitters assessed by proton magnetic resonance spectroscopy: relationship to treatment resistance in major depressive disorder', *Biological psychiatry*. Elsevier, 65(9), pp. 792–800.
- Provencher, S. W. (1993) 'Estimation of metabolite concentrations from localized in vivo proton NMR spectra', *Magnetic resonance in medicine*. Wiley Online Library, 30(6), pp. 672–679.
- Provencher, S. W. (2001) 'Automatic quantitation of localized in vivo 1 H spectra with LCModel', *NMR in Biomedicine*, 14(4), pp. 260–264. doi: 10.1002/nbm.698.
- Snaith, R. P., Hamilton, M., Morley, S., Humayan, A. (1995) 'Snaith, Hamilton, 1995 - A scale for the assessment of hedonic tone the SHAPS', *British Journal of Psychiatry (1995)*, 167, pp. 99–103. doi: 10.1192/bjp.167.1.99.
- Radke, S. *et al.* (2011) 'Mistakes that affect others: An fMRI study on processing of own errors in a social context', *Experimental Brain Research*, 211(3–4), pp. 405–413. doi: 10.1007/s00221-011-2677-0.
- Radulescu, E. *et al.* (2013) 'Effect of Schizophrenia Risk-Associated Alleles in SREB2 (GPR85) on Functional MRI Phenotypes in Healthy Volunteers', *Neuropsychopharmacology*. Nature Publishing Group, 38(2), pp. 341–349. doi: 10.1038/npp.2012.184.
- Raichle, M. E. (1987) 'Circulatory and metabolic correlates of brain function in normal humans', *Handbook of Physiology. The Nervous System. Higher Functions of the Brain*, 1987, p. 643.
- Raichle, M. E. *et al.* (2001) 'A default mode of brain function.', *Proceedings of the National Academy of Sciences of the United States of America*, 98(2), pp. 676–82. doi: 10.1073/pnas.98.2.676.
- Raichle, M. E. and Gusnard, D. A. (2005) 'Intrinsic brain activity sets the stage for expression of motivated behavior', *Journal of Comparative Neurology*. Wiley Online Library, 493(1), pp. 167–176.
- Rajkowska, G. *et al.* (1999) 'Morphometric evidence for neuronal and glial prefrontal cell pathology in major depression', *Biological Psychiatry*, 45(9), pp. 1085–1098. doi: 10.1016/S0006-3223(99)00041-4.
- Rajkowska, G. (2000) 'Postmortem studies in mood disorders indicate altered numbers of neurons and glial cells', *Biological Psychiatry*, 48(8), pp. 766–777. doi: 10.1016/S0006-3223(00)00950-1.

- Rajkowska, G. (2003) 'Depression: what we can learn from postmortem studies.', *The Neuroscientist: a review journal bringing neurobiology, neurology and psychiatry*, 9(4), pp. 273–284. doi: 10.1177/1073858403252773.
- Rajkowska, G. et al. (2005) 'Prominent reduction in pyramidal neurons density in the orbitofrontal cortex of elderly depressed patients', *Biological Psychiatry*. Elsevier, 58(4), pp. 297–306.
- Rajkowska, G. and Stockmeier, C. a (2013) 'Astrocyte pathology in major depressive disorder: insights from human postmortem brain tissue.', *Current drug targets*, 14(11), pp. 1225–36. doi: 10.2174/13894501113149990156.
- Ramadan, S., Lin, A. and Stanwell, P. (2014) 'Glutamate and glutamine: a review of in vivo MRS in the human brain.', *NMR in biomedicine*, 26(12), pp. 1630–1646. doi: 10.1002/nbm.3045.Glutamate.
- Rao, L. K. et al. (2016) 'Role of cytochrome P4502B6 polymorphisms in ketamine metabolism and clearance', *Anesthesiology: The Journal of the American Society of Anesthesiologists*. The American Society of Anesthesiologists, 125(6), pp. 1103–1112.
- Regev, a et al. (1997) 'Thrombotic complications in essential thrombocythemia with relatively low platelet counts.', *American journal of hematology*, 56(3), pp. 168–72. doi: 10.1002/(SICI)1096-8652(199711)56:3<168::AID-AJH6>3.o.CO;2-W.
- Reker, M. et al. (2010) 'Individual differences in alexithymia and brain response to masked emotion faces', *Cortex*. Elsevier Srl, 46(5), pp. 658–667. doi: 10.1016/j.cortex.2009.05.008.
- Rial, D. et al. (2016) 'Depression as a glial-based synaptic dysfunction', *Frontiers in cellular neuroscience*. Frontiers, 9, p. 521.
- Richter, J., Eisemann, M. and Richter, G. (2000) 'Zur deutschsprachigen Version des Temperament- und Charakterinventars', *Z Klin Psychol Psychother*, 29(2), pp. 117–126. doi: https://doi.org/10.1026//0084-5345.29.2.117.
- Ritchie, R. F. et al. (2004) 'Reference Distributions for Alpha2-Macroglobulin: A Practical, Simple and Clinically Relevant Approach in a Large Cohort', *Journal of Clinical Laboratory Analysis*, 18(2), pp. 139–147. doi: 10.1002/jcla.20012.
- Rizvi, S. J. et al. (2014) 'Treatment-resistant depression in primary care across Canada.', *Canadian journal of psychiatry. Revue canadienne de psychiatrie*, 59(7), pp. 349–57. doi: 10.1177/070674371405900702.
- Robinson, J. M. and Vandré, D. D. (1995) 'Stimulus-dependent alterations in macrophage microtubules: increased tubulin polymerization and detyrosination.', *Journal of cell science*, 108 (Pt 2(May)), pp. 645–655.
- Romeo, B. et al. (2018) 'Meta-analysis of central and peripheral γ -aminobutyric acid levels in patients with unipolar and bipolar depression', *Journal of Psychiatry and Neuroscience*, 43(1), pp. 58–66. doi: 10.1503/jpn.160228.
- van Rossum, E. F. C. et al. (2006) 'Polymorphisms of the glucocorticoid receptor gene and major depression', *Biological psychiatry*. Elsevier, 59(8), pp. 681–688.
- Rothman, D. L. et al. (2003) 'In vivo NMR studies of the glutamate neurotransmitter flux and neuroenergetics: implications for brain function.', *Annual review of physiology*, 65(1), pp. 401–427. doi: 10.1146/annurev.physiol.65.092101.142131.
- Rothman, D. L. et al. (2011) '¹³C MRS studies of neuroenergetics and neurotransmitter cycling in humans', *NMR in Biomedicine*, 24(8), pp. 943–957. doi: 10.1002/nbm.1772.
- Rovirosa-Hernández, M. J. et al. (2011) 'Blood parameters are little affected by time of sampling after the application of ketamine in black howler monkeys (*Alouatta pigra*)', *Journal of Medical Primatology*, 40(5), pp. 294–299. doi: 10.1111/j.1600-0684.2011.00474.x.
- Rowland, L. M. et al. (2005) 'Effects of ketamine on anterior cingulate glutamate metabolism in healthy humans: A 4-T proton MRS study', *American Journal of Psychiatry*, 162(2), pp. 394–396. doi: 10.1176/appi.ajp.162.2.394.
- Rush, A. J. et al. (2006) 'Bupropion-SR, sertraline, or venlafaxine-XR after failure of SSRIs for depression', *New England Journal of Medicine*. Mass Medical Soc, 354(12), pp. 1231–1242.
- Russo, S. and Nestler, E. (2013) 'The brain reward circuitry in mood disorders', *Nature Reviews Neuroscience*, 625(September), pp. 609–625. doi: 10.1038/nrn3381.
- Saad, Z. S. et al. (2013) 'Correcting Brain-Wide Correlation Differences in Resting-State fMRI', *Brain Connectivity*, 3(4), pp. 339–352. doi: 10.1089/brain.2013.0156.
- Saland, S. K., Duclot, F. and Kabbaj, M. (2017) 'Integrative analysis of sex differences in the rapid antidepressant effects of ketamine in preclinical models for individualized clinical outcomes', *Current Opinion in Behavioral Sciences*. Elsevier Ltd, 14, pp. 19–26. doi: 10.1016/j.cobeha.2016.11.002.
- Salvadore, G. et al. (2012) 'An investigation of amino-acid neurotransmitters as potential predictors of clinical improvement to ketamine in depression', *The International Journal of Neuropsychopharmacology*, 15(08), pp. 1063–1072. doi: 10.1017/S1461145711001593.
- Sambataro, F. et al. (2014) 'Revisiting default mode network function in major depression: Evidence for disrupted subsystem connectivity', *Psychological Medicine*, 44(10), pp. 2041–2051. doi: 10.1017/S0033291713002596.
- Sanacora, G. et al. (2002) 'Increased occipital cortex GABA concentrations in depressed patients after therapy with selective

- serotonin reuptake inhibitors', *American Journal of Psychiatry*, 159(4), pp. 663–665. doi: 10.1176/appi.ajp.159.4.663.
- Sanacora, G. and Banasr, M. (2013) 'From Pathophysiology to Novel Antidepressant Treatment of Mood Disorders', *Biological Psychiatry*. Elsevier, 73(12), pp. 1172–1179. doi: 10.1016/j.biopsych.2013.03.032.
- Sanacora, G. and Schatzberg, A. F. (2015) 'Ketamine: promising path or false prophecy in the development of novel therapeutics for mood disorders?', *Neuropsychopharmacology*, 40(2), pp. 259–67. doi: 10.1038/npp.2014.261.
- Sanacora, G., Treccani, G. and Popoli, M. (2012) 'Neuropharmacology Towards a glutamate hypothesis of depression An emerging frontier of neuropsychopharmacology for mood disorders', *Neuropharmacology*. Elsevier Ltd, 62(1), pp. 63–77. doi: 10.1016/j.neuropharm.2011.07.036.
- Sánchez-Huertas, C. and Rico, B. (2011) 'CREB-dependent regulation of *gad65* transcription by BDNF/TrkB in cortical interneurons', *Cerebral Cortex*, 21(4), pp. 777–788. doi: 10.1093/cercor/bhq150.
- Sangha, S. *et al.* (2009) 'Deficiency of the 65 kDa isoform of glutamic acid decarboxylase impairs extinction of cued but not contextual fear memory.', *The Journal of neuroscience : the official journal of the Society for Neuroscience*, 29(50), pp. 15713–20. doi: 10.1523/JNEUROSCI.2620-09.2009.
- Sankoh, A. J., Huque, M. F. and Dubey, S. D. (1997) 'Some comments on frequently used multiple endpoint adjustment methods in clinical trials', *Statistics in medicine*. Wiley Online Library, 16(22), pp. 2529–2542.
- Sassi, R. B. *et al.* (2005) 'Reduced NAA levels in the dorsolateral prefrontal cortex of young bipolar patients.', *The American journal of psychiatry*, 162(11), pp. 2109–15. doi: 10.1176/appi.ajp.162.11.2109.
- Satpute, A. B. *et al.* (2013) 'The functional neural architecture of self-reports of affective experience', *Biological Psychiatry*. Elsevier, 73(7), pp. 631–638. doi: 10.1016/j.biopsych.2012.10.001.
- Satterthwaite, T. D. *et al.* (2013) 'An improved framework for confound regression and filtering for control of motion artifact in the preprocessing of resting-state functional connectivity data', *NeuroImage*. Elsevier Inc., 64(1), pp. 240–256. doi: 10.1016/j.neuroimage.2012.08.052.
- Savic, I. *et al.* (2000) 'In vivo measurements of glutamine + glutamate (Glx) and N-acetyl aspartate (NAA) levels in human partial epilepsy.', *Acta neurologica Scandinavica*, 102(3), pp. 179–88. Available at: <http://www.ncbi.nlm.nih.gov/pubmed/10987378>.
- Scharf, S. L., Parikh, S. and Dillon, L. C. (2005) 'Spontaneous bruising as a possible adverse reaction to memantine', *Internal medicine journal*, 35(9), pp. 571–572. doi: 10.1111/j.1445-5994.2005.00874.x.
- Scheidegger, M. *et al.* (2012) 'Ketamine decreases resting state functional network connectivity in healthy subjects: implications for antidepressant drug action.', *PloS one*, 7(9), p. e44799. doi: 10.1371/journal.pone.0044799.
- Scheidegger, M. *et al.* (2016) 'Ketamine administration reduces amygdalo-hippocampal reactivity to emotional stimulation', *Human Brain Mapping*, 37(5), pp. 1941–1952. doi: 10.1002/hbm.23148.
- Schilbach, L. *et al.* (2008) 'Minds at rest? Social cognition as the default mode of cognizing and its putative relationship to the "default system" of the brain.', *Consciousness and cognition*, 17(2), pp. 457–67. doi: 10.1016/j.concog.2008.03.013.
- Schousboe, A. *et al.* (1997) 'Trafficking between glia and neurons of TCA cycle intermediates and related metabolites', *Glia*. Wiley Online Library, 21(1), pp. 99–105.
- Schubert, F. *et al.* (2004) 'Glutamate concentrations in human brain using single voxel proton magnetic resonance spectroscopy at 3 Tesla.', *NeuroImage*, 21(4), pp. 1762–71. doi: 10.1016/j.neuroimage.2003.11.014.
- Schuch, J. J. J. *et al.* (2014) 'Gender differences in major depressive disorder: results from the Netherlands study of depression and anxiety', *Journal of affective disorders*. Elsevier, 156, pp. 156–163.
- Schuff, N. *et al.* (2001) 'Region and Tissue Differences of Metabolites in Normally Aged Brain Using Multislice 1H Magnetic Resonance Spectroscopic Imaging', 907, pp. 899–907.
- Seeley, W. W. *et al.* (2007) 'Dissociable intrinsic connectivity networks for salience processing and executive control.', *The Journal of neuroscience : the official journal of the Society for Neuroscience*, 27(9), pp. 2349–56. doi: 10.1523/JNEUROSCI.5587-06.2007.
- Selby, N. M. *et al.* (2008) 'Obstructive nephropathy and kidney injury associated with ketamine abuse', *NTD plus*, 1(5), pp. 310–312. doi: 10.1093/ndtplus/sfn054.
- Seney, M. L. *et al.* (2013) 'The role of genetic sex in affect regulation and expression of GABA-related genes across species', *Frontiers in Psychiatry*, 4(SEP), pp. 1–18. doi: 10.3389/fpsy.2013.00104.
- Serafini, G. *et al.* (2014) 'Hippocampal neurogenesis, neurotrophic factors and depression: possible therapeutic targets?', *CNS & Neurological Disorders-Drug Targets (Formerly Current Drug Targets-CNS & Neurological Disorders)*. Bentham Science Publishers, 13(10), pp. 1708–1721.
- Setiawan, E. *et al.* (2015) 'Role of Translocator Protein Density, a Marker of Neuroinflammation, in the Brain During Major

- Depressive Episodes', 72(3), pp. 268–275. doi: 10.1001/jamapsychiatry.2014.2427.
- Sheehan, D. V. *et al.* (1998) 'The Mini-International Neuropsychiatric Interview (M.I.N.I.): The development and validation of a structured diagnostic psychiatric interview for DSM-IV and ICD-10', *Journal of Clinical Psychiatry*, 59(SUPPL. 20), pp. 22–33. doi: 10.1016/S0924-9338(99)80239-9.
- Sheline, Y. I. *et al.* (2010) 'Resting-state functional MRI in depression unmasks increased connectivity between networks via the dorsal nexus', *Proceedings of the National Academy of Sciences*, 107(24), pp. 11020–11025. doi: 10.1073/pnas.1000446107.
- Shen, J. *et al.* (1999) 'Determination of the rate of the glutamate/glutamine cycle in the human brain by in vivo ^{13}C NMR.', *Proceedings of the National Academy of Sciences of the United States of America*, 96(14), pp. 8235–40. Available at: <http://www.pubmedcentral.nih.gov/articlerender.fcgi?artid=22218&tool=pmcentrez&rendertype=abstract>.
- Shen, J. (2006) ' ^{13}C magnetic resonance spectroscopy studies of alterations in glutamate neurotransmission', *Biological psychiatry*. Elsevier, 59(10), pp. 883–887.
- Shen, J. (2013) 'Modeling the glutamate–glutamine neurotransmitter cycle', *Frontiers in neuroenergetics*. Frontiers, 5, p. 1.
- Sheth, S. A. *et al.* (2012) 'Human dorsal anterior cingulate cortex neurons mediate ongoing behavioural adaptation', *Nature*. Nature Publishing Group, 488(7410), p. 218.
- Shibata, M. *et al.* (2014) 'Alexithymia is associated with greater risk of chronic pain and negative affect and with lower life satisfaction in a general population: The Hisayama study', *PLoS ONE*, 9(3), pp. 1–8. doi: 10.1371/journal.pone.0090984.
- Shinno, H. *et al.* (2007) 'A decrease in N-acetylaspartate and an increase in myoinositol in the anterior cingulate gyrus are associated with behavioral and psychological symptoms in Alzheimer's disease.', *Journal of the neurological sciences*, 260(1–2), pp. 132–8. doi: 10.1016/j.jns.2007.04.017.
- Short, B. *et al.* (2018) 'Side-effects associated with ketamine use in depression: a systematic review', *The Lancet Psychiatry*. Elsevier Ltd, 5(1), pp. 65–78. doi: 10.1016/S2215-0366(17)30272-9.
- Shulman, R. G. *et al.* (2004) 'Energetic basis of brain activity: Implications for neuroimaging', *Trends in Neurosciences*, 27(8), pp. 489–495. doi: 10.1016/j.tins.2004.06.005.
- Si, X. *et al.* (2004) 'Age-dependent reductions in the level of glial fibrillary acidic protein in the prefrontal cortex in major depression', *Neuropsychopharmacology*, 29(11), pp. 2088–2096. doi: 10.1038/sj.npp.1300525.
- Sierko, E. and Wojtukiewicz, M. Z. (2007) 'Inhibition of platelet function: Does it offer a chance of better cancer progression control?', *Seminars in Thrombosis and Hemostasis*, 33(7), pp. 712–721. doi: 10.1055/s-2007-991540.
- Skudlarski, P., Constable, R. T. and Gore, J. C. (1999) 'ROC Analysis of Statistical Methods Used in Functional MRI: Individual Subjects', *NeuroImage*, 9(3), pp. 311–329. doi: 10.1006/nimg.1999.0402.
- Sladky, R. *et al.* (2013) 'High-resolution functional MRI of the human amygdala at 7 T', *European Journal of Radiology*. Elsevier Ireland Ltd, 82(5), pp. 728–733. doi: 10.1016/j.ejrad.2011.09.025.
- Smith, S. M. *et al.* (2009) 'Correspondence of the brain's functional architecture during activation and rest.', *Proceedings of the National Academy of Sciences of the United States of America*, 106(31), pp. 13040–5. doi: 10.1073/pnas.0905267106.
- Soeiro-de-Souza, M. G. *et al.* (2015) 'Anterior cingulate Glutamate–Glutamine cycle metabolites are altered in euthymic bipolar I disorder', *European neuropsychopharmacology*. Elsevier, 25(12), pp. 2221–2229.
- Soghomonian, J. J. and Martin, D. L. (1998) 'Two isoforms of glutamate decarboxylase: Why?', *Trends in Pharmacological Sciences*, 19(12), pp. 500–505. doi: 10.1016/S0165-6147(98)01270-X.
- Soldin, O. P. and Mattison, D. R. (2009) 'Sex differences in pharmacokinetics and pharmacodynamics', *Clinical Pharmacokinetics*, 48(3), pp. 143–157. doi: 10.2165/00003088-200948030-00001.
- Song, H. R. *et al.* (2012) 'Platelet count alterations associated with escitalopram, venlafaxine and bupropion in depressive patients', *Psychiatry and Clinical Neurosciences*, 66(5), pp. 457–459. doi: 10.1111/j.1440-1819.2012.02355.x.
- Song, X.-W. *et al.* (2011) 'REST: a toolkit for resting-state functional magnetic resonance imaging data processing', *PLoS one*. Public Library of Science, 6(9), p. e25031.
- Song, Y. and Brady, S. T. (2015) 'Post-translational modifications of tubulin: Pathways to functional diversity of microtubules', *Trends in Cell Biology*. Elsevier Ltd, 25(3), pp. 125–136. doi: 10.1016/j.tcb.2014.10.004.
- Speck, O., Stadler, J. and Zaitsev, M. (2008) 'High resolution single-shot EPI at 7T.', *Magnetic Resonance Materials in Physics, Biology and Medicine*, 21(1–2), pp. 73–86. doi: 10.1007/s10334-007-0087-x.
- Spunt, R. P. and Lieberman, M. D. (2012) 'An integrative model of the neural systems supporting the comprehension of observed emotional behavior', *NeuroImage*. Elsevier Inc., 59(3), pp. 3050–3059. doi: 10.1016/j.neuroimage.2011.10.005.

- Stagg, C. J., Bachtiar, V. and Johansen-Berg, H. (2011) 'What are we measuring with GABA magnetic resonance spectroscopy?', *Communicative & integrative biology*, 4(5), pp. 573–575. doi: 10.4161/cib.4.5.16213.
- Stallings, M. C. *et al.* (1996) 'Genetic and environmental structure of the Tridimensional Personality Questionnaire: three or four temperament dimensions?', *Journal of personality and social psychology*, 70(1), pp. 127–140. doi: 10.1037/0022-3514.70.1.127.
- Stanley, J. A. and Raz, N. (2018) 'Functional Magnetic Resonance Spectroscopy: The "New" MRS for Cognitive Neuroscience and Psychiatry Research', *Frontiers in Psychiatry*, 9(March). doi: 10.3389/fpsy.2018.00076.
- Stockmeier, C. a. and Rajkowska, G. (2004) 'Cellular abnormalities in depression: Evidence from postmortem brain tissue', *Dialogues in Clinical Neuroscience*, 6(2), pp. 185–197.
- Stone, J. M. *et al.* (2012) 'Ketamine effects on brain GABA and glutamate levels with 1H-MRS: Relationship to ketamine-induced psychopathology', *Molecular Psychiatry*. Nature Publishing Group, 17(7), pp. 664–665. doi: 10.1038/mp.2011.171.
- Stork, O. *et al.* (2000) 'Postnatal development of a GABA deficit and disturbance of neural functions in mice lacking GAD65', *Brain Research*, 865(1), pp. 45–58. doi: 10.1016/S0006-8993(00)02206-X.
- Straube, T. *et al.* (2009) 'Dynamic activation of the anterior cingulate cortex during anticipatory anxiety', *NeuroImage*. Elsevier Inc., 44(3), pp. 975–981. doi: 10.1016/j.neuroimage.2008.10.022.
- Sturm, V. E. *et al.* (2006) 'Self-conscious emotion deficits in frontotemporal lobar degeneration', *Brain*, 129(9), pp. 2508–2516. doi: 10.1093/brain/awl145.
- Sturm, V. E. *et al.* (2012) 'Role of right pregenual anterior cingulate cortex in self-conscious emotional reactivity', *Social Cognitive and Affective Neuroscience*. doi: 10.1093/scan/nss023.
- Sturm, V. E. and Levenson, R. W. (2011) 'Alexithymia in neurodegenerative disease.', *Neurocase*, 17(3), pp. 242–50. doi: 10.1080/13554794.2010.532503.
- Su, T.-P. *et al.* (2017) 'Dose-Related Effects of Adjunctive Ketamine in Taiwanese Patients with Treatment-Resistant Depression', *Neuropsychopharmacology*. Nature Publishing Group, (April), pp. 1–47. doi: 10.1038/npp.2017.94.
- Suslow, T. *et al.* (2016) 'Alexithymia is associated with attenuated automatic brain response to facial emotion in clinical depression', *Progress in Neuro-Psychopharmacology and Biological Psychiatry*, 65, pp. 194–200. doi: <https://doi.org/10.1016/j.pnpbp.2015.10.006>.
- Swart, M., Kortekaas, R. and Aleman, A. (2009) 'Dealing with feelings: characterization of trait alexithymia on emotion regulation strategies and cognitive-emotional processing.', *PloS one*, 4(6), p. e5751. doi: 10.1371/journal.pone.0005751.
- Takeuchi, H. *et al.* (2013) 'Resting state functional connectivity associated with trait emotional intelligence.', *NeuroImage*. Elsevier Inc., 83, pp. 318–28. doi: 10.1016/j.neuroimage.2013.06.044.
- Taylor, G. J. (2000) 'Recent developments in alexithymia theory and research', *The Canadian Journal of Psychiatry*. SAGE Publications Sage CA: Los Angeles, CA, 45(2), pp. 134–142.
- Taylor, K. S., Seminowicz, D. a and Davis, K. D. (2009) 'Two systems of resting state connectivity between the insula and cingulate cortex.', *Human brain mapping*, 30(9), pp. 2731–45. doi: 10.1002/hbm.20705.
- Taylor, M. *et al.* (2008) 'Differential effects of citalopram and reboxetine on cortical Glx measured with proton MR spectroscopy', *Journal of Psychopharmacology*, 22(5), pp. 473–476. doi: 10.1177/0269881107081510.
- Taylor, M. J., Godlewska, B. R., *et al.* (2012) 'Early increase in marker of neuronal integrity with antidepressant treatment of major depression : 1 H-magnetic resonance spectroscopy of N -acetyl-aspartate', *international journal of ne*, 15(10), pp. 1541–1546. doi: 10.1017/S1461145712000272.
- Taylor, M. J., Tiangga, E. R., *et al.* (2012) 'Lack of effect of ketamine on cortical glutamate and glutamine in healthy volunteers: a proton magnetic resonance spectroscopy study.', *Journal of psychopharmacology (Oxford, England)*, 26(5), pp. 733–7. doi: 10.1177/0269881111405359.
- Taylor, M. J. (2014) 'Could glutamate spectroscopy differentiate bipolar depression from unipolar?', *Journal of affective disorders*. Elsevier, 167, pp. 80–84.
- Taylor, R. *et al.* (2015) 'Increased glutamate levels observed upon functional activation in the anterior cingulate cortex using the Stroop Task and functional spectroscopy', *Neuroreport*. Wolters Kluwer Health, 26(3), p. 107.
- Théberge, J. *et al.* (2002) 'Glutamate and glutamine measured with 4.0 T proton MRS in never-treated patients with schizophrenia and healthy volunteers', *American Journal of Psychiatry*. Am Psychiatric Assoc, 159(11), pp. 1944–1946.
- Théberge, J. *et al.* (2003) 'Glutamate and glutamine in the anterior cingulate and thalamus of medicated patients with chronic schizophrenia and healthy comparison subjects measured with 4.0-T proton MRS', *American Journal of Psychiatry*. Am Psychiatric Assoc, 160(12), pp. 2231–2233.

- Tian, L., Ren, J. and Zang, Y. (2012) 'Regional homogeneity of resting state fMRI signals predicts Stop signal task performance', *NeuroImage*. Elsevier Inc., 60(1), pp. 539–544. doi: 10.1016/j.neuroimage.2011.11.098.
- Tian, X. *et al.* (2016) 'NeuroImage Assessment of trait anxiety and prediction of changes in state anxiety using functional brain imaging: A test – retest study', *NeuroImage*. Elsevier Inc., 133, pp. 408–416. doi: 10.1016/j.neuroimage.2016.03.024.
- de Timary, P. *et al.* (2008) 'Absolute and relative stability of alexithymia in alcoholic inpatients undergoing alcohol withdrawal: Relationship to depression and anxiety', *Psychiatry Research*, 157(1–3), pp. 105–113. doi: 10.1016/j.psychres.2006.12.008.
- van Tol, M.-J. *et al.* (2013) 'Local cortical thinning links to resting-state disconnectivity in major depressive disorder.', *Psychological medicine*, pp. 1–13. doi: 10.1017/S0033291713002742.
- Tomasi, D., Wang, G.-J. and Volkow, N. D. (2013) 'Energetic cost of brain functional connectivity', *Proceedings of the National Academy of Sciences*, 110(33), pp. 13642–13647. doi: 10.1073/pnas.1303346110.
- Torta, D. M. and Cauda, F. (2011) 'Different functions in the cingulate cortex, a meta-analytic connectivity modeling study', *NeuroImage*. Elsevier Inc., 56(4), pp. 2157–2172. doi: 10.1016/j.neuroimage.2011.03.066.
- Torta, D. M. E. *et al.* (2013) 'Parcellation of the cingulate cortex at rest and during tasks: a meta-analytic clustering and experimental study.', *Frontiers in human neuroscience*, 7(June), p. 275. doi: 10.3389/fnhum.2013.00275.
- Triantafyllou, C. *et al.* (2005) 'Comparison of physiological noise at 1.5 T, 3 T and 7 T and optimization of fMRI acquisition parameters', *NeuroImage*, 26(1), pp. 243–250. doi: 10.1016/j.neuroimage.2005.01.007.
- Tweed, W. A., Minuck, M. and Mymin, D. (1972) 'Circulatory responses to ketamine anesthesia', *Anesthesiology*, 37(6), pp. 613–619.
- Tyler, M. W. *et al.* (2017) 'Classics in chemical neuroscience: ketamine', *ACS chemical neuroscience*. ACS Publications, 8(6), pp. 1122–1134.
- Ündar, A. *et al.* (2004) 'Anesthetic induction with ketamine inhibits platelet activation before, during, and after cardiopulmonary bypass in baboons', *Artificial Organs*, 28(10), pp. 959–962. doi: 10.1111/j.1525-1594.2004.07377.x.
- Unschuld, P. G. *et al.* (2009) 'Polymorphisms in the GAD2 gene-region are associated with susceptibility for unipolar depression and with a risk factor for anxiety disorders', *American Journal of Medical Genetics, Part B: Neuropsychiatric Genetics*, 150(8), pp. 1100–1109. doi: 10.1002/ajmg.b.30938.
- Valentine, G. W. *et al.* (2011) 'The antidepressant effect of ketamine is not associated with changes in occipital amino acid neurotransmitter content as measured by [(1)H]-MRS.', *Psychiatry research*. Elsevier Ireland Ltd, 191(2), pp. 122–7. doi: 10.1016/j.psychresns.2010.10.009.
- Vanheule, S. *et al.* (2007) 'Alexithymic depression: Evidence for a depression subtype? [3]', *Psychotherapy and Psychosomatics*, 76(5), pp. 315–316. doi: 10.1159/000104710.
- Veeraiah, P. *et al.* (2014) 'Dysfunctional Glutamatergic and γ -Aminobutyric Acidergic Activities in Prefrontal Cortex of Mice in Social Defeat Model of Depression', *Biological Psychiatry*. Elsevier, 76(3), pp. 231–238. doi: 10.1016/j.biopsych.2013.09.024.
- Van der Velde, J. *et al.* (2014) 'Dissociable morphometric profiles of the affective and cognitive dimensions of alexithymia', *Cortex*, 54(1), pp. 190–199. doi: 10.1016/j.cortex.2014.02.017.
- Velde, J. Van Der *et al.* (2013) 'Neuroscience and Biobehavioral Reviews Neural correlates of alexithymia: A meta-analysis of emotion processing studies', *Neuroscience and Biobehavioral Reviews*. Elsevier Ltd, 37(8), pp. 1774–1785. doi: 10.1016/j.neubiorev.2013.07.008.
- Victor, T. A. *et al.* (2013) 'Changes in the neural correlates of implicit emotional face processing during antidepressant treatment in major depressive disorder', *International Journal of Neuropsychopharmacology*, 16(10), pp. 2195–2208. doi: 10.1017/S146114571300062X.
- Visser, M. *et al.* (2012) 'Both the Middle Temporal Gyrus and the Ventral Anterior Temporal Area Are Crucial for Multimodal Semantic Processing: Distortion-corrected fMRI Evidence for a Double Gradient of Information Convergence in the Temporal Lobes', *Journal of Cognitive Neuroscience*, 24(8), pp. 1766–1778. doi: 10.1162/jocn_a_00244.
- Vogt, B. A. (2005) 'Pain and emotion interactions in subregions of the cingulate gyrus', *Nature Reviews Neuroscience*, 6(7), pp. 533–544. doi: 10.1038/nrn1704.
- Vogt, B. A. (2016) 'Midcingulate cortex: Structure, connections, homologies, functions and diseases', *Journal of Chemical Neuroanatomy*. Elsevier B.V., 74, pp. 28–46. doi: 10.1016/j.jchemneu.2016.01.010.
- Vogt, B. A. *et al.* (1995) 'Human cingulate cortex: Surface features, flat maps, and cytoarchitecture', *Journal of Comparative Neurology*, 359(3), pp. 490–506. doi: 10.1002/cne.903590310.
- Vogt, B. A., Berger, G. R. and Derbyshire, S. W. G. (2003) 'Structural and functional dichotomy of human midcingulate cortex',

- European Journal of Neuroscience*, 18(11), pp. 3134–3144. doi: 10.1111/j.1460-9568.2003.03034.x.
- Vogt, B. aA, Finch, D. M. and Olson, C. R. (1992) 'Functional heterogeneity in cingulate cortex: The anterior executive and posterior evaluative regions', *Cerebral Cortex*, 2(6), pp. 435–443. doi: 10.1093/cercor/2.6.435-a.
- Vogt, B. A. and Palomero-Gallagher, N. (2012) 'Cingulate cortex', in *The Human Nervous System (Third Edition)*. Elsevier, pp. 943–987.
- Vogt, B. A, Vogt, L. and Laureys, S. (2006) 'Cytology and functionally correlated circuits of human posterior cingulate areas.', *NeuroImage*, 29(2), pp. 452–66. doi: 10.1016/j.neuroimage.2005.07.048.
- Volz, H. P. *et al.* (1998) '31P magnetic resonance spectroscopy in the frontal lobe of major depressed patients', *European Archives of Psychiatry and Clinical Neuroscience*, 248(6), pp. 289–295. doi: 10.1007/s004060050052.
- Vorst, H. C. M. and Bermond, B. (2001) 'Validity and reliability of the Bermond–Vorst alexithymia questionnaire', *Personality and individual differences*. Elsevier, 30(3), pp. 413–434.
- Waagepetersen, H. S., Sonnewald, U. and Schousboe, A. (2003) 'Compartmentation of glutamine, glutamate, and GABA metabolism in neurons and astrocytes: functional implications', *The neuroscientist*. SAGE Publications, 9(5), pp. 398–403.
- Wager, T. D. *et al.* (2016) 'Pain in the ACC?', *Proceedings of the National Academy of Sciences*, 113(18), p. 201600282. doi: 10.1073/pnas.1600282113.
- Walter, M. *et al.* (2008) 'Distinguishing specific sexual and general emotional effects in fMRI-Subcortical and cortical arousal during erotic picture viewing', *NeuroImage*, 40(4), pp. 1482–1494. doi: 10.1016/j.neuroimage.2008.01.040.
- Walter, M. *et al.* (2009) 'The Relationship Between Aberrant Neuronal Activation in the Pregenual Anterior Cingulate, Altered Glutamatergic Metabolism, and Anhedonia in Major Depression', *Archives of General Psychiatry*, 66(5), p. 478. doi: 10.1001/archgenpsychiatry.2009.39.
- Walter, M. *et al.* (2018) 'Translational machine learning for psychiatric neuroimaging', *Progress in Neuro-Psychopharmacology and Biological Psychiatry*. doi: <https://doi.org/10.1016/j.pnpbp.2018.09.014>.
- Walter, M., Li, S. and Demenescu, L. R. (2014) 'Multistage drug effects of ketamine in the treatment of major depression', *European Archives of Psychiatry and Clinical Neuroscience*, 264(1), pp. 55–65. doi: 10.1007/s00406-014-0535-3.
- Wang, B. *et al.* (2014) 'Microtubule acetylation amplifies p38 kinase signaling and anti-inflammatory IL-10 production', *Nature communications*, 5(3479), pp. 1–17. doi: 10.1038/ncomms4479.Microtubule.
- Wang, C. *et al.* (2013) 'Brain damages in ketamine addicts as revealed by magnetic resonance imaging.', *Frontiers in neuroanatomy*, 7, p. 23. doi: 10.3389/fnana.2013.00023.
- Weber, H. *et al.* (2012) 'Gender differences in associations of glutamate decarboxylase 1 gene (GAD1) variants with panic disorder', *PLoS ONE*, 7(5), pp. 1–7. doi: 10.1371/journal.pone.0037651.
- White, P. F. *et al.* (1985) 'Comparative pharmacology of the ketamine isomers: Studies in volunteers', *British Journal of Anaesthesia*, 57(2), pp. 197–203. doi: 10.1093/bja/57.2.197.
- Whitney, C. *et al.* (2011) 'The neural organization of semantic control: TMS evidence for a distributed network in left inferior frontal and posterior middle temporal gyrus', *Cerebral Cortex*, 21(5), pp. 1066–1075. doi: 10.1093/cercor/bhq180.
- Wildgruber, D. *et al.* (2006) 'Cerebral processing of linguistic and emotional prosody: fMRI studies. Zerebrale Verarbeitung linguistischer und emotionaler Prosodie', 4, pp. 249–268.
- Williams, N. R. and Schatzberg, A. F. (2016) 'NMDA antagonist treatment of depression', *Current Opinion in Neurobiology*. Elsevier Ltd, 36, pp. 112–117. doi: 10.1016/j.conb.2015.11.001.
- World Medical Association (2002) 'World Medical Association Declaration of Helsinki Ethical Principles for Medical Research Involving Human Subjects, 5th (Edinburgh) amendment and Note of Clarification', pp. 6–9. doi: 10.3917/jib.151.0124.
- Xu, Y. *et al.* (2016) 'Effects of Low-Dose and Very Low-Dose Ketamine among Patients with Major Depression: A Systematic Review and Meta-Analysis', *International Journal of Neuropsychopharmacology*, 19(4), pp. 1–15. doi: 10.1093/ijnp/pyv124.
- Yan, C. G. *et al.* (2013) 'A comprehensive assessment of regional variation in the impact of head micromovements on functional connectomics', *NeuroImage*. Elsevier Inc., 76, pp. 183–201. doi: 10.1016/j.neuroimage.2013.03.004.
- Yanagihara, Y. *et al.* (2003) 'Plasma concentration profiles of ketamine and norketamine after administration of various ketamine preparations to healthy Japanese volunteers', *Biopharmaceutics and Drug Disposition*, 24(1), pp. 37–43. doi: 10.1002/bdd.336.
- Yang, C. *et al.* (2009) 'Cytoskeletal alterations in rat hippocampus following chronic unpredictable mild stress and re-exposure to acute and chronic unpredictable mild stress', *Behavioural Brain Research*, 205(2), pp. 518–524. doi: 10.1016/j.bbr.2009.08.008.

- Yang, C. *et al.* (2013) 'Acute administration of ketamine in rats increases hippocampal BDNF and mTOR levels during forced swimming test.', *Upsala journal of medical sciences*, 118(1), pp. 3–8. doi: 10.3109/03009734.2012.724118.
- Yang, C. *et al.* (2015) 'R-ketamine: a rapid-onset and sustained antidepressant without psychotomimetic side effects', *Translational Psychiatry*, 5(9), p. e632. doi: 10.1038/tp.2015.136.
- Yang, C. *et al.* (2017) '(R)-Ketamine Shows Greater Potency and Longer Lasting Antidepressant Effects Than Its Metabolite (2R,6R)-Hydroxynorketamine', *Biological Psychiatry*. Elsevier Inc., 82(5), pp. e43–e44. doi: 10.1016/j.biopsych.2016.12.020.
- Yang, G. J. *et al.* (2014) 'Altered global brain signal in schizophrenia.', *Proceedings of the National Academy of Sciences of the United States of America*, 111(20), pp. 7438–43. doi: 10.1073/pnas.1405289111.
- Yi, C. *et al.* (2006) 'The changes of cytoskeletal proteins in plasma of acrylamide-induced rats', *Neurochemical Research*, 31(6), pp. 751–757. doi: 10.1007/s11064-006-9079-x.
- Yildiz-Yesiloglu, A. and Ankerst, D. P. (2006) 'Review of 1H magnetic resonance spectroscopy findings in major depressive disorder: a meta-analysis.', *Psychiatry research*, 147(1), pp. 1–25. doi: 10.1016/j.psychres.2005.12.004.
- Yin, H. *et al.* (2016) 'A pilot integrative genomics study of GABA and glutamate neurotransmitter systems in suicide, suicidal behavior, and major depressive disorder', *American Journal of Medical Genetics Part B: Neuropsychiatric Genetics*. Wiley Online Library, 171(3), pp. 414–426.
- Yoo, S. Y. *et al.* (2009) 'Proton magnetic resonance spectroscopy in subjects with high genetic risk of schizophrenia: investigation of anterior cingulate, dorsolateral prefrontal cortex and thalamus', *Schizophrenia research*. Elsevier, 111(1–3), pp. 86–93.
- Yu, C. *et al.* (2011) 'Functional segregation of the human cingulate cortex is confirmed by functional connectivity based neuroanatomical parcellation', *NeuroImage*. Elsevier Inc., 54(4), pp. 2571–2581. doi: 10.1016/j.neuroimage.2010.11.018.
- Yüksel, C. and Öngür, D. (2010) 'Magnetic resonance spectroscopy studies of glutamate-related abnormalities in mood disorders.', *Biological psychiatry*. Elsevier Inc., 68(9), pp. 785–94. doi: 10.1016/j.biopsych.2010.06.016.
- Zakariaez, Y. *et al.* (2016) 'Balance of the Sexes: Addressing Sex Differences in Preclinical Research', *Yale Journal of Biology and Medicine*, 89, pp. 255–259.
- Zang, Y. *et al.* (2004) 'Regional homogeneity approach to fMRI data analysis', *NeuroImage*, 22(1), pp. 394–400. doi: 10.1016/j.neuroimage.2003.12.030.
- Zang, Y. F. *et al.* (2007) 'Altered baseline brain activity in children with ADHD revealed by resting-state functional MRI', *Brain and Development*, 29(2), pp. 83–91. doi: 10.1016/j.braindev.2006.07.002.
- Zanos, P. *et al.* (2016) 'NMDAR inhibition-independent antidepressant actions of ketamine metabolites.', *Nature*. Nature Publishing Group, 533(7604), pp. 1–18. doi: 10.1038/nature17998.
- Zanos, P. and Gould, T. D. (2018) 'Mechanisms of ketamine action as an antidepressant', *Molecular Psychiatry*. Nature Publishing Group, 23(4), pp. 801–811. doi: 10.1038/mp.2017.255.
- Zarate, C. A. *et al.* (2012) 'Relationship of ketamine's plasma metabolites with response, diagnosis, and side effects in major depression', *Biological Psychiatry*. Elsevier Inc., 72(4), pp. 331–338. doi: 10.1016/j.biopsych.2012.03.004.
- Zarate, C. A. *et al.* (2006) 'A randomized trial of an n-methyl-d-aspartate antagonist in treatment-resistant major depression', *Archives of General Psychiatry*, 63(8), pp. 856–864. Available at: <http://dx.doi.org/10.1001/archpsyc.63.8.856>.
- Zarate, C. A. and Machado-Vieira, R. (2017) 'Ketamine: translating mechanistic discoveries into the next generation of glutamate modulators for mood disorders', *Mol Psychiatry*, pp. 1–4. doi: 10.1038/mp.2016.249.
- Zhang, Z. *et al.* (2011) 'Epigenetic suppression of GAD65 expression mediates persistent pain.', *Nature medicine*. Nature Publishing Group, 17(11), pp. 1448–1455. doi: 10.1038/nm.2442.
- Zhao, X.-H. *et al.* (2007) 'Altered default mode network activity in patient with anxiety disorders: An fMRI study', *European Journal of Radiology*, 63, pp. 373–378. doi: 10.1016/j.ejrad.2007.02.006.
- Zhao, X. *et al.* (2007) 'Systematic study of association of four GABAergic genes: Glutamic acid decarboxylase 1 gene, glutamic acid decarboxylase 2 gene, GABAB receptor 1 gene and GABAA receptor subunit $\gamma 2$ gene, with schizophrenia using a universal DNA microarray', *Schizophrenia Research*, 93(1–3), pp. 374–384. doi: 10.1016/j.schres.2007.02.023.
- Zhao, X. *et al.* (2012) 'Simultaneous population pharmacokinetic modelling of ketamine and three major metabolites in patients with treatment-resistant bipolar depression', *British Journal of Clinical Pharmacology*, 74(2), pp. 304–314. doi: 10.1111/j.1365-2125.2012.04198.x.
- Zhou, W. *et al.* (2014) 'Ketamine-induced antidepressant effects are associated with AMPA receptors-mediated upregulation of mTOR and BDNF in rat hippocampus and prefrontal cortex', *European Psychiatry*. Elsevier, 29(7), pp. 419–423.

- Zhu, H. and Barker, P. B. (2011) 'MR spectroscopy and spectroscopic imaging of the brain', in *Magnetic resonance neuroimaging*. Springer, pp. 203–226.
- Zijdenbos, A. P., Forghani, R. and Evans, A. C. (2002) 'Automatic" pipeline" analysis of 3-D MRI data for clinical trials: application to multiple sclerosis', *IEEE transactions on medical imaging*. IEEE, 21(10), pp. 1280–1291.
- Zimmerman, M., Posternak, M. A. and Chelminski, I. (2002) 'Symptom severity and exclusion from antidepressant efficacy trials', *Journal of clinical psychopharmacology*. LWW, 22(6), pp. 610–614.
- Zohar, A. H. *et al.* (2003) 'Tridimensional personality questionnaire trait of harm avoidance (anxiety proneness) is linked to a locus on chromosome 8p21.', *American journal of medical genetics. Part B, Neuropsychiatric genetics : the official publication of the International Society of Psychiatric Genetics*, 117B(August 2002), pp. 66–69. doi: 10.1002/ajmg.b.10029.
- Zou, Q. H. *et al.* (2008) 'An improved approach to detection of amplitude of low-frequency fluctuation (ALFF) for resting-state fMRI: Fractional ALFF', *Journal of Neuroscience Methods*, 172(1), pp. 137–141. doi: 10.1016/j.jneumeth.2008.04.012.
- Zuo, X.-N. *et al.* (2010) 'The oscillating brain: complex and reliable', *Neuroimage*. Elsevier, 49(2), pp. 1432–1445.

Appendix

I. Supplementary Material

I.A. Supplementary Figures

Supplementary Figures of Materials and Methods

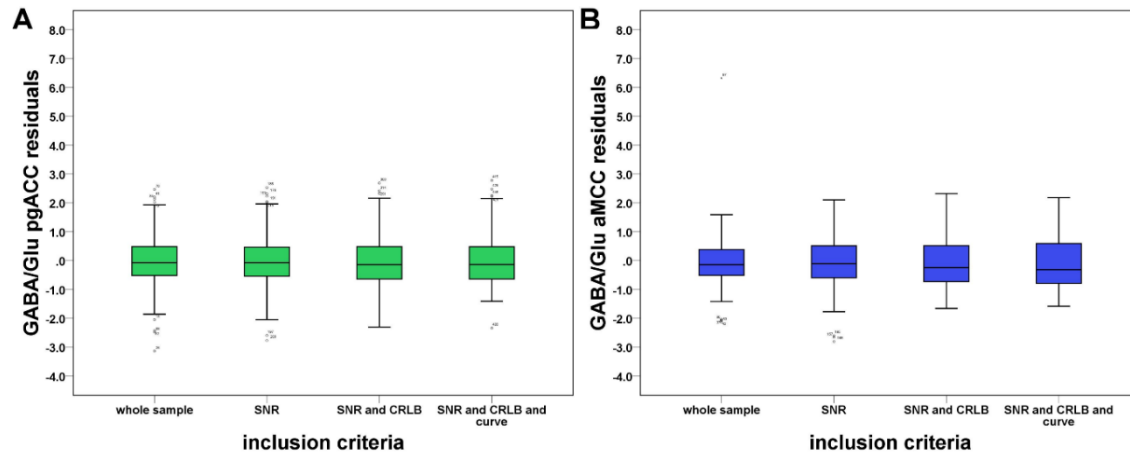


Figure S2. 1. Comparison of inclusion criteria for the GABA/Glu ratio measured in 7T.

A For the pgACC there was no significant difference in variance ($F(1,3) = .209$, $p = .890$), while **B** for the aMCC considering all data yielded different variance as compared to three inclusion criteria ($F(1,3) = 3.69$, $p = .012$). Data is presented in mean \pm SD.

Supplementary Figures of Study 1

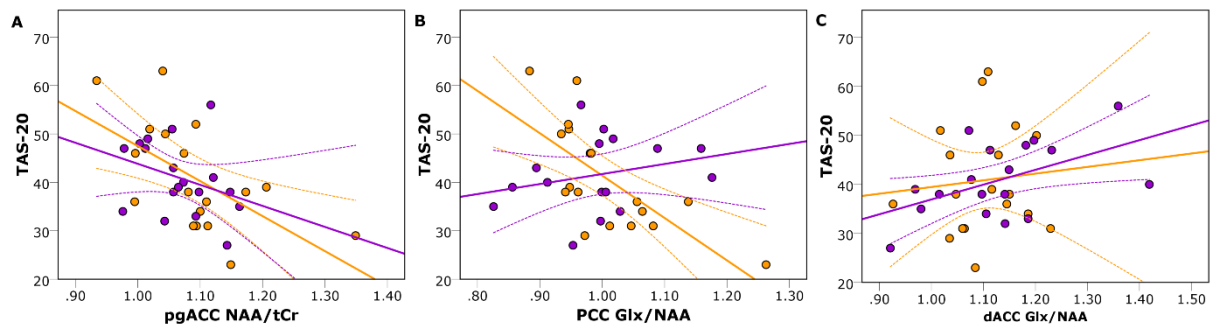


Figure S3. 1. Significant correlations of TAS-20 total score and metabolites.

A with the pgACC NAA/tCr (women: $\rho = -.71$, men: $\rho = -.49$); **B** with the PCC Glx/NAA (women: $\rho = -.72$, men: $\rho = 0.23$); **C** with the dACC Glx/NAA (women: $\rho = 0.03$, men: $\rho = .50$, $p = .07$). Women (orange) and men (purple), data points are not corrected for gray matter partial volume and are presented as mean \pm 95% CI.

Supplementary Figures of Study 2



Figure S4. 1. Additive mediation model with pgACC GABA/Glu and ALFF.

There was no significant direct or indirect effect including both mediators for the whole sample (burgundy, $n = 41$). Total indirect effects were also not significant ($b = -.641$, boot 95% CI = [-3.656, 1.563]); $b =$ effect, CI = 95%.

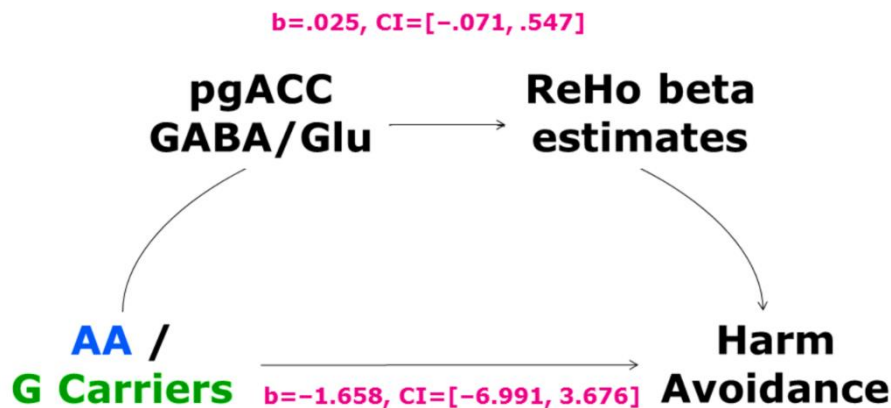


Figure S4. 2. Additive mediation model with pgACC GABA/Glu and ReHo.

There was no significant direct or indirect effect including both mediators for the whole sample (burgundy, $n = 41$). Total indirect effects were also not significant ($b = .114$, boot 95% CI = [-1.966, 2.319]); $b =$ effect, CI = 95%.

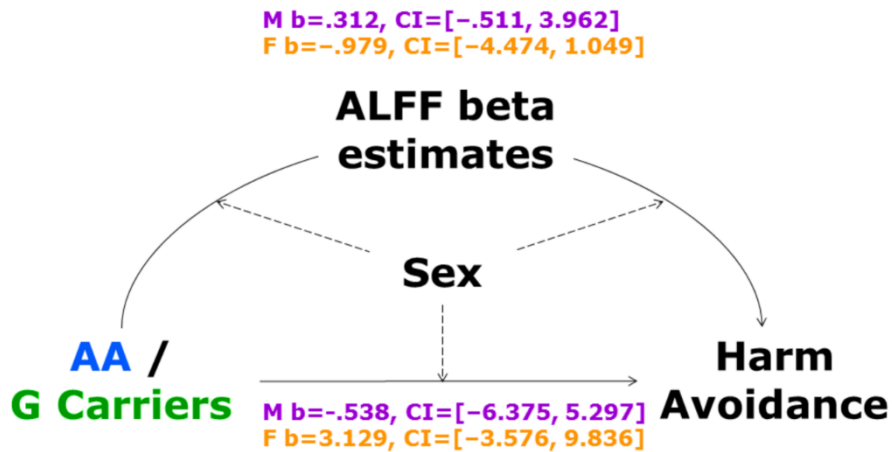


Figure S4. 3. Moderated mediation with ALFF.

Index = -1.291, bootstrapped 95% CI = [-5.369, 1.493] (N = 48); in both sexes the direct effect of GAD65 genotype on harm avoidance was not significant, as well as the indirect effect via ALFF β estimates (curved arrow); M = men (purple), F = women (orange), b = effect, CI = 95%.

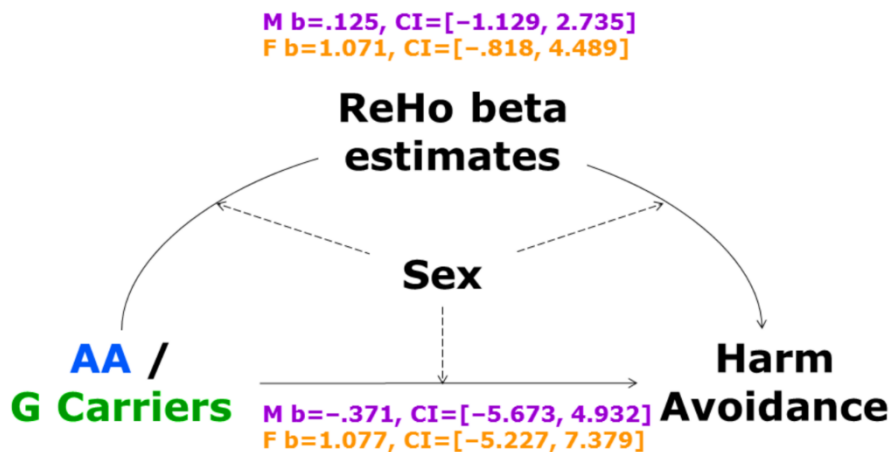


Figure S4. 4. Moderated mediation with ReHo.

Index = .946, bootstrapped 95% CI = [-1.612, 4.937] (N = 48); in both sexes the direct effect of GAD65 genotype on harm avoidance was not significant, as well as the indirect effect via ReHo β estimates (curved arrow); M = men (purple), F = women (orange), b = effect, CI = 95%.

Supplementary Figures of Study 4

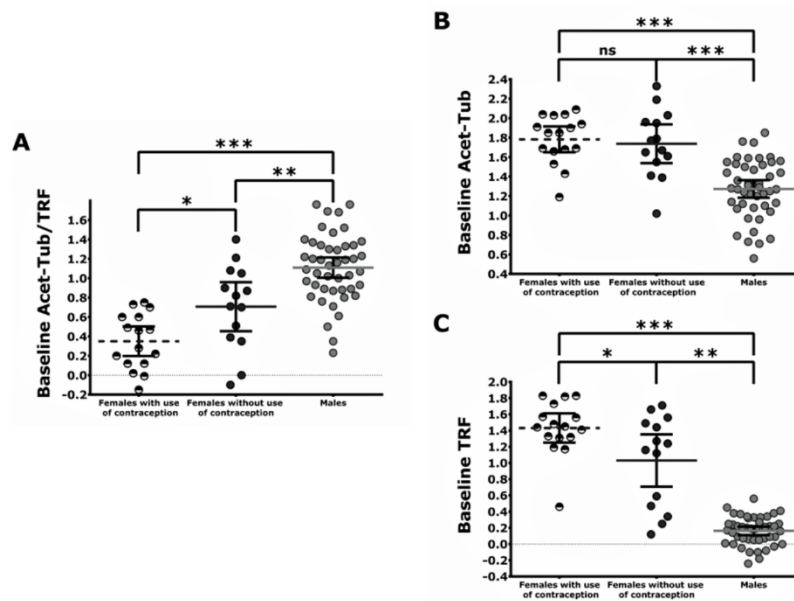


Figure S6. 1. Baseline sex and contraception differences in Acet-Tub/TRF.

Differences in the baseline A Acet-Tub/TRF levels between men and women taking contraceptives ($*** t(59) = -7.784, p < .001$), men and women not using contraceptives ($*** t(57) = -3.540, p = .001$) and two female groups ($* t(28) = 2.666, p = .013$); B Acet-Tub absolute levels between men and women taking contraceptives ($*** t(59) = 6.066, p < .001$), men and women not using contraceptives ($*** t(57) = 4.872, p < .001$) and two female groups ($^{ns} t(28) = -.416, p = .681$); and C TRF absolute levels between men and women taking contraceptives ($*** U > 0.99, p < .001$), men and women not using contraceptives ($*** t(57) = 9.201, p < .001$) and two female groups ($* U = 62.0, p = .038$). Data is ln transformed and is presented in mean \pm 95% CI.

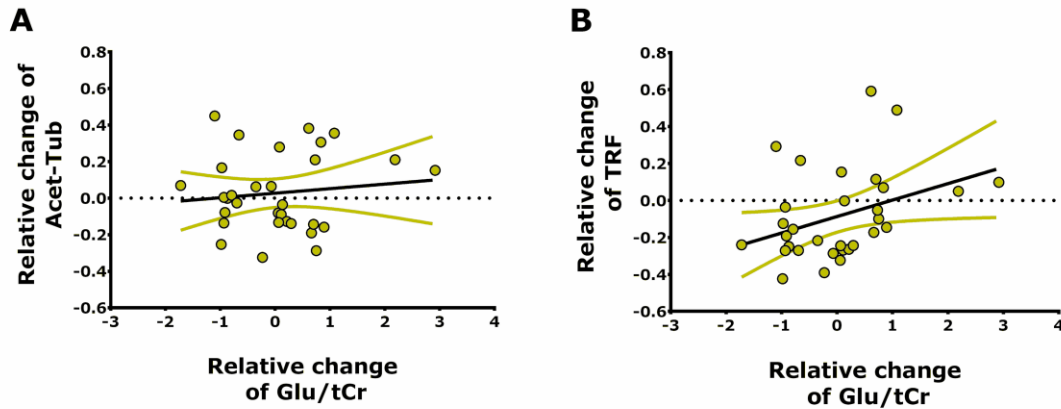


Figure S6. 2. Correlation of the changes in the glutamatergic and the peripheral system 24 h after ketamine.

Correlation of the relative changes of Glu/tCr pgACC residualized for gray partial volume and A Acet-Tub and ($r(28) = .123, p = .518$) and B Transferrin ($\rho(28) = .397, p = .030$) for the whole ketamine group.

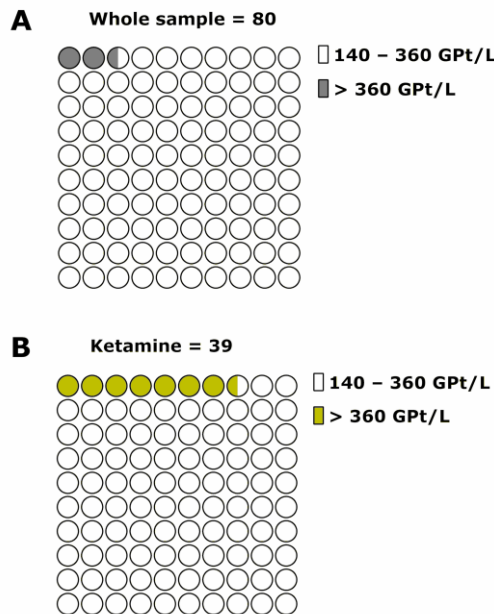


Figure S6. 3. Frequency of participants exceeding reference range for thrombocytes.

Reference range is 140 - 360 GPt/L; A at baseline in the whole sample, 2.5% (black; 2 out of 80 participants) and B at follow-up in the ketamine group, 7.7% (black; 3 out of 39 participants), whereas, in the placebo group, 0% (0 out of 40 participants).

I.B. Supplementary Tables

Supplementary Tables of Study 1

Table S3. 1. Inter scale correlation matrix for the TAS-20 questionnaire for both studies.

	Study	Group	DDF	DIF	EOTS
Total Score		Whole sample	.826	.890	.650
	3T	Women	.892	.937	.777
		Men	.832	.826	.422
	7T	Whole sample	.810	.695	.633
		Women	.780	.755	.498
		Men	.848	.683	.748
DDF	3T	Whole sample		.743	.235
		Women		.885	.474
		Men		.727	-.023
	7T	Whole sample		.633	.290
		Women		.619	.122
		Men		.680	.465
DIF	3T	Whole sample			.326
		Women			.540
		Men			-.038
	7T	Whole sample			.037
		Women			-.016
		Men			.139

3T study: Whole sample $n= 36$, women $n= 18$, Men $n= 18$; 7T study: Whole sample $n= 59$, Women $n= 28$, Men $n= 31$; DDF-Difficulty Describing Feelings; DIF-Difficulty Identifying Feelings; EOTS-Externally Oriented Thinking Style

Table S3. 2. Metabolite and cortical thickness values for the 3T study.

Variables are in mean± SD

Region	Metabolite	Whole sample	Women	Men	Student's t-test or Mann-Whitney test
pgACC	NAA/tCr	1.079± .076	1.092± .092	1.067± .057	$t(34) = .957, p = .345$
	Glx/tCr	1.329± .156	1.323± .149	1.336± .167	$t(34) = -.247, p = .806$
	Glx/NAA	1.233± .134	1.214± .125	1.252± .145	$t(34) = -.828, p = .413$
	CTh	3.680± .201	3.729± .148	3.631± .237	$U = 114, p = .134$
dACC	NAA/tCr	1.093± .064	1.099± .059	1.086± .069	$t(34) = .592, p = .558$
	Glx/tCr	1.219± .132	1.209± .112	1.228± .153	$t(34) = -.408, p = .686$
	Glx/NAA	1.115± .103	1.099± .074	1.130± .126	$t(34) = -.900, p = .375$
	CTh	3.594± .231	3.585± .232	3.602± .236	$t(34) = -.221, p = .826$
PCC	NAA/tCr	1.202± .102	1.181± .085	1.225± .116	$t(33) = -1.273, p = .212$
	Glx/tCr	1.193± .114	1.187± .122	1.200± .108	$t(32) = -.328, p = .745$
	Glx/NAA	.999± .091	1.006± .090	.992± .095	$U = 143, p = .986$
	CTh	3.469± .149	3.442± .136	3.449± .161	$t(33) = -1.150, p = .259$
dIPFC	NAA/tCr	1.380± .125	1.383± .102	1.376± .148	$t(34) = .173, p = .864$
	Glx/tCr	1.171± .153	1.174± .160	1.169± .150	$t(32) = .098, p = .922$
	Glx/NAA	.856± .080	.850± .084	.863± .078	$t(32) = -.462, p = .647$
	CTh	3.164± .258	3.132± .304	3.196± .207	$U = 136, p = .424$

Table S3. 3. Difference in the correlation slopes between women and men for TAS-20 and FC maps of ACC inferior seeds.

There were no significant clusters for superior seeds. Results are considered significant at $p < .05$, FWE cluster level corrected, with an initial threshold of $p < .001$, uncorrected. Other non-significant results (ns) are reported here at cluster size $k > 5$, as to show consistency of the result.

ROI	Contrast	P	k	MNI			Region	
				x	y	z		
L idACC 1	Male > Fem	ns	15	6	6	2	R Caudate	
				8	4	8		
L idACC 2	M > F	.037	82	22	4	12	8	R Caudate
				6	12	0	R Caudate	
L idACC 3	M > F	ns	18	6	6	2	R Caudate	
				6	14	4		
L idACC 4	M > F	.097	65	6	4	4	R Caudate	
				2	2	2		
L idACC 5	M > F	ns	18	6	4	4	R Caudate	
				6	14	10		
R idACC 1	M > F	.071	73	12	16	14	R Caudate	
				4	6	2		R Caudate
R idACC 2	M > F	ns	49	6	16	0	R Caudate	
				8	20	0		
R idACC 3	M > F	ns	14	4	8	2	R Caudate	
				6	14	10		
R idACC 4	M > F	ns	62	4	8	2	R Caudate	
				6	4	4		
R idACC 5	M > F	ns	8	6	4	4	R Caudate	
R idACC 5	M > F	ns	8	8	14	10	R Caudate	

Supplementary Table of Study 2

Table S4. 1. Comparison of the pgACC GABA/Glu levels in women between all five SNPs.

Student's *t*- test or Mann Whitney's *U* test, threshold at $p < .05$.

Polymorphism	<i>n</i> (Homozygotes / Minor allele carriers)	Statistical test
GAD2 rs2236418	24 / 14	$t(36) = -2.19, p = .035 *$
GAD2 rs10508715	18 / 18	$t(34) = -1.14, p = .26$
GAD1 rs3791850	18 / 18	$t(34) = -.69, p = .50$
GAD1 rs769390	21 / 15	$t(34) = .17, p = .86$
GLS rs13035504	29 / 8	$t(35) = .77, p = .46$

* $p < .05$

Supplementary Tables of Study 3

Table S5. 1. Medication list for the 23 MDD patients.

Medication is listed following app NbNomenclature.

Participant	Medication name	Dose	Pharmacology
1	Doxepin	25 mg	Norepinephrine, serotonin
	Opipramol	100 mg	not implemented in app
2	Amitriptyline	25 mg	Norepinephrine, serotonin
	Duloxetine	60 mg	Serotonin, Norepinephrine
	Lithium ret	Tbl	Lithium
3	Escitalopram	15 mg	Serotonin
	Promethazine	missing	Histamine, Dopamine
4	Escitalopram	20 mg	Serotonin
	Suspiresd	100 mg	Dopamine
5	Escitalopram	10 mg	Serotonin
6	Citalopram	30 mg	Serotonin
	Chlorprothixene	50 mg	not implemented in app
7	Duloxetine	120 mg	Serotonin, Norepinephrine
	Trimipramine	25 mg	Serotonin, Dopamine
8	Duloxetine	60 mg	Serotonin, Norepinephrine
	Quetiapine	missing	Glutamate
	Agomelatine	25 mg	Melatonin
9	Doxepin	75 mg	Norepinephrine, Serotonin
10	Levomepromazine	25 mg	not implemented in app
	SSRI	100 mg	Serotonin
11	Mirtazapine	15 mg	Norepinephrine, Serotonin
12	Mirtazapine	15 mg	Norepinephrine, Serotonin
	Escitalopram	10 mg	Serotonin
13	Mirtazapine	15 mg	Norepinephrine, Serotonin
14	Amitriptyline	75 mg	Norepinephrine, Serotonin
	Citalopram	20 mg	Serotonin
15	Quetiapine	300 mg	Dopamine, Serotonin
	Pipamperone	40 mg	not implemented in app
	Duloxetine	60 mg	Serotonin, Norepinephrine
16	Trimipramine	25 mg	Serotonin, Dopamine

17	Lorazepam	missing	GABA
	Venlafaxine	missing	Norepinephrine, Serotonin
18	Venlafaxine	150 mg	Norepinephrine, Serotonin
	Amitriptyline	25 mg	Norepinephrine, Serotonin
19	Venlafaxine	150 mg	Norepinephrine, Serotonin
20	Venlafaxine	150 mg	Norepinephrine, Serotonin
	Venlafaxine	75 mg	Norepinephrine, Serotonin
21	Venlafaxine	150 mg	Norepinephrine, Serotonin
22	Venlafaxine	150 mg ret	Norepinephrine, Serotonin
23	Sertraline	50 mg	Serotonin

Table S5. 2. Demographic and clinical properties of the MDD divided by the HAMD clinical cut-off 18 and control participants.

Data is presented in frequencies or mean± SD.

	HAMD< 18	HAMD> 18	Controls	Statistics
Sex (F/M)	11 / 11	8 / 2	19 / 13	$\chi^2(2) = 2.57, p = .28$
Age	37.23± 14.20	48.90± 8.24 A *** & B *	33.09± 8.24	$\chi^2(2) = 1.81, p = .005 **$
BMI (n=19/10/29)	24.50± 5.83	26.91± 4.64	23.38± 2.80	$\chi^2(2) = 4.50, p = .11$
Smoking (no/yes/quit)	8 / 10 / 2	3 / 3 / 4	13 / 11 / 8	$\chi^2(4) = 4.07, p = .40$
HAMD (n=22/10/31)	11.91± 4.68 A *** & B ***	21.70± 2.95 A *** & B ***	.55± .81	$\chi^2(2) = 52.01, p < .001 ***$
SHAPS (n=19/9/30)	4.89± 3.83 A ***	3.89± 3.89 A ***	.37± .65	$\chi^2(2) = 28.32, p < .001 ***$
gm (%) (n=21/8/32)	.600± .075	.603± .088	.596± .078	$F(2, 58) = .03, p = .97$

Number of participants with available data is shown in brackets, *** $p < .001$.

Post hoc tests: A difference to healthy controls A *** $p < .001$; B difference between HAMD groups B * $p < .05$; B *** $p < .001$

Table S5. 3. Demographic and clinical properties of the MDD divided by the SHAPS cut-off 4 and control participants.

Data is presented in frequencies or mean± SD.

	SHAPS< 4	SHAPS> 4	Controls	Statistics
Sex (F/M)	11 / 5	6 / 6	18 / 12	$\chi^2(2) = 1.01, p = .60$
Age	42.94± 13.16	39.75± 14.49	33.07± 8.47	$\chi^2(2) = 4.19, p = .12$
BMI (n=15/12/27)	25.23± 5.79	25.18± 5.19	23.30± 2.89	$F(2, 2.380) = 1.24, p = .31$
Smoking (no/yes/quit)	4 / 9 / 3	6 / 4 / 2	13 / 9 / 8	$\chi^2(4) = 3.79, p = .44$
HAMD (n=16/12/30)	15.56± 6.10 A ***	15.25± 4.73 A ***	.53± .82	$\chi^2(2) = 44.30, p < .001$ ***
SHAPS (n=16/12/30)	1.81± 1.42 A *** & B ***	8.25± 2.63 A *** & B ***	.37± .81	$\chi^2(2) = 38.97, p < .001$ ***
gm (%) (n=15/10/30)	.594± .086	.605± .069	.597± .080	$F(2, 55) = .06, p = .94$

Number of participants with available data is shown in brackets, *** $p < .001$.*Post hoc* tests: A difference to healthy controls ^A *** $p < .001$; B difference between SHAPS groups ^B *** $p < .001$

Table S5. 4. Demographic and clinical properties of the MDD divided by medication status and control participants.

Data is presented in frequencies or mean± SD.

	No medication	Yes medication	Controls	Statistics
Sex (F/M)	5 / 4	14 / 9	19 / 13	$\chi^2(2)=.08, p= .96$
Age	34.56± 13.58	43.35± 13.16 A **	33.09± 8.24	$\chi^2(2)= 6.99, p= .03 *$
BMI (n=8/21/29)	2.84± 1.38 A * & B **	27.05± 5.51 A * & B **	23.38± 2.80	$\chi^2(2)= 12.68, p= .002 **$
Smoking (no/yes/quit)	4 / 4 / 1	7 / 9 / 5	13 / 11 / 8	$\chi^2(4)= 1.21, p= .88$
HAMD (n=9/23/31)	11.67± 7.35 A *** & B #	16.26± 5.34 A *** & B #	.55± .81	$\chi^2(2)= 47.07, p< .001***$
SHAPS (n=8/20/ 30)	2.63± 2.20 A ** & B *	5.35± 4.07 A *** & B *	.37± .81	$\chi^2(2)= 28.96, p< .001 ***$
gm (%) (n=9/20/32)	.558± .067	.620± .074	.596± .078	$F(2, 60) = 2.12, p= .13$

Number of participants with available data is shown in brackets; * $p < .05$; ** $p < .01$, *** $p < .001$.

Post hoc tests: A difference to healthy controls A * $p < .05$; A ** $p < .01$, A *** $p < .001$

B difference between medication groups B # $.1 > p > .05$; A * $p < .05$; B ** $p < .01$

Supplementary Tables of Study 4

Table S6. 1. Reference ranges for hematological and biochemical values included in the analysis.

Parameter	Unit	Range
Thrombocytes	gigaparticles (10^9) per liter	140 - 360
Erythrocytes (Men)	teraparticles (10^{12}) per liter	4.5 - 6
Erythrocytes (Women)	teraparticles (10^{12}) per liter	4 - 5.3
Leukocytes	gigaparticles (10^9) per liter	4 - 10
Hemoglobin (Men)	millimole (10^{-3}) per liter	8.6 - 11
Hemoglobin (Women)	millimole (10^{-3}) per liter	7.4 - 10
Sodium	millimole (10^{-3}) per liter	135 - 145
Potassium	millimole (10^{-3}) per liter	3.5 - 5.1
Calcium	millimole (10^{-3}) per liter	2.15 - 2.55

Table S6. 2. Results of the linear regression (enter-method) for the baseline measures in the ketamine study.

A Glu/tCr (residualized for gray matter partial volume); B Acet-Tub/TRF levels; C absolute Acet-Tub levels; D absolute TRF levels; E Leukocytes number; F Erythrocytes number; G Thrombocytes number; H Haemoglobin; I Sodium; J Potassium; K Calcium, by the demographic parameters.

A Glu/tCr				
Model summary	<i>R</i> ² change	<i>df</i> ₁	<i>df</i> ₂	sig. <i>F</i> change
	-.016	6	68	.571
Predictors	<i>B</i>	<i>β</i>	<i>t</i>	<i>p</i>
Constant	.377		.351	.727
Age	-.045	-.243	-1.977	.052 #
Sex^A	<.001	<.001	-.002	.998
BMI	.038	.113	.913	.364
Smoking^B	.035	.016	.123	.902
Alcohol usage^C	-.228	-.111	-.823	.413
Drugs^D	.019	.009	.066	.948
Model summary	<i>R</i> ² change	<i>df</i> ₁	<i>df</i> ₂	sig. <i>F</i> change
	< .001	1	28	.916

Predictors	<i>B</i>	β	<i>t</i>	<i>p</i>
Constant	.022		.080	.936
Contraceptives ^E	-.038	-.020	-.107	.992

B Acet-Tub/ TRF

Model summary	<i>R</i> ² change	<i>df</i> 1	<i>df</i> 2	sig. <i>F</i> change
	.372	6	68	< .001
Predictors	<i>B</i>	β	<i>t</i>	<i>p</i>
Constant	.373		.348	.729
Age	.042	.161	1.611	.112
Sex ^A	1.388	.576	5.578	< .001 ***
BMI	.018	.045	.454	.651
Smoking ^B	-.055	-.022	-.200	.842
Alcohol usage ^C	.088	.036	.321	.749
Drugs ^D	-.213	-.087	-.736	.464
Model summary	<i>R</i> ² change	<i>df</i> 1	<i>df</i> 2	sig. <i>F</i> change
	.233	1	28	.007
Predictors	<i>B</i>	β	<i>t</i>	<i>p</i>
Constant	2.203		12.089	< .001
Contraceptives ^E	-.728	-.483	-2.918	.007 **

C Acet-Tub

Model summary	<i>R</i> ² change	<i>df</i> 1	<i>df</i> 2	sig. <i>F</i> change
	.463	6	68	< .001
Predictors	<i>B</i>	β	<i>t</i>	<i>p</i>
Constant	5.783		3.921	< .001
Age	-.029	-.074	-.808	.422
Sex ^A	-2.160	-.602	-6.307	< .001 ***
BMI	.055	.093	1.009	.317
Smoking ^B	-.072	-.019	-.189	.851
Alcohol usage ^C	-.464	-.127	-1.222	.226
Drugs ^D	-.261	-.072	-.656	.514
Model summary	<i>R</i> ² change	<i>df</i> 1	<i>df</i> 2	sig. <i>F</i> change
	.001	1	28	.859
Predictors	<i>B</i>	β	<i>t</i>	<i>p</i>
Constant	5.996		13.050	< .001

Contraceptives^E	.112	.034	.179	.859
-----------------------------------	------	------	------	------

D TRF

Model summary	<i>R</i>² change	<i>df</i>1	<i>df</i>2	sig. <i>F</i> change
	.678	6	68	< .001
Predictors	<i>B</i>	<i>β</i>	<i>t</i>	<i>p</i>
Constant	4.874		4.687	< .001
Age	-.054	-.155	-2.168	.034 *
Sex^A	-2.542	-.778	-1.523	< .001 ***
BMI	.016	.030	.422	.674
Smoking^B	-.155	-.035	-.581	.563
Alcohol usage^C	.002	.001	.009	.993
Drugs^D	-.172	-.052	-.613	.542
Model summary	<i>R</i>² change	<i>df</i>1	<i>df</i>2	sig. <i>F</i> change
	.163	1	28	.027
Predictors	<i>B</i>	<i>β</i>	<i>t</i>	<i>p</i>
Constant	3.195		8.565	< .001
Contraceptives^E	1.192	.404	2.334	.027 *

E Leukocytes

Model summary	<i>R</i>² change	<i>df</i>1	<i>df</i>2	sig. <i>F</i> change
	.041	6	73	.171
Predictors	<i>B</i>	<i>β</i>	<i>t</i>	<i>p</i>
Constant	4.972		3.019	.003
Age	.019	.062	.538	.592
Sex^A	.097	.030	.251	.803
BMI	.028	.050	.439	.662
Smoking^B	1.167	.337	2.711	.008 **
Alcohol usage^C	-.141	-.042	-.333	.740
Drugs^D	-.330	-.097	-.708	.481
Model summary	<i>R</i>² change	<i>df</i>1	<i>df</i>2	sig. <i>F</i> change
	.035	1	31	.299
Predictors	<i>B</i>	<i>β</i>	<i>t</i>	<i>p</i>
Constant	6.613		16.150	< .001
Contraceptives^E	-.586	-.186	-1.056	.299

F Erythrocytes				
Model summary	R² change	df1	df2	sig. F change
	.362	6	73	< .001
Predictors	B	β	t	p
Constant	4.077		1.557	< .001
Age	-.001	-.012	-.120	.905
Sex^A	.483	.531	5.314	< .001 ***
BMI	.022	.144	1.472	.145
Smoking^B	-.102	-.106	-1.006	.318
Alcohol usage^C	.008	.008	.076	.940
Drugs^D	.109	.116	.996	.323
Model summary	R² change	df1	df2	sig. F change
	.052	1	31	.203
Predictors	B	β	t	p
Constant	4.475		55.980	< .001
Contraceptives^E	.141	.228	1.302	.203

G Thrombocytes				
Model summary	R² change	df1	df2	sig. F change
	.144	6	73	.070
Predictors	B	β	t	p
Constant	21.774		3.941	< .001
Age	-.473	-.046	-.410	.683
Sex^A	-32.634	-.300	-2.592	.012 *
BMI	2.685	.149	1.315	.193
Smoking^B	22.106	.193	1.581	.118
Alcohol usage^C	-2.962	-.027	-.215	.830
Drugs^D	-1.082	-.090	-.666	.507
Model summary	R² change	df1	df2	sig. F change
	< .001	1	31	.955
Predictors	B	β	t	p
Constant	263.067		18.281	< .001
Contraceptives^E	1.100	.010	.056	.955

H Haemoglobin				
Model summary	R² change	df1	df2	sig. F change
	.536	6	73	< .001
Predictors	B	β	t	p
Constant	.536	6	73	< .001
Age	B	Beta	t	p
Sex^A	8.088		12.775	< .001
BMI	.011	.066	.791	.431
Smoking^B	1.244	.711	8.347	< .001 ***
Alcohol usage^C	-.007	-.023	-.275	.784
Drugs^D	.184	.100	1.109	.271
Model summary	R² change	df1	df2	sig. F change
	.012	1	31	.546
Predictors	B	β	t	p
Constant	8.373		47.573	< .001
Contraceptives^E	-.146	-.109	-.611	.546

I Sodium				
Model summary	R² change	df1	df2	sig. F change
	.055	6	73	.649
Predictors	B	β	t	p
Constant	139.653		61-679	< .001
Age	-.023	-.057	-.479	.633
Sex^A	.603	.138	1.131	.262
BMI	.012	.017	.142	.887
Smoking^B	.102	.022	.172	.864
Alcohol usage^C	-.542	-.122	-.932	.355
Drugs^D	.714	.158	1.114	.269
Model summary	R² change	df1	df2	sig. F change
	.021	1	31	.425
Predictors	B	β	t	p
Constant	139.533		259.273	< .001
Contraceptives^E	-.589	-.144	-.808	.425

J Potassium				
Model summary	R² change	df1	df2	sig. F change

	.077	6	72	.430
Predictors	B	β	t	p
Constant	.077	6	72	.430
Age	B	Beta	t	P
Sex^A	3.873		12.066	< .001
BMI	.007	.121	1.0202	.311
Smoking^B	-.095	-.151	-1.251	.215
Alcohol usage^C	.007	.070	.593	.555
Drugs^D	-.034	-.051	-.401	.689
Model summary	R² change	df1	df2	sig. F change
	< .001	1	30	.955
Predictors	B	β	t	p
Constant	4.246		47.194	< .001
Contraceptives^E	.001	.001	.007	.995

K Calcium

Model summary	R² change	df1	df2	sig. F change
	.159	6	73	.043
Predictors	B	β	t	p
Constant	2.376		26.413	< .001
Age	.005	.299	2.672	.009 **
Sex^A	.023	.125	1.090	.279
BMI	-.006	-.195	-1.739	.086 #
Smoking^B	.031	.158	1.308	.195
Alcohol usage^C	.014	.073	.594	.554
Drugs^D	.003	.018	.134	.894
Model summary	R² change	df1	df2	sig. F change
	.289	1	31	.001
Predictors	B	β	t	p
Constant	2.439		123.005	< .001
Contraceptives^E	-.095	-.538	-3.551	.001 **

^A women= 0, men= 1; ^B no= 0, yes= 1; ^C <1 drink per week= 0, >1 drink per week= 1;

^D no= 0, yes= 1; ^E women only, n= 33; physical= 0, hormonal= 1.

*** p < .001; ** p < .01; * p < .05

Table S6. 3. Results of the rmANOVA for the absolute peripheral markers.

A Acet-Tub and B TRF absolute levels

Effect	A Acet-Tub	B TRF
Within- participants		
Time point	$F(1, 67) = 2.788, p = .100, \eta^2 = .040$	$F(1, 67) = 1.530, p = .220, \eta^2 = .022$
Time point by sex	$F(1, 67) = 1.136, p = .290, \eta^2 = .017$	$F(1, 67) = 9.725, p = .003, \eta^2 = .127 ***$
Time point by treatment	$F(1, 67) = 1.302, p = .258, \eta^2 = .019$	$F(1, 67) = 4.555, p = .036, \eta^2 = .064 *$
Time point by treatment by sex	$F(1, 67) = .030, p = .862, \eta^2 < .001$	$F(1, 67) = 3.108, p = .082, \eta^2 = .044 \#$
Between- participants		
Sex	$F(1, 67) = 6.317, p < .001, \eta^2 = .474 ***$	$F(1, 67) = 245.530, p < .001, \eta^2 = .786 ***$
Treatment	$F(1, 67) = .010, p = .919, \eta^2 < .001$	$F(1, 67) = .050, p = .823, \eta^2 = .001$
Treatment by Sex	$F(1, 67) = .010, p = .920, \eta^2 < .001$	$F(1, 67) = .312, p = .579, \eta^2 = .005$

*** $p < .001$; * $p < .05$; # $.1 < p < .05$ **Table S6. 4. Results of the repeated measures ANCOVA for blood safety parameters.**

Analysis was controlled for sex, age and BMI.

	Time point by treatment
Thrombocytes (Gpt/L)¹	$F(1, 74) = 13.54, p = .001, \eta^2 = .155$
Erythrocytes (Tpt/L)²	$F(1, 74) = .001, p = .98, \eta^2 = .001$
Leukocytes (Gpt/L)	$F(1, 73) = .09, p = .77, \eta^2 = .001$
Hemoglobin (mmol/L)³	$F(1, 74) = .06, p = .80, \eta^2 = .001$
Sodium (mmol/L)	$F(1, 73) = .53, p = .47, \eta^2 = .007$
Potassium (mmol/L)	$F(1, 74) = .17, p = .68, \eta^2 = .002$
Calcium (mmol/L)	$F(1, 70) = .001, p = .99, \eta^2 = .001$

1 Gpt/L denotes gigaparticles (10⁹) per litre; 2 Tpt/L denotes teraparticles (10¹²) per litre; 3 mmol/ L denotes millimole (10⁻³) per litre; *** $p < .001$; * $p < .05$; # $.1 < p < .05$

Table S6. 5. Results of the linear regression (enter method) for the relative increase of

A residualized Glu/tCr; B Acet-Tub/TRF; C thrombocytes in the whole ketamine group or only women by demographic parameters.

A Glu/tCr								
Model summary	Ketamine = 36				Ketamine women = 14			
	R² change	df1	df2	sig. F change	R² change	df1	df2	sig. F change
	.160	6	29	.494	.372	6	7	.666
Predictors	B	β	t	p	B	β	t	p
Constant	1.688		1.070	.293	-2.377		-.662	.529
Age	.009	.054	.293	.772	.021	.138	.320	.759
Sex^A	.119	.061	.344	.734				
BMI	-.079	-	-.246	.219	.065	.161	.370	.722
Smoking^B	-.501	-	-.234	.277	-1.595	-	-.577	.213
Alcohol use^C	-.240	-	-.124	.589	-.705	-	-.310	.575
Drugs^D	.577	.284	1.161	.255	1.603	.638	1.414	.200
Contraceptive pill^E					.897	.379	.938	.379

B Acet-Tub/TRF								
Model summary	Ketamine = 36				Ketamine women = 14			
	R² change	df1	df2	sig. F change	R² change	df1	df2	sig. F change
	.052	6	28	.952	.588	6	6	.393
Predictors	B	β	t	p	B	β	t	p
Constant	.288		1.014	.319	-2.377		-.622	.529
Age	-.004	-	-.113	.574	.021	.138	.320	.759
Sex^A	.052	.147	.777	.444				
BMI	-.004	-	-.071	.746	.065	.161	.370	.722
Smoking^B	.068	.173	.686	.498	-1.595	-	-.577	.213
Alcohol us^C	.006	.018	.080	.937	-.705	-	-.310	.575

Drugs^D	-.056	-.151	-.536	.596	1.603	.638	1.414	.200
Contraceptive pill^E					.897	.379	.938	.379

C Acet-Tub

Model summary	Ketamine = 36				Ketamine women = 14			
	<i>R</i> ² change	<i>df</i> 1	<i>df</i> 2	sig. <i>F</i> change	<i>R</i> ² change	<i>df</i> 1	<i>df</i> 2	sig. <i>F</i> change
	.115	6	28	.722	.653	6	6	.231
Predictors	<i>B</i>	<i>β</i>	<i>t</i>	<i>p</i>	<i>B</i>	<i>β</i>	<i>t</i>	<i>p</i>
Constant	.548		1.603	.120	1.003		1.546	.173
Age	-.007	-.173	-.903	.374	-.009	-.267	-.527	.617
Sex^A	-.036	-.083	-.454	.653				
BMI	-.014	-.203	-.968	.341	-.029	-.407	-.627	.554
Smoking^B	.129	.266	1.091	.285	.427	.771	1.963	.097
Alcohol usage^C	.004	.008	.038	.970	.001	.001	.003	.998
Drugs^D	-.093	.125	-.744	.463	-.581	1.050	2.137	.076
Contraceptive pill^E					.002	.004	.007	.994

D TRF

Model summary	Ketamine = 36				Ketamine women = 14			
	<i>R</i> ² change	<i>df</i> 1	<i>df</i> 2	sig. <i>F</i> change	<i>R</i> ² change	<i>df</i> 1	<i>df</i> 2	sig. <i>F</i> change
	.052	6	28	.953	.374	6	6	.727
Predictors	<i>B</i>	<i>β</i>	<i>t</i>	<i>p</i>	<i>B</i>	<i>β</i>	<i>t</i>	<i>p</i>
Constant	.296		.766	.450	.111		.160	.878
Age	-.004	-.100	-.502	.620	-.008	-.334	-.491	.641
Sex^A	-.055	-.114	-.603	.551				
BMI	-.010	-.136	-.624	.537	.005	.083	.096	.927
Smoking^B	.043	.081	.322	.750	.063	.142	.269	.797

Alcohol usage^C	-.007	-.015	-.066	.948	-.054	-.145	-.211	.840
Drugs^D	-.001	-.002	-.008	.993	-.231	-.522	-.792	.458
Contraceptive pill^E					.034	.089	.134	.898

E Thrombocytes

Model summary	Ketamine = 36				Ketamine women = 14			
	<i>R</i> ² change	<i>df</i> 1	<i>df</i> 2	sig. <i>F</i> change	<i>R</i> ² change	<i>df</i> 1	<i>df</i> 2	sig. <i>F</i> change
	.148	6	32	.491	.229	6	8	.862
Predictors	<i>B</i>	<i>β</i>	<i>t</i>	<i>p</i>	<i>B</i>	<i>β</i>	<i>t</i>	<i>p</i>
Constant	1.136		.649	.521	.316		.880	.405
Age	.006	.255	1.462	.154	.007	.377	.811	.441
Sex^A	.049	.177	1.058	.298				
BMI	-.011	-.246	1.371	.180	-.021	-.534	1.003	.345
Smoking^B	-.011	-.038	-.183	.856	.129	.412	1.033	.332
Alcohol usage^C	.073	.264	1.253	.219	.071	.282	.487	.639
Drugs^D	-.037	-.127	-.537	.595	-.142	-.502	1.072	.315
Contraceptive pill^E					.047	.176	.396	.702

^A 0= women, 1= men; ^B 0= no, 1= yes; ^C 0= <1 drink per week, 1= > 1 drink per week;

^D 0= no, 1= yes; ^E 0= physical, 1= hormonal.

Table S6. 6. Demographic data for the CADSS groups: there were no differences between the groups.

Data is presented in mean± S.D or frequencies.

	Placebo (N= 40)	< 4 CADSS (N= 16)	>5 CADSS (N= 24)	Kruskal-Wallis or χ^2 interaction test
Age	25.83± 4.98	27.19± 7.24	25.13± 4.26	$\chi^2(2)= 1.031, p= .597$
Sex	17 women	8 women	8 women	$\chi^2(2)= 1.152, p= .562$
BMI	23.76± 2.94	24.78± 2.52	23.17± 3.27	$\chi^2(2)= 3.834, p= .147$
Smoking yes	15	5	6	$\chi^2(2)= 1.083, p= .582$
Alcohol usage A	27	7	16	$\chi^2(2)= 3.004, p= .223$
Drugs yes B	15	4	9	$\chi^2(2)= .879, p= .644$
Contraceptive pill yes C	8	5	5	$\chi^2(2)= .793, p= .673$

^A Frequency of 1-3 drinks per week; ^B Ever consumed drugs; ^C Only for women

II. Publications

Publications included in doctoral thesis

1. Colic, L.* , McDonnell, C.* , Li, M., Woelfer, M., Liebe, T., Kretschmar, M., ...& Walter, M. (2018). Neuronal and peripheral markers of plasticity dynamics change concomitantly after sub-anaesthetic dose of ketamine in humans. *Behavioural Brain Research*, *accepted*.
2. Colic, L., Li, M., Demenescu, L. R., Li, S., Müller, I., Richter, A., ... & Stork, O. (2018). GAD65 promoter polymorphism rs2236418 modulates harm avoidance in women via inhibition/excitation balance in the rostral ACC. *Journal of Neuroscience*, *38(22)*, 5067-5077.
3. Colic, L., Woelfer, M., Colic, M., Leutritz, A. L., Liebe, T., Fensky, L., ... & Walter, M. (2018). Delayed increase of thrombocyte levels after a single sub-anesthetic dose of ketamine - a randomized trial. *European Neuropsychopharmacology*, in press
4. Li, M., Demenescu, L. R., Colic, L., Metzger, C. D., Heinze, H. J., Steiner, J., ... & Walter, M. (2017). Temporal dynamics of antidepressant ketamine effects on glutamine cycling follow regional fingerprints of AMPA and NMDA receptor densities. *Neuropsychopharmacology*, *42(6)*, 1201.
5. Colic, L., Demenescu, L. R., Li, M., Kaufmann, J., Krause, A. L., Metzger, C., & Walter, M. (2015). Metabolic mapping reveals sex-dependent involvement of default mode and salience network in alexithymia. *Social cognitive and affective neuroscience*, *11(2)*, 289-298.

Book chapter

1. Amidfar, M., Colic, L., Walter, M., & Kim, Y. K. (2018). Complex Role of the Serotonin Receptors in Depression: Implications for Treatment. In *Understanding Depression* (pp. 83-95). Springer, Singapore.

Other publications

1. Walter, M., Alizadeh, S., Jamalabadi, H., Lueken, U., Dannlowski, U., Walter, H., ... & Hahn, T. (2018). Translational machine learning for psychiatric neuroimaging. *Progress in Neuro-Psychopharmacology and Biological Psychiatry*, *accepted*
2. Li, M., Woelfer, M., Colic, L., Safron, A., Chang, C., Heinze, H.-J.,... & Walter, M. (2018). Default Mode Network connectivity change corresponds to ketamine's delayed glutamatergic effects. *European Archives of Psychiatry and Clinical Neuroscience*, *accepted*
3. Liebe, T., Li, M., Colic, L., Matthias, H. M., Sweeney-Reed, C. M., Woelfer, M., ... & Walter, M. (2018). Ketamine influences the locus coeruleus norepinephrine network, with a dependency on norepinephrine transporter genotype—a placebo controlled fMRI study. *NeuroImage: Clinical*, *in press*
4. Krause, A. L., Colic, L., Borchardt, V., Li, M., Strauss, B., Buchheim, A., ... & Walter, M. (2018). Functional connectivity changes following interpersonal reactivity. *Human brain mapping*, *39(2)*, 866–879
5. Ristow, I., Li, M., Colic, L., Marr, V., Födisch, C., von Düring, F., ... & Walter, M. (2018). Pedophilic sex offenders are characterised by reduced GABA concentration in dorsal anterior cingulate cortex. *NeuroImage: Clinical*, *18*, 335-341.
6. Liebe, T., Li, S., Lord, A., Colic, L., Krause, A. L., Batra, A., ... & Walter, M. (2017). Factors Influencing the Cardiovascular Response to Subanesthetic Ketamine: A Randomized, Placebo-Controlled Trial. *International Journal of Neuropsychopharmacology*, *20(11)*, 909-918.
7. Amidfar, M., Kim, Y. K., Colic, L., Arbabi, M., Mobaraki, G., Hassanzadeh, G., & Walter, M. (2017). Increased levels of 5HT_{2A} receptor mRNA expression in peripheral blood mononuclear cells of patients with major depression: correlations with severity and duration of illness. *Nordic journal of psychiatry*, *71(4)*, 282-288.
8. Demenescu, L. R., Colic, L., Li, M., Safron, A., Biswal, B., Metzger, C. D., ... & Walter, M. (2017). A spectroscopic approach toward depression diagnosis: local

metabolism meets functional connectivity. *European archives of psychiatry and clinical neuroscience*, 267(2), 95-105.

9. Blazevic, S., Colic, L., Culig, L., & Hranilovic, D. (2012). Anxiety-like behavior and cognitive flexibility in adult rats perinatally exposed to increased serotonin concentrations. *Behavioural brain research*, 230(1), 175-181.

III. Ehrenerklärung

Ich versichere hiermit, dass ich die vorliegende Arbeit ohne unzulässige Hilfe Dritter und ohne Benutzung anderer als der angegebenen Hilfsmittel angefertigt habe; verwendete fremde und eigene Quellen sind als solche kenntlich gemacht.

Ich habe insbesondere nicht wissentlich:

- Ergebnisse erfunden oder widersprüchlich Ergebnisse verschwiegen,
- statistische Verfahren absichtlich missbraucht, um Daten in ungerechtfertigter Weise zu interpretieren,
- fremde Ergebnisse oder Veröffentlichungen plagiiert,
- fremde Forschungsergebnisse verzerrt wiedergegeben.

Mir ist bekannt, dass Verstöße gegen das Urheberrecht Unterlassungs- und Schadensersatzansprüche des Urhebers sowie eine strafrechtliche Ahndung durch die Strafverfolgungsbehörden begründen kann.

Ich erkläre mich damit einverstanden, dass die Arbeit ggf. mit Mitteln der elektronischen Datenverarbeitung auf Plagiate überprüft werden kann.

Die Arbeit wurde bisher weder im Inland noch im Ausland in gleicher oder ähnlicher Form als Dissertation eingereicht und ist als Ganzes auch noch nicht veröffentlicht.

Magdeburg, 26.11.2018.

